

- **The development and hydraulic roughness of subaqueous dunes**

- Antoine Wilbers



Nederlandse Geografische Studies

NGS

Geographical Studies

323

The development and hydraulic roughness of subaqueous dunes

De ontwikkeling en de hydraulische ruwheid van duinen op de rivierbodem

(met een samenvatting in het Nederlands)

PROEFSCHRIFT

Ter verkrijging van de graad van doctor aan de Universiteit Utrecht
op gezag van de Rector Magnificus, Prof. Dr. W.H. Gispen, ingevolge het
besluit van het College voor Promoties in het openbaar te verdedigen op
donderdag 15 januari 2004 des voormiddags te 10:30 uur

Door

Antoine Wilbers

Geboren op 13 januari 1973 te Asten

1272
C

141

S 613.A 37

Promotores:

Prof. Dr. Ir. L.C. van Rijn

Utrecht University

Prof. Dr. E.A. Koster

Utrecht University

Co-promotor:

Dr. J.H. van den Berg

Utrecht University

EX LIBRIS
UNIVERSITATIS
NOVIOMAGENSIS

The development and hydraulic roughness of subaqueous dunes

Nederlandse Geografische Studies / Netherlands Geographical Studies

Redactie / Editorial Board

Prof. Dr. J.M.M. van Amersfoort
Dr. H.J.A. Berendsen
Drs. J.G. Borchert
Prof. Dr. A.O. Kouwenhoven
Prof. Dr. H. Scholten
Dr. P.C.J. Druiven

Plaatselijke Redacteuren / Associate Editors

Drs. J.G. Borchert,
Faculteit Geowetenschappen Universiteit Utrecht
Dr. D.H. Drenth,
Faculteit Beleidswetenschappen Katholieke Universiteit Nijmegen
Drs. F.J.P.M. Kwaad,
Fysich-Geografisch en Bodemkundig Laboratorium Universiteit van Amsterdam
Dr. P.C.J. Druiven,
Faculteit der Ruimtelijke Wetenschappen Rijksuniversiteit Groningen
Dr. L. van der Laan,
Economisch-Geografisch Instituut Erasmus Universiteit Rotterdam
Dr. J.A. van der Schee,
Centrum voor Educatieve Geografie Vrije Universiteit Amsterdam
Dr. F. Thissen,
Instituut voor Sociale Geografie Universiteit van Amsterdam

Redactie-Adviseurs / Editorial Advisory Board

Prof. Dr. G.J. Ashworth, Prof. Dr. P.G.E.F. Augustinus, Prof. Dr. G.J. Borger,
Prof. Dr. J. Buursink, Prof. Dr. K. Bouwer, Dr C. Cortie, Dr. J. Floor,
Drs. J.D.H. Harten, Prof. Dr. G.A. Hoekveld, Dr. A.C. Imeson,
Prof. Dr. J.M.G. Kleinpenning, Dr. W.J. Meester, Prof. Dr. F.J. Ormeling,
Prof. Dr. H.F.L. Ottens, Dr. J. Sevink, Dr. W.F. Slegers,
T.Z. Smit, Drs. P.J.M. van Steen, Dr. J.J. Sterkenburg, Drs. H.A.W. van Vianen,
Prof. Dr.J. van Weesep

ISSN 0169-4839

Netherlands Geographical Studies 323

The development and hydraulic roughness of subaqueous dunes

Antoine Wilbers

Utrecht 2004

The Royal Dutch Geographical Society/
Faculty of Geosciences, Utrecht University

Promotores:

Prof. Dr. Ir L. C. van Rijn Utrecht University

Prof. Dr. E. A. Koster Utrecht University

Co-promotor

Dr. J. H. van den Berg Utrecht University

Examination committee:

Prof. Dr. ir. H. J. de Vriend Faculty of Civil Engineering and Geosciences,
Delft University of Technologie.

Prof. Dr. J. Best School of Earth Sciences, University of Leeds

Prof. Dr. S. J. M. H. Hulscher Department of Civil Engineering, University of Twente

Dr. H. Ogink WL I Delft Hydraulics

Dr. W. B. M. ten Brinke Institute for Inland Water Management and Waste Water
Treatment ("RIZA"), Ministry of Transport, Public Works and
Water Management

ISBN 90-6809-361-4

Copyright © Antoine Wilbers, c/o Faculty of Geosciences, Utrecht University,
2004

Niets uit deze uitgave mag worden vermenigvuldigd en/of openbaar gemaakt door middel
van druk, fotokopie of op welke andere wijze dan ook zonder voorafgaande schriftelijke
toestemming van de uitgevers.

All rights reserved. No part of this publication may be reproduced in any form, by print or
photo print, microfilm or any other means, without written permission by the publishers.

Printed in the Netherlands by Labor Grafimedia b.v. - Utrecht

Voor Bianca en Caithlyn

Contents

List of figures 11

List of plates 15

List of tables 16

Acknowledgements – Voorwoord 17

1 Introduction 21

- 1.1 Background and problem definition 21
- 1.2 Subaqueous dunes 24
 - 1.2.1 Dune formation 24
 - 1.2.2 Dune roughness 25
 - 1.2.3 Dynamic feedback loop 26
- 1.3 Research objectives 27
- 1.4 Organization of the theses 28
- 1.5 References 28

2 Classification of subaqueous bedforms 31

- Abstract 31
- 2.1 Introduction 32
 - 2.1.1 Bars 34
 - 2.1.2 Transverse bedforms 34
- 2.2 Classification according to flow 35
 - 2.2.1 Sediment mobility 35
 - 2.2.1.1 Stable bedforms in sub-critical flow 35
 - 2.2.1.2 Stable bedforms in super-critical flow 37
 - 2.2.2 Sediment mobility in case of a distribution of grain sizes 37
 - 2.2.3 Sediment availability 39
- 2.3 Description of dune and ripple dimensions 40
 - 2.3.1 Ripple dimensions and shapes 40
 - 2.3.2 Dune dimensions 40
 - 2.3.2.1 Steady flow conditions 40
 - 2.3.2.2 Unsteady flow conditions 41
 - 2.3.3 Dune shapes 43
- 2.4 Complicating aspects 43
 - 2.4.1 Low angle dunes 43
 - 2.4.2 Superposition 44
- 2.5 References 45

Part 1 Development of subaqueous dunes 49

3 Bedload transport rate obtained by dune tracking: reliability and optimisation 51

- Abstract 51
- 3.1 Introduction 52
- 3.2 Sediment transport over dunes 53
- 3.3 Dune Tracking technique 55
- 3.4 Use of dune tracking in field situations 56
 - 3.4.1 Difficulties of field measurements 56
 - 3.4.2 Conversion of dune migration to bedload transport rate 59
 - 3.4.2.1 Dune shape 59
 - 3.4.2.2 Point of zero bed-load transport rate 61
 - 3.4.2.3 Closed mass balance between stoss-side erosion and lee-side accretion 61
 - 3.4.2.4 Two dimensional flow 62
 - 3.4.2.5 The bed-load discharge coefficient 62
 - 3.4.3 Superposition of dunes 65
- 3.5 Conclusion 67
- Acknowledgments 68
- Notation 68
- References 68

4 The response of subaqueous dunes to floods in sand and gravel bed reaches of the Dutch Rhine 71

- Abstract 71
- 4.1 Introduction 72
 - 4.1.1 Study area 73
- 4.2 Methods and analyses 74
 - 4.2.1 Collecting dune data 74
 - 4.2.2 Detailed datasets during floods 76
 - 4.2.3 Hydrodynamics 77
 - 4.2.4 Calculation of dune properties 77
 - 4.2.5 Dune propagation and bedload transport 78
- 4.3 Results 79
 - 4.3.1 Dune patterns: spatial variation 79
 - 4.3.2 Dune growth and decay 82
 - 4.3.2.1 Dune length 82
 - 4.3.2.2 Dune height 83
 - 4.3.2.3 Dune migration rate 86
 - 4.3.3 Hysteresis in sediment transport 88
- 4.4 Discussion 88
 - 4.4.1 Dune patterns 88

4.4.1.1	The impact of groynes	90
4.4.1.2	Grain size effects	90
4.4.1.3	Floodplain effects	92
4.4.2	Dune growth and decay	94
4.4.2.1	Relations with shear stress	94
4.4.3	Hysteresis in bedload sediment transport	97
4.5	Conclusions	98
	Acknowledgements	99
	Notation	99
	References	99

5 Predicting dune development during flood waves in the Rhine branches in The Netherlands 103

	Abstract	103
5.1	Introduction	104
5.2	Review of existing prediction methods	105
5.2.1	Steady, uniform flow conditions	107
5.2.2	Unsteady, non-uniform flow conditions	110
5.3	Development of a prediction method for the Rhine branches	112
5.3.1	Equilibrium predictors	112
5.3.2	Adaptation constant	115
5.3.3	The prediction method for the Rhine branches	116
5.4	Discussion	119
5.4.1	Adaptation constant	119
5.4.2	Two equilibrium predictors	120
5.4.3	The Waal near Druten	121
5.5	Conclusion	121
	Acknowledgements	122
	Notation	122
	References	123
	Appendix 5.I	125
	Shinohara & Tsubaki (1959)	125
	Tsuchiya & Ishizaki (1967)	125
	Allen (1968)	126
	Van Rijn (1984)	126
	Appendix 5. II	126
	Dune height around Pannerdensche Kop	127
	Dune length around Pannerdensche Kop	127
	Dune height near Druten	128

Part 2 The hydraulic roughness of subaqueous dunes 129

6 Invariable flow separation zone characteristics at the lee sides of subaqueous bedforms 131

Abstract 131

6.1 Introduction 132

6.2 Review of past research 134

6.2.1 Separation length versus dune dimensions 134

6.2.2 Separation length versus flow and grain size 135

6.3 Parameterisation of the flow separation zone 135

6.3.1 Data quality 137

6.4 Results 137

6.5 Discussion 140

6.5.1 Point of flow separation 142

6.6 Conclusions 143

Acknowledgement 144

Notation 144

References 144

7 Predicting the hydraulic roughness of subaqueous dunes 147

Abstract 147

7.1 Introduction 148

7.2 Measurement data 150

7.2.1 Flume experiments 151

7.2.2 Field measurements 156

7.3 Method of analysis 157

7.3.1 Statistical analysis 159

7.4 Results 160

7.5 Discussion 164

7.5.1 Summing k_s 166

7.5.2 Improving the Vanoni & Hwang predictor 168

7.5.3 Field situations 168

7.6 Conclusion 170

Acknowledgements 171

Notation 171

References 173

Appendix 7.I 174

8 Synthesis, application of the results and implications for future research 177

8.1 Introduction 177

8.2 Conclusions of this thesis 178

8.2.1 Bedload transport and migrating dunes 178

8.2.2	Observed and predicted dune development	179
8.2.3	The relation between flow separation and hydraulic roughness	180
8.2.4	Predicting the hydraulic roughness of dunes	180
8.2.5	Superposition of subaqueous dunes	181
8.3	Combining predictors	183
8.3.1	Step 1	184
8.3.2	Step 2	184
8.3.3	Step 3	185
8.3.4	Step 4	186
8.3.5	Step 5	188
8.4	Conclusions	189
8.5	Future research	190
8.6	References	192

Appendix A Dune development data 195

Appendix B Hydraulic roughness data 206

Summary 215

Samenvatting 220

Curriculum Vitae 225

Publications 226

Figures

1.1. The physiography of the rivers in The Netherlands (a) and the influence of this regulated state versus the natural state on water levels during floods (b). 21

1.2. Dune patterns in the Rhine near the bifurcation of the Pannerdensche Kop in The Netherlands on 4 November 1998 during the peak of a flood. PK is Pannerdensche Kanaal, and BR is Bovenrijn. 23

1.3. Example of the phase shift (δ) between flow velocity (U) and bedload sediment transport in an unstable situation. $Z(t)$ is the bed-elevation at time t , $z(t+\Delta t)$ the bed-elevation after some time and d is the average water depth (after Kennedy, 1969). 25

1.4. The expansion and separation of the flow over the lee-side trough of a dune. 26

1.5. A dynamic feedback loop between flow, sediment transport and dunes. 27

2.1. Classification scheme of bedforms described in this study. 32

2.2. Schematic representation of bedform types present in the Dutch Rhine. Flow convergence and divergence between opposite groynes creates a sand wave or bar-like feature called a groyne-bar. Other bedforms, like dunes, are superimposed on these groyne-bars. 33

2.3. Conceptual explanatory stability diagram for bedforms and sediment transport, relating grain size and flow strength under the assumption that the riverbed consists of grains of one specific size only. Grain size is represented by a dimensionless particle parameter and flow strength by a dimensionless mobility parameter. After Chabert & Chauvin (1963); Guy *et al.* (1966); Southard & Boguchwal (1990); Van den Berg & Van Gelder (1993, 1998). A) bedform stability in lower flow regime ($Fr < 1$). B) bedform stability in upper flow regime ($Fr > 1$). Diagonal black lines indicate $Fr \approx 0.8$ and $Fr = 1.0$ at an arbitrary water depth. Grey lines indicate $Fr \approx 0.8$ and $Fr = 1.0$ at a larger water depth ($h = >$) and at a smaller water depth ($H = <$). C) type of sediment transport. D) relation between ripples or dunes and the thickness of the viscous sub-layer (δ_v), after Allen (1985). 36

2.4. Conceptual explanatory model for the occurrence of bedforms in sediment supply-limited conditions, after Kleinhans *et al.* (2002). 38

2.5. A plot of height (H) versus length (L) of 1491 flow transverse subaqueous bedforms from different environments including flumes (after Flemming, 1988), showing a clear gap between ripples and dunes. 39

2.6. A plot of dune height (a) and dune length (b) versus the average water depth in many flume tests (Laursen, 1958; Shinohara & Tsubaki, 1959; Znamenskaya, 1963; Stein, 1965; Guy *et al.*, 1966; Crickmore, 1970; Engel & Lau, 1980; Livesey *et al.*, 1995), and rivers (Shinohara & Tsubaki, 1959; Stückrath, 1969; Nasner, 1974; Havinga, 1982; Mahmood *et al.*, 1984; Mahmood, 1987; Julien, 1992), including the data from the Rhine and Waal in The Netherlands. Dashed lines indicate a factor 2 variation. 41

2.7. Examples of time-lag of dune height and length in changing flow conditions. a) time-lag defined as a phase difference between maximum flow and maximum dune height or length. b) time-lag defined as a transition-period between the equilibrium dune dimensions during one steady flow condition and the equilibrium dune dimensions during the next. 42

2.8. Differences between measuring the lee side slope of a steep dune with high or low resolution. Dunes are not drawn to scale. a) difference between steepest slope and average slope (between crest and trough). b) difference between the real steepest slope and the measured steepest slope in low resolution measurements. 44

3.1. Flow and sediment transport over a dune. The sediment transport is divided into zones and the interactions between different zones are shown with arrows. A₁ is the suspension transport zone over the stoss-side, and A₂ the bedload transport zone. B₁ is the suspension transport zone over de separation zone, B₂ is zone with downstream flow just above the separation zone, B₃ is the zone of upstream moving water in the separation zone, B₄ is the zone where material avalanches down the lee-side, and B₅ is the zone where upstream moving water causes an upstream moving bedload transport. This schematisation is modified from figures of Allen (1965) and Bennet & Best (1995). 53

3.2. Dune profile definition sketch. For explanation of letters see text. 55

3.3. The number of points per dune versus the maximum relative error of the real value of dune height, length and volume. 57

3.4. Relative error in calculating the dune migration distance as a function of the real migration distance and the spatial resolution. 58

3.5. The ambiguous correlation of dunes when the temporal resolution is to large. 58

3.6. A) Histogram of all measured form factors (Table 1). B) Histogram of factor a , calculated with the relations of Engel & Lau (1981). 59

3.7. Histograms and scatterplots of the logarithmic relative differences between β_c and β_f . The relative values and β values are also shown. a) using equation 3.16. b) using equation 3.17. 63

3.8. Changes in dune dimensions, migration rate and calculated bedload transport in the Rhine during the flood of 1998. a) dune height. b) dune length. c) migration rate. d) bedload transport rate. For explanation about assumed migration rates see text. 66

4.1. The tributaries of the Rhine River in The Netherlands. The numbers in (B) and (A) indicate the different sections and subsections where echosoundings were made; with Section 1 being the Bovenrijn, Section 2 being the Pannerdensche Kop, a bifurcation of the Bovenrijn (2C) into the Waal (2A) and the Pannerdensche Kanaal (PK) (2B) and Section 3 being halfway down the Waal. Figure (D) shows the changes in median grain size (D_{50}) along the Rhine, Bovenrijn and Waal. 72

4.2. Grain size distributions of the different sections and subsections. For Section 3, two distributions are provided to show the difference between the northern and southern halves of the river. 73

4.3. Flow discharges of the floods of 1995, 1997 and 1998 at Lobith, and the days within the flood waves for which data on dunes are available. 76

4.4. Typical dune shape defining the characteristics as calculated with DT2D. 78

4.5. The difference between two successive multibeam echosoundings (time step is 24h) in the Waal (Section 3), showing erosion on the stoss sides and deposition on the lee-sides. The flow is from right to left. 79

4.6. Small part of a bed profile from Subsection 2C (fig. 4.1C) on 16 February 1998 showing large dunes (grey) which are superimposed by small dunes on the stoss and lee-sides. 80

4.7. Phase diagrams of changing dune length in all three sections using all available data from Table 4.1. Filled and open triangles distinguish between single and multibeam measurements respectively. Filled and open squares and dots, respectively, distinguish between primary and secondary dunes in Sections 1 and 2A. The arrows going to the right indicate the average development during rising discharge, whereas arrows going to the left indicate the development during falling discharge for specific floods. For Section 3, the dune length of both the large dunes in the northern half and the small dunes in the southern half is shown. 82

4.8. Phase diagrams of changing dune height in all three sections using all available data from Table 4.1. Filled and open triangles distinguish between single and multibeam measurements respectively. Filled and open squares and dots, respectively, distinguish between primary and secondary dunes in Sections 1 and 2A. The arrows going to the right indicate the average development during rising discharge, whereas arrows going to the left indicate the development during falling discharge for specific floods. For Section 3, the dune height of both the large dunes in the northern half and the small dunes in the southern half is shown. 83

4.9. Phase diagrams of changing migration rate in all three sections using all available data from Table 4.1. Filled and open triangles distinguish between single and multibeam measurements respectively. Filled and open squares and dots, respectively, distinguish between primary and secondary dunes in Sections 1 and 2A. The arrows going to the right indicate the average development during rising discharge, whereas arrows going to the left indicate the development during falling discharge for specific floods. For Section 3, migration rates were only calculated for the large dunes from the northern half of the river. 86

4.10. Phase diagrams of changing bedload transport rate in all three sections using all available data from Table 4.1. Filled and open triangles distinguish between single and multibeam measurements respectively. Filled and open squares and dots, respectively, distinguish between primary and secondary dunes in Sections 1 and 2A. The arrows going to the right indicate the average development during rising discharge, whereas arrows going to the left indicate the development during falling discharge for specific floods. For Section 3, bedload transport rates were only calculated for the large dunes from the northern half of the river. 87

4.11. The variation of the length of protrusion of the groynes on both sides of the river. 89

4.12. The variability in discharge through the floodplain and the flow velocity in the main channel of the Bovenrijn – Waal during the flood of 1995 calculated with SOBEK. 91

4.13. The changes in bed shear stress from SOBEK in the three sections during rising discharges. 92

4.14. The changes in grain-related shear stress from SOBEK in the three sections during rising discharges. 93

4.15. Relations between dimensionless bed shear stress and dune height (A), dune length (B), dimensionless migration rate (C) and dimensionless bedload transport rate (D). Only measurements during rising discharges are used. The middle solid lines show the fitted power functions along with the power function, the outer solid lines define the 100% deviation range from this power function. 96

4.16. Relations between dimensionless grain-related shear stress and dune height (A), dune length (B), dimensionless migration rate (C) and dimensionless bedload transport rate (D). Only measurements during rising discharges are used. The middle solid lines show the fitted power functions along with the power function, the outer solid lines define the 100% deviation range from this power function. 97

5.1. The development of dune height and length related to the changing bed shear stress near the Pannerdensch Kop, Sections 1 and 2 (a) and near Druten, Section 3 (b). Dates indicate the year in which the flood occurred. In all cases hystereses was anti-clock wise. 105

5.2. The measured dune heights (a) and lengths (b) of the Rhine branches plotted in diagrams of Allen, (1968). Frequency (N) histograms of the dune height, length and water depth of the Rhine data are drawn to show that the most frequent characteristics are predicted with the predictor of Allen, (1968). 107

5.3. Evaluation of several predictors in predicting dune height (a) and dune length (b) in the Bovenrijn for the flood of 1998. A value of 1 in H_p/H_o denotes a perfect prediction. The predictors are named by the authors and their publication date, and the graphs are split to distinguish between primary and superimposed secondary dunes. 109

5.4. Example of reaction and relaxation time. 110

5.5. The rate of adaptation of a dune characteristic (D) depends on the difference between the dune dimensions before the change in flow conditions (D_0) and the new equilibrium dimensions (D_∞). See also eq. 5.1. 111

5.6. Exponential fit of the proportion of change in dune height as a function of time step (days) between measurements for the Bovenrijn during the flood of 1998. 115

5.7. Examples of observed and predicted dune development: a) in the Bovenrijn (Section 1) for 1995. b) the Pannerdensch Kanaal (Section 2b) for 1998. c) the Waal near the Pannerdensch Kop (Section 2c) for 1997. d) the Waal near Druten (Section 3) for 1997. 117

5.8. Comparison between observed and predicted dimensions. The line at a 45° angle denotes a perfect simulation. a) Bovenrijn (Sections 1 and 2a). b) Pannerdensch Kanaal (Section 2b). c) Waal near Pannerdensch Kop (Section 2c). d) Waal near Druten (Section 3). 118

5.9. Influence on the prediction of equilibrium dune height of a hypothetical change in D_{50} of transportable material in the Bovenrijn (Section 2a) during the flood of 1998. 120

6.1. Example of the average flow over a dune (not to scale). The arrow lines indicate stream lines, while vertical lines show the location of velocity profiles. 132

6.2. a) definition of the bed form characteristics. b) definition of the separation zone characteristics. c) detail of the upper part of a smoothly curving lee-side. In all three figures the vertical scale is exaggerated compared to the horizontal scale. 133

6.3. The point of zero velocity is calculated from vertical velocity profiles by calculating a regression line through the three points nearest to the zero velocity. a) a typical velocity profile near the crest of a dune. b) a typical velocity profile in the separation zone. c) a typical velocity profile on the stoss-side of a dune downstream of the reattachment point. 136

6.4. The angle of the zero velocity line in all measurements plotted against the quality of the data (see table 6.1 for abbreviations). 137

6.5. Examples of the shape of the flow separation zone in case of: a) a solitary backward step. b) multiple solid dunes. c) a sinuous dune for a case without a free water surface. The points along the vertical lines represent examples of velocity profiles which were measured at every location marked at the top of each figure. The points along the diagonal lines indicate the zero-velocity points at each velocity profile location. The diagonal lines approximate the zero-velocity lines by connecting the separation point and the reattachment point. 138

6.6. a) relation between the height of an obstacle and the separation length. b) relation between the separation height and the separation length. c) the relation between separation height and total separation length. Solitary forms are represented by squares and multiple forms by diamonds, the grey filling indicating the quality of the data. 139

6.7. a) relation between dimensionless separation length (L_s/H) and the Reynold's number. The original figure was created by Kadota & Nezu (1999), but the results of the present analysis have been added. Solitary forms are thereby represented as squares and multiple forms as diamonds, the grey filling indicating the quality of the data. The small squares and diamonds are the data points of Kadota & Nezu, (1999) and the lines are the relations they created. b) relation between dimensionless separation length (L_s/H) and form steepness (H/L). the original figure was created by Engel (1981), but the results of the present analysis have been added. Only the tests with multiple forms were used. The numbers beside each point show the dimensionless grain size (D_{50}/H), and the lines show the relations created by Engel (1981). 141

7.1. Definition of several dune characteristics, including the areas of superposition and grain roughness. $H_{b,s}$ and L_s are the brinkpoint height and dune length of the superimposed secondary forms. 150

7.2. Bedform configurations in the tests of Ogink (1989). 151

7.3. Bedform configurations in the tests of Kornman (1995). 153

7.4. Grain-size distribution of the sand in the flume during the tests of Van Enckevoort & Van der Slikke (1996). 154

7.5. The non-linear energy height and velocity slopes in one of in the tests of Van Enckevoort & Van der Slikke (1996). Due to non-uniform flow conditions resulting in differences in dune size along the flume, the velocity slope can be divided into 3 sections with slopes that differ from the overall slope. Along with this the energy slope can also be divided into 3 sections to approximate its non-linear shape. For this

example the second section was used as the dominant part, and flow velocity, energy slope, and bed form characteristics were determined from this section. The average sand bed height was about 40 cm above the bottom of the flume. 155

7.6. Predicted roughness versus observed roughness using the original (a) and the adapted (b) predictor of Vanoni & Hwang (1967). The larger diamonds in the cases from the Nile indicate the average values over the full width of the river. 161

7.7. Predicted roughness versus observed roughness using the original (a) and the adapted (B) predictor of Engelund (1977). The larger diamonds in the cases from the Nile indicate the average values over the full width of the river. 162

7.8. Predicted roughness versus observed roughness using the original (a) and the adapted (b) predictor of Van Rijn (1984). The larger diamonds in the cases from the Nile indicate the average values over the full width of the river. 163

7.9. Predicted roughness versus observed roughness using the original (a) and the adapted (b) predictor of Van Rijn (1984) but now with $f=f'+f''$ instead of $k_s=k_s'+k_s''$. 165

7.10. Observed roughness of bedforms versus dune characteristics and water depth similarly to Vanoni & Hwang (1967). 167

7.11. Relation between the brinkpoint height as a proportion of the dune height and the dune height. The fitted functions were created after assuming that the points which plot beneath the lines can be ignored due to low measurement resolution. 169

7.12. Relations between the abundance of superimposed dunes and the steepness of the primary dunes for both flume and field situations. 170

8.1. A visual representation on how the predictors formulated in Chapters 5 and 7 of this thesis fit into the feedback loop between flow conditions, sediment transport, and dune development. 177

8.2. A hypothetical flood wave with a maximum of $16.000 \text{ m}^3\text{s}^{-1}$, defined according to the largest known flood wave in the Rhine at the Dutch-German border from 1995. 183

8.3. The relation between the discharge and the water depth of the main channel according to SOBEK-calculations. 184

8.4. Development of water depth, flow velocity, bed shear stress, and Chezy value during the hypothetical flood wave according to SOBEK-calculations. 185

8.5. Development of dune length and height of primary and secondary dunes as predicted with the models described in Chapter 5. The development of the brinkpoint height was calculated with the function shown in fig. 8.6. 186

8.6. Relation between the brinkpoint height as a proportion of the dune height and the dune height. The fitted function indicates the relation used in the analysis, after assuming that the points which plot beneath the line can be ignored due to low measurement resolution. 187

8.7. Relation between the abundance of superimposed dunes and the steepness of the primary dunes for the Bovenrijn during the flood of 1998. 187

8.8. Development of the Chezy value during the hypothetical flood wave according to the models of Chapter 5 and 7 describing the dune development and dune related hydraulic roughness and also according to the SOBEK-calculations. 188

Plates

4.1. Maps showing the spatial development of dunes in Section 1 during the flood of 1995. (A – D) bed elevation at the beginning of the flood, at peak discharge, at maximum dune height and at the end of the flood respectively. Below map C, three profiles are plotted to show the differences in dune shape over the width of the river. m+NAP refers to an elevation in meters above the Dutch ordnance datum. 81

4.2. Maps showing the spatial development of dunes in Section 2 during the flood of 1998. (A – D) bed elevation at the beginning of the flood, at peak discharge, at maximum dune height and at the end of the flood respectively. Below map C, three profiles are plotted to show the differences in dune shape over the width of the Bovenrijn. m+NAP refers to an elevation in meters above the Dutch ordnance datum. 84

4.3. Maps showing the spatial development of dunes in Section 3 during the flood of 1997. (A – D) bed elevation at the beginning of the flood, at peak discharge, at maximum dune height and at the end of the

flood respectively. Below map C, three profiles are plotted to show the differences in dune shape over the width of the river. The large arrow follows one dune during the flood to show the changes in plan form. m+NAP refers to an elevation in meters above the Dutch ordnance datum. 85

Tables

- 3.1. Factor values (minimum – average – maximum) of the datasets that were used. β values have been recalculated using the reported data on dune characteristics and direct bedload transport measurements. The values of a are calculated using the diagram by Engel & Lau, 1981. n/a means that data is not available. 60
- 4.1. A list of campaigns on measuring dune properties and bedload transport (dune tracking) carried out in the Dutch Rhine (Bovenrijn - Waal reach) between 1982 and 2002, together with the discharge ranges during the campaigns. 75
- 5.1. Overview of general characteristics of the Rhine branches and the different measurement periods. 106
- 5.2. The selected steady, uniform flow predictors of dune height and dune length tested in the unsteady, non-uniform flow conditions of the Rhine, divided into theoretical and empirical based. 108
- 5.3. The values of bed shear stress during the initiation of dune growth, dune decline and superposition near the Pannerdensche Kop (Sections 1 and 2) and the bed shear stress values at the moments of changing development rates in the Waal near Druten (Section 3). 114
- 5.4. Adaptation constants for dune height and length in every Rhine branch during the rising and falling limbs of different floods. 116
- 6.1. Summary of the collected data sources. The bedforms are classified in 6 types, Backward step, Sinuous dune, Solid dune (dunes which are solidified forms of migration dunes, using glue, resin or cement, or artificial dune models with a more natural shape than Triangle dunes), Trench (not really a bedform but in shape similar to backward steps), Triangle dune (an artificial dune model with a triangular shape) and Migrating sand dune (dunes that are actively migrating downstream during the measurements). The abbreviations are used in fig. 6.4. 134
- 7.1. Data on flow and bedform characteristics during the tests of Ogink (1989), Kornman (1995), Van Enckevoort & Van der Slikke (1996), and measurements in the Nile (Abdel-Fattah, 1997) and in the Rhine (Julien *et al.*, 2002; Wilbers and Ten Brinke, 2003; Chapter 4). 152
- 7.2. Statistical results on all data points. The centre values for f and k_s of all observed roughness values are 0.073 and 0.325 respectively. 164
- 7.3. Statistical results on the data points of test D and the tests by Kornman. The centre values for f and k_s of Test D are 0.078 and 0.093 respectively, and for the tests by Kornman, 0.042 and 0.047. 164
- 7.4. Statistical results on a comparison between using $k_s = k_s' + k_s''$ or $f = f' + f''$ in the method of Van Rijn (1984). The centre values for f and k_s of all observed roughness values are 0.073 and 0.325 respectively. 167
- 7.5. Statistical results on improving the predictor of Vanoni & Hwang (1967). The centre value for f of all observed roughness values is 0.073. 168

Acknowledgments – Voorwoord

In het begin van de zomer van 1997 was ik druk bezig met het afronden van mijn veldwerkscriptie zodat ik kon afstuderen als Fysisch Geograaf, toen ik werd gebeld of ik interesse had om een maand of vier te werken onder begeleiding van Janrik van den Berg. Het ging om een contract voor Rijkswaterstaat, RIZA-Arnhem, waarbij bodemmetingen gedaan in maart 1997 in de Bovenrijn en Midden-Waal moesten worden verwerkt om te bepalen wat het bodemtransport was. Hierna volgden nog verschillende andere contracten om steeds andere metingen op een vergelijkbare manier te verwerken. De verkregen data bleek uniek en al snel werd het idee geboren om er meer mee te gaan doen in een promotieonderzoek. Samen met Janrik van den Berg en Professor van Rijn heb ik een onderzoeksvoorstel geschreven en dat werd eind 1998 geaccepteerd. In Februari 1999 begon ik als AIO bij Fysische Geografie in Utrecht.

Voor u ligt nu het resultaat van 4 jaar analyseren, deduceren, redeneren en concluderen. Dat heb ik echter niet allemaal alleen gedaan. Zonder de hulp van velen was dit alles niet tot stand gekomen. Ten eerste wil ik iedereen bij RIZA-Arnhem bedanken. Samen met de Directie Oost-Nederland en de meetdienst van Oost-Nederland hebben zijn gezorgd dat ik alle data tot mijn beschikking had die ik noodzakelijk achtte. Met name ben ik dankbaar voor de hulp van Wilfried ten Brinke. Hij was altijd een vast aanspreekpunt, bezorgde mij alle data die ik wilde, maar ook zorgde hij voor de contracten waarin ik de gegevens van nieuwe metingen kon uitwerken. Wilfried stond ook altijd klaar voor discussies over elk aspect van mijn onderzoek, of het nu ging om technische problemen of inhoudelijke hypothesen. Wilfried nogmaals hartelijk dank voor alle hulp en ik hoop dat het rekenvoorbeeld in hoofdstuk 8 je niet te veel heeft laten schrikken maar dat het je kan helpen in de toekomst. Een ander persoon zonder wie ik niet tot deze resultaten was gekomen is Henk van de Kaay. Henk was degene die me alle ins en outs van de multibeam heeft geleerd en die me heeft geholpen enkel zeer vreemde resultaten van multibeam metingen te verklaren. Henk, hartelijk bedankt, zonder jouw hulp was de nauwkeurigheid van mijn onderzoek beduidend slechter uitgevallen. Verder wil ik Claus van den Brink, Eric-Jan Houwing, Leonie Bolwidt, Arjan Sieben, Klaas-Jan Douben en alle anderen die bij RIZA in Arnhem en Dordrecht, bij Directie Oost-Nederland en bij de Meetdiensten werken bedanken voor al hun hulp in het verzamelen van gegevens, het analyseren daarvan en het discussiëren over de resultaten.

Naast de personen die me aan de data hielpen ben ik natuurlijk ook veel dank verschuldigd aan iedereen binnen de Universiteit die mij heeft geholpen. Allereerst Janrik van den Berg natuurlijk. Zonder hem was ik nooit met duinen begonnen. Hij zorgde ervoor dat ik contractwerk had, dat alle faciliteiten voor mij klaar stonden, dat ik aan mijn promotie kon beginnen maar vooral zorgde hij ervoor dat ik binnen mijn doelstelling bleef, dat ik niet teveel zijpaadjes ging bewandelen en dat mijn hypothesen en conclusies die ik verzon ook fysisch uitvoerbaar waren. Janrik was voor mij een metaaldetector om Professor van Rijn te vinden, zorgde ervoor dat ik naar congressen ben geweest in Genua (Italië) en Lincoln (USA) en sleepte mij mee naar alle vergaderingen en symposia waarvan hij dacht dat mijn onderzoek daar wel interessant gevonden zou worden. Janrik ik ben je zoveel dank verschuldigd voor alle hulp die je me hebt gegeven voorafgaand, tijdens maar ook na mij promotie dat ik enkele pagina's vol kan schrijven. Ik denk echter

dat je dat veel te veel ophef vind en dat je liever een simpel dank je wel wilt. Daarom hierbij, dank je wel voor alles. Als tweede wil ik Professor van Rijn bedanken. Hij was bereid om promotor te zijn van mijn promotieonderzoek ook al was het onderwerp ambitieus en de financiële ondersteuning ietwat moeizaam. Beste Leo, in het begin ging onze samenwerking niet vlekkeloos en moest ik terugvallen op Janrik, maar bij de laatste loodjes was je zeer behulpzaam. Je opmerking, "We gaan samen ervoor zorgen dat er een goed proefschrift uitkomt", gaf me nieuwe moed op een moment dat ik voor de zoveelste keer verschillende hoofdstukken grotendeels moest veranderen. Je opmerkingen die je maakte bij de tekst kwamen vaak hard aan maar waren altijd gerechtvaardigd. De analyse kon ook vaak wat scherper, of de opzet van een hoofdstuk kan veel duidelijker. Daarom wil ik je heel hartelijk danken en ik hoop dat je het niet erg vind dat ik het niet altijd eens ben met jouw conclusies uit het verleden. Naast Leo van Rijn wil ik natuurlijk ook Ward Koster hartelijk bedanken. Hij was mij tweede promotor en ondanks dat hij inhoudelijk geen kaas had gegeten van mijn onderwerp (zoals hij dat zelf zei) was hij toch een grootte hulp bij het schrijven van dit proefschrift. Ward, zonder jou was dit proefschrift alleen te lezen door echte experts (en die zijn er maar een tiental in deze wereld). Jij zorgde ervoor dat ik mijn teksten zo verbeterde dat iemand die er zijdelings iets vanaf wist het ook nog kon begrijpen. Daarvoor ben ik je bijzonder dankbaar, alleen bij de samenvattingen zul je altijd weer zeggen, "te beknopt en onduidelijk" en daar heb je gelijk in maar samenvattingen schrijven blijkt niet mijn specialiteit te zijn.

Een ander persoon zonder wie dit promotieonderzoek duidelijk in kwaliteit had ingeboet is Maarten Kleinhans. Hij was al eerder begonnen aan een promotie naar sedimenttransport in de Rijn, maar omdat wij beiden gebruik maakten van dezelfde metingen hadden we veelvuldig contact. Na veel discussies, snelle analyses, verdere discussies, data uitwisseling en samen hypothesen opstellen en weer verwerpen kwamen we vaak tot de conclusie dat onze onderwerpen zeer dicht bij elkaar lagen. Beste Maarten, ik wil je hartelijk danken voor al deze discussies die we samen hebben gehad. Soms vond ik je daarbij zeer vervelend omdat jij weer eens gelijk had en ik niet (grrrr), maar daarvoor heb ik je terug gepakt doordat ik veelvuldig van conclusie veranderde tijdens een analyse waardoor jij telkens je proefschrift moest aanpassen (hihihi). Dit maakte onze discussies echter levendig ("kunnen jullie niet wat minder luidruchtig discussiëren!") en ze hebben me erg geholpen om mijn eigen ideeën over duinen, sedimenttransport en hydraulische ruwheid steeds weer aan te scherpen en te verbeteren. Veel dank ben ik ook verschuldigd aan Cees Wesseling. Hij was het die al voordat ik met mijn eerste contract was begonnen, een computerprogramma moest schrijven om de metingen van Rijkswaterstaat te verwerken en te zorgen dat ik er het bodemtransport mee kon berekenen. Geen van beiden wisten wij hoe je zoiets het beste kunt aanpakken en het heeft dus heel wat verbeteringen en aanpassingen gekost voordat het programma zo goed was dat ik er nauwkeurige getallen uit kon krijgen. Arme Cees, DT2D en vooral mijn voortdurende vragen, opmerkingen, problemen en aanpassingen moeten je vele slapeloze nachten hebben bezorgd. Ik weet dat we momenteel bij versie 3.03 zijn maar ik ben de tel van alle vorige versies volledig kwijt. Soms waren we constant met elkaar aan het e-mailen en volgden de nieuwe versies elkaar in hoogtempo op, totdat jij een slepend probleem volkomen had opgelost. In ieder geval was dit onderzoek nooit zo snel afgerond zonder al de hulp van jouw. DT2D is en blijft noodzakelijk voor dit soort werk

omdat anders het jaren duurt om al die megabytes aan meetdata te analyseren. Ik weet dat wij niet de rechten van het programma bezitten maar ik denk dat DT2D toch altijd een beetje ons kindje zal blijven.

Natuurlijk zijn er veel meer mensen binnen de Universiteit die ik dankbaar ben voor al hun hulp en voor de gezelligheid. Allereerst mijn verschillende kamergenoten, Andre van Gelder, Nico Willemse, Daniel Mourad en Hanneke Schuurmans. Andre, het was knus maar altijd gezellig. Co, je was er lange tijd niet maar daarna was het zeker gezellig en je was een grootte hulp bij het maken van mijn eerste figuren. Daniel en Hanneke, leuk dat jullie het niet erg vonden dat ik op het laatst nog een hoekje van jullie kamer in gebruik had. Ganggenoten, ook die wil ik bedanken omdat ik er altijd even kon binnenlopen voor een praatje als afleiding. Rutger, Menno, Esther, Kim, Leo, Wim, Annika, Jeroen en iedereen die ik nog vergeet, hartelijk bedankt voor de gezelligheid. Ik moet natuurlijk niet Roy Frings vergeten. Hij is er nog maar pas, maar hij is de opvolger van mij en Maarten binnen de rivierprocessen club. Beste Roy, Janrik en ik hadden je uitgekozen vanwege je puntenlijst om een klein klusje voor ons te doen. Maar we hadden niet verwacht dat je zo enthousiast in een voor jouw onbekend onderwerp zou duiken. Je hebt samen met Janrik en Maarten een promotieplaats weten te krijgen van Rijkswaterstaat en ik weet zeker dat de uitkomsten van dat onderzoek indrukwekkend en zeer goed onderzocht zullen zijn. Ik wens je veel succes de komende jaren. Ook Irene en Anina van het secretariaat wil ik hartelijk bedanken, jullie stonden altijd klaar om mijn te helpen als ik iets nodig had, iets wilde versturen of iemand niet kon vinden. En natuurlijk mag ik alle mensen van de Facultaire Automatisering Dienst niet vergeten. Ik had veel data en dus krachtige computers nodig om die data mee te verwerken. Maar krachtige computers vergen veel onderhoud en daarvoor stonden de mensen van het FAD altijd klaar. Ook voor raad en daad over printen, scannen, animatie maken, internetpagina's en netwerken kon ik altijd een beroep op ze doen. Daarom, Maarten, Harm, Gerlach en de velen die er werkten tijdens mijn promotietijd, hartelijk dank voor de hulp.

Ook van buiten de Universiteit waren er personen die ik altijd om hulp kon vragen. Daarom wil ik Astrid Blom, Sanne Niemann, Gerrit Klaassen, Henk Ogink, Jim Best, Randy Dinehart, David Abraham en Pierre Julien hartelijk bedanken voor hun tijd, interesse en hulp. Jim, Randy, Sanne, David and Pierre, many thanks for all your time, interest and help with my research and I hope you enjoy reading this thesis. Jorgen de Kramer wil ik niet bedanken omdat hij direct geholpen heeft met het promotieonderzoek. Ik wil hem echter heel hartelijk bedanken omdat hij een vriend is die altijd een gewillig oor heeft voor de onderzoeksgelateerde problemen. Ook zorgde hij ervoor dat ik elke zomer afleiding vond in de rivier de Allier. Beste Jorgen, bedankt voor alles. Net als jij ben ik ook verknocht aan de Allier en ik hoop (maar ik denk dat, dat wel zal lukken) dat we er nog vaak naar toe zullen gaan.

Als laatste en zeker niet als minste wil ik mijn familie bedanken. Martijn, Els, Alex, Colette, Mario, Monique, Koos, Astrid, papa en mama, ondanks dat jullie helemaal niets begrijpen van mijn onderzoek waren jullie altijd geïnteresseerd in wat ik aan het doen ben en hoe het ermee stond. Ik dank jullie voor al jullie steun en hoop dat als jullie de Nederlandse samenvatting lezen dat jullie toch een beetje begrijpen dat dit onderzoek ook voor jullie belangrijk was. Ook mijn kat Tiggr wil ik bedanken, dat klinkt misschien vreemd maar hij zorgde ervoor dat ik me thuis nooit verveelde en was altijd een gewillig

publiek als ik weer eens een presentatie moest oefenen (van hem kwam nooit enige kritiek). Degene die ik echt niet mag vergeten te bedanken is natuurlijk mijn vriendin, vrouw en moeder van Caithlyn, Bianca. Bianca, ik heb geen idee hoe ik jou moet bedanken voor alles wat je voor mij hebt gedaan in de afgelopen jaren. Wat ik ook zou opschrijven zou bij lange na niet goed genoeg zijn, daarom hou ik het simpel. Dank je wel en ik hou ontzettend veel van je.

Antoine Wilbers

Ps. Caithlyn, natuurlijk ben ik jou niet vergeten. Je bent er pas net, maar je bent nu al het belangrijkste van allemaal. Ik hoop dat je ooit dit boek zult lezen en zult begrijpen dat je vader niet voor niets altijd maar weer naar rivieren, bergen en zeeën wil gaan kijken tijdens een vakantie.

1 General introduction

1.1 Background and problem definition

Natural alluvial rivers by definition bear the threat of flooding. However, the presence of water and the fertility of floodplains has always attracted mankind. Presently many of these areas are heavily populated, and in order to prevent the rivers from flooding or eroding their banks, and to increase the navigation possibilities, the physiography of many of these rivers has been altered. In The Netherlands, already in medieval times, dikes were build to protect the homes and agricultural fields (Edelman *et al.*, 1950; Egberts, 1950; Pons, 1957; Hesselink, 2002). Later on, channels were straightened and arrays of groynes constructed, in order to increase navigability and enhance drainage of high discharge peaks (Bosch & Van der Ham, 1998). All these changes resulted in confined and regulated rivers, in which higher water levels are reached than was possible in their former natural state, especially during large floods (fig. 1.1).

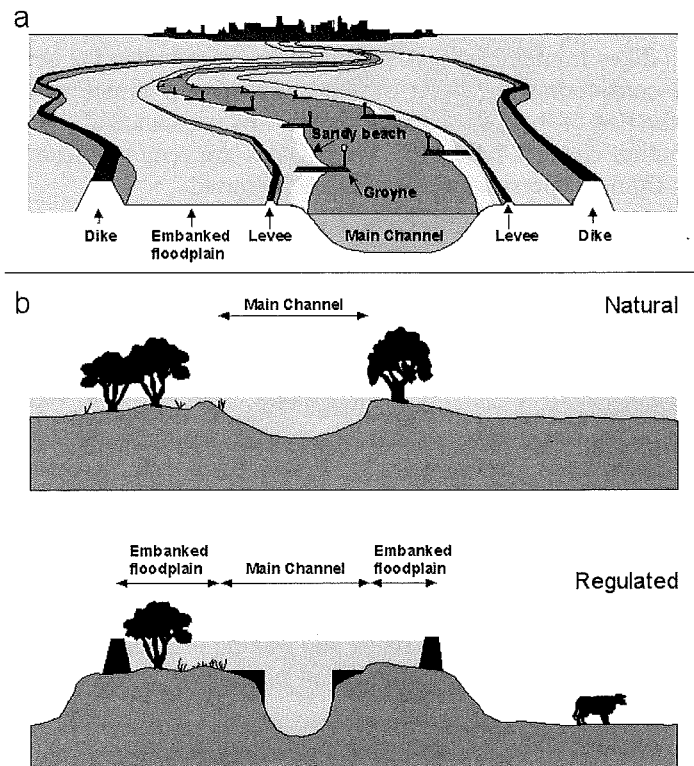


Figure 1.1. The physiography of the rivers in The Netherlands (a) and the influence of this regulated state versus the natural state on water levels during floods (b).

Every year more evidence is found that the climate is changing worldwide (IPCC, 2001). For the river basins drained by the Dutch rivers, the probable consequences of this changing climate are; an increase in temperature and, more importantly, an increase in precipitation (Kwadijk, 1993; Middelkoop, 1997, Middelkoop, 2000; Middelkoop *et al.*, 2001). Consequently, more water has to be transported by the rivers, probably in more and larger floods. In the lower Rhine branches (The Netherlands), this may lead to an increase of high water levels by 25 to 30 cm (Silva *et al.*, 2000). A predictable first response to this threat would be to increase the height of the dikes. However, in the long run this would increase the chance for a catastrophic dike breach. In addition, a further increase of the height of the dikes might cause damage to the valuable cultural and scenic aspects of the area (Silva *et al.*, 2000). Therefore, in The Netherlands, a number of alternatives is considered that will reduce the water level at high discharge. Two types of measures can be distinguished, the enlarging of the flow cross-sectional area between the dikes, by lowering or widening of the floodplain or the river bed, and, secondly, the reduction of the flow resistance. Generally, this resistance is denoted as hydraulic roughness. Hydraulic roughness is caused by any protruding element in the flow that produces shear stresses and turbulence. Natural roughness is caused by sediment particles at the bed surface, bed forms and vegetation. In addition, artificial obstacles such as groynes may add considerably to the flow resistance.

A number of measures to reduce the flow resistance at high discharge involves the removal of small dikes from the embanked floodplains or reducing the height of groynes. However, when considering the effect of such measures, it is necessary to know the contribution of the bed of the main channel to the flow resistance of the river, assuming that this contribution changes only little as obstacles are removed from the embanked floodplains. It is from this perspective that this study started.

The bed of the main channel of the Rhine and the Meuse consists of loose sand and gravel. This bed may be flat in which case the hydraulic roughness is caused by the coarse fraction of the grain size distribution of the bed material (Van Rijn, 1984). However, during many flow conditions (especially during flood waves) the bed of these rivers becomes covered with subaqueous dunes. Dunes protrude much higher into the flow of water than single grains and therefore produce a form resistance that is larger than the bed grain roughness (Van Rijn, 1984). Dunes also increase in height as the discharge rises during a flood, further increasing their hydraulic roughness.

Thus, as soon as dunes appear on the riverbed they determine most of the hydraulic roughness. The form resistance of a dune is related to the turbulence produced in the wake downstream of it, which in turn is related to the size and shape of the dune. Therefore, in order to analyse dune generated roughness, it is necessary to know the geometric characteristics of the dunes that are present on the bed and to know how these dune characteristics develop during the rising and waning of a flood. The present study is aimed at investigating the dune development in non-steady flows and to calculate the hydraulic roughness of these dunes.

In the following sections a short introduction is given of the present state of knowledge on the formation and development of subaqueous dunes and their relation to flow conditions and sediment transport. After that, a number of scientific questions are presented that will be addressed in this thesis along with a number of restrictions

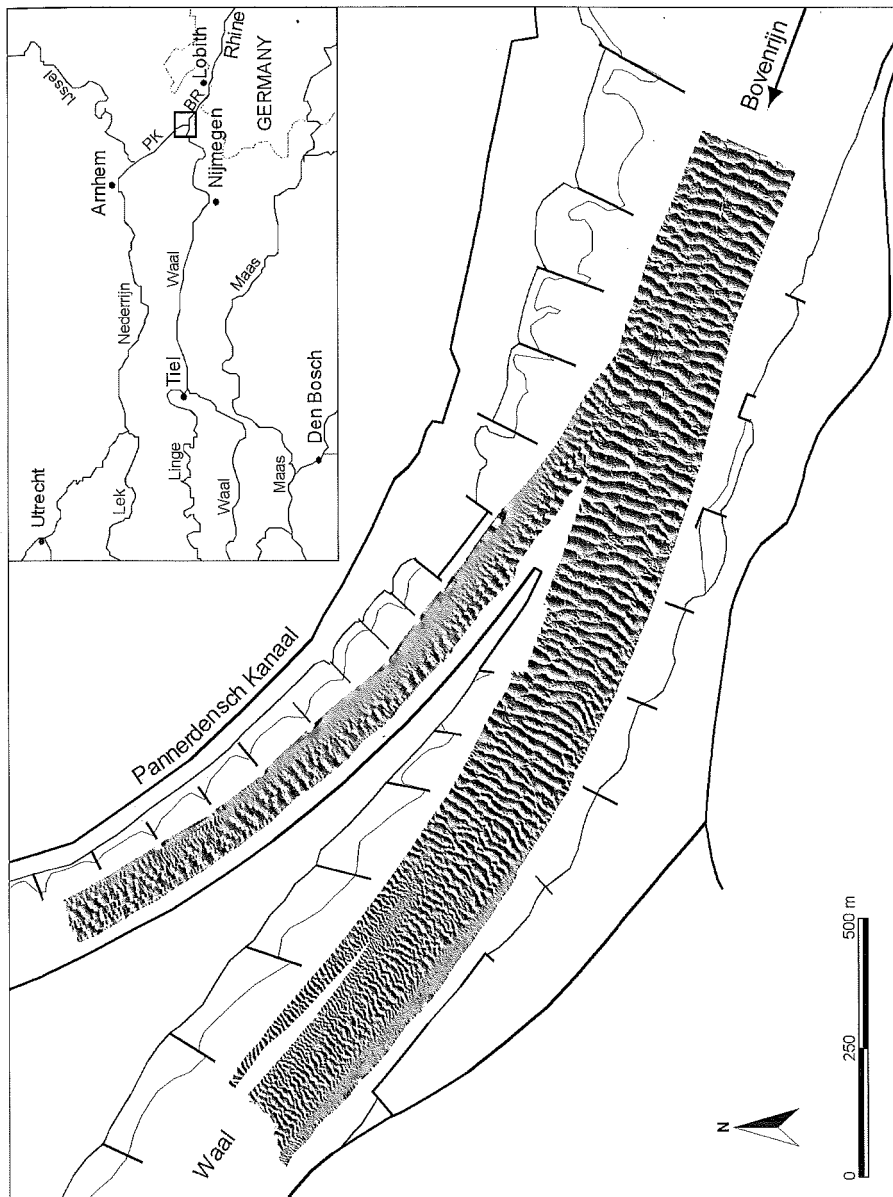


Figure 1.2. Dune patterns in the Rhine near the bifurcation of the Panmerdensch Kanaal, and BR is Bovenrijn. PK is Panmerdensch Kanaal, and BR is Bovenrijn.

concerning topics that will not be addressed. The present state of knowledge will help to explain the choice of the scientific questions and the restrictions.

1.2 Subaqueous dunes

Dunes are basically triangular bed forms moulded by the flow in loose, non cohesive sediments. They form repetitive patterns in the bed and may be several meters to hundreds of meters long en decimetres to meters high (see Chapter 2 for a more detailed definition used throughout this thesis). Dunes grow or reduce in length and height as the bed load transport increases respectively decreases, and they migrate downstream because material is eroded from the stoss side and deposited on the lee side.

Dunes are common features in many rivers. In small rivers with sandy beds, the dunes are relatively small. For instance, the Calamus river in the USA, 15–20 m wide, 0.35–0.6 m deep and bed material of 0.35 mm sand, has dunes of 0.1–0.2 m high and 2–4 m long (Gabel, 1993). In larger rivers with sandy beds such as the Elbe and Weser in Germany, the Mississippi in the USA and the Orinoco in Venezuela, much larger dunes are found. At a specific location, for example, the Orinoco is 1200 m wide and 13–27 m deep and the dunes are 10–225 m long and 0.2–3.2 m high (Nordin and Perez-Hernandez, 1989). Dunes are also present in gravel bed rivers. In the North Fork Toutle River (USA), the dunes are 2.5–13 m long and 0.15–0.75 m high (Dinehart, 1989). Therefore, it is not surprising that especially during floods, the sand and sand-gravel beds of the Rhine branches in The Netherlands are generally also covered with patterns of dunes (fig. 1.2).

1.2.1 Dune formation

The initiation of dunes is generally explained by the so-called “stability theory” (Kennedy, 1969, 1980; Reynolds, 1976; Richards, 1980; Engelund and Fredsøe, 1982). In this theory, the initiation of dunes is seen as a result of the instability of the sand and water interface. If a bed is slightly perturbed so that flow and sediment transport are disturbed, two directions of development are possible (Engelund and Fredsøe, 1982):

1. In a stable situation, the disturbed flow and sediment transport will diminish the perturbation so that a stable plane bed will again be formed.
2. In an unstable situation, the disturbed flow and sediment transport will increase the perturbation in time by eroding in the depression and depositing on the higher parts.

Whether a situation is stable or unstable depends on a phase shift between bed elevation and especially bed roughness, flow velocity and sediment transport (fig. 1.3). Gravitational forces, local turbulences and water surface waves may also play a role.

In an unstable situation, the phase shift (δ) manifests itself by the fact that the flow velocity (u , in fig. 1.3) is at its maximum just downstream of the maximum bed-elevation $z(t)$ but the bed-load transport is not at its maximum until just upstream of the next maximum bed-elevation (fig. 1.3). This phase shift between flow velocity and bed-load

transport causes deposition just after the top of the perturbation and scour in and just downstream of the trough. With a phase shift as shown in fig. 1.3 the perturbation will move downstream. If the phase shift is somewhat smaller, the perturbation will grow and in case of a very small perturbation, it can even move upstream (Kennedy, 1969).

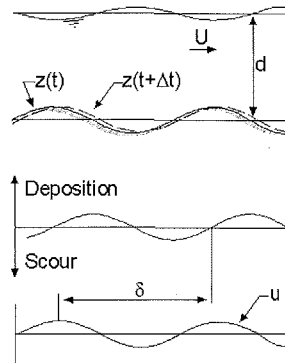


Figure 1.3. Example of the phase shift (δ) between flow velocity (U) and bedload sediment transport in an unstable situation. $Z(t)$ is the bed-elevation at time t , $z(t+\Delta t)$ the bed-elevation after some time and d is the average water depth (after Kennedy, 1969).

There is still much unknown about how and why these phase shifts occur. Probably they are created by local turbulence, and related to dune shapes. Therefore, much of the current research is focussed on sediment transport over dunes (Venditti & Bennett, 2000; Cellino & Graff, 2000; Kleinhans & Van Rijn, 2002) and turbulent structures (Van Mierlo & De Ruiter, 1988; McLean *et al.*, 1994; Nelson *et al.*, 1995; Bennett & Best, 1995; Venditti & Bennett, 2000). There is much less research focussing on the shape and development of dunes, especially in unsteady conditions. This is one of the major issues of the present study. The present state of knowledge on shape and development of subaqueous dunes will be addressed in Chapter 2. These investigations will eventually bring us closer to understanding how and why dunes are created and how they develop from initiation. Whether this understanding will make it easier to predict this behaviour outside controlled flume conditions is, however, still very uncertain (ASCE Task Committee on flow and transport over dunes, 2002).

1.2.2 Dune roughness

Dunes contribute to hydraulic roughness due to turbulence produced in the wake that develops downstream of a dune. On the one hand, this turbulence is produced by expansion over the lee-side trough (Carnot equation, in: Van Rijn, 1994), while on the other hand, the steep decline of the surface elevation at the lee-side causes the flow to separate from the surface, creating a re-circulating flow in the flow separation zone. In this separation zone, large turbulent eddies are created that dissipate energy by transferring it, to the bed to pick up sediment, or to the water surface to create boils and waves (Müller & Gyr, 1986; Kostaschuk & Villard, 1996; Kadota & Nezu, 1999) (fig. 1.4).

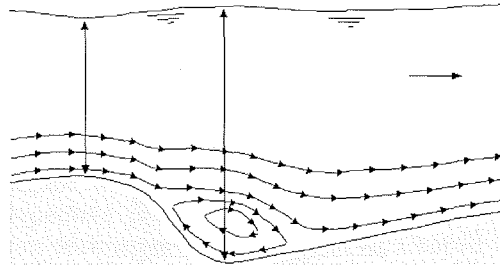


Figure 1.4. The expansion and separation of the flow over the lee-side trough of a dune.

The hydraulic roughness is strongly related to the height of the dunes. When a dune increases in height, the flow expansion behind it becomes larger, dissipating more energy. A larger flow separation zone means that larger and more turbulent eddies are produced, as was clearly documented in a number of flume experiments (Müller & Gyr, 1986; McLean & Wolfe, 1993; Bennett & Best, 1995). However, not only dune height is important, the hydraulic roughness of a field of dunes in a river is also influenced by the dune shape, dune length and frequency of occurrence.

Results of investigations on the expansion of the flow over the lee-side trough and on the creation and type of turbulent eddies that are formed in the separation zone (Müller & Gyr, 1986; McLean & Wolfe, 1993; Bennett & Best, 1995) have been used to test sophisticated flow models with build-in prediction methods for turbulence (for example $K-\epsilon$ or $K-\omega$, Rodi, 1984). However, the shape and size of the flow separation zone and the location of the separation point can still not be predicted accurately and these flow models still require a large computational power. These models therefore are not yet practical to investigate and predict the hydraulic roughness of dunes in rivers.

Other investigators used flume and field measurements of dunes and hydraulic roughness to create empirical predictors for the dune roughness (Vanoni & Hwang, 1967; Van Rijn, 1984). These predictors perform reasonably well in controlled flume condition and in the steady flows of small rivers. However, in large rivers the results are much less impressive (Julien *et al.*, 2002), probably caused by the non-steady development of the dunes in the non-steady flows (hystereses and superposition) or by a misrepresentation of the dune and flow characteristics that determine the hydraulic roughness of dunes.

1.2.3 Dynamic feedback loop

Dunes are moulded by bed load sediment transport and exert a significant hydraulic roughness and flow retardation. This hydraulic roughness however, reduces the bed-load transport which, in turn, changes the dune morphology (Kleinhans, 2002). Thus, there is a strong dynamic feedback loop between flow, sediment transport and dunes (Müller & Gyr, 1986; Simons & Sentürk, 1992; Best, 1993; Kleinhans, 2002). When one of these three factors changes, it also changes the other two and eventually even itself (fig. 1.5). This means that an analysis of the development of dunes and the hydraulic roughness related to dunes, must take the complete feedback loop into account.

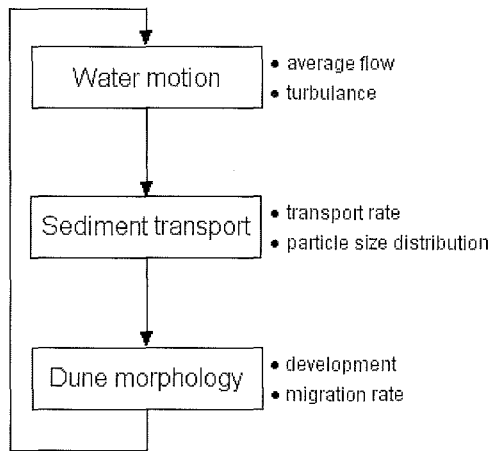


Figure 1.5. A dynamic feedback loop between flow, sediment transport and dunes.

1.3 Research objectives

This study is focused on the development and hydraulic roughness of dunes in non-steady flows during floods in medium-sized rivers with sand or sand-gravel beds like the Rhine and Meuse. The specific goals are:

1. To predict the development of dune shape and size in non-steady flows during floods.
2. To predict the hydraulic roughness caused by dunes using the characteristics of dune shape, size, and flow conditions.

To achieve these goals the following research questions are answered, bearing in mind the dynamic interaction between flow, sediment transport and dune development.

- How do sediment transport and dunes interact and how is the migration of dunes related to the bed load transport?
- How do the dunes in the Dutch rivers change during the unsteady flow conditions and how can these changes be predicted?
- What is the relation between dune shape and size, the dimensions of the flow separation zone, and the hydraulic roughness of a dune?
- How can the hydraulic roughness of dunes be predicted with dune characteristics?
- What is the cause of the superposition of dunes in the Dutch rivers and how does this superposition influence the bed load transport, dune development, and hydraulic roughness?

Answering these research questions is done within certain constraints as not all aspects of subaqueous dunes can be analysed.

- The only bed forms that are considered are dunes, as defined in chapter 2. Other bed forms are considered to be absent, undetectable or not important unless stated otherwise.
- This also means that the morphological and temporal scales of the studied processes are related to the dimensions and migration rates of these dunes.
- Although sediment transport is an integral part of the feedback loop the detailed processes and predictive formulae will not be given much attention as this has been extensively studied by Kleinhans (2002).

1.4 Organization of the thesis

The thesis is divided in two parts; Part 1 concentrates on the development of dunes during non-steady flows, and Part 2 concentrates on the hydraulic roughness of dunes. First in Chapter 2 the classification of different bed forms and a definition of dunes is addressed, as this term is used throughout the thesis to describe the bed forms that are studied. Attention will also be paid to the relations between bed form types and flow velocity, bed form types and flow patterns, plan form differences of bed forms, and the occurrence of superposition.

Part 1 starts with Chapter 3 which addresses part of the interaction between sediment transport and dunes by studying how dune shape changes the pathways of sediment transport and how dune migration can be used to calculate the bed load transport. Chapter 4 provides a comprehensive description of the measurements that were used for the study of dune development in the Dutch rivers, and in Chapter 5 the non-linear development of the dunes in the Dutch rivers during floods is analysed, together with the possibility of accurately predicting this development from unsteady flow conditions.

Part 2 starts with Chapter 6 concerning the relation between dune dimension, the dimension of the flow separation zone on the lee-side, and the hydraulic roughness of a dune. Relating dune dimensions to hydraulic roughness probably becomes more reliable if the size and shape of the flow separation zone is considered first. The results from Chapter 6 are used in Chapter 7 to answer the question: How can the hydraulic roughness be predicted on the basis of dune characteristics? Finally, in Chapter 8, the results and conclusions of the project are summarized. An analysis is presented of predicted dune development and hydraulic roughness during a virtual extreme flood in the Rhine River, together with scientific recommendations for future research. The question regarding the influence of superposition is also addressed in this chapter.

1.5 References

- ASCE TASK COMMITTEE ON FLOW AND TRANSPORT OVER DUNES (2002) Flow and transport over dunes. *Journal of Hydraulic Engineering*, 128, 726-728.
- BENNETT, S.J. & BEST, J.L. (1995) Mean flow and turbulence structure over fixed, two-dimensional dunes: implications for sediment transport and bedform stability. *Sedimentology*, 42, 491-513.

- BEST, J.L. (1993) On the Interactions between turbulent flow structure, sediment transport and bedform development: some considerations from recent experimental research. In: *Turbulence: perspectives on flow and sediment transport* (Ed. by N.J. Clifford *et al.*), pp. 61-92. Wiley and Sons, Chichester.
- BOSCH, A. & VAN DER HAM, W. (1998) Twee eeuwen Rijkswaterstaat, 1798 - 1998. Europese Bibliotheek, Zaltbommel, The Netherlands
- CELLINO, M. & GRAFF, W.H. (2000) Experiments on suspension flow in open channels with bed forms. *Journal of Hydraulic Research*, 38, 289-298.
- DINEHART, R.L. (1989) Dune migration in a steep, coarse-bedded stream. *Water Resources Research*, 25, 911-923.
- EDELMAN, C.H., ERINGA, L., HOEKSEMA, K.J., JANTZEN, J.J., & MODDERMAN, P.J.R. (1950) Een bodemkartering van de Bommelerwaard boven den Meidijk. *Verslagen van Landbouwkundige Onderzoekingen*, 56.18.
- EGBERTS, H. (1950) De bodemgesteldheid van de Betuwe. *Verslagen van Landbouwkundige Onderzoekingen*, 56.19.
- ENGELUND, F. & FREDSE, J. (1982) Sediment ripples and dunes. *Annual Review in Fluid Mechanics*, 14, 13-37.
- GABEL, S.L. (1993) Geometry and kinematics of dunes during steady and unsteady flows in the Calamus River, Nebraska, USA. *Sedimentology*, 40, 237-269.
- HESSELINK, A.W. (2002) History makes a river: Morphological changes and human interference in the river Rhine. *Netherlands Geographical Studies* 292, 200 pp.
- IPCC (2001) *Climate Change 2001: The Scientific Basis*, Cambridge University Press, Cambridge.
- JULIEN, P.Y., KLAASSEN, G.J., TEN BRINKE, W.B.M., & WILBERS, A.W.E. (2002) Case study: Bed resistance of the Rhine River during the 1998 flood. *Journal of Hydraulic Engineering*, 128, 1042-1050.
- KADOTA, A. & NEZU, I. (1999) Three-dimensional structure of space-time correlation on coherent vortices generated behind dune crest. *Journal of Hydraulic Research*, 37, 59-80.
- KENNEDY, J.F. (1969) The formation of sediment ripples, dunes and antidunes. *Annual Review in Fluid Mechanics*, 1, 147-168.
- KENNEDY, J.F. (1980) Bed forms in alluvial streams: some views on current understanding and identification of unresolved problems. In: *Application of stochastic processes in sediment transport* (Ed. by H.W. Shen & H. Kikkawa), pp. 1-13. Water Resources Publications, Fort Collins.
- KLEINHANS, M.G. (2002) Sorting out sand and gravel: Sediment transport and deposition in sand-gravel bed rivers. *Netherlands Geographical Studies* 293, 320 pp.
- KLEINHANS, M.G. & VAN RIJN, L.C. (2002) Stochastic prediction of sediment transport in sand-gravel bed rivers. *Journal of Hydraulic Engineering*, 128, 412-425.
- KOSTASCHUK, R.A. & VILLARD, P.V. (1996) Flow and sediment transport over large subaqueous dunes: Fraser River, Canada. *Sedimentology*, 43, 849-863.
- KWADIJK, J. (1993) The impact of climate change on the discharge of the River Rhine. *Netherlands Geographical Studies* 171.
- MCLEAN, S.R., NELSON, J.M., & WOLFE, S.R. (1994) Turbulence structure over two-dimensional bed forms: implications for sediment transport. *Journal of Geophysical Research*, 99, 12729-12747.
- MCLEAN, S.R. & WOLFE, S.R. (1993) Mean flow and turbulence fields over two-dimensional bed forms. *Water Resources Research*, 29, 3935-3953.
- MIDDELKOOP, H. (1997) Embanked floodplains in The Netherlands: geomorphological evolution over various time scales. *Netherlands Geographical Studies* 224.
- MIDDELKOOP, H. (2000) The impact of climate change on the River Rhine and the implications for water management in The Netherlands., 2000.010, RIZA, Arnhem, The Netherlands.
- MIDDELKOOP, H., DAAMEN, K., GELLENS, D., GRABS, W., KWADIJK, J., LANG, H., PARMET, B.W.A.H., SCHÄDLER, B., SCHULLA, J., & WILKE, K. (2001) Impact of climatic change on hydrological regimes and water resources management in the Rhine Basin. *Climatic Change*, 49, 105-128.
- MÜLLER, A. & GYR, A. (1986) On the vortex formation in the mixing layer behind dunes. *Journal of Hydraulic Research*, 24, 375.
- NELSON, J.M., SHREVE, R.L., MCLEAN, S.R., & DRAKE, T.G. (1995) Role of near-bed turbulence structure in bed load transport and bed form mechanics. *Water Resources Research*, 31, 2071-2086.

- NORDIN, C.F. & PEREZ-HERNANDEZ, D. (1989) Sand waves, bars and wind-blown sand of the Rio Orinoco, Venezuela and Colombia. US Geological Survey Water supply Paper, 2326-A.
- PONS, L.J. (1957) De geologie, de bodenvorming en de waterstaatkundige ontwikkeling van het Land van Maas en Waal en een gedeelte van het Rijk van Nijmegen. Verslagen van Landbouwkundige Onderzoekingen, 63.11.
- REYNOLDS, A.J. (1976) A decade's investigation of the stability of erodible stream beds. *Nordic Hydrology*, 7, 161-180.
- RICHARDS, K.J. (1980) The formation of ripples and dunes on an erodible bed. *Journal of Fluid Mechanics*, 99, 597-618.
- RODI, W. (1984) Turbulence models and their application in hydraulics. International association for hydraulic research, Delft
- SILVA, W., KLIJN, F., & DIJKMAN, J. (2000) Ruimte voor Rijntakken. Wat onderzoek ons geleerd heeft., 2000.026, RIZA, Lelystad, The Netherlands
- SIMONS, D.B. & SENTÜRK, F. (1992) Sediment transport technology: water and sediment dynamics. Water Resources Publications, Littleton
- VAN MIERLO, M.C.L.M. & DE RUITER, J.C.C. (1988) Turbulence measurements above artificial dunes Report on measurements., Q789, Delft hydraulics,
- VAN RIJN, L.C. (1984) Sediment transport; Part 3: bed forms and alluvial roughness. *Journal of Hydraulic Engineering*, 110, 1733-1754.
- VAN RIJN, L.C. (1994) Principles of fluid flow and surface waves in rivers, estuaries, seas, and oceans. Aqua Publications, Oldemarkt, The Netherlands
- VANONI, V.A. & HWANG, L.S. (1967) Relation between bed forms and friction in streams. *Journal of the Hydraulics Division*, 93, 121-144.
- VENDITTI, J.G. & BENNETT, S.J. (2000) Spectral analysis of turbulent flow and suspended sediment transport over fixed dunes. *Journal of Geophysical Research*, 105, 22035-22047.

2 Classification of subaqueous bedforms

Abstract

This chapter provides a bedform classification which uses both descriptive and conditional terms with the special aim to classify the bedforms, that are observed in the environmental settings used throughout this thesis. Dunes in river channels are asymmetrical transverse bedforms with a gentle stoss side slope and a steep lee side slope. They occur as repetitive forms of similar size and shape, and cover large parts of a river bed. Their dimensions are strongly related to water depth and flow strength and are in the order of 1 m to hundreds of meters long and 10 cm to many meters high. In most cases dunes are 3 dimensional shapes, but straight almost 2 dimensional shapes have been reported also.

Other bedforms such as, bars, ripples, anti-dunes, stripes and barchans are also briefly described in this chapter to indicate that they occur in different conditions to dunes and that they have a different shape or size. Finally attention is given to the discussion on low-angle dunes and the superposition of dunes. Both are related to the same flow conditions as dunes. However they both fall outside the classification provided here.

2.1 Introduction

When considering the river bed as completely flat, any undulation of, or accumulation on this bed might be called a bedform. Many different types of bedforms are distinguished, ranging from very small high ripples in sand bed rivers (Mahmood *et al.*, 1984), and bed load sheets in gravel-bed rivers (Whiting *et al.*, 1988), or sand ribbons in mixed sand-gravel bed rivers (Kleinhans *et al.*, 2002), to very large forms such as scroll bars or alternating bars in large rivers (Smith, 1974; Hein & Walker, 1977). However describing and naming a bedform requires a uniform bedform classification scheme usable in all situations where bedforms are found.

A classification of bedforms should identify distinct forms according to size and shape and should be practical in both active and fossil settings. However, bedforms are observed in many different environments such as rivers, coastal embayments and continental shelves (ASCE, 1966; Ashley, 1990). In these environments, bedforms range in dimension from centimetres to several hundred meters, in shape from symmetrical to asymmetrical in profile view, and from straight to either convex or concave in plan form (Harms, 1969; Costello & Southard, 1981). Hence, both bedform, size, and shape form a continuous range without objective boundaries to classify bedforms on purely descriptive terms (Yalin, 1964; Kennedy, 1969; Allen & Collinson, 1974). Over the past decades this resulted in the vast variety of bedform names, created by different investigators, including numerous duplicates, overlapping definitions and conflicting terms (ASCE, 1966; Ashley, 1990). The main goal of this chapter is therefore to create a bedform classification which uses both descriptive, and conditional terms, to describe the bedforms that are observed in the environmental settings used throughout this thesis.

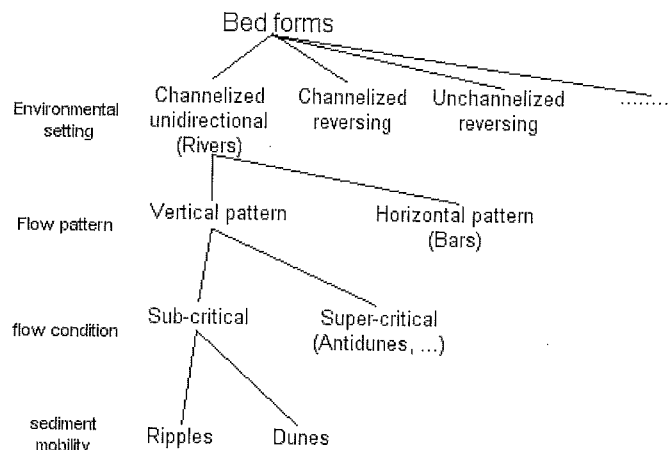


Figure 2.1. Classification scheme of bedforms described in this study.

In the bedform classification proposed in this study, bedforms are divided, first of all, into groups according to their environmental setting (fig. 2.1). A distinction is made

between channelized and unchannelized environments with unidirectional or reversing flows. Secondly, bedforms in river settings, are divided according to their relation with horizontal or vertical flow patterns. Bedforms that are related to horizontal flow patterns are called bars, while bedforms related to vertical flow patterns which are called transverse bedforms, are further divided according to conditions of sub-critical and super-critical flow. Finally, bedforms in sub-critical flows are classified according to their size, shape, and the flow conditions in which they occur (fig 2.1). This classification scheme is different, but uses the desirable attributes as noted by Bridge (1987) and the Society for Sedimentary Geology (SEPM) Symposium of 1990 (Ashley, 1990).

In this study only the channelized river setting with unidirectional flow will be considered. The other settings, which include coastal embayments and continental shelves, are excluded. Because this study focuses on subaqueous dunes, which are, as will be shown later, a kind of transverse bedform, bars were also ignored in all analyses of this thesis. However, a short description on genesis, shape and relevance for the Rhine setting in the Netherlands is provided before focussing on transverse bedforms.

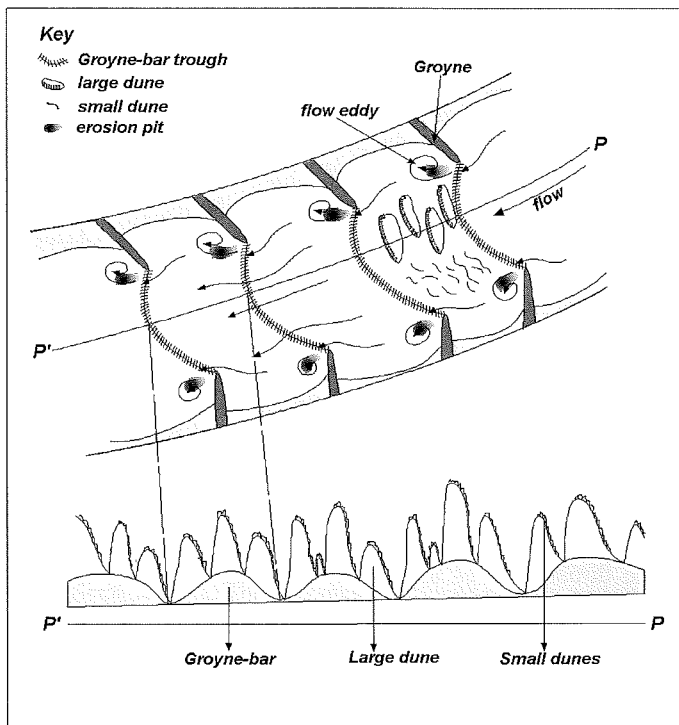


Figure 2.2. Schematic representation of bedform types present in the Dutch Rhine. Flow convergence and divergence between opposite groynes creates a sand wave or bar-like feature called a groyne-bar. Other bedforms, like dunes, are superimposed on these groyne-bars.

2.1.1 Bars

Bars are created in places of flow divergence behind obstacles, in inner bends or in suddenly widening channels. At these locations the flow direction changes and the velocity decreases resulting in the deposition of sediment (Smith, 1974; Church & Jones, 1982; Bridge, 1993). Since these changes in flow directions are directly related to the dimensions of the channel, the size and shape of the bars scale with these channel dimensions.

In the Rhine branches in the Netherlands only the asymmetrical bed profile, associated with point-bar development, occurs. Large emerging bars in the main channel do not exist. However, a bedform resembling a bar that does occur is the so-called a groyne-bar (fig. 2.2). This type of bar is specific to the Dutch Rhine. It develops because the flow narrows between two opposite groynes, which increases the flow velocity and creates a depression (trough) by eroding the bed. This depression curves between the groynes, and extends downstream in the centre of the channel. Between two opposite inter-groyne areas, the river expands and the bed is elevated by sedimentation. In a profile (fig. 2.2), these groyne-bars show up as symmetrical undulations with wavelengths in the same order as the groyne spacing and heights up to a meter. Superimposed on these bars, dunes may exist or develop. Because these groyne-bars are not related to changing flow conditions but more to the plan-form of the main channel, they have also been excluded in this study.

2.1.2 Transverse bedforms

Unlike bars, transverse bedforms always have a front which is more or less perpendicular to the flow direction, and their shape and dimensions are related to vertical gradients in the flow rather than horizontal changes. Transverse bedforms always form patterns of similar size and shape, whereas bars are more or less solitary forms. In classifying and describing these transverse bedforms, two questions need to be considered.

1. What kind of stable bedforms can exist under specific flow conditions?
In order to answer this, flow conditions have to be related to sediment mobility and sediment availability.
2. What are the dimensions of a specific bedform, and how are these dimensions related to the flow and sediment conditions?

The main part of this chapter will answer these questions in order to create a general classification for these transverse forms in channelized unidirectional flows. After that some attention will be paid to the ongoing discussions in literature on low-angle dunes and superposition.

2.2 Classification according to flow.

2.2.1 Sediment mobility

Transverse bedforms are formed by bed load transport, and the nature of bed load transport is determined by the relation between flow strength and the size and composition of the bed material. To review this relation in its simplest form, it is assumed here that the bed material consist of grains of one specific size only, this in contrast to natural conditions where different grain sizes are usually mixed together.

2.2.1.1 Stable bedforms in sub-critical flow

Grains of a specific size have a specific threshold that defines the flow strength necessary to lift them from the bed surface. Below this initiation threshold grains cannot move and the bed remains flat (fig. 2.3A and 2.3C) (for example, the threshold curve designed by Shields (1936) or one of the later derivatives). Above this, all the grains are transported (fig. 2.3C) and bedforms can develop. Sediment transport usually is a combination of bed load and suspension transport. Very coarse grains are transported as bed load because the flow strength usually is too low to sustain suspension (fig 2.3C), while very fine material is transported only in suspension with no bed load transport at all (fig. 2.3C). This means that there are two further thresholds specifying, the beginning of suspension transport (initial-suspension; for example, the threshold curve designed by Engelund (1965)) where bed load and suspension coexist, and full suspension where suspension is the only mode of transport (for example, the threshold curve designed by Bagnold (1966)). This last threshold applies to all grain sizes but the flow strength necessary to transgress it increases strongly with coarser grains. In principle, this full-suspension threshold probably defines the upper reach of flow strengths in which bedforms can occur (fig. 2.3A).

In the range where bed load transport can occur (exclusively or in combination with suspension) two types of bedforms exist: ripples and dunes. In both cases, these bedforms consist of series of similar triangular forms, with steep lee sides, that migrate downstream. Ripples, however, are smaller than dunes and are considered to be a distinct bedform type (see Section 2.3). The threshold between ripples and dunes coincides with flow conditions in which the thickness of the viscous sub-layer has the same dimensions as the grains themselves (fig. 2.3D; Allen, 1985).

This viscous sub-layer is a thin layer of laminar flow at the bed below the fully turbulent flow. The thickness of the viscous sub-layer is defined as:

$$\delta_v = \frac{11.6\nu}{u_*} \quad (2.1)$$

where δ_v is the thickness of the viscous sub-layer [m], ν is kinematic viscosity [m^2s^{-1}], and u_* is bed shear velocity [ms^{-1}]. It has a strong relation with the dimensionless Reynolds number (Re_*) and thus with grain size (Shields, 1936; Middleton & Southard, 1986):

$$Re_* = \frac{u_* D}{\nu} = 11.6 \frac{D}{\delta_v} \quad (2.2)$$

where Re_* is the dimensionless Reynolds-number for grains [-] and D is the grain size [m]. This relation implies that, when $D < \delta_v$ (hydraulically smooth bed), the turbulence of the turbulent flow layer cannot influence the grains at the bed (fig. 2.3D). When $D > \delta_v$ (hydraulically rough bed), the grains protrude through the viscous sub-layer and the

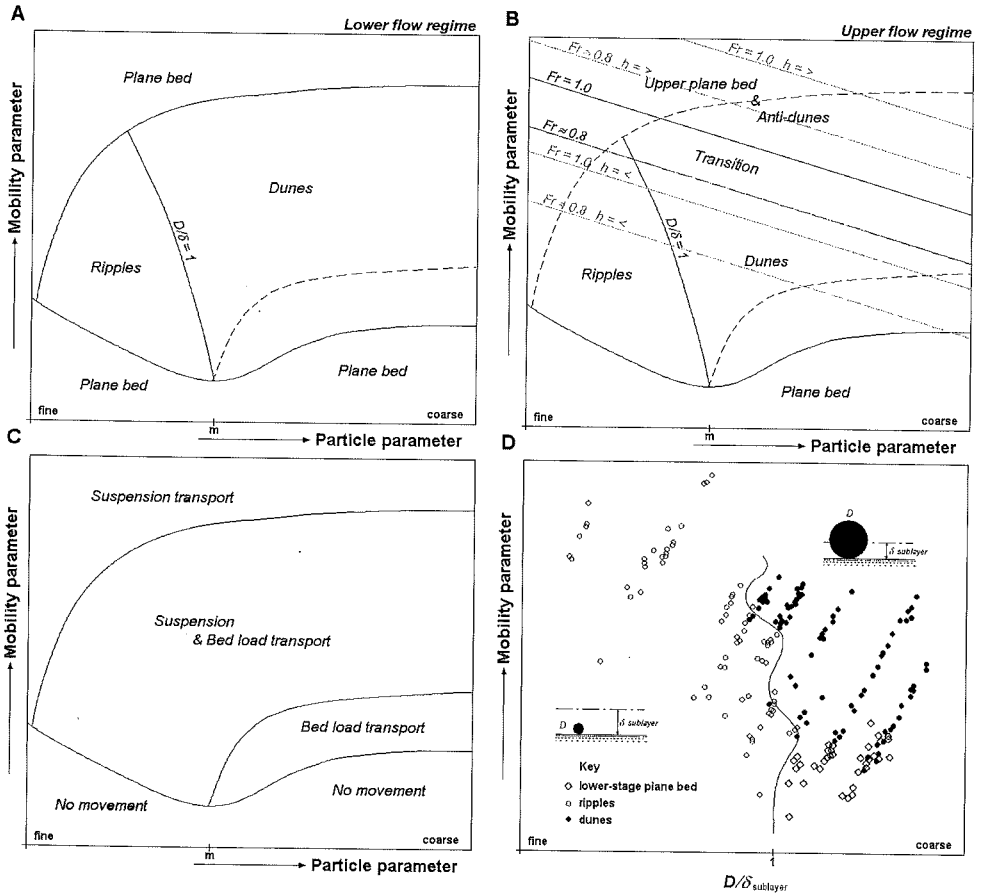


Figure 2.3. Conceptual explanatory stability diagram for bedforms and sediment transport, relating grain size and flow strength under the assumption that the riverbed consists of grains of one specific size only. Grain size is represented by a dimensionless particle parameter and flow strength by a dimensionless mobility parameter. After Chabert & Chauvin (1963); Guy *et al.* (1966); Southard & Boguchwal (1990); Van den Berg & Van Gelder (1993, 1998).

A) bedform stability in lower flow regime ($Fr < 1$).

B) bedform stability in upper flow regime ($Fr > 1$). Diagonal black lines indicate $Fr \approx 0.8$ and $Fr \approx 1.0$ at an arbitrary water depth. Grey lines indicate $Fr \approx 0.8$ and $Fr \approx 1.0$ at a larger water depth ($h = >$) and at a smaller water depth ($h = <$).

C) type of sediment transport.

D) relation between ripples or dunes and the thickness of the viscous sub-layer (δ_v), after Allen (1985).

turbulence can amplify the erosion of the bed particles (fig. 2.3D). The condition where $D = \delta_v$, was empirically shown to approximate the transition between ripples and dunes (Allen, 1985), allowing ripples to be stable in conditions with a hydraulically smooth bed and dunes with a hydraulically rough bed.

2.2.1.2 Stable bedforms in super-critical flow

In describing the various sediment transport and bedform stability-fields above, it was assumed that the water depth was sufficiently high to maintain sub-critical flow. If the flow strength increases but the water depth remains small, the Froude number will increase:

$$Fr = \frac{U}{\sqrt{gh}} \quad (2.3)$$

where Fr is the Froude number [-], U is the average flow velocity [ms^{-1}], g is the acceleration of gravity [ms^{-2}], and h is the water depth [m]. As long as $Fr \ll 1$, the flow stays sub-critical and ripples and dunes are the only bedforms that can exist. However, if $Fr \approx 0.8$ or higher existing bedforms of sand particles will be washed out in a transition phase up to $Fr = 1.0$ (fig. 2.3B), and when $Fr > 1.0$, the flow becomes super-critical and the bed will be flat (upper flat bed), or moulded into in-phase waves or anti-dunes (fig. 2.3B), depending on flow velocity (Cheel, 1990).

Because water depth is not included in either the dimensionless mobility parameter or the dimensionless particle parameter in the stability diagrams of figs. 2.3A to C, the position of the lines indicating $Fr \approx 0.8$ and $Fr = 1.0$ is not fixed. At larger water depths, these boundaries move up, and at smaller water depths downwards, decreasing the range where ripples and dunes can exist as stable bedforms. This unstable position of the threshold to super-critical flow, created much confusion in earlier stability diagrams (e.g. Guy *et al.*, 1966; Southard & Boguchwal, 1990), that showed large areas of overlap between ripples and dunes, and the bedforms in super-critical flows. Van den Berg and Van Gelder (1993, 1998) showed that much of this overlap was caused by data from flumes and rivers with water depths less than a meter, which moves the Froude threshold significantly downwards.

In large and deep rivers, flow conditions never reach the threshold of $Fr > 0.8$. Therefore, this study pays no further attention to bedforms in super-critical flows. For a more in-depth discussion, see Simons & Richardson (1963), Termes (1986), and Cheel (1990).

2.2.2 Sediment mobility in case of a distribution of grain sizes

When defining the stability fields of bedforms and sediment transport above, it was assumed that the bed material consists of grains of one particular size only. However, in natural conditions, bed material will always be a mixture of many different grainsizes. If this particle distribution is narrow (consisting of closely related grain sizes), it can be well represented with a single grain size, for example median grain size (D_{50} [m]), and the above-described boundaries can be approximated with empirically determined

relations. The Shields curve (Shields, (1936)) can be used as an approximation of the initiation-threshold, the threshold between bed load transport and the beginning of suspension transport (initial-suspension) can be approximated by the suspension criterion of Engelund, (1965), and finally, the threshold to full-suspension can be approximated by the criterion of Bagnold, (1966).

If the distribution of grain sizes is much wider or even bimodal, incorporating portions of silt, sand and gravel, it cannot be represented with a single grain size, and the boundaries become diffuse. In this case, the initiation of grain movement becomes a stochastic problem (Bridge and Bennett, (1992); Van Rijn, (1993); Kleinhans and Van Rijn, (2002)). Finer fractions may start to move sooner than coarser fractions and not all grains of a specific fraction will begin to move at the same time. There can be a large difference between the flow strength necessary to move a few fine grains, and the strength that is required to move all the grains (Graff and Pazis, (1977), Anon., (1982)). The same applies to the threshold of suspension. As some of the fractions may go into suspension already at small flow strengths, coarser fractions may never reach the suspension stage at all. Consequently, these diffuse thresholds, complicate the creation of a generally applicable stability-diagram for bedforms and sediment transport (Chabert and Chauvin, (1963); Guy *et al.*, (1966); Southard and Boguchwal, (1990); Van den Berg and Van Gelder, (1993), 1998). It is impossible to represent the grain size distribution in such a way that processes such as armouring, hiding-exposure and selective transport are fully integrated (Kleinhans, (2001)).

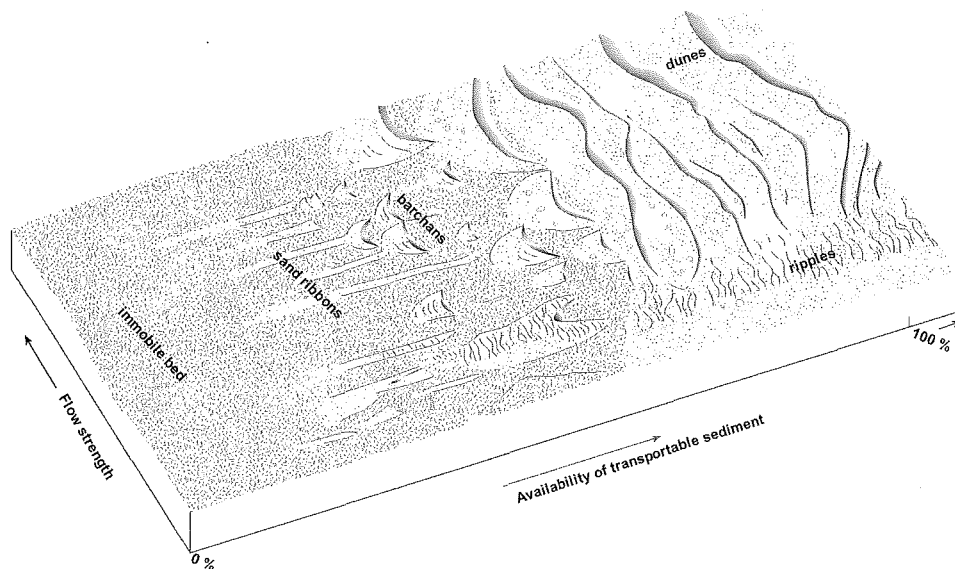


Figure 2.4. Conceptual explanatory model for the occurrence of bedforms in sediment supply-limited conditions, after Kleinhans *et al.* (2002).

2.2.3 Sediment availability

In many rivers with bed material of sand-gravel mixtures, the bed becomes armoured at low to moderate flows as the finer fractions are washed from the surface of the bed, leaving a layer of coarse grains prohibiting the erosion of finer sand fractions from deeper in the bed. Although, in these cases, the flow strength is high enough to enable sand transport and create bedforms, there is not enough erodable sand available and therefore no bedforms will occur. Similar situation can also occur in case the bed is made of non-erodable clays or rock.

In natural conditions, there will usually be some material available, either from upstream or from the riverbanks. This creates a very specific range of bedforms (fig. 2.4), depending on how much material is available compared to how much can be transported (Kleinhans *et al.*, 2002). If very little sediment is available, sand-ribbons evolve. These are flow parallel ribbons, only a few grains thick and in the order of 0.1 m wide. As the availability increases, these ribbons increase in width and eventually transform into individual barchans. Flow transverse barchans have a crescent shape with horns pointing downstream, and their height and length is similar to dunes. If the sediment availability increases even further, these barchans grow and merge, eventually becoming dunes or ripples, covering the immobile (armoured) bed almost completely. If the amount of

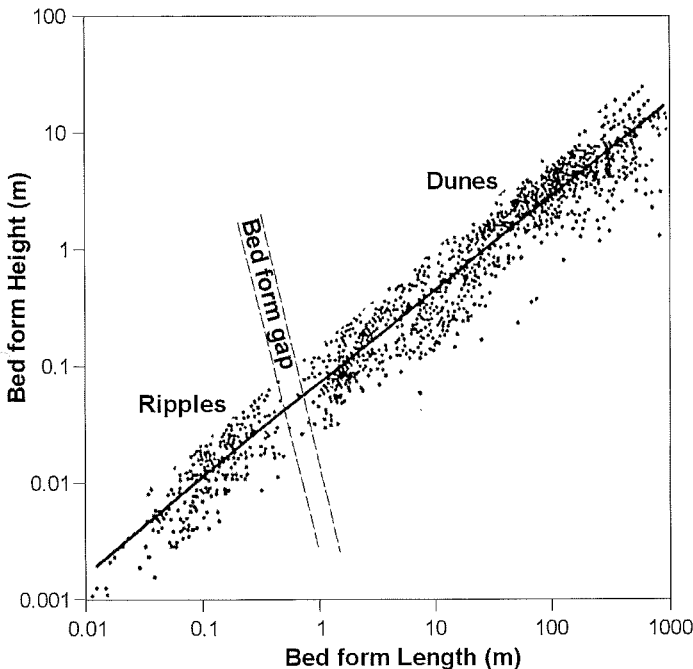


Figure 2.5. A plot of height (H) versus length (L) of 1491 flow transverse subaqueous bedforms from different environments including flumes (after Flemming, 1988), showing a clear gap between ripples and dunes.

available sediment is higher than the transport capacity, the normal bedforms will develop as described previously.

Sand-ribbons, barchans, and even the complete range of bedforms described above, were found in many rivers (McCulloch & Janda, 1964; Carling *et al.*, 2000a, 2000b; Kleinhans *et al.*, 2002), but not in the Rhine branches. In these branches armouring is probably too weak or spatially incomplete and the supply of finer material from upstream large enough to create normal dunes (Kleinhans, 2002).

2.3 Description of dune and ripple dimensions

Ripples and dunes have similar shapes, and the only difference seems to be the dimensions. It has long been a serious discussion if ripples and dunes are truly separate forms or just the same bedforms in a continuum of sizes. However, a diagram by Flemming (1988) plotting the heights and lengths of ripples and dunes from all available sources, clearly shows a gap between ripples and dunes in the region of 0.5 – 1.0 m long (fig. 2.5). This demonstrates that ripples and dunes do not form a continuum, but are separate forms in dimensions as well as flow conditions (see also section 2.2.1.1).

2.3.1 Ripple dimensions and shapes

Ripples occur in hydraulically smooth conditions where grains are smaller than the viscous sub-layer. Therefore ripples are probably related to small-scale turbulence and differences in viscosity, and it is therefore not surprising that ripple dimensions are strongly related to grain size (Yalin, 1985):

$$\begin{aligned} H_r &= 50 \text{ to } 200 D_{50} \\ L_r &= 500 \text{ to } 1000 D_{50} \end{aligned} \tag{2.4}$$

Ripples are much less related to water depth and flow strength (Van Rijn, 1993). Especially in faster flows, ripples become more irregular in shape, height and spacing, yielding three-dimensional ripples. These shapes are called lunate or linguoid, according to the concave or convex front of the ripples. Linguoid ripples are thereby mostly found in shallow water depths, and lunate ripples in large water depths (Baas, 1993). Two-dimensional ripples (straight or fairly straight fronts) are only found in non-equilibrium conditions where there is insufficient time to develop the three-dimensionality.

2.3.2 Dune dimensions

2.3.2.1 Steady flow conditions

In steady flow conditions, and a hydraulically rough bed, dunes with a specific dimension will develop. To predict these equilibrium dimensions many equations have been proposed (Shinohara & Tsubaki, 1959; Allen, 1968; Gill, 1971; Yalin, 1972; Ranga Raju

& Soni, 1976; Fredsøe, 1980, 1982; Van Rijn, 1984; Julien & Klaassen, 1995). These equations relate dune height and dune length to one or a combination of parameters, such as flow strength (θ or τ), water depth, grain size, and Froude number. Grain size is, however, much less important than for ripples (Van Rijn, 1993). Flow strength and water depth seem to be more important. Flow strength determines how much material can be transported as bed load, thereby shaping and maintaining the dunes. Water depth defines the vertical space shared by dunes and large turbulent eddies. Finally, the Froude number is only important if it exceeds a value of about 0.8.

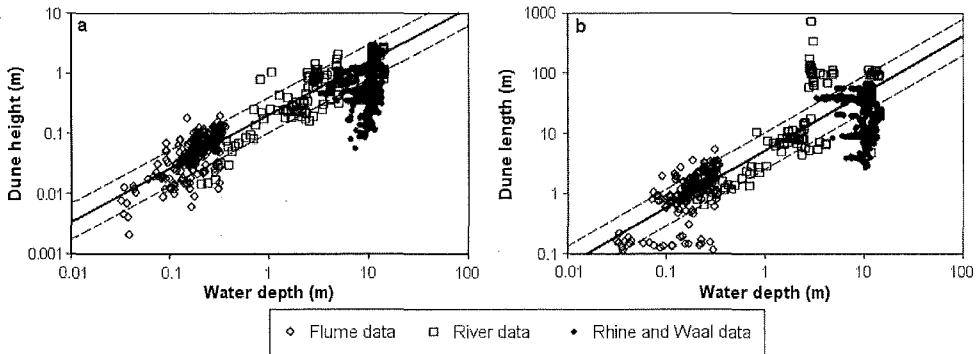


Figure 2.6. A plot of dune height (a) and dune length (b) versus the average water depth in many flume tests (Laursen, 1958; Shinohara & Tsubaki, 1959; Znamenskaya, 1963; Stein, 1965; Guy *et al.*, 1966; Crickmore, 1970; Engel & Lau, 1980; Livesey *et al.*, 1995), and rivers (Shinohara & Tsubaki, 1959; Stückrath, 1969; Nasner, 1974; Havinga, 1982; Mahmood *et al.*, 1984; Mahmood, 1987; Julien, 1992), including the data from the Rhine and Waal in The Netherlands. Dashed lines indicate a factor 2 variation.

The strong relations between water depth and dune height and length are shown in fig. 2.6. Using data from 8 flume and 8 river sources, the equilibrium dune height seems to be $1/2$ to $1/15$ of the water depth, and the dune length 3 to 15 times the water depth. However, in shallow waters (i.e. less than 1 m) the water depth is more important than in deep rivers (i.e. 10 to 20 m). A small water depth limits the height of the dunes since water is forced to flow over the crests, where the flow accelerates, eroding this dune crest. Although higher dunes could exist due to the flow strength alone, there has to be enough vertical space to build these dunes. In deep rivers (for example in the Rhine) the water depth is less important. A change of 1 or 2 meters in water depth on a total of 10 to 15 m changes the dune height about 10 to 20 cm, in a situation where dunes are already 0.8 to 1.2 m high. This change in dune height is of the same order of magnitude as the natural range of dune heights in this situation.

2.3.2.2 Unsteady flow conditions

River discharge and flow velocity change over time. Especially during floods, flows are constantly changing (rising and falling stages) causing the dune dimensions never to reach equilibrium. Ripples can respond rapidly to new conditions but dunes have longer response times and therefore a considerable phase lag may occur, which increases for

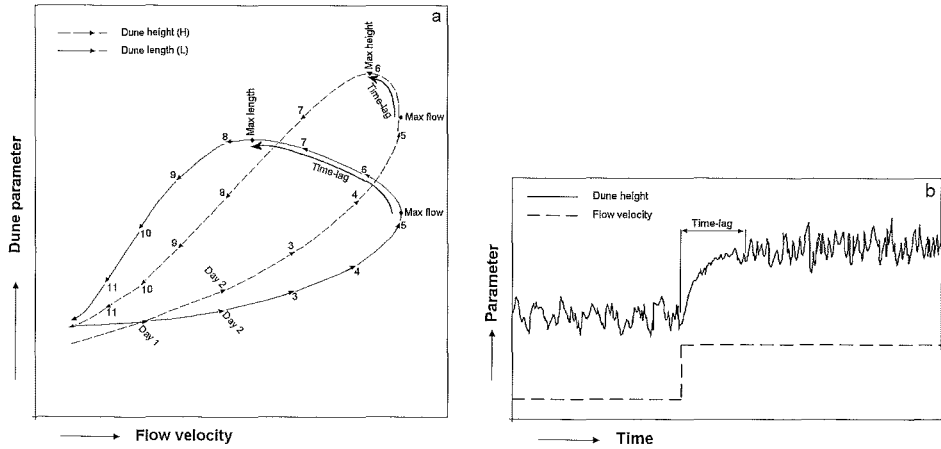


Figure 2.7. Examples of time-lag of dune height and length in changing flow conditions.

a) time-lag defined as a phase difference between maximum flow and maximum dune height or length.

b) time-lag defined as a transition-period between the equilibrium dune dimensions during one steady flow condition and the equilibrium dune dimensions during the next.

larger forms (Allen, 1976b; Fredsøe, 1979, 1982; Wijnbenga & Klaassen, 1981; Tsujimoto & Nakagawa, 1983; Iseya, 1984; Van Rijn, 1989; Wijnbenga, 1990). This phase lag can be defined as the time difference between maximum flow and maximum dune dimension (fig. 2.7A), or as the transition-period T between the equilibrium dune dimension at one flow stage and the equilibrium dimension at the next flow stage (fig 2.7B). This transition-period relates the ratio of change in cross-sectional area of the dune to the average bed load transport during the transition-period (Van Rijn, 1989):

$$T = \alpha \frac{(H_2 L_2 - H_1 L_1)}{(q_{b,1} + q_{b,2})} \quad (2.5)$$

in which H_1 , L_1 , is the equilibrium dune height [m], length [m] at stage 1; H_2 , L_2 , is the equilibrium dune height [m], length [m] at stage 2; and $q_{b,1}$, $q_{b,2}$ is the equilibrium bed load transport rates [m^2s^{-1}] at stage 1, 2. α is an empirical coefficient [-] which is about 4 according to Van Rijn (1989).

Independent of the definition used, Wijnbenga (1990) concluded that in general the time lag

- is larger for large bedforms,
- is larger for bedform length than for bedform height (fig. 2.7A),
- depends on the discharge variability (shape of the hydrograph),
- is relatively small during increasing discharge (rising stage), but relatively large during decreasing discharge (falling stage),
- and is primarily related to variations in flow velocity; variations in grain size and water depth are less important.

2.3.3 Dune shapes

While ripples are always three-dimensional under equilibrium conditions, dunes have been described with both two-dimensional and three-dimensional shapes (Dalrymple *et al.*, 1978; Costello & Southard, 1981; Harms *et al.*, 1982; Middleton & Southard, 1986; Boguchwal & Southard, 1990). 2-D forms can adequately be represented by a transect parallel to flow, but 3-D forms must be defined in three dimensions because they are characterized by scour pits and curved fronts. Two dimensional dunes are found in flumes (with small widths) during low flow velocities, while 3-D dunes are reported especially at larger flow velocities. Two and three-dimensional dunes have also been discovered in many rivers (Nasner, 1974; Dinehart, 2002; Chapter 4 of this thesis). It is however unclear whether the described 2-D dunes that are found are indeed equilibrium forms. It is possible that these dunes are 2-D, just because there was insufficient time to fully adapt to the changing flows.

2.4 Complicating aspects

This review on bedform classification shows that, at least in a theoretical sense, subaqueous bedforms can be classified according to flow conditions and bedform dimensions. In practical situations this is more difficult, especially in cases where the bed consists of a wide or bimodal grainsize distribution, and when the sediment supply is smaller than the transport capacity. However, concerning the dimensions and shapes of different bedforms that have been described, two important aspects, low angle dunes and the concept of superposition, have not been mentioned yet. These complicating aspects prompted a lot of discussion recently on their occurrence and cause (Ashley, 1990; Best & Kostaschuk, 2002). Some attention has to be paid to these discussions at the end of this review because of their relevance to the problems of bedform classification.

2.4.1 Low angle dunes

Low angle dunes or wave type bedforms have been classified as a separate type of bedform by several investigators (Julien & Klaassen, 1995; Kostaschuk & Villard, 1996; Roden, 1998). However, these low angle dunes occur in many different situations, and are therefore not considered as a separate type of bedform in the classification presented here. In some cases, like in the Mississippi river, low angle dunes are forms that are washed out when flow conditions approach the upper flow regime ($Fr > 0.8$, fig. 2.3B; Julien & Klaassen, 1995). In other cases, low angle dunes are found in estuarine conditions where the flow reversal of the tides alters the dune shape; during high tide, erosion of the lee-side creates low angle forms (Boersma & Terwindt, 1981; Van den Berg *et al.*, 1995). Low angle dunes are probably also found in conditions with large concentrations of suspended sediment (i.e. the region near the threshold of full suspension transport, fig. 2.3A). In this case, it is assumed that the vertical concentration gradient of suspended matter hinders flow separation in the lee-trough, resulting in

suspended material being deposited on the lee-side and creating a smoother slope (J.H. van den Berg, personal communication).

However, it appears that low angle dunes may also be the result of either calculation errors or measurements at low resolution (in space and time). If the angle of the lee-side is calculated as an average between dune crest and trough, the result will be a low value, since most of the lee-side actually has a low angle near the crest and near the trough (fig. 2.8A). The steepest part of a lee-side, which is close to the angle of repose, is very short. If a dune is about 1 m high and 30 m long, the length of the lee-side is about 6 m. The steepest part, at an angle of about 30 degrees is however, not much longer than about 20 cm. In order to accurately measure the angle of this steepest part requires at least 2 measurement points spaced not more than 10 cm apart. In data of natural dunes, this resolution is almost never obtained, which means that the angle of the steepest parts of the lee-side is generally not determined correctly (fig 2.8B).

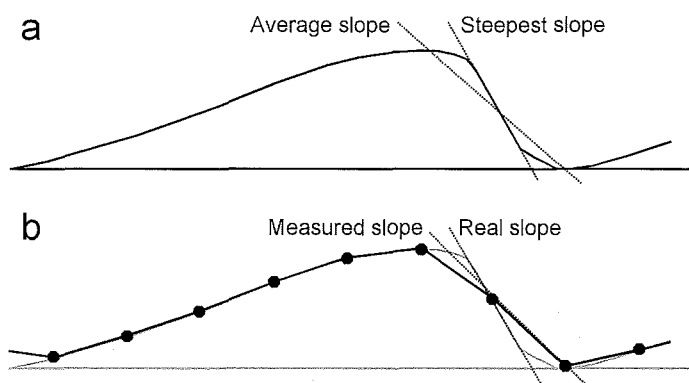


Figure 2.8. Differences between measuring the lee side slope of a steep dune with high or low resolution. Dunes are not drawn to scale.

- a) difference between steepest slope and average slope (between crest and trough).
- b) difference between the real steepest slope and the measured steepest slope in low resolution measurements.

2.4.2 Superposition

Ripples and dunes are not only found as fields of bedforms of similar size but also superimposed on each other in many different situations (Allen & Collinson, 1974; Nasner, 1974; Havinga, 1982; Dinehart, 1989; Nordin & Perez-Hernandez, 1989; Gabel, 1993; Harbor, 1998; Carling *et al.*, 2000a; Chapter 4 of this thesis). A good example of superimposing bedforms was described by Coleman (1969), who found four types of bedforms superimposed on each other. He found “sand waves” (hundreds of meters long and meters high) with superimposed “dunes” (ten of meters long) with superimposed “mega ripples” (meters long and decimetres to a meter high) with superimposed “ripples” (less than a meter long and less than a decimetre high).

Superimposed dunes are generally about an order of a magnitude less in height and length than the dunes they are superimposed on (Allen, 1976a), and occur only when there is

enough space and time to be developed on the larger forms (Ashley, 1990). However, it is unclear why superposition occurs. The stability diagrams show that only one bedform can be stable in a certain flow condition. One possibility is that the superimposed dunes are the forms that should be present under the reigning flow conditions and that the dunes they are superimposed upon are relict forms of previous conditions. The conditions changed so fast that the development of the largest forms could not keep up and they became relicts as new, smaller dunes, developed (Allen & Collinson, 1974). These superimposed smaller dunes in these cases cover both the stoss and lee-side of the large relict forms. Another possibility is that the largest bedforms alter the flow locally in such a way that bedforms with smaller dimensions or even other types of bedforms can develop on top of the larger ones. In this case both forms are active and the superimposed forms mostly just cover part of the stoss-side of the larger dune. Whatever the cause, the resulting superposition effects the way in which dunes develop, as well as how hydraulic roughness is predicted, and how bed load transport has to be calculated using the migration of the bedforms.

2.5 References

- Anon. (1982) Initiation of motion and suspension, development of concentration profiles in a steady, uniform flow without initial sediment load., M1531-III, Delft hydraulics, Delft, The Netherlands
- ALLEN, J.R.L. & COLLINSON, J.D. (1974) The superposition and classification of dunes formed by unidirectional aqueous flows. *Sedimentary Geology*, 12, 169-178.
- ALLEN, J.R.L. (1968) Current ripples. North-Holland Publishing Company, Amsterdam
- ALLEN, J.R.L. (1976a) Bedforms and unsteady processes: some concepts of classification and response illustrated by common one-way types. *Earth Surface Processes*, 1, 361-374.
- ALLEN, J.R.L. (1976b) Computational models for dune time-lag: general ideas, difficulties and early results. *Sedimentary Geology*, 15, 1-53.
- ALLEN, J.R.L. (1985) Sliding, rolling, leaping and making sand waves. In: *Principles of physical sedimentology* pp. 55-79. George Allen & Unwin, London.
- ASCE TASK FORCE ON BEDFORMS IN ALLUVIAL CHANNELS OF THE COMMITTEE ON SEDIMENTATION (1966) Nomenclature for bedforms in alluvial channels. *Journal of the Hydraulics Division*, 92, 51-64.
- ASHLEY, G.M. (1990) Classification of large-scale subaqueous bedforms: a new look at an old problem. *Journal of Sedimentary Petrology*, 60, 160-172.
- BAAS, J.H. (1993) Dimensional analysis of current ripples in recent and ancient depositional environments. *Faculteit Aardwetenschappen, Universiteit Utrecht, Utrecht, The Netherlands*, -199 pp.
- BAGNOLD, R.A. (1966) An approach to the sediment transport problem from general physics. *Geological Survey Professional Paper*, 422-I.
- BEST, J.L. & KOSTASCHUK, R.A. (2002) An experimental study of turbulent flow over a low-angle dune. *Journal of Geophysical Research*, 107, 18-1-18-19.
- BOERSMA, J.R. & TERWINDT, J.H.J. (1981) Neap-spring tide sequences of intertidal shoal deposits in a mesotidal estuary. *Sedimentology*, 28.
- BOGUCHWAL, L.A. & SOUTHARD, J.B. (1990) Bed configurations in steady unidirectional water flows. Part 1. Scale model study using fine sands. *Journal of Sedimentary Petrology*, 60, 649-657.
- BRIDGE, J.S. & BENNETT, S.J. (1992) A model for entrainment and transport of sediment grains of mixed sizes, shapes and densities. *Water Resources Research*, 28.
- BRIDGE, J.S. (1987) Descriptive classification of fluvial bedforms: SEPM Classification of Large-scale Flow-transverse Bedforms Symposium.
- Ref Type: Unpublished Work

- BRIDGE, J.S. (1993) The interaction between channel geometry, water flow, sediment transport and deposition in braided rivers. In: Braided rivers (Ed. by J.L. Best & C.S. Bristow).
- CARLING, P.A., GÖLZ, E., ORR, H.G., & RADECKI-PAWLIK, A. (2000a) The morphodynamics of fluvial sand dunes in the River Rhine, near Mainz, Germany. 1. Sedimentology and morphology. *Sedimentology*, 47, 227-252.
- CARLING, P.A., WILLIAMS, J.J., GÖLZ, E., & KELSEY, A.D. (2000b) The morphodynamics of fluvial sand dunes in the River Rhine, near Mainz, Germany. 2. Hydrodynamics and sediment transport. *Sedimentology*, 47, 253-278.
- CHABERT, J. & CHAUVIN, J.L. (1963) Formation des dunes et des rides dans les modelés fluviaux. Bulletin du Centre de Recherches et d'Essais de Chatou, 4.
- CHEEL, R.J. (1990) Horizontal lamination and the sequence of bed phases and stratification under upper-flow-regime conditions. *Sedimentology*, 37, 517-529.
- CHURCH, M.A. & JONES, D. (1982) Channel-bars in gravel bed rivers. In: Gravel-bed rivers (Ed. by R.D. Hey *et al.*), Wiley, Chichester.
- COLEMAN, J.M. (1969) Brahmaputra river: channel processes and sedimentation. *Sedimentary Geology*, 3, 129-239.
- COSTELLO, W.R. & SOUTHARD, J.B. (1981) Flume experiments on lower-flow-regime bedforms in coarse sand. *Journal of Sedimentary Petrology*, 51, 849-864.
- CRICKMORE, M.J. (1970) Effects of flume width on bed form characteristics. *Journal of the Hydraulics Division*, 96, 473-496.
- DALRYMPLE, R.W., KNIGHT, R.J., & LAMBAISE, J.J. (1978) Bedforms and their hydraulic stability relationships in a tidal environment, Bay of Fundy, Canada. *Nature*, 275.
- DINEHART, R.L. (1989) Dune migration in a steep, coarse-bedded stream. *Water Resources Research*, 25, 911-923.
- DINEHART, R.L. (2002) Bedform movement recorded by sequential single-beam surveys in tidal rivers. *Journal of Hydrology*, 258, 25-39.
- ENGEL, P. & LAU, Y.L. (1980) Computation of bed load using bathymetric data. *Journal of the Hydraulics Division*, 106, 369-380.
- ENGELUND, F. (1965) A criterion for the occurrence of suspended load. *La Houille Blanche*, 8.
- FLEMMING, B.W. (1988) Zur klassifikation subaquatischer, strömungstransversaler transportkörper. *Bochumer Geologische und Geotechnische Arbeiten*, 29, 44-47.
- FREDSØE, J. (1979) Unsteady flow in straight alluvial streams: modification of individual dunes. *Journal of Fluid Mechanics*, 91, 497-512.
- FREDSØE, J. (1980) The formation of dunes.
- FREDSØE, J. (1982) Shape and dimensions of stationary dunes in rivers. *Journal of the Hydraulics Division*, 108, 932-947.
- GABEL, S.L. (1993) Geometry and kinematics of dunes during steady and unsteady flows in the Calamus River, Nebraska, USA. *Sedimentology*, 40, 237-269.
- GILL, M.A. (1971) Height of sand dunes in open channel flows. *Journal of Hydraulic Engineering*, 97, 2067-2074.
- GRAFF, W.H. & PAZIS, G.C. (1977) Les phénomènes de déposition et d'érosion dans un canal alluvionnaire. *Journal of Hydraulic Research*, 15.
- GUY, H., SIMONS, D.B., & RICHARDSON, E.V. (1966) Summary of alluvial channel data from flume experiments, 1956-61. US Geological Survey Professional Paper, 462-I.
- HARBOR, D.J. (1998) Dynamics of bedforms in the lower Mississippi river. *Journal of Sedimentary Research*, 68, 750-762.
- HARMS, J.C. (1969) Hydraulic significance of some sand ripples. *Bulletin of the Geological Society of America*, 80, 363-396.
- HARMS, J.C., SOUTHARD, J.B., & WALKER, R.G. (1982) Structure and sequence in clastic rocks. SEPM short course, 9
- HAVINGA, H. (1982) Bed load determination by dune tracking., 82.3, Rijkswaterstaat, Arnhem, the Netherlands
- HEIN, F.J. & WALKER, R.G. (1977) Bar evolution and development of stratification in the gravelly braided Kicking Horse River, B.C. *Canadian Journal of Earth Sciences*, 14.

- ISEYA, F. (1984) Experimental study of dune development and its effect on sediment suspension. Environmental research center papers, 5, Environmental research center, Ibaraki, Univ. of Tsukuba
- JULIEN, P.Y. & KLAASSEN, G.J. (1995) Sand-dune geometry of large rivers during floods. *Journal of Hydraulic Engineering*, 121, 657-663.
- JULIEN, P.Y. (1992) Geometry of bed forms in large rivers., Q1386, Delft Hydraulics, Delft
- KENNEDY, J.F. (1969) The formation of sediment ripples, dunes and antidunes. *Annual Review in Fluid Mechanics*, 1, 147-168.
- KLEINHANS, M.G. & VAN RIJN, L.C. (2002) Stochastic prediction of sediment transport in sand-gravel bed rivers. *Journal of Hydraulic Engineering*, 128, 412-425.
- KLEINHANS, M.G. (2001) The key role of fluvial dunes in transport and deposition of sand-gravel mixtures, a preliminary note. *Sedimentary Geology*, 143, 7-13.
- KLEINHANS, M.G. (2002) Sorting out sand and gravel: Sediment transport and deposition in sand-gravel bed rivers. *Netherlands Geographical Studies* 293,
- KLEINHANS, M.G., WILBERS, A.W.E., DE SWAAF, A., & VAN DEN BERG, J.H. (2002) Sediment supply-limited bedforms in sand-gravel bed rivers. *Journal of Sedimentary Research*, 72, 629-640.
- KOSTASCHUK, R.A. & VILLARD, P.V. (1996) Flow and sediment transport over large subaqueous dunes: Fraser River, Canada. *Sedimentology*, 43, 849-863.
- LAURSEN, E.M. (1958) The total sediment load of streams. *Journal of the Hydraulics Division*, 84, 1530-1-1530-36.
- LIVESEY, J., BENNETT, S.J., ASHWORTH, P.J., & BEST, J.L. (1995) Flow, Sediment transport and bedform dynamics in bimodal sediments. In: 4th international workshop on gravel-bed rivers .
- MAHMOOD, K. (1987) ACOP canals equilibrium runs computerized base., IWRI-87-4, International Water Resources Institute, Washington
- MAHMOOD, K., MEHRDAD, M.H., HAQUE, M.I., & ASUD CHOUDRI, A. (1984) Bedform data in Acop canals 1977 - 1980. *Civ. Eng. Dep., George Washington Univ., Washington*
- MCCULLOCH, D.S. & JANDA, R.J. (1964) Subaqueous river channel barchan dunes. *Journal of Sedimentary Petrology*, 34, 694.
- MIDDLETON, G.V. & SOUTHARD, J.B. (1986) Mechanics of sediment movement. Short course, 3, SEPM, Binghamton
- NASNER, H. (1974) Über das verhalten von transportkörpern im tidegebiet. *Mitteilungen des Franzius Instituts für Grund- und Wasserbau der Technischen Universität Hannover*, 40, 1-149.
- NORDIN, C.F. & PEREZ-HERNANDEZ, D. (1989) Sand waves, bars and wind-blown sand of the Rio Orinoco, Venezuela and Colombia. *US Geological Survey Water supply Paper*, 2326-A.
- RANGA RUJU, K.G. & SONI, J.P. (1976) Geometry of ripples and dunes in alluvial channels. *Journal of Hydraulic Research*, 14, 241-249.
- RODEN, J.E. (1998) The sedimentology and dynamics of mega-dunes, Jamuna River, Bangladesh. Department of Earth Sciences and School of Geography, University of Leeds, Leeds, UK, 310 pp.
- SHIELDS, A. (1936) Anwendung der anhnlichkeitsmechanik und der turbulenzforschung auf die geschiebebewegung. *Mitteilungen der Preussischen Versuchsanstalt für Wasserbau und Schiffbau*, 26.
- SHINOHARA, K. & TSUBAKI, T. (1959) On the characteristics of sand waves formed upon the beds of open channels and rivers. *Reports of Research Institute for Applied Mechanics*, 7, 15-45.
- SIMONS, D.B. & RICHARDSON, E.V. (1963) Forms of bed roughness in alluvial channels. *ASCE Transactions*, 14.
- SMITH, N.D. (1974) Sedimentology and bar formation in the upper Kicking Horse Rivers: a braided outwash stream. *Journal of Geology*, 82.
- SOUTHARD, J.B. & BOGUCHWAL, L.A. (1990) Bed configurations in steady unidirectional water flows. Part 2. Synthesis of flume data. *Journal of Sedimentary Petrology*, 60, 658-679.
- STEIN, R.A. (1965) Laboratory studies of total load and apparent bed load. *Journal of Geophysical Research*, 70, 1831-1842.
- STÜCKRATH, T. (1969) Die bewegung van großriffeln an der sohle des rio Parana. *Mitteilungen des Franzius Instituts für Grund- und Wasserbau der Technischen Universität Hannover*, 32, 267-293.
- TERMES, A.P.P. (1986) dimensions of bedforms under steady flow at high sediment transport rates., M2130, Delft Hydraulics, Delft
- TSUJIMOTO, T. & NAKAGAWA, H. (1983) Time lag appering in unsteady flow with sand waves. *Journal of Hydrosience and Hydraulic Engineering*, 1, 83-95.

- VAN DEN BERG, J.H. & VAN GELDER, A. (1993) A new bedform stability diagram, with emphasis on the transition of ripples to plane bed in flows over fine sand and silt. In: Special Publication of the International Association of Sedimentologists 28, 11-21.
- VAN DEN BERG, J.H. & VAN GELDER, A. (1998) Discussion: Flow and sediment transport over large subaqueous dunes: Fraser River, Canada. *Sedimentology*, 45, 217-221.
- VAN DEN BERG, J.H., ASSELMAN, N.E.M., & RUESSINK, B.G. (1995) Hydraulic roughness of tidal channel bedforms, Westerschelde estuary, The Netherlands. In: Tidal signatures in modern and ancient sediments (Ed. by B.W. Flemming & A. Bartholomae).
- VAN RIJN, L.C. (1984) Sediment transport; Part 3: bedforms and alluvial roughness. *Journal of Hydraulic Engineering*, 110, 1733-1754.
- VAN RIJN, L.C. (1989) Handboek sediment transport by currents and waves., report H461, Delft Hydraulics, Delft
- VAN RIJN, L.C. (1993) Principles of sediment transport in Rivers, Estuaries and Coastal seas. Aqua Publications, Amsterdam
- WHITING, P.J., DIETRICH, W.E., LEOPOLD, L.B., DRAKE, T.G., & SHREVE, R.L. (1988) Bedload sheets in heterogeneous sediment. *Geology*, 16.
- WIJBENGA, J.H.A. & KLAASSEN, G.J. (1981) Changes in bedform dimensions under steady flow conditions in a straight flume. In: Second international conference on fluvial sediments 260.
- WIJBENGA, J.H.A. (1990) Flow resistance and bedform dimensions for varying flow conditions; a literature review (main text and annexes)., Q785, Delft hydraulics,
- YALIN, M.S. (1964) Geometrical properties of sand waves. *Journal of the Hydraulics Division*, 90, 105-119.
- YALIN, M.S. (1972) *Mechanics of sediment transport*. Pergamon Press, Oxford
- YALIN, M.S. (1985) On the determination of ripple geometry. *Journal of Hydraulic Engineering*, 3.
- ZNAMENSKAYA, N.S. (1963) Experimental study of dune movement of sediment. *Transactions of the State Hydrologic Institut*, 108, 89-114.

Part 1 Development of subaqueous dunes

In part 1 of this thesis (Chapters 3-5) the main objective is to predict the development of dune shape and size in non-steady flows during floods. An important factor in the development of dunes is bedload transport, which directly influences the shape and size of dunes. In Chapter 3 therefore this bedload transport is described in relation to the migration of dunes. Dunes migrate due to material being eroded from their stoss-side, which is then deposited on the lee-side. Consequently, the migration rate and size of the dunes can be used to calculate bedload transport rates in a river. This so-called Dune Tracking technique is reviewed and analysed in Chapter 3 in view of its performance in field situations.

Chapter 4 describes the dune characteristics during several floods and low to moderate flow conditions in the Rhine branches as they were measured in the last decades. The development of dune size, migration rate and bedload transport rate is reviewed for the different river sections and related to the flow conditions in those sections. A qualitative analysis investigates which factors are influencing the dune development in the Rhine branches and what are the causes of the differences in dune development between the studied river sections.

Finally, in Chapter 5 the prediction of dune development is discussed. Several existing methods are reviewed and tested. These tests show that a new prediction method is necessary to predict the dune development in the Rhine branches. Using the measurements described in Chapter 4 this new method is created.

3 Bedload transport rate obtained by dune tracking: reliability and optimalization

Abstract

It is difficult to get a realistic estimate of the bedload transport rate in a river by using a bedload sampler. An attractive alternative therefore is to calculate it from the migration of dunes as revealed from successive echo-sounding of the river bed. Many researchers successfully tested this dune tracking technique by comparing calculated bedload transport rates with direct measurements of bedload. In this paper the factors that influence the reliability of the dune tracking technique in field situations are analysed, and recommendations are made about the conditions which have to be met for the reliable use of dune tracking. These factors involve the spatial en temporal resolution of the measurements necessary to accurately determine the dune characteristics and the dune migration rate, together with the correct positioning of profiles and the problems associated with dune superposition. In addition, the influence of dune shape and complex sediment transport fluxes are investigated to see to what extent these factors influence the calculations and how they have to be incorporated in the dune tracking equation.

This chapter has been submitted to the Journal of Hydraulic Engineering.

3.1 Introduction

Generally, sediment transport of bed material is divided into suspended and bedload transport. Bedload transport is defined as the transport of sediment particles by rolling, sliding or saltating in a bedload transport layer with a thickness of a few particle diameters (Van Rijn, 1984), while suspended particles stay in the flowing water and hardly ever reach the bed again. In case of a fine sand as bed material, most of the particles are transported in the suspended mode. This transport rate can be measured relatively easily, by measuring flow velocity and sediment concentration, either from samples of the water and sediment mixture or indirectly by using an acoustic device, such as the Acoustic Sand Transport Meter (Van den Berg 1984). In the case of coarser sediment, bedload is the principal mode of transport, but direct measurement of it is much more difficult. The bedload transport rate can be measured using bedload traps, however, the efficiency of these traps is difficult to determine. Kleinhans (2002), for example, showed that, because of an uncertain sand-trap efficiency-coefficient for the adapted Helley-Smith that was used in the Waal near the Dutch-German border during a flood in 1998, the measured bedload transport rates could deviate up to 200%. In addition to this efficiency, the precise positioning of the trap, in case the bed is covered with subaqueous dunes, is important because the bedload transport rates differ much over the length of a dune (Kleinhans & Ten Brinke, 2001).

Fortunately, in many rivers, during periods of significant sediment transport, the bed is covered by migrating dunes and it was suggested by several researchers that a reliable estimate of the bedload transport rate can be obtained from their downstream movement (Jinchi, 1992; Ten Brinke *et al.*, 1999; Wilbers & Ten Brinke, 1999; Ten Brinke & Wilbers, 1999). This indirect method of determination of bedload transport rate is called dune tracking, and many investigators have successfully used it under various conditions (Stückrath, 1969; Nasner, 1974; Crickmore, 1970; Engel & Lau, 1980, 1981; Van den Berg, 1987; Jinchi, 1992; Ten Brinke *et al.*, 1999; Dinehart, 2002), indicating that dune tracking could be a reliable alternative for direct measurements.

The use of dune tracking is, however, still not widespread in river engineering. This may be due to the fact that it can be difficult to perform the necessary measurements in a river (Ten Brinke *et al.*, 1999). Bed profiles have to be measured, using for example echosounding equipment, with sufficient spatial and temporal resolution to determine the dune characteristics and dune migration rates. In addition, these measurements have to be done in a field situation that allows a simple conversion of dune migration rate into bedload transport rate (Engel & Lau, 1981; Van den Berg, 1987; Ten Brinke *et al.*, 1999). It is, however, still unclear which factors, and to what extent, determine this conversion. The objective of the present analysis is to review the dune tracking technique and the assumptions associated with the conversion, to find out in which river situations this technique can be considered reliable enough to determine bedload transport rate. This is addressed by looking first at how sediment is transported over a dune and describe the basic dune tracking technique as provided by previous investigators. After that several factors which influence the reliability of the dune tracking technique in river situations

are analysed, such as: measurement resolution, complex sediment transport fluxes, dune superposition and the choice of a bedload discharge coefficient. The analysis is carried out by using new data on dunes and dune tracking from the Rhine in The Netherlands, and reanalysing published data of other researchers.

3.2 Sediment transport over dunes

When the bed of a stream is covered with subaqueous dunes, the usual division of sediment transport into bedload and suspended load is not always correct. Over dunes, sediment transport follows complex flow patterns, eroding material in some places and depositing it elsewhere, which results in the migration of the dunes. In addition, the near-bed turbulence varies over the dune morphology creating large spatial variations in

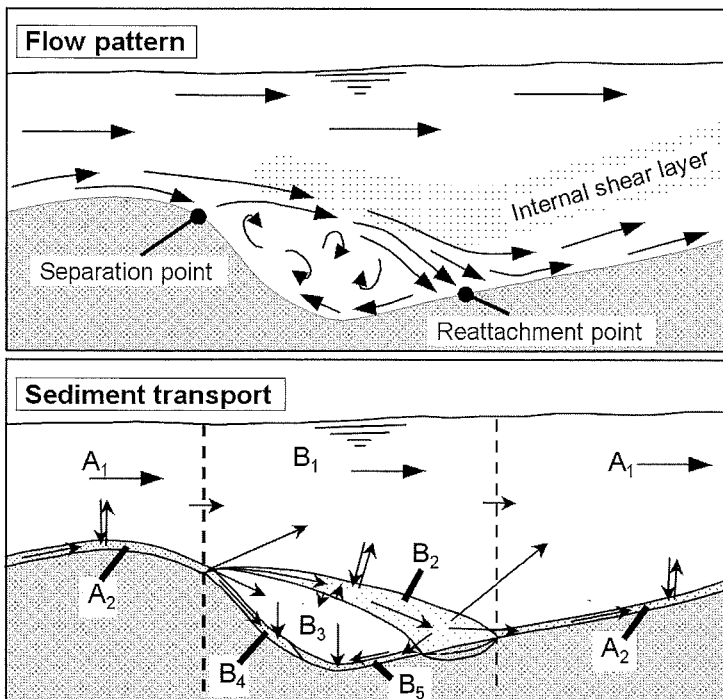


Figure 3.1. Flow and sediment transport over a dune. The sediment transport is divided into zones and the interactions between different zones are shown with arrows.

A_1 is the suspension transport zone over the stoss-side, and A_2 the bedload transport zone.

B_1 is the suspension transport zone over the separation zone, B_2 is zone with downstream flow just above the separation zone, B_3 is the zone of upstream moving water in the separation zone, B_4 is the zone where material avalanches down the lee-side, and B_5 is the zone where upstream moving water causes an upstream moving bedload transport.

This schematisation is modified from figures of Allen (1965) and Bennet & Best (1995).

bedload transport rate and suspended sediment concentration. These complex flow patterns can be divided into zones in which the direction and velocity of the sediment transport is different. In fig. 3.1 (modified after Allen (1965) and Bennet & Best (1995)) the different zones of flow over a dune are shown together with every possible interaction, transporting a particle from one zone to another (Allen, 1965, 1968; Jopling, 1964, 1965; Mercer, 1964; Havinga, 1982; Carling & Glaister, 1987; Bennet & Best, 1995; Best, 1996). In dune tracking, it is implicitly assumed that dune migration is only a function of sediment erosion from the stoss-side, transporting it as bedload towards the dune brink and depositing it in avalanches on the dune lee-side. The reality, however, may be more complicated (Engel & Lau, 1981; Van den Berg, 1987; Ten Brinke *et al.*, 1999).

Starting at the reattachment point, where the separated flow from a previous dune reattaches to the bed, strong turbulent bursts originating from the separation zone collide with the bed. These bursts erode large amounts of material and transport it as suspended or bedload transport in zone A (fig. 3.1). Zone A covers the stoss-side of a dune where the flow is comparable with the flow over flat bed, resulting in the usual division of sediment transport into bedload and suspended transport. When a particle, eroded and transported this way, arrives at the flow separation zone (Zone B), the flow is divided into 5 different sub-zones (fig 3.1) and a particle can pass into either of these. To analyse if the sediment transport involved in dune migration is equal to the actual bedload transport, it is crucial to know which path the majority of particles take through zone B. The five most important paths (in order of the relative number of particles) are from sub-zone:

- A_1 to B_1 : particles in suspension over zone A will most likely stay in suspension over zone B.
- A_2 to B_4 : particles from bedload transport in zone A are mostly deposited just below the flow separation point and avalanche down slope in sub-zone B_4 . Erosion at the reattachment point and deposition in sub-zone B_4 causes the downstream migration of the dune, and therefore these particles are regarded here as the bedload transport in zone B.
- A_2 to B_2 : some particles from sub-zone A_2 are not deposited in sub-zone B_4 but are transported in semi-suspension through sub-zone B_2 directly to the next reattachment point and probably into the next sub-zone A_2 . The material, that was in bedload transport over the stoss-side, therefore does not contribute to the migration of the dune. In the present analysis this material is not regarded as being bedload or suspended transport but something in between, called semi-suspension transport or trough bypassing transport.
- A_2 to B_1 : a few particles are swept from bedload transport into suspension at the separation point.
- A_1 or B_1 to B_4 : also a few particles fall from suspension over the flow separation zone being deposited on the lee-side (B_4).

These five paths of sediment transport show that the migration of dunes is not simply a function of bedload material transported over the stoss-side being deposited on the lee-side. There are other fluxes that either decrease or increase the migration rate and also the

calculated bedload transport rate. Therefore, it is important to know which fluxes are accounted for in the dune tracking technique when the calculated bedload transport rates are to be compared with rates from direct measurements.

3.3 Dune Tracking technique

The indirect determination of the bedload transport rate from dune migration data is nothing new. Exner (1931) already developed a working equation for windblown sand dunes. Crickmore (1970) and Engel & Lau (1980, 1981) formulated an equation to be used for subaqueous dunes. They assumed that:

- dunes can be considered triangular (fig. 3.2),
- the point where the bedload transport rate is zero is located in the trough of the dune,
- all material eroded from the stoss-side is deposited on the dune lee-side,
- and the flow, the dunes and the sediment transport can be simplified to a 2 dimensional situation, as presented in fig. 3.1.

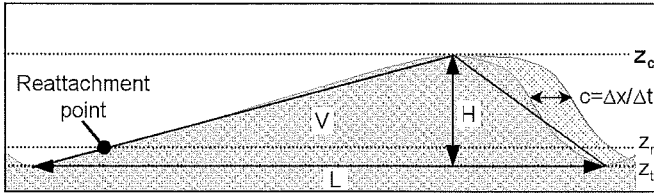


Figure 3.2. Dune profile definition sketch. For explanation of letters see text.

Under these assumptions, the conservation of volume implies

$$\frac{\partial q_b}{\partial x} + \frac{\partial z}{\partial t} = 0 \quad (3.1)$$

where q_b is the bedload transport rate [m^2s^{-1}] including pore space, x is distance in flow direction [m], z is bed level [m] and t is time [s]. Assuming undisturbed propagation of the dunes at a celerity $c = \Delta x / \Delta t$

$$z(x, t + \Delta t) = z(x - c\Delta t, t) \quad (3.2)$$

and thus

$$z(x, t) + \frac{\partial z}{\partial t} \Delta t = z(x, t) - \frac{\partial z}{\partial x} \Delta x \quad (3.3)$$

resulting in

$$\frac{\partial z}{\partial t} = -c \frac{\partial z}{\partial x} \quad (3.4)$$

Combining equations 3.1 and 3.4 leads to

$$\frac{\partial q_b}{\partial x} - c \frac{\partial z}{\partial x} = 0 \quad (3.5)$$

Integration yields

$$\int_0^x \frac{\partial q_b}{\partial x} dx = c \int_0^x \frac{\partial z}{\partial x} dx \quad (3.6)$$

Hence

$$q_b = c(z(x) - z_0) \quad (3.7)$$

where z_0 is the height of the bed where $q_b(x)=0$. The average bedload transport rate over one dune wavelength (L) results from the integration of equation 3.7

$$q_b = \frac{1}{L} \int_0^L q_b(x) dx = \frac{c}{L} \int_0^L (z(x) - z_0) dx \quad (3.8)$$

When the shape of a dune is approximated by a triangle and the position of zero bedload is the trough ($z_0 = z_t$), as stated above (Stückrath 1969, Nasner 1974), then equation 3.8 becomes

$$q_b = \frac{1}{2} Hc \quad (3.9)$$

where H is dune height ($z_c - z_t$) [m]. Generally, dunes do not have a perfect triangular shape and the value $\frac{1}{2}$ is replaced by a so called bedload discharge coefficient (β) which has a value that deviates from 0.5.

3.4 Use of dune tracking in field situations

After describing the sediment transport over dunes and the basic principles of the dune tracking technique, the difficulties in using this technique in field situations can be analysed in more detail, providing guidelines to avoid or account for them. First, the difficulties related to the measurement of dune characteristics and migration rates are discussed, then the difficulties related to the conversion of the migration rate into the bedload transport rate resulting from the four assumption in the basic dune tracking technique, and finally the superposition of dunes.

3.4.1 Difficulties of field measurements

According to equation 3.9, two characteristics of the dunes have to be determined to enable dune tracking, the dune height (H) and the migration rate (c). As will be shown later, dune length (L) and dune volume (V) are also important. The method of measuring, and the measurement resolution therefore, has a significant influence on the reliability of the dune tracking technique. However, these factors were hardly ever considered by other researchers. Generally, in field measurements, the dune characteristics are obtained from echo sounding profiles (Dinehart 1992, 2002, Gabel 1993, Ten Brinke *et al.* 1999). From these profiles, the dune dimensions and migration rates are calculated.

The accuracy of the obtained dune height (H) and length (L) and dune volume (V), depends more on the spatial resolution of the measured points along a profile, rather than on the method used to extract the characteristics from the sounded profile. The spatial

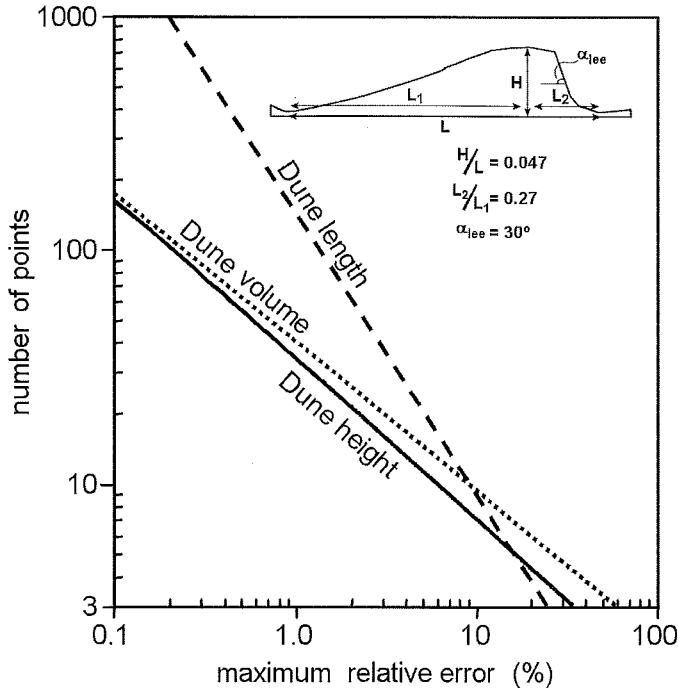


Figure 3.3. The number of points per dune versus the maximum relative error of the real value of dune height, length and volume.

resolution determines the number of points measured along a dune and therefore, determines the accuracy at which the dune shape is represented. After sampling an analytical continuous dune shape (of a common dune) with various number of points (at regular but slightly varying intervals), and comparing the calculated characteristics with the actual values, fig. 3.3 shows the number of points necessary on a dune for the accurate determination of dune characteristics. To accurately determine the characteristics of, for example, a dune of about 10 m long and 0.3 m high, with an relative error smaller then 10%, the dune has to be covered with 7-10 points. This means that the spatial resolution of the measured points in the profile has to be about one point per 1-1.4 m. However, the dunes on the bed of a river do not all have the same shape as the dune used here, and any measurement method results in a spatial variation of the resolution, which means that in practice, the spatial resolution determined from fig. 3.3 only provides a lowest estimate.

The accuracy of the dune migration rate (c) depends both on the spatial resolution and on the time span between consecutive measurements. This is shown in fig. 3.4, where the spatial resolution is represented as the number of points used to measure a 10 m long dune, and the temporal resolution is represented as the relative migration distance (c/L). Figure 3.4 also shows that when the temporal resolution is high than the relative error in the migration distance is also high. Although the absolute error in the migration distance might be low, the relative error will also occur in the migration rate and bedload transport

rate. On the other hand, the migration distance of a dune can only be calculated if the same dune can be recognized in both measurements. If a dune migrates over a distance of

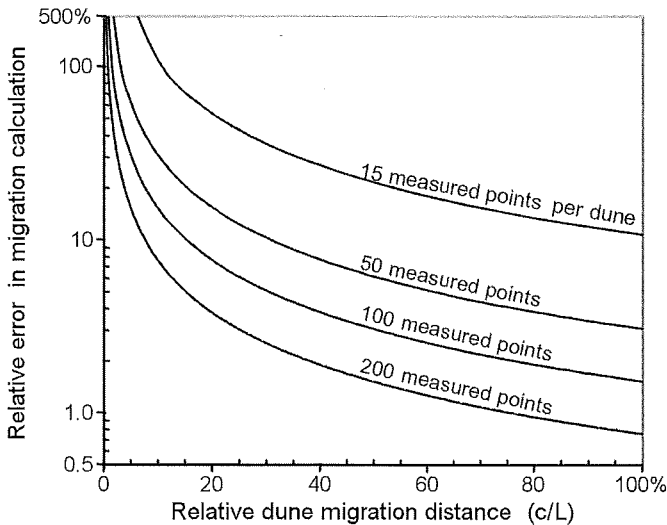


Figure 3.4. Relative error in calculating the dune migration distance as a function of the real migration distance and the spatial resolution.

more than one dune length, the migration distance becomes ambiguous. This is shown in fig. 3.5, where two profiles are compared in which the dunes have migrated more than one dune length. The calculated migration distance can for example be $1.1L$ or $2.1L$, $3.1L$ or more, as one dune cannot be distinguished from another. This means that the time between two measurements (the temporal resolution) should be small enough so that the dunes will not have migrated more than one dune length (Wilbers & Kleinhans, 1999). But the time between two measurements should be even smaller, because dunes change in shape as they migrate downstream. Extensive analyses by Wilbers & Kleinhans (1999) of migrating dunes of numerous shapes and configurations showed that the best temporal resolution lies between a dune migrating more than 20% and less than 80% of its dune

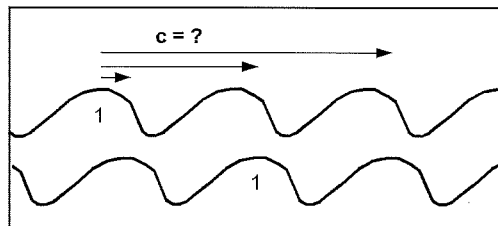


Figure 3.5. The ambiguous correlation of dunes when the temporal resolution is too large.

length. According to fig. 3.4 this however also means that the spatial resolution will have to be much higher than was determined from fig. 3.3.

Both the determination of spatial resolution from fig. 3.3 and the temporal resolution from fig. 3.4 require some previous knowledge on the dune size and migration rate in the

river of interest. In a new field situation, therefore, a trial-measurement has to provide information that will help to determine the minimal spatial and temporal resolution, before the real measurement campaign is carried out.

Besides the spatial and temporal resolution, the accuracy of the obtained dune characteristics and migration rate can also be influenced by the positioning and direction of the profile in the river. If the profile is not perpendicular to the crests of the dunes, then dune length and volume will be overestimated, and the migration rate underestimated, resulting in falsely calculated bedload transport rates. Especially in meander bends, dunes are usually rotated in the direction of the inner bend (Dietrich and Smith, 1984) . Profiles following the bend are therefore not perpendicular to the dune crests and the calculated bedload transport rates will be underestimated. This problem is normally avoided by performing the measurements in a almost straight section of the river, where the flow patterns are straight and the dune crests perpendicular to the banks.

3.4.2 Conversion of dune migration to bedload transport rate

The resolution and positioning of the profiles are not the only factors that can influence the reliability of the dune tracking technique. The most obvious factors are the four assumptions used in deriving equation 3.9. All four assumptions can be shown to be invalid in most conditions.

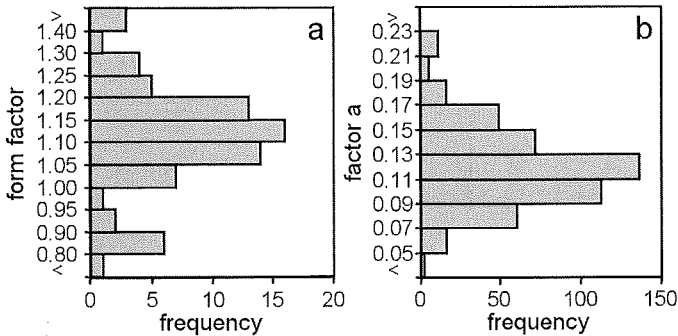


Figure 3.6. A) Histogram of all measured form factors (Table 3.1). B) Histogram of factor a , calculated with the relations of Engel & Lau (1981).

3.4.2.1 Dune shape

The shape of a dune is not equal to a triangle. Therefore, a form factor (f) was introduced by Stückrath (1969), Crickmore (1970), Van den Berg (1987), Jinchi (1992) and ten Brinke *et al.* (1999). Adding to equation 3.9, the form factor f is defined as:

$$q_b = \frac{1}{2} f H c = \frac{1}{2} \left(\frac{2V}{HL} \right) H c \quad (3.10)$$

This form factor implies that also the dune length and volume have to be measured and calculated accurately, resulting in a higher spatial resolution than for only calculating

Table 3.1. Factor values (minimum – average – maximum) of the datasets that were used. β values have been recalculated using the reported data on dune characteristics and direct bedload transport measurements. The values of a are calculated using the diagram by Engel & Lau, 1981. n/a means that data is not available. *Only total sediment transport rate was available.

Author	Conditions	β	Form factor (f)	Factor a	Factor b	F_i	F_p
Shinohara & Tsubaki 1959	Flume	0.41 - 0.81 - 1.21	n/a	0.09 - 0.16 - 0.23	n/a	n/a	n/a
Znamenskaya 1963	Flume	0.24 - 0.50 - 1.97	n/a	0.04 - 0.11 - 0.22	n/a	n/a	n/a
Stein 1965	Flume	0.20 - 0.91 - 1.84*	n/a	0.07 - 0.10 - 0.14	n/a	n/a	n/a
Guy et al. 1966	Flume	0.008 - 0.39 - 25.7	n/a	0.05 - 0.13 - 0.22	n/a	n/a	n/a
Crickmore 1970	Flume	0.33 - 0.38 - 0.49	Assumed 1.43	0.120 - 0.128 - 0.135	n/a	n/a	n/a
Engel & Lau 1980, 1981	Flume	0.28 - 0.44 - 0.62	Assumed 1.00	0.11 - 0.14 - 0.18	n/a	n/a	n/a
Shinohara & Tsubaki 1959	Hii River	0.19 - 0.78 - 6.3	1.09 - 1.13	0.06 - 0.11 - 0.17	n/a	n/a	n/a
Stueckrath 1969	Parana River	n/a	Assumed 1.00 - 1.33	0.08 - 0.09 - 0.10	n/a	n/a	n/a
Nasner 1974	Elbe and Weser Rivers	n/a	Assumed 1.00	0.07 - 0.11 - 0.17	n/a	n/a	n/a
Havinga 1982	IJssel River	0.41 - 1.24 - 2.47	Assumed 1.00	n/a	n/a	n/a	n/a
Dinehart 1992	North Fork Toutle River	0.27 - 0.28 - 0.29	n/a	n/a	n/a	n/a	n/a
Jinchi 1992	Shen Shui, Guang Dong Zhenjiang, and Guang Dong Dongjan Rivers	n/a	0.39 - 1.12 - 2.86	0.09 - 0.16 - 0.23	n/a	n/a	n/a
Gabel 1993	Calamus River	0.29 - 0.61 - 1.36	n/a	0.13 - 0.15 - 0.17	n/a	n/a	n/a
Wilbers 1999	Rhine River	n/a	1.04 - 1.14 - 1.30	0.06 - 0.11 - 0.13	n/a	n/a	n/a

dune height (fig. 3.3). Form factors (f) were measured by several investigators (Table 3.1), and a histogram made from all these form factors (fig. 3.6a) shows that f cannot be assumed 1, as was proposed by Nasner (1974), Engel & Lau (1980, 1981) and Havinga (1982). In most cases, the form factor has a value between 1.10 and 1.15, indicating a cross-section area of the dune which is larger than the cross-section area of a triangle between troughs and crest. The small peak in the histogram between 0.8 and 0.9 is caused by data from Jinchi (1992). Probably his dune dimensions were not calculated accurately enough as an f smaller than 1 is not realistic in unidirectional flows. A dune cross-sectional area smaller than a triangle is probably only possible in wave-ripples.

3.4.2.2 Point of zero bedload transport rate

Crickmore (1970) and Engel & Lau (1980, 1981) showed that the position of zero bedload transport rate is not the trough but the point of reattachment ($z_0 = z_r$). Upstream of this point the sediment transport is directed to the toe of the lee side (fig. 3.1, sub-zone B₅). Thus bedload transport in a downstream direction only takes place over a depth of $(1-a)H$ instead of H , where a is the part of the dune height below the point of reattachment ($z_0 - z_t$ in fig. 3.2). Adding this factor to equation 3.10, it becomes:

$$q_b = \frac{1}{2} f (1-a) H c \quad (3.11)$$

The factor a was calculated with a relation provided by Engel & Lau (1981). The calculations were done for all the available data with a steepness (H/L) between 0.01 - 0.08 and a D_{50}/H between 0 - 0.09. Of the 428 available data-points, only 29 were outside these ranges. A histogram (fig. 3.6b) shows that, in most cases, a has value between 0.11 and 0.13.

3.4.2.3 Closed volume balance between stoss-side erosion and lee-side accretion

As was shown above, there are several fluxes that prevent a closed volume balance between the erosion on the stoss-side and the deposition on the lee-side. Some material, which is bedload over the stoss side, is transported in semi-suspension over the flow separation zone (sub-zone B₂, fig. 3.1) without being deposited on the lee side or in the trough. This trough-bypassing transport has been observed by several investigators (i.e. Allen, 1965, 1968; Jopling, 1964, 1965; Carling & Glaister, 1987) but has unfortunately never been quantified. It could be argued that part of the bedload volume, transported over the crest, contains a volume of bypassing material of a previous dune, and that most this material will be deposited on the lee-side instead of the dune's own material bypassing the lee side now. At first sight, because of this balance in volume between material imported from a previous dune, and material exported from this dune, this factor for bypassing could be considered negligible. However, the velocity of the trough bypassing material averaged over a dune length is higher than the velocity of the particles in the bedload mode (which are buried for long periods in the dunes themselves), making it an important factor in calculating the transport rate. The bypassing flux is added as a

factor b to equation 3.11:

$$q_b = \frac{1}{2} fb(1-a)Hc \quad (3.12)$$

In case of the volume balance hypothesis the value of b would be 1, otherwise the value would be larger than 1 because the bedload transport rate calculated with dune tracking would otherwise underestimate the rate measured with a direct measurement instrument, as this instrument will capture also the volume of bypassing material transported as bedload over most of the dune length. 3.1 indicates that no measured values of b are currently available, but it's importance and average value will be analysed in the next section.

Other fluxes counteracting the assumption of a volume balance between erosion on the stoss-side and deposition on the lee-side are the interactions between bedload and suspended transport (between sub-zones A₁, A₂, B₁ and B₄). Material is transferred from bedload into suspension and visa versa. All these individual interactions are difficult to quantify and these fluxes are therefore incorporated into a single factor F_i .

$$q_b = F_i \frac{1}{2} fb(1-a)Hc \quad (3.13)$$

If measurements are done in non-erosive and non-aggrading conditions, it is assumed here that the volumes deposited and eroded by the fluxes are in dynamic equilibrium, and that the value of F_i can be assumed 1.

3.4.2.4 Two dimensional flow

Finally, the fact that flow, sediment transport, and dune geometry are 3D instead of 2D features, has to be taken into account. Locally, sediment transport direction over dunes will deviate from the mean flow direction. Kisling-Møller (1993), for example, found that there were small secondary dunes in the troughs of the large dunes migrating perpendicular to the primary dune and mean flow. If there is only one profile or the sounded profiles are far apart, this perpendicular bedload transport can create a third volume imbalance by inputting extra material in a trough or extracting material from a trough in a profile. However, if measurements are done in straight sections of a river, it is assumed here that the input and output perpendicular to the main migration path will probably be in dynamic equilibrium. The factor F_p describing this flux, can therefore be assumed to have a value of 1 in carefully selected field sites.

$$q_b = F_p F_i \frac{1}{2} fb(1-a)Hc = \beta Hc \quad (3.14)$$

3.4.2.5 The bedload discharge coefficient

In most situations, it is very difficult to adequately determine the five factors added to equation 3.9 in the sections above. Therefore, a bedload discharge coefficient β was introduced (Engel & Lau, 1981; Van den Berg, 1987; Ten Brinke *et al.*, 1999) which combines all these factors (equation 3.14). This coefficient is estimated by comparing the bedload transport rate calculated using equation 3.9 (without any factor included) with

the bedload transport rate measured with some kind of direct measurement technique. Hence:

$$\beta = \frac{q_b \text{ measured}}{Hc} \quad (3.15)$$

To analyse the range of possible β values and the importance of the different factors combined in β , data from various studies were used (Table 3.1). The form factor (f) was measured in some cases or could be assumed to be between 1.10 and 1.15 in others, factor a could be calculated, and factors F_i and F_p were assumed to be 1. The only

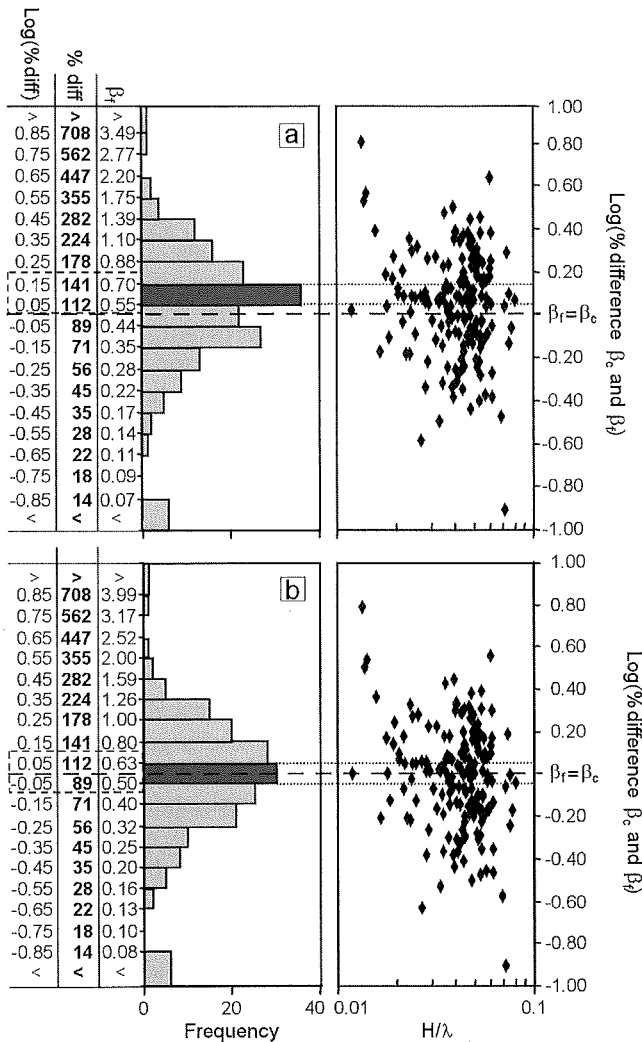


Figure 3.7. Histograms and scatterplots of the logarithmic relative differences between β_c and β_f . The relative values and β values are also shown.

a) using equation 3.16.

b) using equation 3.17.

uncertain factor was factor b . In a first approximation b was therefore assumed to be 1, as proposed by Engel & Lau (1980, 1981), and the bedload discharge coefficient (β) was calculated with:

$$\beta_f = F_p F_i^{\frac{1}{2}} f b (1-a) = 1 * 1 * \frac{1}{2} * f * 1 * (1-a) = \frac{1}{2} f (1-a) \quad (3.16)$$

in which β_f is the β calculated using all the factors. This β_f was then compared with the β_c calculated with equation 3.15 (the β values in Table 3.1). The relative deviations between β_f and β_c (converted to a logarithmic scale) were used to create a histogram (fig. 3.7a) to analyse how much most of the calculated bedload transport rates deviated from the measured bedload transport rates. Figure 3.7a shows that the bedload discharge coefficient varies considerably over different measurements, but it also shows that the distribution of β_f is shifted compared to β_c , indicating that the values of β_f are higher than the values of β_c . The interval with the highest frequency (mode) shows that β_f deviates from β_c by 12 – 41 %. In terms of equation 3.15 this means that the calculated bedload transport rate (H_c) is relatively underestimated compared to the measured bedload transport rate (q_b measured). Somehow, more material is measured moving downstream than is transported within the dunes. The only likely explanation is that in directly measuring bedload transport rate, the faster moving semi-suspension transport material is also captured.

Factor b therefore has to be larger than 1. On average the value of b should eliminate the shift between β_f and β_c in fig. 3.7a. That shift was between 12 and 41 % which can be recalculated into a average value of 1.12 to 1.41 for factor b . To calculate the individual factor b values for every single measurement is however impossible without measurements of the semi-suspension transport rates over the flow separation zones. If the most frequent values of both factor a (0.11 – 0.13, fig. 3.6b) and factor b are used in equations 3.14 or 3.16 it appears that on average these factors are each others opposite. Although the processes behind the factors a and b are not related physically, the empirical fact that these factors are each others opposite probably makes it possible to eliminate both factors from the calculation of β . Hence:

$$\beta = \beta_f = \frac{1}{2} f \quad (3.17)$$

To test this elimination of both factors a and b in equation 3.17, a second histogram was made, similar to fig. 3.7a, by using equation 3.17 for calculating β_f (fig. 3.7b). This histogram shows the same distribution of bedload discharge coefficients as fig. 3.7a, but the shift between β_f and β_c now lies between -11 and 12 %, meaning that on average the β_f is equal to β_c , and the elimination of factors a and b is at least empirically a possibility. This seems to contradict the results found by Engel & Lau (1980, 1981). They had good results in comparing the bedload transport rates measured in the flume with the transport rates calculated with dune tracking after they introduced the factor a (without using factor b). They found an average underestimation of bedload transport rate of about 3 % (when run 6 is excluded). However, because they did not use the factor b , they should have found an average underestimation of 12 - 41 %, according to the analysis above. The discrepancy between the results of Engel & Lau and this study can probably be explained by the fact that their study was done in a flume with no suspended transport and only small bedload transport rates (except in run 6). In most runs, the semi-suspended

transport was probably non-existent so calculating β with equation 3.16 would result in a good approximation of the bedload transport rate. However, in one case, run 6, the bedload transport rate was underestimated by 29.5%. In this run, the measured bedload transport was about twice as high as in all other runs. Semi-suspended transport was probably present in this run so they should have calculated β with equation 3.17.

Therefore, in field situations where the values of factors a and b are unknown (but both bedload and suspended transport are present), and the bedload discharge coefficient can not be calculated by comparing with measured bedload transport rates, the β can be calculated using equation 3.17. In cases where even the form factor cannot be calculated, the β can be assumed to have a value between 0.50 and 0.63 (fig 3.7b) with a best estimate of 0.57, see equation 3.9.

3.4.3 Superposition of dunes

One final issue that can make the use of dune tracking in field situations difficult is the superposition of dunes. In many rivers, smaller secondary dunes are superimposed on larger primary dunes (Pretious and Blench, 1951; Coleman, 1969; Allen and Collinson, 1974; Dinehart, 1989; ten Brinke *et al.*, 1999). This superposition complicates the calculation of the dune characteristics and dune migration rate, but more importantly, superposition can cause a problem in the translation of dune migration rate to the bedload transport rate.

In a situation with superposition, it is very important to determine whether to use the primary or the secondary dunes for calculating the bedload transport rate. In cases where superimposed secondary dunes are only present on the stoss-sides of the primary forms, most of the material transported by these secondary forms is deposited on the lee-sides of the primary forms. In such a case, the bedload transport rate calculated with the secondary forms is the same as the transport rate calculated with the primary forms. However, if the superimposed secondary dunes are present on both the stoss and the lee-sides of the primary forms (so covering the complete primary dune), not all the material transported by the secondary forms will be deposited on the lee-sides of the primary forms. In the latter case, the bedload transport rates calculated with the separate dune types are not the same.

This can clearly be shown with data from the Rhine (Wilbers, 1999). During a large flood in November 1998 detailed dune tracking measurements were done near a bifurcation called Pannerdensche Kop in the Rhine in The Netherlands. In a section of 1 km in length, the bed was measured twice a day with multibeam echo sounders for 17 days, resulting in a spatial resolution of about 15-20 points/m² (Wilbers, 1999). The dune characteristics and migration rate were calculated with a computer program; DT2D (Ten Brinke *et al.*, 1999), which determines the troughs of individual dunes in profiles extracted from the multibeam measurements. The dune length is the distance between 2 troughs and the dune height is the difference in elevation between the base-line (connecting the troughs) and the dune crest. In case of superposition, DT2D can be used to either locate the troughs of the primary dunes or the troughs of secondary dunes, by

providing a longer or shorter minimum distance required between two consecutive troughs.

The characteristics from DT2D (H in fig. 3.8a, λ in 3.8b and c in 3.8c) show that the dunes were relatively small at the start of the flood. However, they were already migrating fast. As the discharge rose, the dunes became higher and longer up to a few days after the maximum discharge. The migration rate just increased a little as the dunes became larger but slowed already down before peak discharge was reached. After 7 November 1998, during the falling stage, the dune height decreased again but the length kept on increasing. From 12 November on, these long and low dunes became superimposed with smaller secondary dunes. The migration rate of these secondary dunes could not be determined from the measurements, but it was assumed that the migration rate of the secondary dunes had the same order of magnitude (between 50 and 60 m/day) as the migration rate of the dunes at the start of the flood which had comparable dimensions. The calculated bedload transport rate of these secondary dunes, after assuming a migration rate of 55 m/day, appeared to be about 1.5 times higher than was calculated with the larger dunes (fig. 3.8d), showing that using only the primary dunes for calculating bedload transport rate would have led to an underestimation during the final days of the flood.

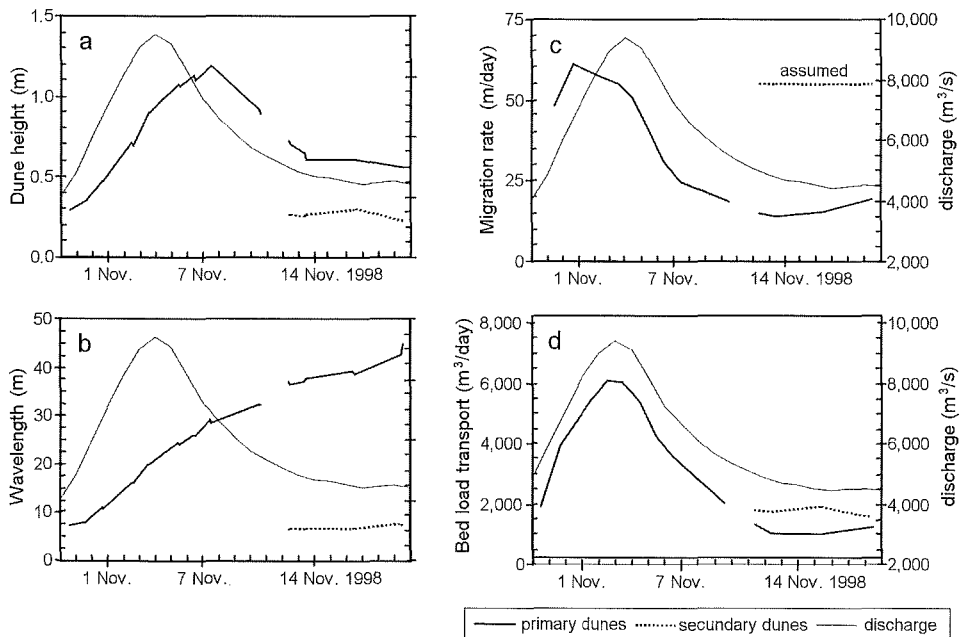


Figure 3.8. Changes in dune dimensions, migration rate and calculated bedload transport in the Rhine during the flood of 1998.

- a) dune height.
- b) dune length.
- c) migration rate.
- d) bedload transport rate.

For explanation about assumed migration rates see text.

Another example of what happens when the wrong dunes are chosen for calculating bedload transport rates is the analysis of Havinga (1982) of bedload transport in the IJssel in The Netherlands. In reviewing the measured profiles plotted by Havinga, it can be seen that there probably were small secondary dunes superimposed on both the stoss and lee sides of the primary forms. However, instead of using these smaller dunes, Havinga removed the secondary forms from the profiles using a filtering procedure, before calculating the bedload transport rate. Therefore, the bedload transport rate was probably underestimated, which would explain the large bedload discharge coefficients he found (Table 3.1) in comparing his calculations with the measured transport rates.

3.5 Conclusion

As direct measurements of bedload transport rates in rivers can be difficult and expensive, because of uncertain trap-efficiency coefficients (Kleinhans, 2002), precise determination of measurement location on a dune, and the amount of measurements necessary for accurate rates (Kleinhans and Ten Brinke, 2001), dune tracking can be a useful tool in many field situations (Stückrath, 1969; Nasner, 1974; Crickmore, 1970; Engel & Lau, 1980, 1981; Van den Berg, 1987; Jinchi, 1992; Ten Brinke *et al.*, 1999; Dinehart, 2002). The description of sediment transport over dunes and the basic dune tracking technique presented here, together with the analyses of various difficulties in using this dune tracking technique in field situations, shows that dune tracking can produce reliable results even without direct measurements. However, to use dune tracking correctly several factors have to be taken into account:

the location of the sounded profiles should be in an almost straight stretch of river and their direction should be parallel to the banks but perpendicular to the dune crests,

the spatial and temporal resolution of the measurements should be based on the expected dune characteristics and dune migration rates. The chosen resolutions should be high enough to accurately determine dune height, length, volume and migration rate, for example a spatial resolution of more than 15 points per dune and a temporal resolution that allows the dunes to migrate 20% to 80% of their dune length between two measurements,

the conditions during the measurements should be such that suspension transport is present and that 3D flow patterns can be neglected. Otherwise the factors a and b will not cancel each other out, and the factors F_i and F_p can not be assumed to have a value of 1,

finally, in case of superposition of dunes, those dunes (either the primary or the secondary) have to be used in dune tracking, that are most active in transporting bedload material as they migrate downstream.

If all these factors are accounted for, the bedload transport rate (including pore space) can be calculated from migrating dunes using:

$$q_b = \frac{1}{2} f H c \quad (3.18)$$

taking $\frac{1}{2} f = \beta = 0.57$ as a best estimate in case the form factor (f) cannot be calculated.

Acknowledgments

The work from which the experience with dune tracking and its problems came was done for the National Institute for Inland Water Management and Waste Water Treatment and the Department of Physical Geography of the Utrecht University in The Netherlands. Therefore, I am indebted to Dr. W.B.M. ten Brinke and Dr. J.H. van den Berg for their help, advice and encouragement. I am also grateful to Dr. A. van Gelder, Dr. E. A. Koster, Dr. Ir. L.C. van Rijn and Dr. M. Kleinhans for their comments on this paper.

Notation

- β = bedload discharge coefficient
- β_c = β calculated by comparing with measured bedload transport rates
- β_f = β calculated with all five factors (a , b , f , F_i , F_p)
- a = fraction of the dune height below the point of reattachment
- b = bypassing transport factor
- c = migration rate [ms^{-1}]
- D_{50} = median grain size [m]
- f = form factor
- F_i = factor for interactions between bedload and suspended transport
- F_p = factor for 3D flow patterns
- H = dune height ($z_c - z_t$) [m].
- L = dune wavelength [m]
- q_b = bedload transport rate [m^2s^{-1}] including pore space
- t = time [s].
- V = dune volume in profile [m^2]
- x = distance in flow direction [m]
- z = bed level [m]
- z_0 = height of the bed where $q_b(x)=0$ [m]
- z_t = height of dune trough [m]
- z_r = height of reattachment point [m]

References

- ALLEN, J.R.L. (1965) Sedimentation to the lee of small underwater sand waves: an experimental study. *Journal of Geology*, 73, 95-116.
- ALLEN, J.R.L. (1968) The accumulation of sediment in the lee of ripples and dunes, and the thickness of bottomset deposits. *Geological Magazine*, 105, 166-176.
- ALLEN, J.R.L. & COLLINSON, J.D. (1974) The superposition and classification of dunes formed by unidirectional aqueous flows. *Sedimentary Geology*, 12, 169-178.
- BENNETT, S.J. & BEST, J.L. (1995) Mean flow and turbulence structure over fixed, two-dimensional dunes: implications for sediment transport and bedform stability. *Sedimentology*, 42, 491-513.
- BEST, J.L. (1996) The fluid dynamics of small-scale alluvial bedforms. In: *Advances in fluvial dynamics and stratigraphy* (Ed. by P.A. Carling & M.R. Dawson), pp. 67-125. John Wiley & Sons, Chichester.

- CARLING, P.A. & GLAISTER, M.S. (1987) Rapid deposition of sand and gravel mixtures downstream of a negative step: the role of matrix-infilling and particle-overpassing in the process of bar-front accretion. *Journal of the geological society of London*, 144, 543-551.
- COLEMAN, J.M. (1969) Brahmaputra river: channel processes and sedimentation. *Sedimentary Geology*, 3, 129-239.
- CRICKMORE, M.J. (1970) Effects of flume width on bed form characteristics. *Journal of the Hydraulics Division*, 96, 473-496.
- DIETRICH, W.E. & SMITH, J.D. (1984) Bed load transport in a river meander. *Water Resources Research*, 20, 1355-1380.
- DINEHART, R.L. (1989) Dune migration in a steep, coarse-bedded stream. *Water Resources Research*, 25, 911-923.
- DINEHART, R.L. (1992) Evolution of Coarse gravel bed forms: Field measurements at flood stage. *Water Resources Research*, 28, 2667-2689.
- DINEHART, R.L. (2002) Bedform movement recorded by sequential single-beam surveys in tidal rivers. *Journal of Hydrology*, 258, 25-39.
- ENGEL, P. & LAU, Y.L. (1980) Computation of bed load using bathymetric data. *Journal of the Hydraulics Division*, 106, 369-380.
- ENGEL, P. & LAU, Y.L. (1981) Bed load discharge coefficient. *Journal of the Hydraulics Division*, 107, 1445-1454.
- EXNER, F.M. (1931) Zur dynamik der bewegungsformen auf der erdoberfläche. *Ergebnisse der Kosmischen Physik*, 1. Band.
- GABEL, S.L. (1993) Geometry and kinematics of dunes during steady and unsteady flows in the Calamus River, Nebraska, USA. *Sedimentology*, 40, 237-269.
- GUY, H., SIMONS, D.B., & RICHARDSON, E.V. (1966) Summary of alluvial channel data from flume experiments, 1956-61. *US Geological Survey Professional Paper*, 462-I.
- HAVINGA, H. (1982) Bed load determination by dune tracking., 82.3, Rijkswaterstaat, Arnhem, The Netherlands
- JINCHI, H. (1992) Application of sandwave measurements in calculating bed load discharge. In: *Erosion and Sediment transport monitoring programmes in river basins* 210, 63-70.
- JOPLING, A.V. (1964) Laboratory study of sorting processes related to flow separation. *Journal of Geophysical Research*, 69, 3403-3418.
- JOPLING, A.V. (1965) Hydraulic factors controlling the shape of laminae in laboratory deltas. *Journal of Sedimentary Petrology*, 35, 777-791.
- KISLING-MØLLER, J. (1993) Bedform migration and related sediment transport in a meander bend. *Special Publications of the International Association of Sedimentology*, 17, 51-61.
- KLEINHANS, M.G. (2002) Sorting out sand and gravel: Sediment transport and deposition in sand-gravel bed rivers. *Netherlands Geographical Studies* 293.
- KLEINHANS, M.G. & TEN BRINKE, W.B.M. (2001) Accuracy of cross-channel sampled sediment transport in large sand-gravel-bed rivers. *Journal of Hydraulic Engineering*, 127, 258-269.
- LAI, N.T. (1998) Bedforms in the Waal river. Characterization and hydraulic roughness., 024, International institute for infrastructural, hydraulic and environmental engineering (IHE), Delft, The Netherlands
- MERCER, A.G. (1964) Characteristics of sand ripples in low froude number flow. *University of Minnisota, Minneapolis*,
- NASNER, H. (1974) Über das verhalten von transportkörpern im tidegebiet. *Mitteilungen des Franzius Instituts für Grund- und Wasserbau der Technischen Universität Hannover*, 40, 1-149.
- PRETIOUS, E.S. & BLENCH, T. (1951) Final report on special observations of bed movement in the lower Fraser river at Ladner Reach during 1950., *Freshet. Natl. Res. Counc. Can., Vancouver*
- ROBERT, A. (1988) Statistical properties of sediment bed profiles in alluvial channels. *International Association for Mathematical Geology*, 205-225.
- SHINOHARA, K. & TSUBAKI, T. (1959) On the characteristics of sand waves formed upon the beds of open channels and rivers. *Reports of Research Institute for Applied Mechanics*, 7, 15-45.
- STEIN, R.A. (1965) Laboratory studies of total load and apparent bed load. *Journal of Geophysical Research*, 70, 1831-1842.
- STÜCKRATH, T. (1969) Die bewegung van großriffeln an der sohle des rio Parana. *Mitteilungen des Franzius Instituts für Grund- und Wasserbau der Technischen Universität Hannover*, 32, 267-293.

- TEN BRINKE, W.B.M. & WILBERS, A.W.E. (1999) Spatial and temporal variability of dune properties and bedload transport during a flood at a sand bed reach of the Dutch Rhine river system. In: IAHR Symposium on river, coastal and estuarine morphodynamics 2, 309-318.
- TEN BRINKE, W.B.M., WILBERS, A.W.E., & WESSELING, C. (1999) Dune growth, decay and migration rates during a large-magnitude flood at a sand and mixed sand-gravel bed in the Dutch Rhine river system. In: Fluvial Sedimentology VI, Special Publication of the International Association of Sedimentologists (Ed. by N.D. Smith & J. Rogers), 28, 15-32.
- VAN DEN BERG, J.H. (1984) The determination of suspended sand concentration. In: The closure of tidal basins (Ed. by J.C. Huis in 't Veld *et al.*), pp. 203-212. Delft University Press, Delft, The Netherlands.
- VAN DEN BERG, J.H. (1987) Bedform migration and bedload transport in some rivers and tidal environments. *Sedimentology*, 34, 681-698.
- VAN RIJN, L.C. (1984) Sediment transport; Part 2: suspended load transport. *Journal of Hydraulic Engineering*, 110, 1613-1641.
- WILBERS, A.W.E. (1999) Bodemtransport en duinontwikkeling in de Rijntakken: bodempeilingen hoogwater november 1998. ICG: Netherlands Centre for Geo-ecological Research, 99/10, Utrecht University, Utrecht
- WILBERS, A.W.E. & KLEINHANS, M.G. (1999) Gevoeligheidsanalyse dune tracking in 2 dimensies. ICG: Netherlands Centre for Geo-ecological Research, 99/8, Utrecht University, Utrecht, The Netherlands
- WILBERS, A.W.E. & TEN BRINKE, W.B.M. (1999) Development of subaqueous dunes in the Rhine and Waal, The Netherlands. A preliminary note. In: IAHR Symposium on river, coastal and estuarine morphodynamics 1, 303-312.
- ZNAMENSKAYA, N.S. (1963) Experimental study of dune movement of sediment. *Transactions of the State Hydrologic Institut*, 108, 89-114.

4 The response of subaqueous dunes to floods in sand and gravel bed reaches of the Dutch Rhine.

Abstract

The branches of the river Rhine in The Netherlands, characterised by a sand-gravel bed in the upstream part and a sand bed in the downstream part of the river system, show migrating dunes, especially during floods. In the last 20 years, these dunes have been studied extensively. High-resolution echo-sounding measurements of these dunes, made with single and multi-beam equipment, were analysed for three different sections of the Rhine River system, during several floods. This analysis was done to quantify the growth and decay and the migration rates of the dunes during floods. In addition, the migrating dunes were used to calculate bedload transport rates with dune tracking.

The results of dune growth and decay and migration rate are shown to be very different for the various sections during the various floods, and these differences are related to differences in grain size of the bed and to differences in the distribution of discharge over the main channel and the floodplain. The relations are used to show that the growth and migration rate of dunes, and the calculated bedload transport rates, during the rising stage of a flood wave can be predicted from the mobility of the bed material with simple power relations.

This Chapter is an extended version of: Wilbers, A.W.E. & Ten Brinke, W.B.M. (2003). The response of subaqueous dunes to floods in sand and gravel bed reaches of the Dutch Rhine. Sedimentology , - .

The extra information comprises of a detailed account on the relations between dune development, migration, and bedload transport rates and the grain-related shear stress. In most field situations, where no well-calibrated flow-models are available, the grain-related shear stress is easier to determine than the bed shear stress, which requires difficult but accurate measurements of water-surface slopes or overall Chezy values. In the case described here, however, the bed shear stress was known more accurately than the grain-related shear stress due to the use of a one-dimensional flow model (SOBEK) calibrated for the Rhine branches, and the lack of measurements on grain size changes of the bed material during floods.

4.1 Introduction

A sand or mixed sand-gravel bed river is generally characterized by the presence of subaqueous dunes during floods (Reid & Frostick, 1994). These dunes can be described by their heights, lengths, plan form and migration rates. Dunes are defined as bed forms present in subcritical flows, that are more than a decimetre high and have a length many times the water depth (Ashley, 1990). Knowledge of dune properties at successive time steps has proved to be a successful and powerful tool for quantifying bedload sediment transport (Engel & Lau, 1980; Havinga, 1982; Van den Berg, 1987; Ten Brinke *et al.*, 1999a). Also, the presence of dunes significantly increases the hydraulic roughness (Leeder, 1983; McLean *et al.*, 1994; Bennett & Best, 1995; Nelson *et al.*, 1995). Thus, information on dune dimensions may be very important for studies on hydraulic roughness as well. In fact, sediment transport, dune dimensions, and flow structures over dunes influence one another in a complicated way (Simons & Sentürk, 1992; Best, 1993).

In The Netherlands, dunes in the Rhine River have been studied extensively over the last 20 years, mainly for analysis of sediment transport (Ten Brinke *et al.*, 1999a, Kleinhans, 2002a, b) and hydraulic roughness (Van Urk, 1982; Moll *et al.*, 1987; Julien & Klaassen, 1995; Julien *et al.*, 2002). These studies on dune dimensions have been carried out during different discharges, and especially during rising and falling stages of flood waves. In the

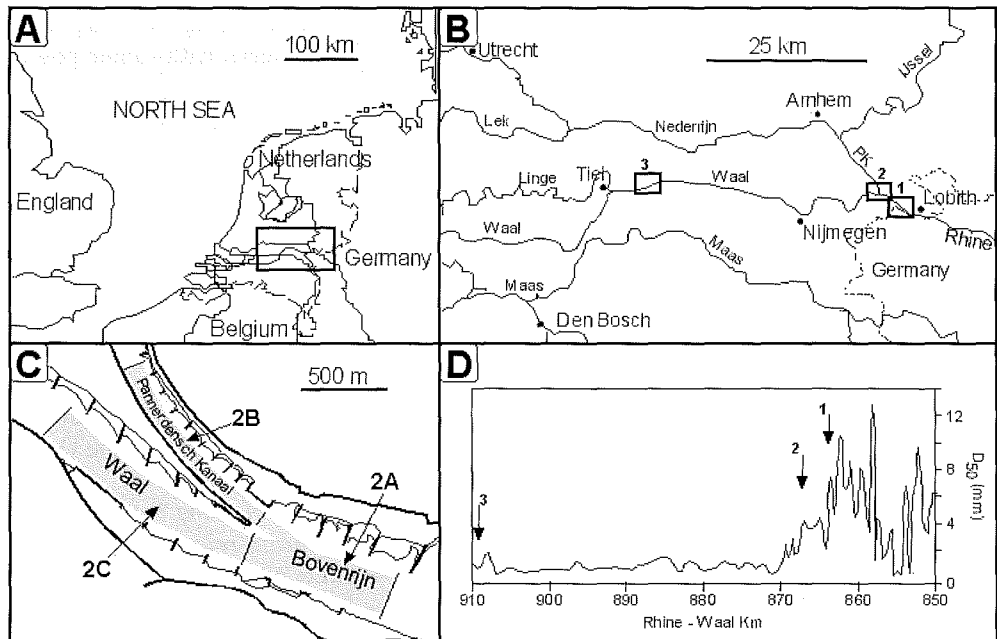


Figure 4.1. The tributaries of the Rhine River in The Netherlands. The numbers in (B) and (A) indicate the different sections and subsections where echosoundings were made; with Section 1 being the Bovenrijn, Section 2 being the Pannerdensch Kop, a bifurcation of the Bovenrijn (2C) into the Waal (2A) and the Pannerdensch Kanaal (PK) (2B) and Section 3 being halfway down the Waal. Figure (D) shows the changes in median grain size (D_{50}) along the Rhine, Bovenrijn and Waal.

Dutch Rhine, dunes are common phenomena during floods in all reaches of the river system. However, during low to moderate discharges, dunes are only observed in the middle and lower sandy reaches of the river system, while the bed in the upper mixed sand-gravel reaches is almost completely flat.

The first goal of this study was to quantify the growth and decay and the migration rates of dunes in the Dutch Rhine in both the sand and mixed sand-gravel bed reaches. A second goal was to calculate bedload sediment transport rates using the principles of dune tracking. Results are discussed in view of dune properties lagging behind changing hydrodynamic conditions during the rise and fall of flood waves, and the resulting hysteresis of the bedload sediment transport. In addition, the impact of bed grain size and the variable distribution of discharge between the main channel and the floodplain on dune growth and decay is discussed. Data from three different floods in three different sections of the Dutch Rhine are used for this analysis, together with data from the low to moderate discharges that act as a reference for conditions not measured during floods.

4.1.1 Study area

The River Rhine originates in the Alps and flows through Switzerland and Germany to The Netherlands. In The Netherlands, the Rhine river system consists of three major distributaries; the Waal, Nederrijn-Lek and IJssel, originating from the River Rhine at two bifurcations, just after the Rhine has passed the Dutch-German border (fig. 4.1). The

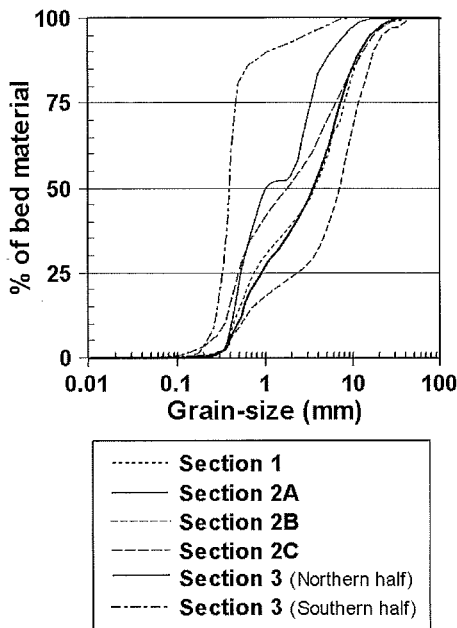


Figure 4.2. Grain size distributions of the different sections and subsections. For Section 3, two distributions are provided to show the difference between the northern and southern halves of the river.

discharge ratio between these distributaries is approximately 6:2:1. All three distributaries have embankments and groynes constructed along their entire length. These groynes extend 40-80 m into the main channel and are spaced 150-200 m apart.

The yearly average discharge of the Rhine near the Dutch-German border is $2300 \text{ m}^3\text{s}^{-1}$, stemming from both rain and snowmelt. In January to February 1995, the River Rhine experienced a maximum discharge of $12,000 \text{ m}^3\text{s}^{-1}$, among the highest Rhine discharges ever recorded.

The data on dunes have been collected in several sections in the Bovenrijn – Waal reach (fig. 4.1B and C, and Table 4.1. See also Appendix A). Along this reach, the river changes from a gravel bed river in Germany into a sand bed river in the Waal (fig. 4.1D). Besides considerable differences in grain size between the different sections, the grain size also differs considerably within some sections (fig. 4.2). In Section 3, for example, the top 5 cm of the bed in the northern half of the main channel is composed of coarse sand with some fine gravel ($D_{50}=1.0 \text{ mm}$) while the southern half is composed of sand ($D_{50}=0.5 \text{ mm}$) (Ten Brinke *et al.*, 1999a). This segregation between a coarse, northern river-half and a fine, southern river-half is present over some 10 km independent of the presence of inner and outer bends (Ten Brinke & Wilbers, 1999). In Section 2, the bed material of Subsection 2B is much coarser than of Subsections 2A and 2C.

The average water depth of the Bovenrijn – Waal reach during yearly average discharge is about 5 m. The width of the river branches in between the groynes (the wetted cross-section at yearly average discharge) is about 340 m for the Bovenrijn (Sections 1 and 2A) and about 260 m for the Waal (Sections 2C and 3). The bed gradient in all sections is in the order of 1.1×10^{-4} .

4.2 Methods and analyses

4.2.1 Collecting dune data

Between 1980 and 2000, a large number of dune measurements using echo-sounder equipment was carried out in the Dutch Rhine branches, during several campaigns (Table 4.1). During 1982 - 1997, all echosoundings of dunes in the Dutch Rhine were made with a digital reading, single-beam echosounder (Atlas Deso 10 until 1985, Atlas Deso 20 from 1985 until 1989 and Atlas Deso 25 from 1989 onwards). These echosoundings consisted of several tracks parallel to the banks, which were regularly distributed over the entire wetted cross-section in between the groynes, generally about 50 m apart.

Since 1997, echo-soundings of dunes are made, when possible, by means of multibeam echosounders (Simrad, Seabat 8101 or Seabat 9001). These multibeam echosounders consist of several sensors within one system underneath the centre point of the vessel that scan the bed topography in a line perpendicular to the boat's track. With a multibeam echosounder a certain width of the bed is scanned in one sweep, being a few to several times the water depth, depending on the number of sensors. The Simrad echosounder for example, consists of 128 sensors. Each sensor transmits a 95kHz signal with a beam width of 1.5° . The beam width of all sensors combined is 150° . This way the river bed is

scanned over a width of five times the water depth. The Seabat 8101 has 100 sensors, being able to scan the bed over a width of six times the water depth. The Seabat 9001 has 60 sensors, resulting in a scanned width of twice the water depth. Several boat tracks parallel to the banks have to be sounded in order to completely cover the whole bed of the river with a consistent density of points. An overlap of 10-50 % between two parallel tracks is preferred. All three multibeam systems include automatic correction for the movements of the vessel (pitch, roll, heath, heading) and the influence of salinity and temperature on sound velocity.

During both single-beam and multibeam echosounder surveys a two-dimensional horizontal positioning system (before 1993: Artemis, Polarfix and Polartrack successively; since 1993: differential global positioning system (DGPS)) is used and the measurement ship follows preset survey tracks. Deviations from these preset tracks are computed and presented directly to the helmsman of the ship to enable him to correct the course immediately. The actual position, together with the related water depth, is stored and later processed on a computer.

Table 4.1. A list of campaigns on measuring dune properties and bedload transport (dune tracking) carried out in the Dutch Rhine (Bovenrijn - Waal reach) between 1982 and 2002, together with the discharge ranges during the campaigns.

* Lat., average distance between points in a lateral direction, Long., average distance between points in a longitudinal direction. (SB), Single-beam echosounder, (MB), Multibeam echosounder.

Location	Period	Discharge range at Lobith (m^3s^{-1})	Equipment	Resolution Lat. & long.*
Bovenrijn (Section 1)	Jan - Feb 1982	3000 - 8000	Atlas Deso 10 (SB)	Unknown
	Mar - Apr 1988	4200 - 10 000	Atlas Deso 20 (SB)	Unknown
	Jan 1994	3600 - 5400	Atlas Deso 25 (SB)	50 and 0.6
	Dec 1994 - Apr 1995	2500 - 11 900	Atlas Deso 25 (SB)	50 and 0.6
Pannerdensche Kop (Section 2)	Feb - Mar 1997	2700 - 6900	Atlas Deso 25 (SB)	10 and 0.6
	Oct - Nov 1998	4100 - 9500	Atlas Deso 25 (SB)	10 and 0.6
			Seabat 8101 (MB)	0.1 and 0.3
			Seabat 9001 (MB)	0.2 and 0.4
Waal (Section 3)	Jan 1989 - Mar 1990	1000 - 2900	Atlas Deso 25 (SB)	50 and 0.8
	Mar 1992	2800 - 3700	Atlas Deso 25 (SB)	50 and 0.8
	Jan 1994	3400 - 4100	Atlas Deso 25 (SB)	50 and 0.6
	Jan - Feb 1995	4300 - 11 000	Atlas Deso 25 (SB)	50 and 0.6
	Feb - Mar 1997	2100 - 6900	Atlas Deso 25 (SB)	10 and 0.6
			Simrad (MB)	0.4 and 0.4
	Nov 1998	3200 - 9400	Seabat 8101 (MB)	0.1 and 0.3
	Mar 1998 - Dec 1999	1400 - 9100	Seabat 8101 (MB)	0.1 and 0.3

In 1982, 1988, 1995, 1997 and 1998 measurements were done during floods (Table 4.1). In most cases these measurements were done once a day, and the data spanned the entire flood wave, starting at the beginning of the rising limb of the discharge curve and ending at the end of the falling limb. In 1982, 1988 and 1995 these measurements were done in Section 1 (fig. 4.1B) and, in 1997 and 1998 they were done in Sections 2 and 3. The measurements during the flood of 1998 in Section 2 were made twice a day, which improved the calculation of bedload transport rate.

Between January 1989 and March 1990 and between March 1998 and December 1999 measurements were done during low to moderate discharges (Table 4.1). These echo-

soundings were made of 1-2 km long reaches within Section 3 (fig. 4.1B). The echo soundings of 1989 and 1990 were done every month on three consecutive days for the purpose of calculating the bedload transport. The echo soundings of 1998 and 1999 were done once a month for determining dune dimensions. Surveys in Table 4.1 that have not mentioned yet, refer to occasional measurements that provided additional information on dune dimensions.

4.2.2 Detailed data sets during floods

In this study, when possible, all available data (Table 4.1) have been used for the calculation of dune characteristics and bedload transport. Special attention, however, has been given to the measurements done during the floods of 1995, 1997 and 1998. These three floods were different from one another in duration and peak discharge (fig. 4.3) but for all three flood events the datasets obtained covered the entire wetted cross-section in between the groynes at regular time intervals such that the growth, decay and migration of individual dunes could be traced throughout the flood wave in great detail.

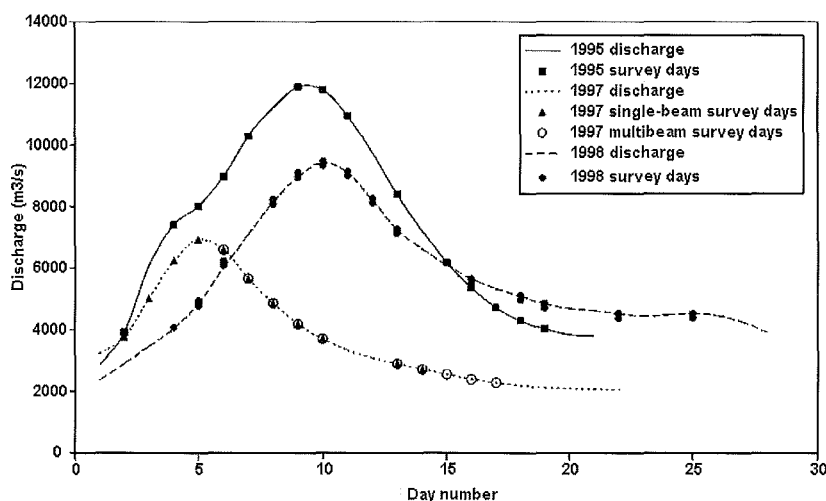


Figure 4.3. Flow discharges of the floods of 1995, 1997 and 1998 at Lobith, and the days within the flood waves for which data on dunes are available.

During the flood of 1995, echosoundings were made of a 3 km long reach of the Bovenrijn near the Dutch-German border, upstream of the first river bifurcation in the Dutch Rhine system (Section 1, fig. 4.1B). The sounded single-beam tracks were 50 m apart and were mostly measured once a day.

The data from the flood of 1997 that were measured over a 1km reach halfway down the Waal were used for Section 3 (fig. 4.1B). This reach was sounded once a day along tracks parallel to the banks with two different types of echosounders. A single-beam echosounder was used between 27 February and 11 March and a multibeam echosounder was used between 3 and 14 March

The data from the flood of 1998 were used for Section 2, the bifurcation called “Pannerdensche Kop”, where the Bovenrijn bifurcates into the Waal and the Pannerdensch Kanaal (fig. 4.1B and C). Echosoundings were made of connecting 1km subsections in each of the three branches. In the Pannerdensch Kanaal (Subsection 2B) a single-beam echosounder (Atlas Deso 25) was used. Twice a day, 10 tracks spaced 10 meters apart and parallel to the banks were measured. The Bovenrijn (Subsection 2A) and Waal (Subsection 2C) were measured twice a day with three different echosounders. Mostly, the Seabat 8101 or the Seabat 9001 multibeam systems were used depending on which survey vessel was available. For a few days no multibeam system was available and a single-beam echosounder (Atlas Deso 25) was used instead.

4.2.3 Hydrodynamics

During all measurement campaigns, not only the echosoundings were made but the local water depths and discharges from nearby stations were also collected. In 1998, in Section 2, some measurements were also done of flow velocities using ADCP current profilers (Julien *et al.*, 2002). In addition to these hydrodynamic measurements, flow velocity discharge and shear stress discharge relations (both bed shear stress and grain-related shear stress) were used, based on calculations with a one-dimensional flow model (SOBEK) for the Dutch Rhine system (Van der Veen, 2002), which is calibrated to reproduce stage levels at various stations along the Rhine branches. These relations were created for each of the three sections in fig. 4.1B, and were then used to calculate the flow velocities and shear stresses related to the echo-sounding measurements done at different discharges. For the calculation of the grain-related shear stress a constant grain size was used in the different sections, as no information was available on the changes in grain size distribution of the bed during a flood.

4.2.4 Calculation of dune properties

Using a computer program called DT2D (Dune Tracking in two Dimensions) the dune characteristics were calculated from all the available measurements except for the data from the floods of 1982 and 1988. In DT2D a dune is defined as any shape in a (non-filtered) bed profile between two (local) minima in bed elevation (troughs). However, a dune needs to be measured, at least, at 10 positions in order to be able to accurately calculate the dune characteristics (Wilbers, 1997; Chapter 3). Thus, the density of measurement points determines the lower bound of dune length that can be determined with DT2D: 3-6 m in the datasets used here (Table 4.1). In DT2D dune length is defined as the length of a line connecting the two troughs (in three dimensions), and dune height is the length of the line perpendicular to the line connecting the troughs up to the dune crest (fig. 4.4). After calculation, the characteristics of all the separate dunes in every profile from a measurement are averaged for an entire study area. Because this averaging assumes homogeneity of all dunes in an area, some of the profiles near the heads of the groynes (the outer profiles) were not used. A visual inspection of these outer profiles

showed that no dunes were present there. The calculated characteristics of the various measurement campaigns are listed in Appendix A.

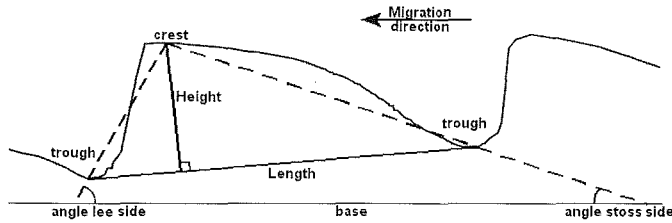


Figure 4.4. Typical dune shape defining the characteristics as calculated with DT2D.

The data from the floods of 1982 and 1988 were copied from the reports of Van Urk (1982) and Wijbenga (1991) respectively. They both calculated length and height by a different method. This means that the absolute values of the length and height do not always compare well with the absolute values calculated with DT2D from other surveys. However, the trends describing the changing dune characteristics in response to discharge should be comparable for the different methods.

4.2.5 Dune propagation and bedload transport

The propagation of dunes can be used to quantify bedload sediment transport (Engel & Lau, 1980; Ten Brinke *et al.*, 1999a) with:

$$q_s = \beta c H \quad (4.1)$$

where H = dune height (dune crest - dune trough) (m); c = dune migration rate (ms^{-1}); β = bedload discharge coefficient (-).

The coefficient β combines corrections for the dune shape, flow separation, and effects such as suspended particles settling in the dune troughs, being suspended at the dune front, or jumping from crest to crest and therefore not taking part in the bedload calculated from the migration of the dunes. This coefficient has to be determined by comparing the calculated bedload transport rate (Eq. 4.1) with the bedload transport rate quantified from measurements with bedload samplers. In the 1980s, pending further information, bedload was calculated with a β coefficient of 0.5. This means that bedload was schematised as the displacement of triangular dunes and other effects, such as the exchange between suspended and bedload, were neglected. In the literature, other values for β are presented, determined from flume experiments, field conditions and combinations of both. From a comparison of these data, Ten Brinke *et al.* (1999a) concluded that, at present, a bedload discharge coefficient β for the Dutch Rhine distributaries of 0.55 is most likely. This value was used for all the dune track calculations on the measurements available for this study. As with the dune characteristics the bedload transport rates were calculated for every profile in a measurement and thereafter combined to determine the integrated bedload transport rate over the full width of a section.

The calculation of the migration rate of dunes is based on the comparison of echo-sounded bed profiles of a set of dunes at times T_1 and T_2 . The time interval between successive echosoundings has to be small enough for the same dunes to be recognizable from T_1 to T_2 . For the relatively large dunes in the Dutch Rhine, echosoundings that were made on a day-to-day basis generally satisfied this condition (fig. 4.5). The migration rate of the dunes follows from the dune migration distance between the echo-sounded profiles T_1 and T_2 , calculated by cross-correlation (Ten Brinke *et al.*, 1999a). The match between certain profiles at times T_1 and T_2 , for which the maximum cross-correlation is calculated, is the dune migration distance from T_1 to T_2 . The dune migration rate is this distance divided by ΔT ($\Delta T = T_1 - T_2$).

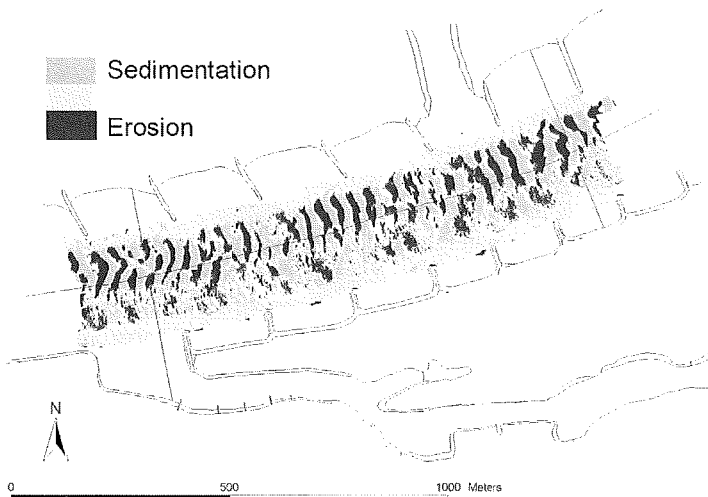


Figure 4.5. The difference between two successive multibeam echosoundings (time step is 24h) in the Waal (Section 3), showing erosion on the stoss sides and deposition on the lee-sides. The flow is from right to left.

4.3 Results

4.3.1 Dune patterns: spatial variation

The echo-sounding measurements during the floods covered the entire width of the river between the groynes. Therefore, the growth and decay, plan form and spatial variation of the dunes are illustrated with four bed elevation maps for each of the three Sections (Plates. 4.1 - 4.3). The four maps each show the bed at a specific time during a flood wave; (A) at the beginning of the flood; (B) at peak discharge; (C) at maximum dune height; and (D) just after the flood. These maps were all made by resampling or interpolating the measurement points to a 1x1 m grid. Below every map made of the time at which the dune height was maximal, three longitudinal profiles are shown; near the north bank (I); the river axes (II); and near the south bank (III).

In Section 1 (Plate 4.1), at the beginning of the flood of 1995 (26 January 1995, map A), the entire bed of the Bovenrijn was covered by small dunes. These dunes probably had sinuous fronts. In Plate 4.1A, however, the dune fronts appear straight because the map was interpolated from single beam tracks that were 50 m apart. During rising and peak discharge (31 January 1995, map B), the bed was covered with large dunes with almost straight fronts over the entire width of the river. A few days after the peak discharge (4 February 1995, map C) the dunes were at their maximum height, and these heights were the same for the deep and shallow parts of the river (profiles I-III in map C). During the falling discharges (10 February 1995, map D), the dunes increased in length but decreased in height. These dunes had a very irregular plan form and (although not visible in this map) were completely covered with small secondary dunes.

In Section 2 (Plate 4.2), at the beginning of the flood of 1998 (30 October 1998, map A), the entire bed of the Bovenrijn (Subsection 2A) near the bifurcation was covered by dunes. Although hardly visible in map A, these dunes had a sinuous plan form. The bed of the Waal (Subsection 2C) and Pannerdensche Kanaal (Subsection 2B) was almost completely flat. During rising and peak discharge (4 November 1998, map B), the bed in all branches was covered with large dunes with straight or slightly sinuous fronts over the entire width of the river. A few days after the peak discharge (6 November 1998, map C) the dunes were at their maximum height and these heights were the same for the deep and shallow parts of the river (profiles I-III in map C). During the falling discharges (16 November 1998, map D), the dunes in all three branches increased in length but decreased in height. These dunes had a very irregular plan form and, although hardly visible in this map, were completely covered with small secondary dunes (fig. 4.6).

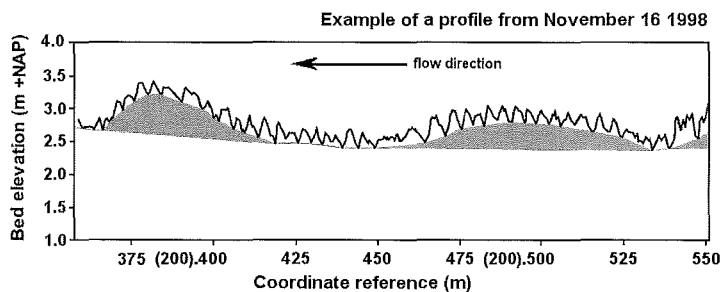


Figure 4.6. Small part of a bed profile from Subsection 2C (fig. 4.1C) on 16 February 1998 showing large dunes (grey) which are superimposed by small dunes on the stoss and lee-sides.

In Section 3, the entire bed of the Waal was covered by dunes during all stages of the flood of 1997 (Plate 4.3). The average length and height of these dunes hardly changed during the flood. There were large dunes in the northern part of the river and much smaller dunes in the southern part (profiles I-III in map C). Both large and small dunes had a more three dimensional plan form, which changed drastically as the dunes migrated downstream (see the shape of the dune near the arrow in all four maps). The large undulating forms that are visible in Profile III below map C are not dunes. These forms do not migrate downstream and are closely related to the location of groynes. The large depressions in Profile III refer to scour holes behind the heads of the groynes clearly visible on map C.

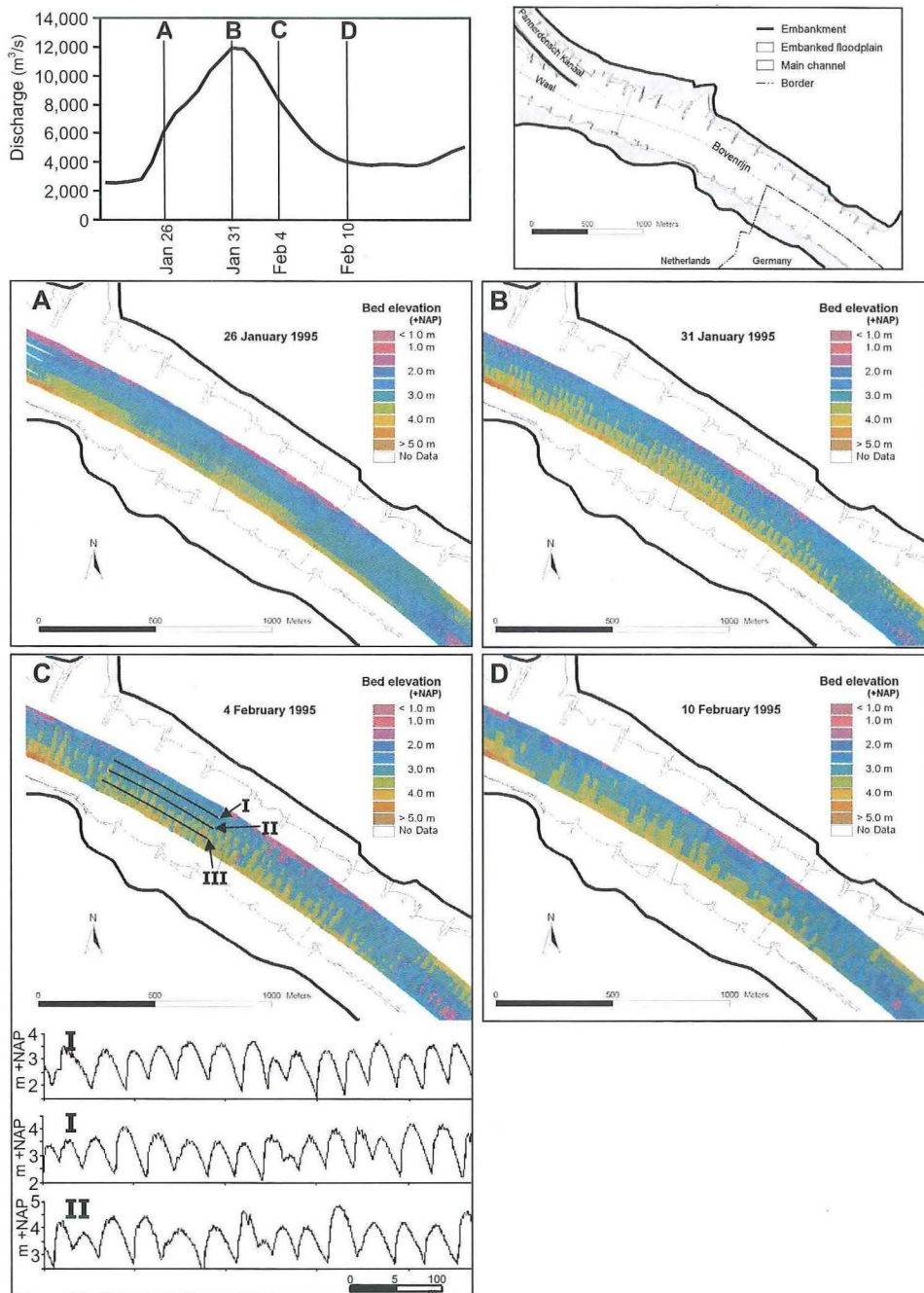


Plate 4.1. Maps showing the spatial development of dunes in Section 1 during the flood of 1995. (A – D) bed elevation at the beginning of the flood, at peak discharge, at maximum dune height and at the end of the flood respectively. Below map C, three profiles are plotted to show the differences in dune shape over the width of the river. m+NAP refers to an elevation in meters above the Dutch ordnance datum.

4.3.2 Dune growth and decay

The dune characteristics over the full width of the sections were averaged for each survey moment in order to investigate the growth and decay of dunes in time in more detail (all these averages are listed in Appendix A of this thesis). The characteristics were related to the discharge in phase diagrams. For these diagrams, all available measurements were used. This allows for comparisons between the three sections of the growth and decay of the dunes (figs. 4.7 and 4.8), the migration rates (fig. 4.9) and the bedload transport rates (fig. 4.10) calculated with dune height and migration rate.

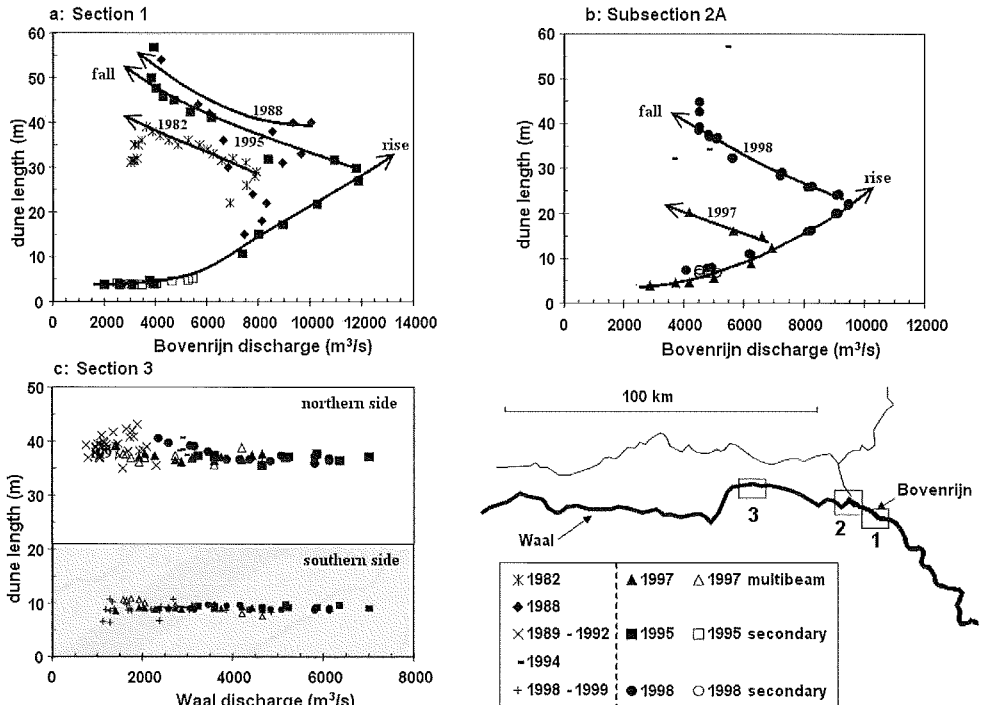


Figure 4.7. Phase diagrams of changing dune length in all three sections using all available data from Table 4.1. Filled and open triangles distinguish between single and multibeam measurements respectively. Filled and open squares and dots, respectively, distinguish between primary and secondary dunes in Sections 1 and 2A. The arrows going to the right indicate the average development during rising discharge, whereas arrows going to the left indicate the development during falling discharge for specific floods. For Section 3, the dune length of both the large dunes in the northern half and the small dunes in the southern half is shown.

4.3.2.1 Dune length

During low to moderate discharges, the dunes in Section 1 and Subsection 2A were relatively short (fig. 4.7A and B). As the discharge increased during a flood, the length of

the dunes increased greatly. The length of the dunes even increased further during the falling discharges until long after the maximum discharge. During the final stages of a flood, secondary dunes appeared on the elongated primary ones with lengths comparable to the dunes present during the low to moderate discharges at the beginning of the flood. In Section 3 (fig. 4.7C), two types of dunes were always present, long dunes in the northern part and shorter dunes in the south. Both types of dunes did not change in average length in response to discharge.

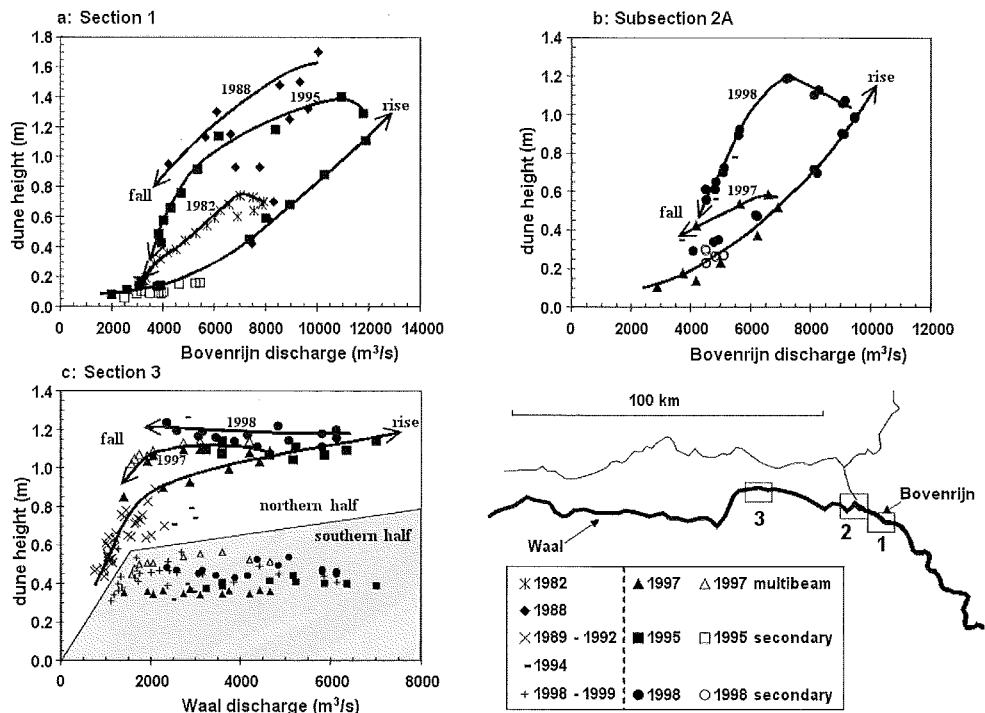


Figure 4.8. Phase diagrams of changing dune height in all three sections using all available data from Table 4.1. Filled and open triangles distinguish between single and multibeam measurements respectively. Filled and open squares and dots, respectively, distinguish between primary and secondary dunes in Sections 1 and 2A. The arrows going to the right indicate the average development during rising discharge, whereas arrows going to the left indicate the development during falling discharge for specific floods. For Section 3, the dune height of both the large dunes in the northern half and the small dunes in the southern half is shown.

4.3.2.2 Dune height

During low to moderate discharges, the height of the dunes in Section 1 and Subsection 2A was small (fig. 4.8a and b). In Section 3 (fig. 4.8c), at low discharge, the dunes in the northern part were lower than during high discharges but they were still much higher than the dunes in the southern part. As the discharge increased during a flood, the height of the dunes in all sections increased greatly. In Sections 3, however, the rate of height increase

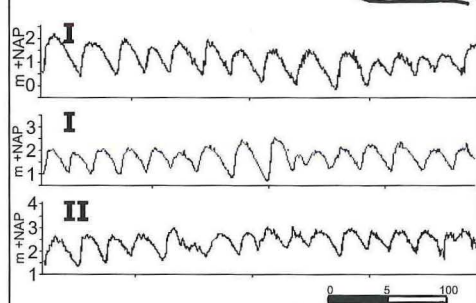
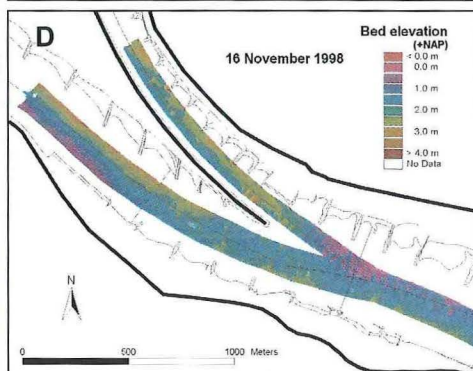
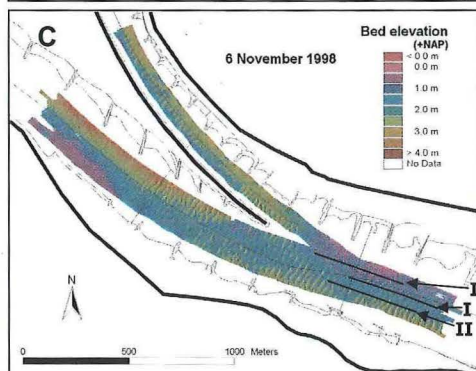
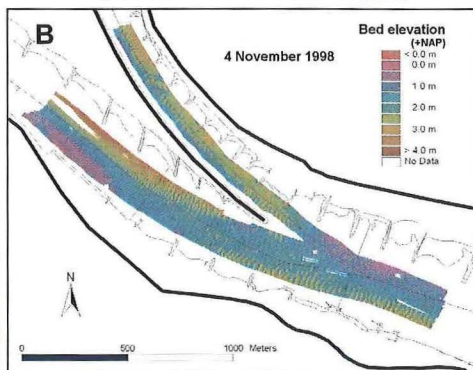
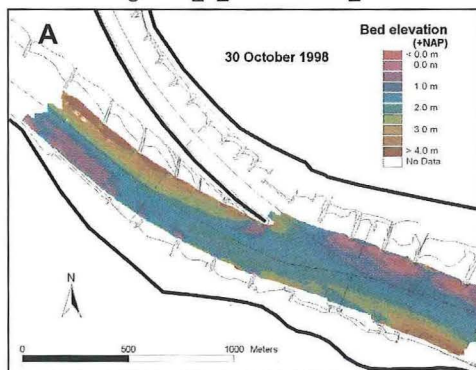
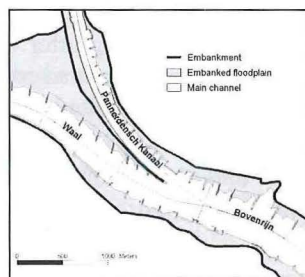
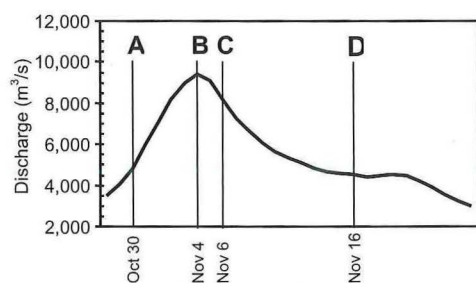


Plate 4.2. Maps showing the spatial development of dunes in Section 2 during the flood of 1998. (A – D) bed elevation at the beginning of the flood, at peak discharge, at maximum dune height and at the end of the flood respectively. Below map C, three profiles are plotted to show the differences in dune shape over the width of the Bovenrijn. m+NAP refers to an elevation in meters above the Dutch ordnance datum.

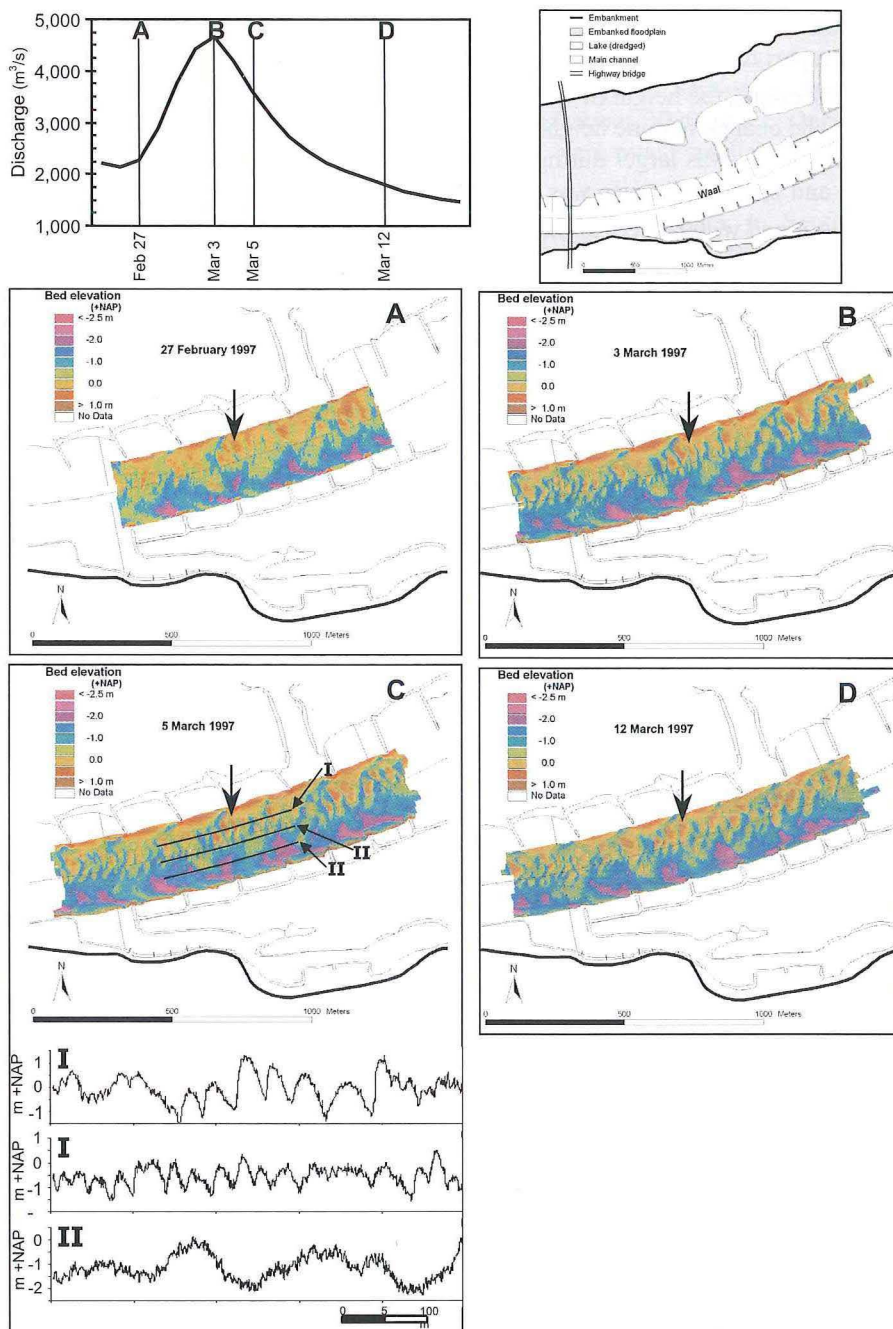


Plate 4.3. Maps showing the spatial development of dunes in Section 3 during the flood of 1997. (A –D) bed elevation at the beginning of the flood, at peak discharge, at maximum dune height and at the end of the flood respectively. Below map C, three profiles are plotted to show the differences in dune shape over the width of the river. The large arrow follows one dune during the flood to show the changes in plan form. m+NAP refers to an elevation in meters above the Dutch ordnance datum.

became slower above a local discharge of about $2000 \text{ m}^3 \text{ s}^{-1}$. The height of the dunes in the southern part of Section 3 did not change at all in response to discharge changes.

In all three sections, the height of the dunes increased until a few days after the maximum discharge. The change in dune height lagged the change in discharge creating a hysteresis effect. Dune height was larger during falling discharges than during rising discharges. In Sections 1 and 2, this difference was much larger than in the northern part of Section 3.

As was mentioned with respect to dune length, in Section 1 and Subsection 2A, at the end of a flood, secondary dunes appeared on the high primary ones. These secondary dunes had heights comparable to the heights of the dunes during the low to moderate discharges at the beginning of the flood.

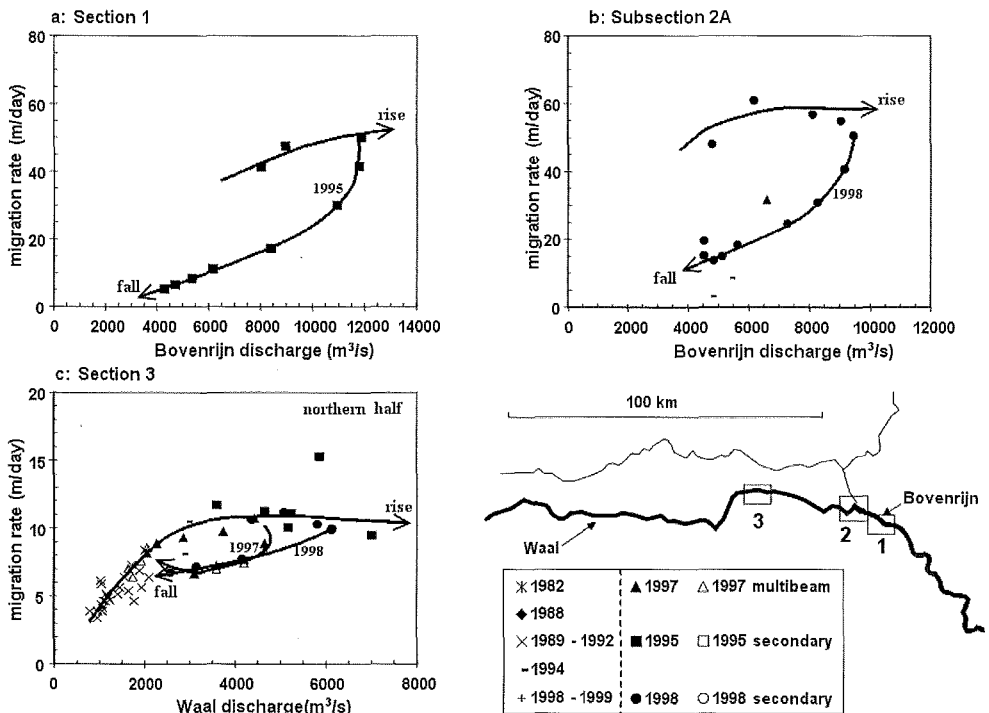


Figure 4.9. Phase diagrams of changing migration rate in all three sections using all available data from Table 4.1. Filled and open triangles distinguish between single and multibeam measurements respectively. Filled and open squares and dots, respectively, distinguish between primary and secondary dunes in Sections 1 and 2A. The arrows going to the right indicate the average development during rising discharge, whereas arrows going to the left indicate the development during falling discharge for specific floods. For Section 3, migration rates were only calculated for the large dunes from the northern half of the river.

4.3.2.3 Dune migration rate

During low to moderate discharges, no migration rates^t could be determined for the dunes in Section 1 and Subsection 2A (fig. 4.9A and B) because the dunes that were present were small and probably migrated much too fast between two consecutive measurements.

In Section 3 (fig. 4.9C), the migration rates were smaller during low to moderate discharges than during high discharges. During the rising discharges of a flood, the migration rates showed an increase in all three sections. In Section 3, however, the migration rate stabilized above a local discharge of about $3000 \text{ m}^3 \text{ s}^{-1}$. During falling discharge, the migration rates decreased greatly and were much smaller (in all sections) than during rising discharge.

No migration rates could be calculated for the secondary dunes in Section 1 and Subsection 2A or for the dunes in the southern part of Section 3. These dunes were all small and probably migrated so fast between two measurements that individual dunes could not be identified between consecutive measurements. In addition, as the calculation of the migration rate depends on the cross-correlation technique, the average migration calculated in case of superposition represents only the migration of the largest forms and not the superimposed forms (Wilbers & Kleinans, 1998).

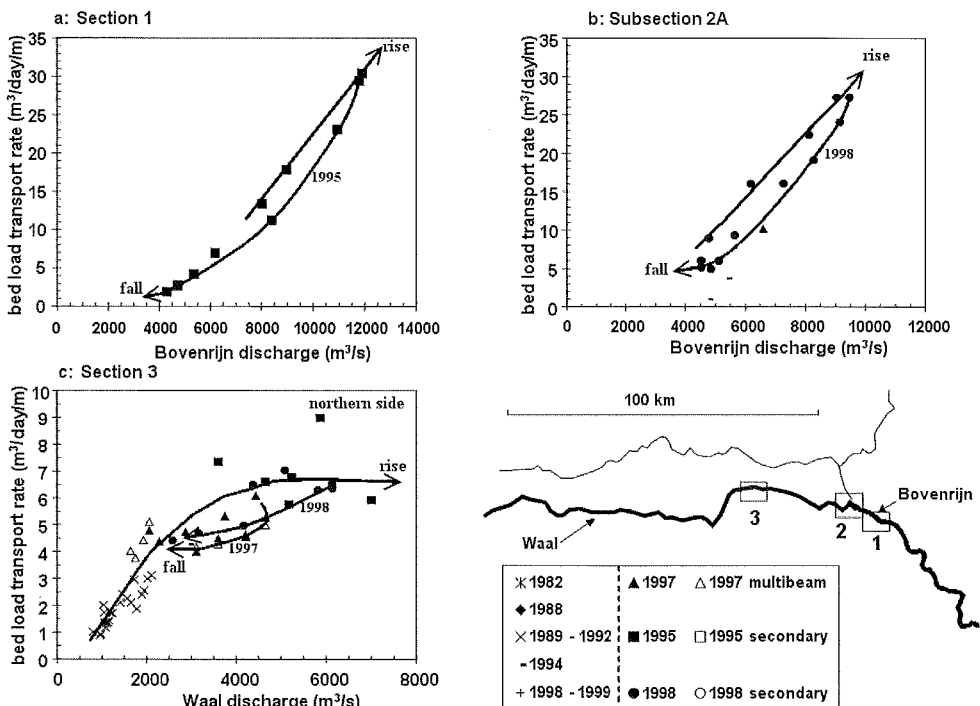


Figure 4.10. Phase diagrams of changing bedload transport rate in all three sections using all available data from Table 4.1. Filled and open triangles distinguish between single and multibeam measurements respectively. Filled and open squares and dots, respectively, distinguish between primary and secondary dunes in Sections 1 and 2A. The arrows going to the right indicate the average development during rising discharge, whereas arrows going to the left indicate the development during falling discharge for specific floods. For Section 3, bedload transport rates were only calculated for the large dunes from the northern half of the river.

4.3.3 Hysteresis in sediment transport

The measurements, from which both dune height and migration rate were determined were used to calculate bedload transport rates using dune tracking (Eq. 4.1). In Section 3 (fig. 4.10C), bedload transport rate could only be calculated for the northern part of the river because no migration rate could be calculated for the small dunes in the southern part. During low to moderate discharges, these rates were much lower than during high discharges. In Section 1 and Subsection 2A, no bedload transport rate could be calculated during low to moderate discharges because the migration rates were unknown.

During the rising stage of a flood, the bedload transport rate increased sharply in all three sections. However, in the northern part of Section 3, the bedload transport rate stabilized above a local discharge of about $4000 \text{ m}^3 \text{ s}^{-1}$. During falling stages, the bedload transport rate decreased sharply in all three sections and was somewhat smaller than during the same discharges on the rising limb of the flood wave. In Section 1 and Subsection 2A (fig. 4.10A and B), the bedload transport rate decreased to almost zero, whereas in Section 3, the transport fell back to the level reached at $2000 \text{ m}^3 \text{ s}^{-1}$ during the rising discharge. No bedload transport rate could be calculated for the secondary dunes in Section 1 and Subsection 2A, which appeared at the end of a flood because it was not possible to calculate the dune migration rate.

During the flood of 1998, the bedload transport rate in Subsection 2C unexpectedly still increased during the falling limb of the discharge. This deviant behaviour is not considered here, as it was treated in detail by Kleinhans (2002a).

4.4 Discussion

The results presented in this paper mainly focus on dunes during three flood waves. These flood waves were very different in their duration and peak discharge. In addition, the results on observed dunes during these flood waves refer to three different sections in the Bovenrijn and Waal reaches of the Dutch Rhine. For each section, a different flood wave was studied in detail. This may complicate the comparison of the dune patterns, dune growth and decay, and bedload transport hystereses for these sections as differences may result from different conditions in river plan form, grain size or energy conditions of the driving hydrodynamic force. However, looking carefully at the hydrodynamics during the floods in combination with the growth and decay of dunes, sufficient information can be obtained on the impact of local conditions vs. variations in flood characteristics. Furthermore, additional information on dunes is available for Section 2 from the 1997 flood (Ten Brinke *et al.*, 1999a; Kleinhans & Ten Brinke, 2001; Kleinhans, 2002a) and for Section 3 from the 1998 flood (Wilbers, 1999).

4.4.1 Dune patterns

Sections 1 and Subsection 2A both refer to the same reach of the Dutch Rhine river system and are only a few kilometres apart. The geometry of the channel and floodplain,

and the grain-size composition of the bed in both sections are comparable. The results for Section 1 refer to the large flood of 1995 while the results for Sub-section 2A refer to the flood of 1998, with additional information on the 1997 flood based on Ten Brinke *et al.* (1999a), Kleinhans & Ten Brinke (2001) and Kleinhans (2002a). Section 3 is located further downstream and is characterized by a much finer bed grain-size. The results for this section refer to the flood of 1997, with additional information on the 1998 flood based on Wilbers (1999).

Sections 1 and 2 (Plates 4.1 and 4.2) showed similar dune patterns during the different stages of a flood wave. At the beginning and directly after the flood wave, the bed was almost flat, whereas large dunes developed during the rising limb and over the peak discharge with the dunes being most pronounced a few days after peak discharge. Dune growth and decay responded quite rapidly to changes in hydrodynamics. In addition, dune patterns were regular with more or less straight fronts perpendicular to the river banks. There was no remarkable variation in dune height and length across the river. The results in Section 3 were very different. Dunes were already present at the beginning of the flood, and the bed did not flatten after the flood wave. Besides, dune size varied greatly across the river.

The combined dune results published here and in previous publications for Subsection 2A and Section 3 refer to the same floods. However, although the different floods in Section 1 and Subsection 2A result in similar dune growth, decay, shape and spatial variation patterns, the floods of 1997 and 1998 result in very different dune properties in Subsection 2A and Section 3. From this observation, it may be concluded that it is not the differences between the three floods but the differences in the conditions between Section 1, Subsection 2A and Section 3 that largely determine the observed differences in dune properties over time.

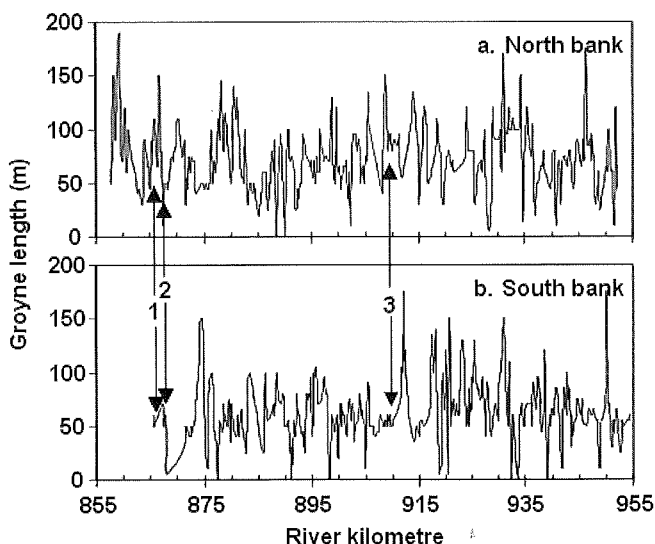


Figure 4.11. The variation of the length of protrusion of the groynes on both sides of the river.

4.4.1.1 The impact of groynes

The presence of groynes leaves its marks upon the morphology of the river bed. Turbulence behind the groyne heads causes scour holes that protrude and fade towards the river axis in downstream direction. This phenomenon is most apparent in Section 3, where this erosion shows as 'flames' on the coloured depth maps (Plate 4.3). In between these flames the river bed is slightly higher due to the increase of the wetted cross-section in between the groynes. The river bed, therefore, shows an undulation with a wave length equal to the spacing of the groynes, which, along the Bovenrijn – Waal, is generally 200 m. These undulations are fixed and do not interact with the superimposed moving bed forms (Wilbers, 1999). The length of protrusion of the groynes into the river does also not vary systematically along the river (fig. 4.11). It is therefore unlikely that differences between the sizes of groynes or groyne fields have influenced the observed differences in the behaviour of the dunes between the sections.

4.4.1.2 Grain size effects

The process of dune growth and decay will depend on the ratio between the strength of the river currents and the grain size of the bed. At a certain stage bed forms are formed more easily when the sediment of the bed is finer grained. Thus, the comparison of sections with different grain size of the bed during the same floods may show dunes to be more pronounced in the finer grained sections than in the coarse-grained ones. This seems to apply to Section 3 when compared with Section 1 and Subsection 2A. In the finer grained Section 3, dunes are always present, whereas in Sections 1 and 2, they only occur during a major flood. In the coarse-grained sections, dune growth during a flood wave may be further retarded due to armouring of the top layer of the bed. The energy conditions first have to reach the threshold for breaking-up the armour layer before bedload transport may be increased and dunes may grow.

When the bed does not become fully mobile, because part of the bed material is too coarse grained relative to the strength of the flow, dune growth is determined by the availability of finer grained sediment on top of the inactive sediments. The movement of small dunes of fine sand as individual dunes on top of an armour layer is common for the German Niederrhein, upstream of Section 1 (Carling *et al.*, 2000). The presence of small dunes at low flows in Section 1 and Subsection 2A also points to this process.

The aspect of the influence of the availability of fine-grained sediments on dune growth may explain the difference of dune properties between the northern and the southern part of the river at Section 3. In this section large dunes are present and moving actively in the shallow, northern part, whereas much smaller dunes occur in the deeper, southern part. Normally the shallow parts, being the inner bends in a meandering river, have finer grained sediments than the outer bends. Hence, the presence of large, moving dunes in this slightly-curved inner bend on the north side of Section 3 makes sense. The deeper part on the south side should be coarser grained and may even be armoured. The presence of small moving dunes in this part is probably due to a shallow fine-grained sand layer on top of sediments that are too coarse to allow dunes to be formed. Thus, the growth of

these small dunes into larger ones is hindered by the restricted availability of these fine-grained sediments.

This theory agrees very well with the morphodynamic behaviour of sandy beaches in between the groynes along the river. Research has shown that these beaches deliver fine-grained sand to the channel (river bed) due to erosion by draw down currents induced by the passage of large vessels (Ten Brinke *et al.*, 1999b). Shipping density in this reach is among the highest of all the waterways in the world. The erosion of the beaches is a continuous process that results in the transport of fine-grained sand to the river bed during most of the year (low – average discharge). This loss of sediment is compensated during large floods when deposition of sand on these beaches takes place. This process significantly influences sediment transport in the river because it results in the sediment of the top layer of the bed being relative fine-grained in those parts of the river bed where the erosion of the beach during low – average discharge is strongest (Ten Brinke *et al.*, 1998). This is typically the southern half of the river bed, due to the way shipping is arranged on this river. This shipping is mainly characterized by heavily loaded vessels sailing from Rotterdam harbour to Germany, and vessels with little or no cargo returning to Rotterdam. The vessels sailing to Germany generally follow the south bank, and the vessels going back to Rotterdam follow the north bank. The currents induced by shipping are much stronger for upstream-moving, heavily loaded vessels than for downstream-moving ones (Bhowmik *et al.*, 1995). Thus, the impact of navigation traffic on erosion of the groyne field beaches is strongest in the southern part of the river and results in these beaches being a source of relatively fine-grained sediment for the main channel during most of the time (Ten Brinke *et al.*, 1999b).

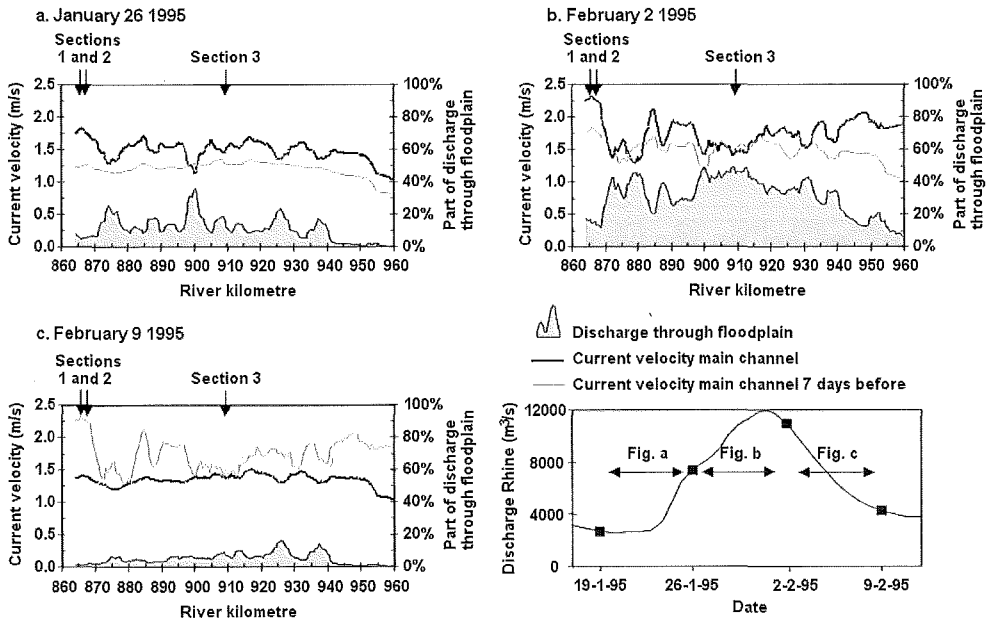


Figure 4.12. The variability in discharge through the floodplain and the flow velocity in the main channel of the Bovenrijn – Waal during the flood of 1995 calculated with SOBEK.

4.4.1.3 Floodplain effects

A second important difference between Sections 1 and 2 and Section 3 is the way the discharge is distributed over the wetted cross-section of main channel and floodplain during floods, and the effect of this distribution on the hydrodynamic force in the main channel at different discharges. This aspect is particularly relevant in The Netherlands since Dutch rivers are embanked. A typical cross-section of a Dutch river landscape consists of a main channel, levees on both banks, and the floodplain between the levees and the main dikes. At low to moderate discharge, the floodplain is drained and in use as meadows and nature reserves. During a flood, the floodplain is submerged and, gradually, more discharge is diverted through the floodplain. The area of floodplain and the height of the levees vary along the river; thus, the part of the discharge that flows through the floodplain varies both in space (along the river) and in time (during the flood). This results in relationships between river discharge and main channel current velocity (and bed, and grain-related shear stress) that differ from one point to another.

For the Bovenrijn – Waal reach this effect was studied with the one-dimensional SOBEK model simulating the 1995 flood. At four instances during the rise and fall of the flood, the part of the discharge that flows through the floodplain was calculated along with the flow velocity in the main channel. The results are shown in fig. 4.12. During peak discharge up to 50% of the discharge flows through the floodplain (fig. 4.12B). This

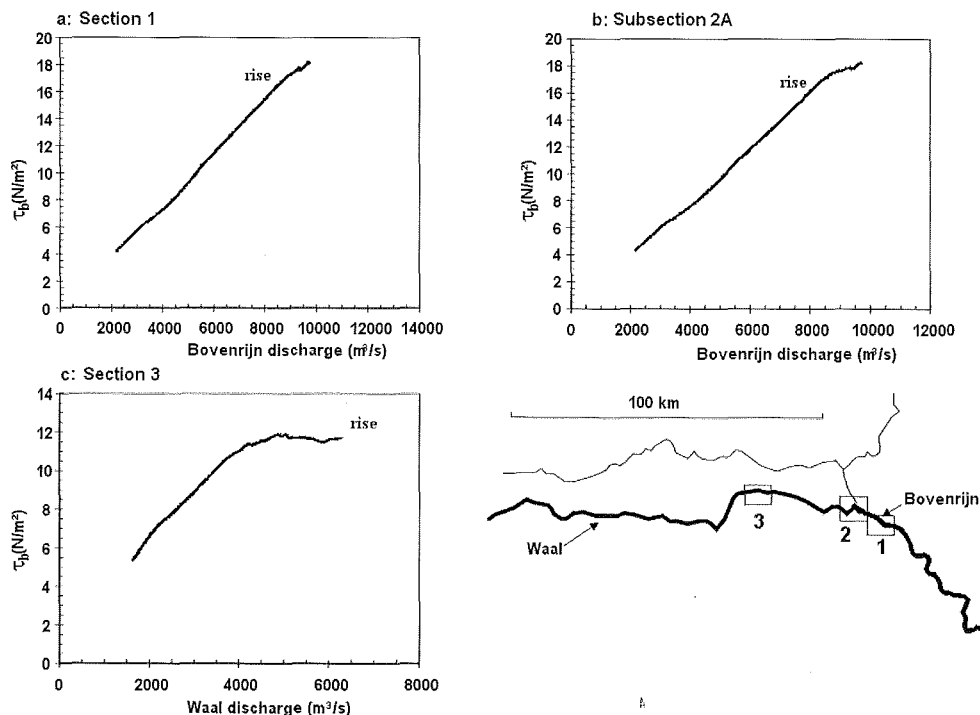


Figure 4.13. The changes in bed shear stress from SOBEK in the three sections during rising discharges.

percentage varies greatly along the river. Floodplain discharge is highest in the middle part of the Bovenrijn – Waal reach, corresponding to Section 3, and smallest in the upstream (near Sections 1 and 2) and downstream parts. The along-stream variation in floodplain discharge is directly reflected in the along-stream variation of main channel flow velocity. During peak discharge (fig. 4.12B), main channel flow velocity is highest in the upstream part (near Sections 1 and 2).

The importance of the floodplain for diverting the river discharge varies during the flood wave such that certain parts of the main channel lose so much water to the floodplain that main channel flow velocity no longer increases during the rising limb of the flood. This is shown clearly in fig. 4.12A-C. In the first part of the rising limb of the flood (fig. 4.12A), most of the river discharge is still accommodated in the main channel, and flow velocity increase is about the same all along the river. In the second part of the rising limb (fig. 4.12B), the floodplain is accommodating more and more water, and the further increase in main channel flow velocity varies greatly along the river, being large near Sections 1 and 2 and negligible near Section 3. During the fall of the flood (fig. 4.12C), the reverse takes place, and main channel flow velocity at Sections 1 and 2 drops again.

This effect of the floodplain flow on the energy conditions in the main channel is expressed in the relationship between bed shear stress of the main channel and river discharge for the Sections 1-3 (fig. 4.13), and the relationship between grain-related shear

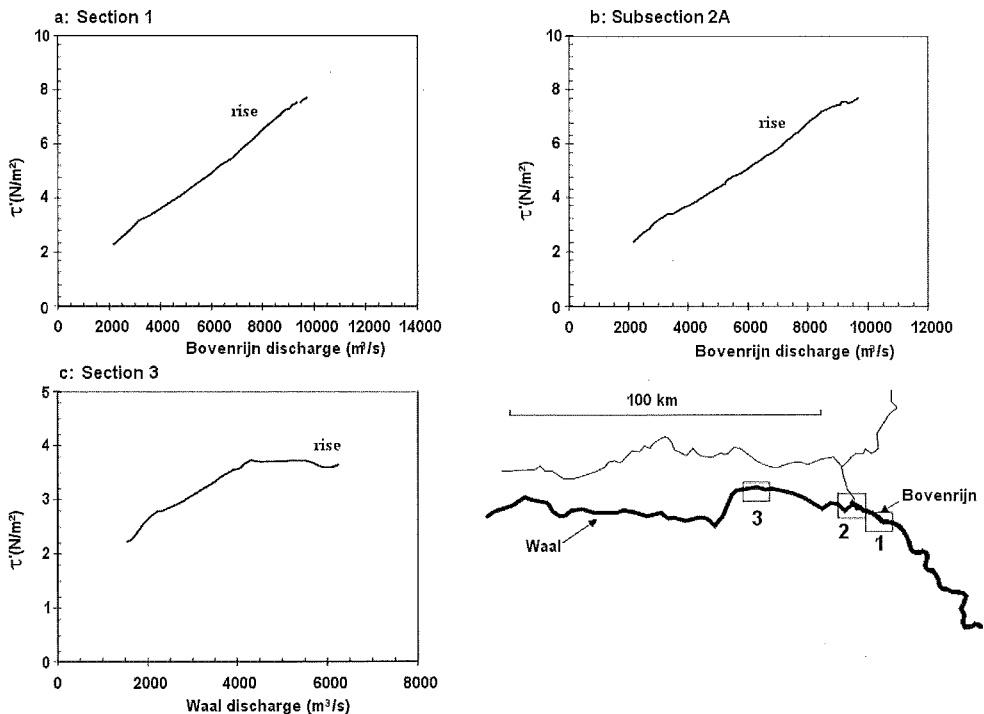


Figure 4.14. The changes in grain-related shear stress from SOBEK in the three sections during rising discharges.

stress of the main channel and river discharge in fig 4.14. In Sections 1 and 2, an increase of river discharge results in a steady increase of bed and of grain-related shear stress. In Section 3, the bed and the grain-related shear stress increases during low to moderate discharges but becomes constant at high discharges.

4.4.2 Dune growth and decay

The results show that there is a clear distinction between the dune growth and decay patterns in Sections 1 and 2 and Section 3. In Sections 1 and 2, the dunes increase greatly in size, whereas in Section 3, the dune size and migration rate show no further increase above a local discharge of $3000\text{--}4000\text{ m}^3\text{s}^{-1}$. In all three sections, dune height vs. discharge shows a counter-clockwise hysteresis pointing at dune height lagging the flood wave. This hysteresis is very clear for Sections 1 and Subsection 2A, and obscured for Section 3. In Sections 1 and Subsection 2A, the dune length also lags the flood wave, but in a somewhat peculiar way: the dune length continues to increase during the falling limb of the flood until the dunes gradually disappear because their heights approach zero. This may be due to material in the top part of the dunes being eroded and then deposited in the troughs. This causes some dunes to aggregate and to form long, very low dunes. In Section 3, the dune length does not change in response to discharge.

At the end of a flood, the flow conditions over the long and low dunes in Sections 1 and Subsection 2A become favourable for smaller, steeper dunes superimposed on the long dunes. The long primary dunes become totally covered with these smaller secondary dunes (fig. 4.6). Once this has happened, the migrating secondary dunes represent all the bedload transport activity and are the only forms that influence the hydraulic roughness (Kleinhans, 2002a; Chapter 7).

4.4.2.1 Relations with shear stress

In the foregoing discussion, it was shown that both grain-size and shear stress variation along the river play an important role in determining along-stream variation in dune characteristics and their variation in time. The observed differences between the dune characteristics of Section 3 with respect to Sections 1 and 2 are very similar to the differences in the shear stress – discharge relations in figs. 4.13 and 4.14. Apparently, the discharge distribution over the main channel and the floodplain greatly influences the bed, and the grain-related shear stress in the main channel, which determines dune behaviour and bedload transport. The difference in grain size is less important but probably determines the energy needed for dune creation and the dune's ability to respond to the changing flows.

The shear stress and grain size differences between the three sections can be combined in the Shields' mobility parameter (dimensionless bed shear stress, θ , or dimensionless grain-related shear stress θ') and related to the development of dune length, height and dimensionless migration rate C^* in all three sections (figs. 4.15 A-D and 4.16 A-D).

$$\theta = \frac{\tau_b}{(\rho_s - \rho)gD_{50}} \quad (4.2)$$

$$\theta' = \frac{\tau'}{(\rho_s - \rho)gD_{50}}$$

Where τ_b = bed shear stress (N m^{-2}); τ' = grain-related shear stress (N m^{-2}); ρ_s = density of sediment (kg m^{-3}); ρ = density of water (kg m^{-3}); g = gravitational acceleration (m s^{-2}); D_{50} = median grain-size (m). The grain related shear stress is defined as:

$$\tau' = \rho g \left(\frac{U}{C'} \right)^2 \quad (4.3)$$

where U = average flow velocity (ms^{-1}); C' = Chezy value related to grain roughness ($\text{ms}^{-0.5}$) which is defined as:

$$C' = 18 \log \left(\frac{12h}{1D_{90}} \right) \quad (4.4)$$

where h = average water depth (m); D_{90} = 90 percentile of the grain-size distribution (m). A grain related roughness height of $1D_{90}$ was chosen over $3D_{90}$ because the bed material in all branches has a significant amount of gravel.

A dimensionless migration rate C^* is defined as:

$$C^* = \frac{cL}{D_{50} \sqrt{\frac{(\rho_s - \rho)}{\rho} g D_{50}}} \quad (4.5)$$

Where L = dune length (m). The dune length was used in the dimensionless migration rate instead of the more obvious dune height (Eq. 4.1), because changing the length of a dune involves more transport of material than changing the dune height. In addition, it takes more time to change the length of longer dunes than of smaller dunes, thus creating a clear relation between dune length and migration rate. Other ways of creating a dimensionless migration rate (for example without L or H) did not result in a clear relation with dimensionless shear stress.

Relating dimensionless bed shear stress, or dimensionless grain-related shear stress to dune development would probably work best for rising discharges. During falling discharge, other processes, such as lagging of dune development behind changes in flow conditions, grain-sorting processes in dunes and bedload transport (Kleinhans, 2002a), and the development of superimposed dunes, also effect dune development, thus disturbing the possible relation between dimensionless shear stress and dune development.

Dune height as well as length and migration rate (figs. 4.15 and 4.16) show reasonably good relations with dimensionless bed shear stress, and dimensionless grain-related shear stress during rising discharges in the range of θ between 0.07 and 0.5 and θ' between 0.04 and 0.2. The data from Subsection 2C (the Waal branch of the bifurcation in Section 2) during the flood of 1998 were not used in creating the power relations for dune length and height, as they clearly plot below the other data sets. It seems that the development of the dunes in this section is delayed during rising discharges, possibly indicating that the

bed was armoured before the flood of 1998. An armour layer may have been intact in this section until a few days after the initial rise of the flood and, from that moment, the dunes may have had a large delay with respect to the development in other sections, which may have kept the dunes relatively small.

The different sections represented in figs. 4.15 and 4.16 form separate clusters, especially those from Section 3, which cluster in the upper right part of the graphs (figs. 4.15 A and B, and 4.16 A and B). In addition, there is a distinction between the three subsections of Section 2. This clustering is a clear indication of the differences in mobility of the graded bed material in the different sections. In Section 3, the bed material is better sorted with much more sand available than in the other sections, causing a higher mobility during similar bed shear stress conditions. The same holds true for Subsection 2A (the Bovenrijn), which has a mixed sand-gravel bed, whereas the bed in Subsection 2B (the Pannerdensch Kanaal) has more gravel than sand.

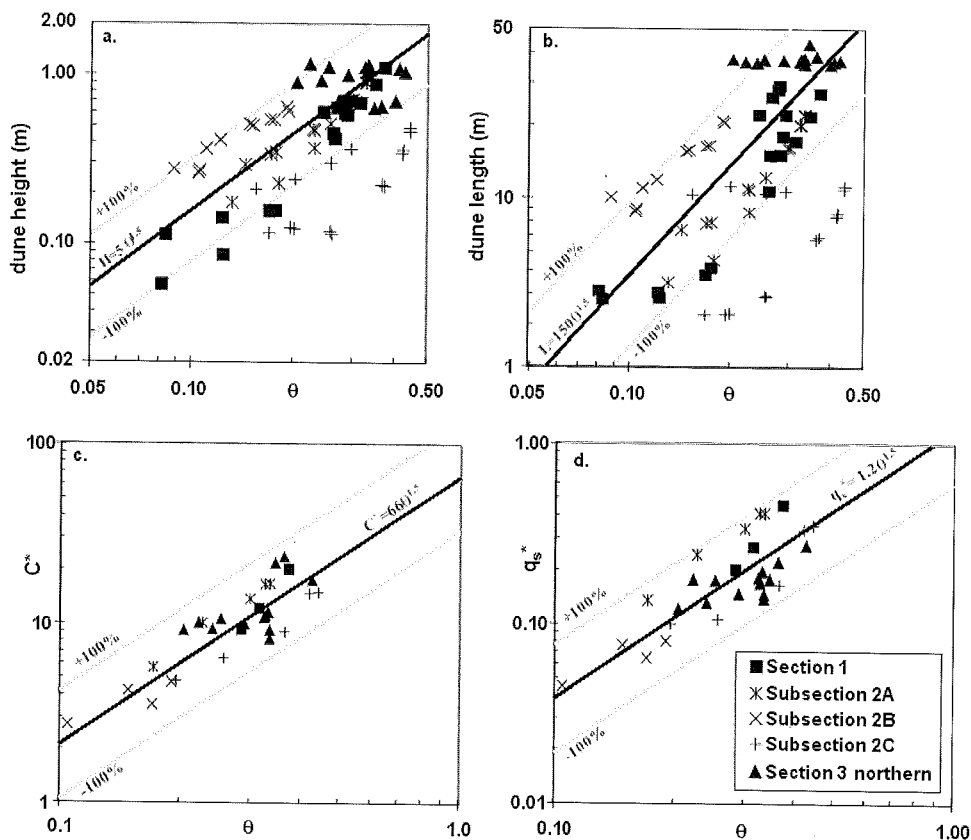


Figure 4.15. Relations between dimensionless bed shear stress and dune height (A), dune length (B), dimensionless migration rate (C) and dimensionless bedload transport rate (D). Only measurements during rising discharges are used. The middle solid lines show the fitted power functions along with the power function, the outer solid lines define the 100% deviation range from this power function.

4.4.3 Hysteresis in bedload sediment transport

Similar to the dune height, length and migration rate, the calculated bedload transport rate was also related to θ , and θ' for rising discharges. For this the bedload transport rate is made dimensionless using:

$$q_s^* = \frac{q_s}{D_{50} \sqrt{\frac{(\rho_s - \rho)}{\rho}} g D_{50}} \quad (4)$$

where q_s = bedload transport rate calculated with dune tracking ($\text{m}^3 \text{s}^{-1} \text{m}^{-1}$). The relations between q_s^* and θ , and between q_s^* and θ' for the rising stage of the flood wave, are power functions with an exponent of 1.5 (figs. 4.15D and 4.16D). This corresponds well with Meyer-Peter-Müller (1948) and Van Rijn (1984) (in Kleinhans and Van Rijn, 2002). Therefore, during rising discharge, bedload transport rate can be predicted. During falling

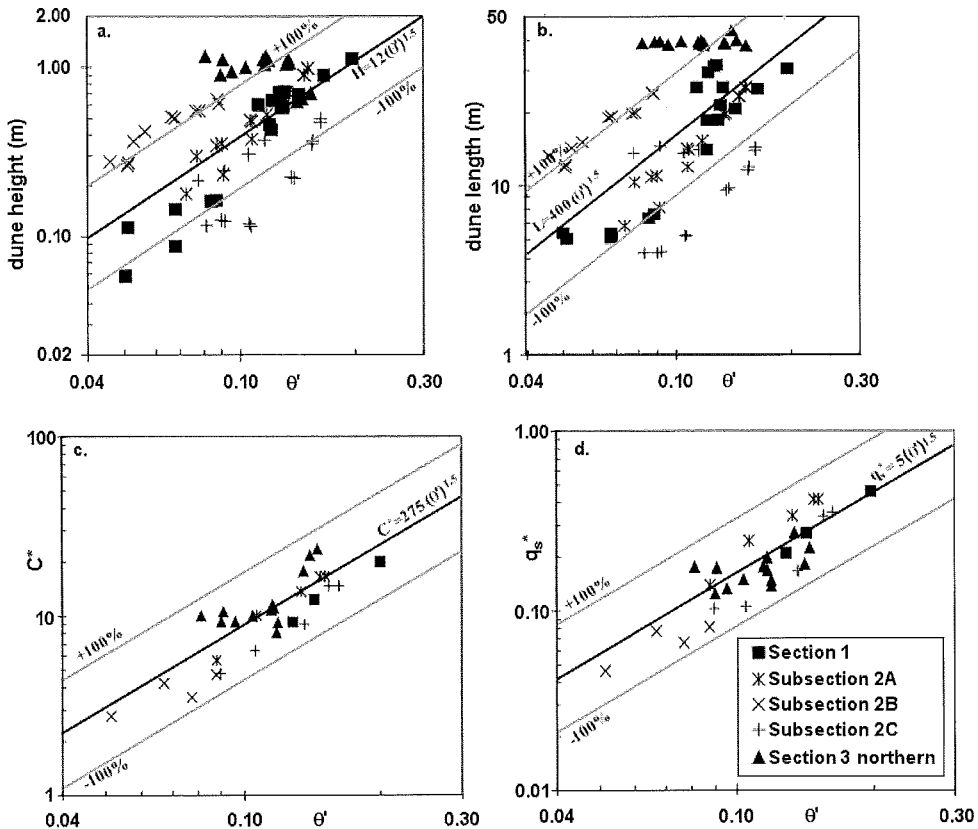


Figure 4.16. Relations between dimensionless grain-related shear stress and dune height (A), dune length (B), dimensionless migration rate (C) and dimensionless bedload transport rate (D). Only measurements during rising discharges are used. The middle solid lines show the fitted power functions along with the power function, the outer solid lines define the 100% deviation range from this power function.

discharge the bedload transport rate is slightly lower than during the rising stages of a flood at similar discharges (fig. 4.10), and a different relation will be necessary to predict the bedload transport rate during these falling stages. The lower transport rates during falling discharge result from the fact that, although the dunes are higher, they migrate slower. This hysteresis is probably due to more energy dissipation by form drag on the falling limb of the discharge curve because of the lagging of the dunes. The smaller dunes also may play an important role in the hydraulic roughness and energy loss (Julien, *et al.*, 2002). Thus, at similar discharge, less energy may be available for bedload transport after the peak discharge (Kleinhans, 2002a)

The small dunes in the southern part of Section 3 and the secondary dunes in Sections 1 and 2 are not considered because their migration rates could not be determined. These dunes most likely migrated much faster than the larger dunes that were present at the same time. For Section 3, this means that the bedload transport in the southern part probably is at least the same amount and maybe even more than in the northern part. For Sections 1 and 2, this means that the bedload transport rate at the end of a flood should have been calculated using the secondary dunes instead of the primary ones as done here. This may have resulted in larger bedload transport rates during the final stages of a flood.

4.5 Conclusions

In this study the growth and decay of the dunes and the related bedload transport in the Dutch Rhine were analysed from echosoundings collected during several floods and during periods of low to moderate discharges. In particular, dunes were analysed during three major floods (1995, 1997 and 1998) for three separate sections of the Bovenrijn and Waal, and the results show how dunes appear, grow and decay during a flood in the different sections. Dune development appears to be very different for the various sections in response to discharge. This is primarily due to grain-size differences and a variable discharge distribution over the main channel and the floodplain. The influence of differences in shape and duration of the flood waves on the spatial variation in dune characteristics seems to be less important.

The variable discharge distribution over channel and floodplain causes a clearly different development of bed shear stress and grain-related shear stress in the main channel of the three sections, which is reflected in the way dunes develop. Combining the differences in grain-size and the differences in either bed shear stress or grain-related shear stress development into the Shields mobility parameter or the dimensionless grain-related shear stress, results in reasonably good power relations that predict dune height, length and migration rate for the given conditions. The dune dimensions and bedload transport rate correlate equally well with grain-related shear stress as with overall bed shear stress.

Dune size and migration rates were also used to calculate the bedload transport rates in the three sections using the dune tracking technique. The results of these calculations, when related to the mobility parameter, showed a clear power relation, similar to the bedload predictors of Meyer-Peter-Müller (1948) and Van Rijn (1984).

Acknowledgements

This research was supported financially by the Directorate Eastern Netherlands (DON) and the Head Office of Rijkswaterstaat. The authors wish to thank the crew of the vessels *Krayenhoff*, *Beyerinck*, *Conrad*, *Onderzoeker* (DON) and *Wijtvliet* (Directorate Zeeland) as well as their supervisors for carrying out the echosoundings, R. van de Veen for providing the SOBEK-results, L. C. van Rijn and E. A. Koster for their comments on an earlier draft of the manuscript, and J. H. Van den Berg and M. G. Kleinhans (Utrecht University) for their assistance during analyses and many helpful suggestions and discussions about this article and countless related subjects. We also would like to thank the reviewers, R. Dinehart, R. Kuhnle and S. Bennett for their constructive remarks.

Notation

β	Bedload discharge coefficient (-)
ρ	Density of water (kg m^{-3})
τ_b	Bed shear stress (N m^{-2})
τ'	Grain related shear stress (N m^{-2})
θ	Shields' mobility parameter (dimensionless bed shear stress)
θ'	Dimensionless grain-related shear stress
ρ_s	Density of sediment (kg m^{-3})
c	Dune migration rate (m s^{-1})
C'	Chezy value related to grain roughness ($\text{ms}^{-0.5}$)
C^*	Dimensionless migration rate (-)
D_{50}	Median grain-size (m)
D_{90}	90 percentile of the grain-size distribution (m)
g	Gravitational acceleration (m s^{-2})
h	Average water depth (m)
H	Dune height (dune crest - dune trough) (m)
L	Dune length (m)
q_{s*}	Bedload transport rate calculated with dune tracking ($\text{m}^3 \text{s}^{-1} \text{m}^{-1}$)
q_s	Dimensionless bedload transport rate calculated with dune tracking
U	Average flow velocity (ms^{-1})

References

- ASHLEY, G.M. (1990) Classification of large-scale subaqueous bedforms: a new look at an old problem. *Journal of Sedimentary Petrology*, 60, 160–172.
- BENNETT, S.J. & BEST, J.L. (1995) Mean flow and turbulence structure over fixed, two-dimensional dunes: implications for sediment transport and bedform stability. *Sedimentology*, 42, 491–513.
- BEST, J.L. (1993) On the interactions between turbulent flow structure, sediment transport and bedform development: some considerations from recent experimental research. In: *Turbulence, Perspectives on Flow and Sediment Transport* (Eds. N.J. Clifford, J.R. French and J. Hardisty), pp. 61–93. John Wiley & Sons, Chichester.

- BHOWMIK, N.G., XIA, R., MAZUMDER, B.S. & SOONG, T.W. (1995) Return flow in rivers due to navigation traffic. *Journal of Hydraulic Engineering*, 121, 914–918.
- CARLING, P.A., GÖLZ, E., ORR, H.G. & RADECKI-PAWLIK, A. (2000) The morphodynamics of fluvial sand dunes in the River Rhine, near Mainz, Germany. Part I Sedimentology and morphology. *Sedimentology*, 47, 227–252.
- ENGEL, P. & LAU, Y.L. (1980) Computation of bedload using bathymetric data. *Journal of the Hydraulics Division*, 107 (11), 1445–1454.
- HAVINGA, H. (1982) Bedload determination by dune tracking. Report 82.3, Rijkswaterstaat, Arnhem.
- JULIEN, P. Y. & KLAASSEN, G.J. (1995) Sand-dune geometry of large rivers during floods. *Journal of Hydraulic Engineering*, 121, 657–663.
- JULIEN, P.Y., KLAASSEN, G.J., TEN BRINKE, W.B.M. & WILBERS, A.W.E. (2002) Bed resistance of the Bovenrijn River during the 1998 flood. *Journal of Hydraulic Engineering*, 128 (12), 1042–1050.
- KLEINHANS, M. G. (2002a) Sorting out sand and gravel; sediment transport and deposition in sand-gravel bed rivers. PhD Thesis, Faculty of Geographical Sciences, Utrecht University, Utrecht, The Netherlands, 314 pp.
- KLEINHANS, M. G. (2002b) The key role of fluvial dunes in transport and deposition of sand-gravel mixtures, a preliminary note. *Sedimentary Geology*, 143 (1-2), 7–13.
- KLEINHANS, M. G. & TEN BRINKE, W. B. M. (2001) Accuracy of cross-channel sampled sediment transport in large sand-gravel-bed rivers. *Journal of Hydraulic Engineering*, 127 (4), 258–269.
- KLEINHANS, M. G. & VAN RIJN, L. C. (2002) Stochastic prediction of sediment transport in sand-gravel bed rivers. *Journal of Hydraulic Engineering*, 128 (4), 412–425.
- LEEDER, M.R. (1983) On the interactions between turbulent flow, sediment transport and bedform mechanics in channelized flows. *Spec. Publ. Int. Ass. Sedimentol.*, 6, 5–18.
- MCLEAN, S.R., NELSON, J.M. & WOLFE, S.R. (1994) Turbulence structure over two-dimensional bed forms: implications for sediment transport. *Journal of Geophysical Research*, 99 (C6), 12729–12747.
- MEYER-PETER, E. & MÜLLER, R. (1948) Formulas for bedload transport. In: *Proceedings of the second IAHR congress in Stockholm, Sweden*. 2, 39–64. IAHR.
- MOLL, J.R., SCHILPEROORT, T. & DE LEEUW, A.J. (1987) Stochastic analysis of bedform dimensions. *Journal of Hydraulic Research*, 25, 465–478.
- NELSON, J.M., SHREVE, R.L., MCLEAN, S.R. & DRAKE, T.G. (1995) Role of near-bed turbulence structure in bedload transport and bed form mechanics. *Water Resources Research*, 31, 2071–2086.
- REID, I. & FROSTICK, L.E. (1994) Fluvial sediment transport and deposition. In: *Sediment Transport and Depositional Processes* (Ed. K. Pye), pp. 89–155. Blackwell Scientific Publications, Oxford.
- SIMONS, D.B. & SENTÜRK, F. (1992) *Sediment Transport Technology: Water and Sediment Dynamics*. Water Resources Publications, Littleton, 897 pp.
- TEN BRINKE, W.B.M., SCHOOR, M.M., SORBER, A.M. & BERENDSEN, H.J.A. (1998) Overbank deposition by large magnitude floods in the Dutch sand-bed Rhine River system. *Earth Surface Processes and Landforms* 23, 809–824.
- TEN BRINKE, W.B.M., WILBERS A.W.E. & WESSELING, C. (1999a) Dune growth, decay and migration rates during a large-magnitude flood at a sand and mixed sand-gravel bed in the Dutch Rhine river system. In: *Fluvial sedimentology VI. Int. Assoc. Sedimentol. Spec. Publ.*, 28, (Eds N.D. Smith and J. Rogers), pp. 15–32.
- TEN BRINKE, W.B.M., KRUYT, N.M., KROON, A. & VAN DEN BERG, J.H. (1999b) Erosion of sediments between groynes in the river Waal as a result of navigation traffic. In: *Fluvial sedimentology VI. (Eds N.D. Smith and J. Rogers)*, *Int. Assoc. Sedimentol. Spec. Publ.*, 28, 147–160.
- TEN BRINKE, W.B.M. & WILBERS A.W.E. (1999) Spatial and temporal variability of dune properties and bedload transport during a flood at a sand bed reach of the Dutch Rhine river system. In: *Proceedings of IAHR Symposium on river, coastal and estuarine morphodynamics*. 2, 309–318. University of Genova; Department of Environmental Engineering, Genova.
- VAN DEN BERG, J.H. (1987) Bed form migration and bedload transport in some rivers and tidal environments. *Sedimentology*, 34, 681–698.
- VAN DER VEEN, R. (2002) Calibration and validation of a hydraulic model (in Dutch). RIZA, Arnhem, The Netherlands.
- VAN RIJN, L. C. (1984) Sediment transport; Part 1: bedload transport. *Journal of Hydraulic Engineering*, 110 (10), 1431–1456.

- VAN URK, A. (1982) Bedforms in relation to hydraulic roughness and unsteady flow in the Bovenrijn branches (The Netherlands). In: The mechanics of sediment transport. pp. 151-157. Euromech 156.
- WIJBENGA, J.H.A. (1991) Analyses prototype measurements (non-) permanent roughness (in Dutch). report Q1302, Delft Hydraulics, Delft, The Netherlands.
- WILBERS, A.W.E. (1997) Dune characteristics and dune tracking during a flood in the Rhine (in Dutch). ICG Report, 97/8, ICG, Utrecht University, Utrecht, The Netherlands.
- WILBERS, A.W.E. (1999). Bedload transport and dune development in the Rhine: echo-soundings from the flood of November 1998 (in Dutch). ICG Report, 99/10, ICG, Utrecht University, Utrecht, The Netherlands.
- WILBERS, A.W.E. & KLEINHANS, M.G (1998) Analyses of sensitivity of Dune Tracking in 2 Dimensions (DT2D) (in Dutch). ICG Report, 99/8, ICG, Utrecht University, Utrecht, The Netherlands.

5 Predicting dune development during flood waves in the Rhine branches in The Netherlands.

Abstract

To determine the influence of hydraulic roughness on the water levels in a river the size of dunes on the river bed must be known as well as their growth rate during flood events. A review of existing prediction methods reveals that these are not applicable in the unsteady, non-uniform flow conditions of the Rhine. Therefore in this study a new method is presented to predict the dune dimensions in several branches of the River Rhine in The Netherlands. This method is based on the ideas of Allen (1974, 1976a, 1976b) whereby the rate of dune development depends on the difference between the dune dimensions before a change in flow conditions and the new equilibrium dimension belonging to those flow conditions. However due to lack of measurement data on changes in grain size during flood events, the grain size had to be presumed constant. This resulted in the fact that not one equilibrium equation but a set of two equilibrium equations had to be used, together with threshold values defining their use. The difference in the development of dune height and length in the Rhine also resulted in two different average adaptation constants, one for dune height and one dune length.

Together these necessary adaptations to the generic method resulted in three calculation models (a set of functions, thresholds and adaptation constants) for the Rhine branches. There is a calculation model for the dune height and one for the dune length applicable near the Pannerdensche kop. And there is a calculation model for dune height, applicable in the Waal near Druten. A comparison between the simulations of the models and the observations from individual flood events in individual sections showed that the models accurately simulate the trends of dune development, the moments of maximum dune dimensions, and the occurrence of superposition of secondary dunes. Even the actual dune height and length was simulated accurately several cases.

5.1 Introduction

Dunes are common features on the bed of most rivers not in the least the Rhine branches, Bovenrijn, Waal, and Pannerdensch Kanaal, in The Netherlands (Chapter 4). During floods these subaqueous dunes grow in length and height and become major obstacles, thereby increasing the hydraulic roughness in the river and creating higher water levels (Van Rijn, 1984). To accurately predict these water levels during flood events, with regard to designing criteria for flood protection plans, detailed and reliable predictions of the dune dimensions are necessary. Previously, several investigators constructed prediction methods for dune dimensions in steady and uniform flow conditions, relating them to flow strength, water depth, and grain size of the bed material (e.g. Shinohara & Tsubaki, 1959; Ranga Raju & Soni, 1976; Allen, 1978; Fredsøe, 1982; Van Rijn, 1984; and Karim, 1999; see also the review section below). However, in river situations there are strong feedback relations between those factors and the hydraulic roughness causing unsteady and non-uniform flow conditions especially during a flood wave. In those conditions it is not easy to predict the dune dimensions at specific moments, as they do not only depend on the reigning flow conditions of that moment but also on the development of the flow conditions before that moment. Prediction methods for these conditions were formulated by other investigators, however, those methods cannot readily be used in the Rhine branches (see the review section below). Therefore, the objective of the present analysis is, to develop a new method, adapting the ideas of other investigators, which predicts the dimensions of dunes during the unsteady, non-uniform flow conditions of a flood wave in the Rhine branches.

Before developing this new prediction method, the existing predictors are first reviewed and tested. Both this review and the development of the new prediction method use measurements of dune dimensions in the Rhine branches made during the last decade, extensively described in Chapter 4. These data refer to the Bovenrijn (Section 1 or Section 2a), the Pannerdensch Kanaal (Section 2b) and the Waal (Section 2c) near the bifurcation called the Pannerdensche kop, and in the Waal near Druten (Section 3) (fig. 4.1). Average dune dimensions were determined for 0.5 to 1 kilometre long river sections in all of these locations during the floods of 1995, 1997 and 1998 (Table 5.1), together with discharge and water depth. Flow velocity and bed shear stress values (Table 5.1) were obtained from a well-tested flow model designed for the Rhine branches in The Netherlands (Van der Veen, 2002; Chapter 4). The average grain size of the bed material was determined from extensive drilling and grab-sampling by Rijkswaterstaat (Ten Brinke, 1997; TNO-NITG, 2000). As no information was available on the changes in grain size during these flood event, the grain size had to be assumed constant for each section during all flood events (fig 4.2, Table 5.1). The observed dune development in the different river sections and during different flood events are shown in figure 5.1.

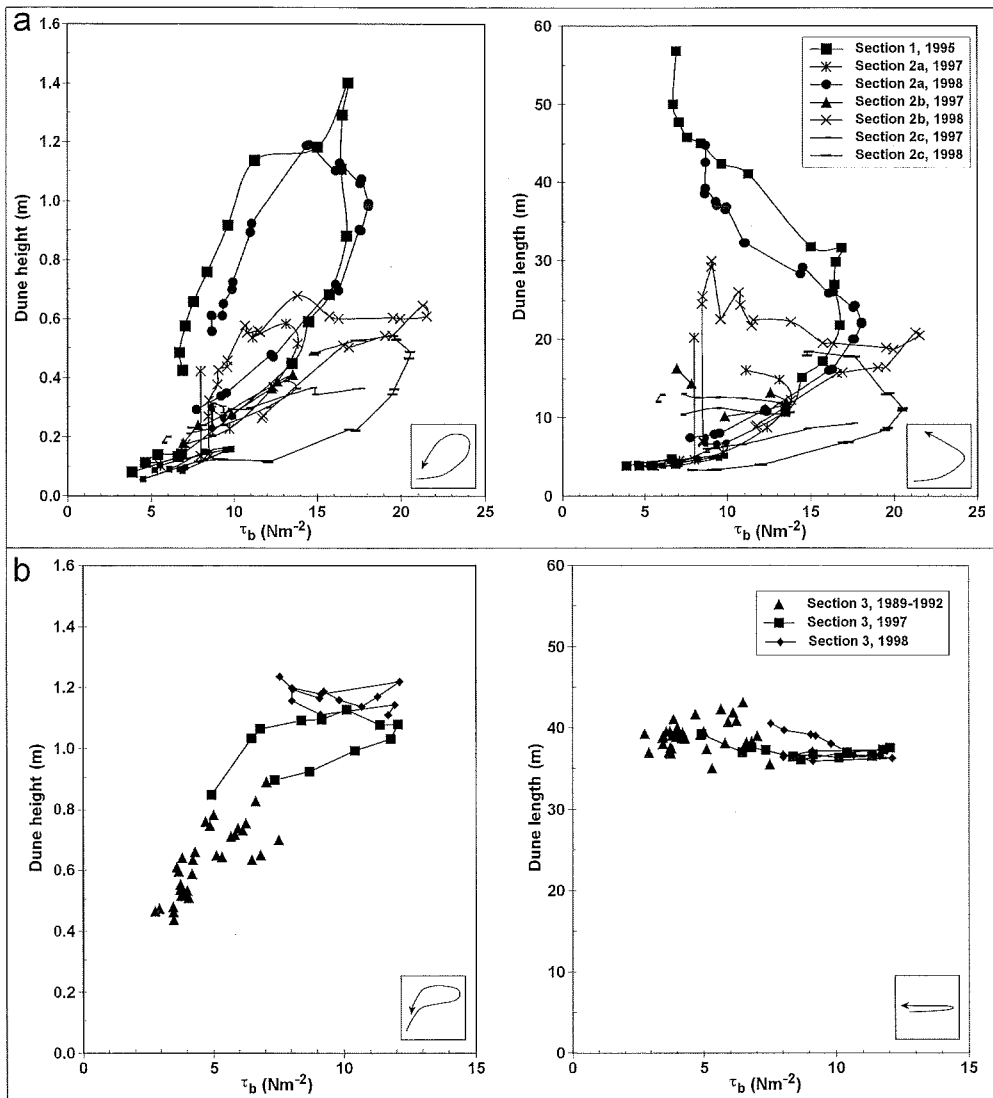


Figure 5.1: The development of dune height and length related to the changing bed shear stress near the Pannerdensche Kop, Sections 1 and 2 (a) and near Druten, Section 3 (b). Dates indicate the year in which the flood occurred. In all cases hystereses was anti-clock wise.

5.2 Review of existing prediction methods

As was said in the introduction several investigators formulated methods for the prediction of dune dimensions. In most cases these methods were made for steady and uniform flow conditions. This means that there is a unique dune height and length for each specific combination of flow characteristics, independent of previous conditions.

Table 5.1. Overview of general characteristics of the Rhine branches and the different measurement periods.

* discharge at nearest measurement station; Lobith for Bovenrijn, Pannerdensch Kop for Waal and Pannerdensch Kanaal, and Tiel for Waal near

Druuten.

** mostly 3 days of measurements every month during low discharges.

grain size in the right river half.

& grain size in the left river half.

Branch	Width [m]	Average grain size [mm]			Period	Discharge [m ³ s ⁻¹]*		Water depth [m]		Flow velocity [ms ⁻¹]		Bed shear stress [Nm ⁻²]	
		Excl. groynes	D ₁₀	D ₅₀		Min	max	Min	max	Min	max	Min	max
Bovenrijn	360	0.53	3.34	10.79	Jan - Apr 1995	2500 - 11900		5.28 - 11.63		1.14 - 2.43		4.54 - 16.90	
					27 Feb - 11 Mar 1997	2700 - 7000		5.48 - 9.49		1.23 - 1.84		5.26 - 13.86	
					29 Oct - 19 Nov 1998	4100 - 9500		7.13 - 10.73		1.45 - 2.13		7.77 - 18.11	
Pannerdensch Kanaal	150	0.73	6.89	16.56	27 Feb - 11 Mar 1997	850 - 2300		3.15 - 6.92		1.14 - 1.69		5.23 - 13.57	
					29 Oct - 19 Nov 1998	1500 - 3300		5.17 - 8.02		1.39 - 2.15		8.47 - 21.57	
Waal	260	0.41	2.86	13.24	27 Feb - 11 Mar 1997	1900 - 4600		5.65 - 9.42		1.19 - 1.66		5.68 - 13.75	
					29 Oct - 19 Nov 1998	2700 - 6200		7.21 - 10.52		1.36 - 1.98		7.89 - 20.57	
Waal near Druuten	250	0.55 0.38	1.62 0.73	5.08 [#] 4.15 ^{&}	Jan 1989 - Mar 1990**	750 - 2100		3.28 - 6.44		0.94 - 1.28		2.76 - 7.03	
					27 Feb - 21 Mar 1997	1400 - 4700		4.82 - 9.10		1.12 - 1.56		4.92 - 12.06	
					1 Nov - 24 Nov 1998	2400 - 6100		6.75 - 10.04		1.31 - 1.57		7.55 - 12.14	

Steady and uniform flow therefore makes it possible to predict the dune dimensions with a single function. For unsteady, non-uniform flow conditions only a few prediction methods were made. In unsteady, non-uniform flows, a specific combination of flow characteristics does not result in the same unique dune dimensions. Instead, the dune dimensions at a specific moment are greatly influenced by previous flow characteristics and dune development. In the next sections both types of prediction methods are reviewed and tested. Then this analysis will be used to formulate a new method applicable in the conditions of the Rhine branches.

5.2.1 Steady, uniform flow conditions

For steady, uniform flow conditions, equations have been developed for dune length, dune height and sometimes dune steepness (H/L). These equations can be divided into

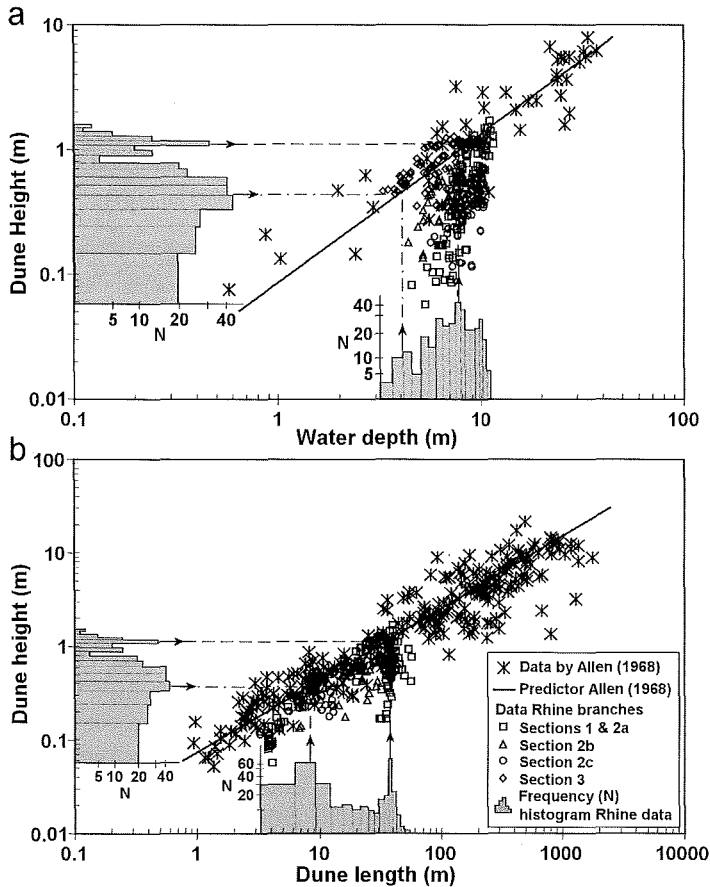


Figure 5.2: The measured dune heights (a) and lengths (b) of the Rhine branches plotted in diagrams of Allen, (1968). Frequency (N) histograms of the dune height, length and water depth of the Rhine data are drawn to show that the most frequent characteristics are predicted with the predictor of Allen (1968).

several groups, depending on the factors used in the relations, whether their development is based on theoretical or empirical grounds, or whether the predictions result in average or equilibrium dune dimensions. In most equations the dune dimensions are related to a combination of flow strength (either flow velocity or a type of shear stress), water depth, and grain size (e.g. D_{50} , or D_{90}). Examples of such equations were made by Shinohara & Tsubaki (1959) (see Appendix 5.I), Ranga Ruju & Soni (1976), Allen (1978), Fredsøe (1982), Van Rijn (1984), and Karim (1999). Others use only one or two of these factors. Anderson, (1953), Stein, (1965), Tsuchiya & Ishizaki (1967), Gill (1971), Yalin (1972), and Kennedy & Odgaard (1990) for example use only water depth and flow strength, while Allen (1968) (see Appendix 5.I) and Mohrig (1994) only use the water depth. Some investigators incorporated very specific parameters in their predictors, which are often difficult to obtain in field situations. The equation of Kennedy (1969), for example, requires the critical flow velocity, the equation of Fredsøe (1980) needs the shear stress at the top of a dune, and the equation of Karim (1995) requires the shear velocity and fall velocity to predict dune dimensions.

Table 5.2. The selected steady, uniform flow predictors of dune height and dune length tested in the unsteady, non-uniform flow conditions of the Rhine, divided into theoretical and empirical based.

	Dune Length	Dune height
Theoretical	Anderson (1953)	Tsuchiya & Ishizaki (1967)
	Tsuchiya & Ishizaki (1967)	Gill (1971)
	Yalin (1972)	Karim (1999)
	Shinohara & Tsubaki (1959)	Shinohara & Tsubaki (1959)
Empirical	Yalin (1964)	Allen (1968)
	Allen (1968)	Ranga Ruju & Soni (1976)
	Van Rijn (1984)	Van Rijn (1984)
	Julien & Klaassen (1995)	Julien & Klaassen (1995)
		Karim (1995)

Most predictors are based on empirically fitted functions through data from different flume, river and estuary measurements (Shinohara & Tsubaki, 1959; Stein, 1965; Allen, 1968; Ranga Ruju & Soni, 1976; Allen, 1978; Van Rijn, 1984; Mohrig, 1994; Julien & Klaassen, 1995; Karim, 1995). Others, like those of Anderson (1953), Tsuchiya & Ishizaki (1967), Kennedy (1969), Gill (1971), Yalin (1972), Fredsøe (1982), Kennedy & Odgaard (1990), and Karim (1999) are based on more theoretical considerations. Independent of the fact whether the equations are based on empirical or theoretical analyses, some equations result in an average value for dune dimensions (i.e. Allen, 1968), while others predict more or less equilibrium dune dimensions (i.e. Tsuchiya & Ishizaki, 1967, or Van Rijn, 1984 (see Appendix 5.I)). The equations that result in average dune values, like the one from Allen (1968), predict the range of dune dimensions that can be expected in a certain river during all stages. Figure 5.2 shows, for example, that the data from the Rhine branches plot well within the data cloud collected

by Allen, and that the most common dune lengths and heights (dotted lines) are correctly predicted by the equation of Allen.

To test the reliability of the equations for steady, uniform flow during the unsteady, non-uniform flows of the Rhine branches, several predictors were selected as indicated in Table 5.2. Others were excluded on the grounds that they either; 1) were based on only a small range of dune sizes (Mohrig, 1994), 2) were only available as diagrams (Stein, 1965; Fredsøe, 1982) and therefore required a full reanalysis of the original data to determine the mathematical functions, or 3) were using parameters that are very difficult to measure in field situations (Kennedy, 1969; Fredsøe, 1980). Figure 5.3 shows an example of the prediction capabilities of five of these predictors for dune height and dune length for Section 2a during the flood of 1998. Only the results of these five equations are shown because they produced the best predictions. Some of these five predictors appear to perform well during low discharges (before and after a flood), such as Karim (1995) for dune height and Tsuchiya & Ishizaki (1967) for dune length. Others predict well the size of the dunes as they reach their maximum dimensions, for example Shinohara & Tsubaki (1959) and Van Rijn (1984) for both dune height and length. The dimensions of the secondary dunes are best predicted by Tsuchiya & Ishizaki, (1967). However, none of the predictors correctly predicts dune dimensions during the complete flood event. This

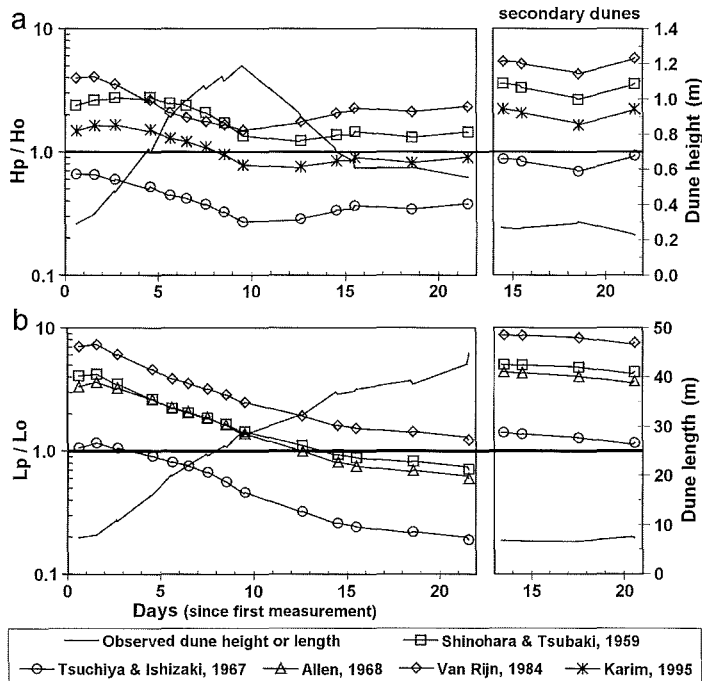


Figure 5.3: Evaluation of several predictors in predicting dune height (a) and dune length (b) in the Bovenrijn for the flood of 1998. A value of 1 in H_p/H_o denotes a perfect prediction. The predictors are named by the authors and their publication date, and the graphs are split to distinguish between primary and superimposed secondary dunes.

demonstrates the inapplicability of these predictors, which were made for steady and uniform flow conditions, in the unsteady, non-uniform conditions of the Rhine branches.

5.2.2 Unsteady, non-uniform flow conditions

The predictors proposed for steady, uniform flow conditions are inadequate in unsteady, non-uniform flow situations because they neglect two important processes, reaction and relaxation (Allen, 1974; 1976a; 1976b). Both result in dune dimensions lagging behind the values expected according to the prevailing flow conditions. The first process, reaction, occurs when the dune dimensions cannot change until a specific condition is reached. For example, in case of an armoured riverbed, during an increase in flow strength, the dunes cannot change until the armour layer is broken. Only at that time will there be enough bedload transport to increase the size of the dunes (fig 5.4). The existence of such a condition therefore results in a reaction time which is part of the total lag time of the dunes. However, as this reaction process only occurs in special situations it was neglected in all unsteady prediction methods. Conversely, the relaxation process is always present when the dune dimensions are changing from one flow condition to the next. It takes time to rework the required volume of sediment to establish new dune dimensions through bedload transport. Every time the conditions (a combination of flow and grain size) change, the dune height and length will slowly adapt to these changes and eventually reach an equilibrium value valid for the prevailing conditions (fig. 5.4), resulting in a relaxation time which normally is the major part of the total lag time.

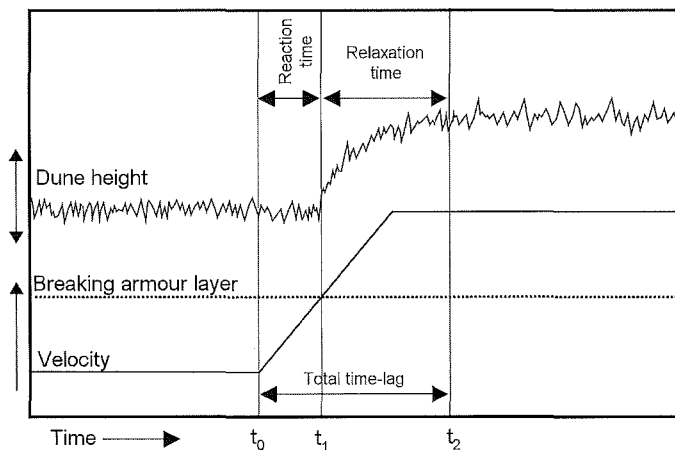


Figure 5.4: Example of reaction and relaxation time.

Several investigators developed prediction methods incorporating this process of relaxation (Allen, 1976a; 1976b; 1976c; Fredsøe, 1979; Van Rijn, 1989). They did this in such a way that the rate of adaptation depends on the difference between the dune dimensions before the change in flow condition and the new equilibrium dimensions (fig. 5.5, Allen, 1976a; 1976b; 1976c). Hence:

$$\frac{\partial D}{\partial t} = a(D_{\infty} - D_0) \quad (5.1)$$

Where D = any type of dune dimension; a = adaptation constant; D_{∞} = equilibrium dune dimension; D_0 = dune dimension before any change (at $t=0$). The equilibrium dimensions are thereby predicted with a function:

$$D_{\infty} = f(h, \tau, D_*) \quad (5.2)$$

Where h = water depth; τ = shear stress and D_* = a particle parameter. Allen, Fredsøe, and

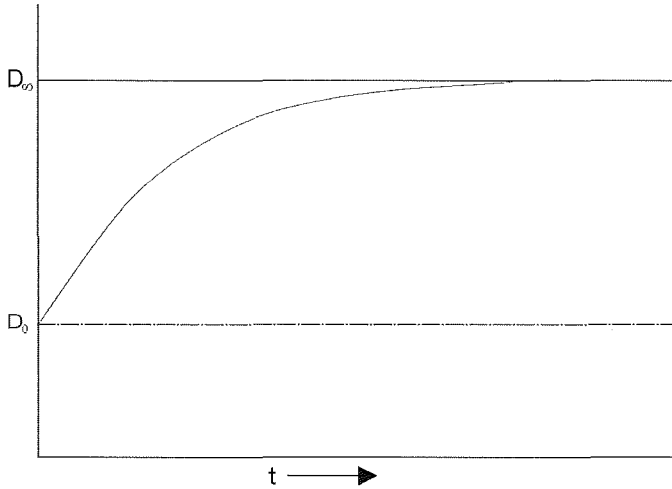


Figure 5.5: The rate of adaptation of a dune characteristic (D) depends on the difference between the dune dimensions before the change in flow conditions (D_0) and the new equilibrium dimensions (D_{∞}). See also eq. 5.1.

Van Rijn all defined the adaptation constant in their own way. Allen (1976a, 1976b, 1976c), for example, used a dune excursion factor for it, which determines the life span of individual dunes in a population. However, to determine the life span of individual dunes, one has to know the migration rate of every dune, which is difficult to establish in field situations. Fredsøe (1979) used an adaptation coefficient that was closely related to the Meyer-Peter & Müller (1948) transport equation thereby relating dune development to bedload transport. In field situations, however, bedload sediment transport is difficult to measure or predict (Kleinhans & Ten Brinke, 2001) making it difficult to determine the value of the adaptation constant. Van Rijn (1989) did not use eq. 5.1 directly but first defined a dune transition period based on the amount of sediment transport that is necessary to change the volume of a dune. He then used this transition period to define the adaptation constants for dune height and dune length. However, to calibrate this dune transition period and both adaptation constants, one needs large amounts of accurate measurements over time which are generally not available in field situations. None of the required data necessary to calibrate these three methods was available for the Rhine branches. The methods of Allen, Fredsøe, and Van Rijn could therefore not be tested, and therefore are not practical prediction methods for the unsteady, non-uniform conditions in the Rhine branches.

5.3 Development of a prediction method for the Rhine branches

Instead of redefining the adaptation constant (a), like was done by Allen (1976a, 1976b, 1976c), Fredsøe (1979), and Van Rijn (1989), in this analysis it is proposed to determine this constant directly from the measurement data. Integration of eq. 5.1 yields:

$$D(t) = D_0 + (1 - e^{-at})(D_\infty - D_0) \quad (5.3)$$

Which can be approximated, to provide the dune dimensions at any given time, with:

$$D(t) = D_{(t-1)} + (1 - e^{a\Delta t})(D_{\infty,t} - D_{(t-1)}) \quad (5.4)$$

where $D(t)$ = dune dimension at time t ; a = adaptation constant; Δt = time step; $D_{\infty,t}$ = equilibrium dune dimension at time t ; $D_{(t-1)}$ = dune dimension at previous time step. Assuming it is possible to define a function describing the equilibrium dune dimensions at a given time (as if the flow was steady), it would be possible to determine the adaptation constant from:

$$1 - e^{-a\Delta t} = \frac{D(t) - D_{(t-1)}}{D_{\infty,t} - D_{(t-1)}} \quad (5.5)$$

in which a is a function of the time step between two measurements (Δt), and the quotient of the difference between two measurements ($D(t) - D_{(t-1)}$) and the maximum difference between $t=t\Delta t$ and equilibrium ($D_{\infty,t} - D_{(t-1)}$). In the situation of the Rhine branches this means that first a function or a set of functions has to be defined that accurately describes the equilibrium dune dimensions (D_∞) for the different Rhine branches. Secondly using these equilibrium predictors in eq. 5, the adaptation constants for the different branches, and for respectively dune height and dune length has to be determined from the available measurements.

In chapter 4, the development of dune length and dune height is described and compared for the different sections in the Rhine branches (fig. 5.1). It showed that the dune development is comparable for all the branches near the Pannerdensche kop (Sections 1 and 2), but that the development in the Waal near Druten (Section 3) is very different from Sections 1 or 2. It also showed that the development of dune height is different from the development of dune length. This probably means that implementing the new calculation method will result in a different set of equilibrium functions and adaptation constants for both dune length and dune height as well as for the sections near the Pannerdensche Kop (Section 1 and 2) and the section in the Waal near Druten (Section 3). Hereafter, such a set of equilibrium functions and an adaptation constant, applicable for either dune height or length in one of the river sections, will be called a calculation model. All the different calculation models that are created are transcribed in Appendix 5.II.

5.3.1 Equilibrium predictors

Equilibrium predictors are predictors made for steady, uniform flow conditions and predict the dune dimensions when the dunes are fully adjusted to the prevailing flow

conditions. In a river situation like the Rhine there are two moments when the dunes may reach this situation. First, if the flow conditions in a river are almost constant for a long period of time. In the Rhine this period of almost constant flow conditions occurs during the summer months when the discharges are low. This means that generally just before the start of the first flood wave in autumn or winter the dunes present on the bed will be at their equilibrium dimensions. The second moment of equilibrium dimensions occurs during a flood wave. As the discharge rises during a flood, the dunes will grow in length and height but will be smaller than their equilibrium dimensions. During the falling limb of the flood wave, the equilibrium dune dimensions will decrease. However, the observed dunes will still increase in size as they still are smaller than their equilibrium dimensions. A few days after the maximum discharge the dunes will stop growing as they reach the decreasing equilibrium dimensions. After this moment the observed dune size will decrease because the dunes are now somewhat larger than the equilibrium dimensions. The second moment where the dunes approximate their equilibrium dimensions therefore coincides with the observed maximum dune height or length.

With these two moments, a predictor (originally made for steady flow) can be selected that predicts the equilibrium height or length of the dunes in the different branches. However, the analysis of the steady flow predictors in the review section (fig. 5.3) showed that there is no single predictor that predicts the observed dune height or length at both moments correctly during any flood event. Some predictors perform reasonably well during low flow conditions, while others can predict the maximum dune height or length. This means that with the available dataset the equilibrium dune dimensions can not be predicted with one method but a set of two predictors has to be used during a flood wave. To determine when to use which predictor certain threshold values have to be defined. These thresholds should be related to observed flow conditions that occur at the moments when the dune development in a river section changes significantly. Examples of such changes in Sections 1 and 2 are, the start of dune growth, the start of dune decline, and the start of superposition (fig. 5.1). In Section 3, a threshold has to be defined at the change in rate of dune development during both dune growth and decline. Table 5.3 shows the bed shear stress values during the floods present at the moment the mentioned changes occurred in the different branches. The bed shear stress (τ_b) was used instead of the grain shear stress (τ_b') or the dimensionless shear stress (θ) because the grain size of the bed in the different branches had to be assumed constant during all flood events. Both the use of grain shear stress and dimensionless shear stress resulted in more variable threshold values compared to the bed shear stress values in Table 5.3. The average values from Table 5.3 show that near the Panterdenschekop (Section 1 and 2), dunes start to grow in height and length as the bed shear stress exceeds 10 Nm^{-2} , during the falling limb of a flood the dune height starts to decrease as the bed shear stress drops below 13 Nm^{-2} , and the initiation of superposition occurs at the moment the bed shear stress declines again below 10 Nm^{-2} . In the Waal near Druten (Section 3) the growth of the dune height slows down considerably as the bed shear stress increases above 7 Nm^{-2} , and on the falling limb, the rate of decline increases again as bed shear stress declines below 7 Nm^{-2} .

After defining the thresholds for the different Rhine branches, the two equilibrium predictors that will be used in the new prediction method were determined from the analysis used in the review section. The best predictors were selected by comparing

their predictions with the observations for either low flow conditions or for maximum dune dimensions. As a maximum dune length was almost never observed during any of the flood events, here the predictors were selected that predicted closest to, but still higher than, the longest dune length that was observed. For superimposed dunes a separate predictor for dune length and height was selected that best predicted these dimensions. Unfortunately, none of the functions that were tested was able to predict the equilibrium dune length in Section 3 because the dune length hardly changes in this section during any part of a flood event. Creating a calculation model for the dune length development in the Waal near Druten (Section 3) was therefore not attempted. A possible reason for this lack of change in dune length in this section will be discussed later. In Section 1 and 2, the dune height and length during low flows were best predicted by the method of Tsuchiya & Ishizaki (1967), while in Section 3, the dune height during low flows was best predicted by method of Allen (1968). Both these methods are described in detail in Appendix 5.I. The best equilibrium predictor for dune height in Sections 1 and 2 for rising and high flows was the method of Shinohara & Tsubaki (1959), while the method of Van Rijn (1984) was second best. For dune length in Sections 1 and 2, the equation of Van Rijn (1984) was the best option. In section 3, the prediction method for dune height of Van Rijn (1984) performed the best. To develop a prediction method that is consistent for all the branches, the equations of Van Rijn (1984) were chosen as the best high flow equilibrium predictors. However, In Appendix 5.I both the prediction method of Shinohara & Tsubaki (1959) and of Van Rijn (1984) are described.

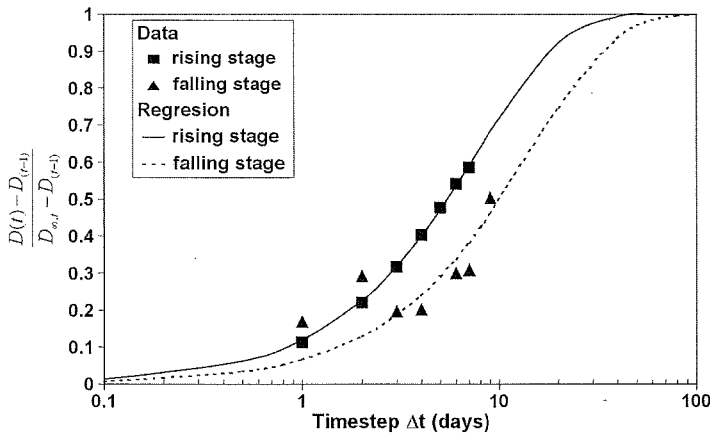


Figure 5.6: Exponential fit of the proportion of change in dune height as a function of time step (days) between measurements for the Bovenrijn during the flood of 1998.

5.3.2 Adaptation constant

The next step in making a new prediction method for the Rhine branches is to determine the adaptation constant of eq. 5.4 using eq. 5.5. In Figure 5.6 the right part of eq. 5.5 $(\frac{D(t) - D_{(t-1)}}{D_{\infty,t} - D_{(t-1)}})$ is plotted against the time step (Δt , in days) from the left part of eq. 5.5. This

was done separately for measurements during rising and falling discharges and the adaptation constants were calculated by fitting the function $1-e^{-a\Delta t}$. Table 5.4 shows the results for the different river sections and for the different flood events. In all sections and during all flood events the adaptation constants were very similar. As the difference between rising and falling discharges was minor, it was ignored. This resulted in an average value for the adaptation constant of 0.12 for the dune height and 0.05 for dune length valid for all river sections and any flood event.

Table 5.4. Adaptation constants for dune height and length in every Rhine branch during the rising and falling limbs of different floods.

* The values for Section 3 were excluded from the average values.

** No adaptation constants for Section 3 were determined as the dune length does not change at this location during a flood event.

Dune height	Rising limb			Falling limb			Avg. Rise	Avg. Fall	Overall Avg.
	1995	1997	1998	1995	1997	1998			
Section 1 and 2a	0.12	0.09	0.13	0.12		0.07	0.11	0.10	0.11
Section 2b		0.11	0.08			0.18	0.09	0.18	0.14
Section 2c		0.04	0.05		0.19	0.22	0.05	0.20	0.12
Section 3*		0.30			0.05		0.30	0.05	0.17
Average	0.12	0.08	0.09	0.12	0.19	0.16	0.08	0.16	0.12
Dune Length	Rising limb			Falling limb			Avg. Rise	Avg. Fall	Overall Avg.
	1995	1997	1998	1995	1997	1998			
Section 1 and 2a	0.05	0.05	0.05			0.07	0.05	0.07	0.06
Section 2b		-0.03	0.05				0.01		0.01
Section 2c			0.04				0.04		0.04
Section 3**									
Average	0.05	0.01	0.05			0.07	0.03	0.07	0.05

5.3.3 The prediction method for the Rhine branches

Selecting the equilibrium predictors together with the thresholds that define when to use which predictor, and combining that with the calculated adaptation constants, resulted in three different calculation models for predicting dune dimensions in the Rhine branches (Appendix 5.II). One model for dune height and one for dune length applicable in Sections 1 and 2, and one model for dune height applicable in Section 3. This last calculation model is only applicable for the large dunes that are normally found in the right half of the river (Wilbers & Ten Brinke, 2003), see the discussion section for further explanation. Every simulation can thereby start with either a measured dune height or length, or with a value predicted with the low flow predictor. In this last case it is assumed that low flow conditions lasted long enough before a flood event for the dunes to have reached equilibrium dimensions.

As no other data is available besides the data used here to create the calculation models for the Rhine branches, validation of these models is not possible. However, because the models were made by averaging the results from all branches and all flood events, it is possible to test their applicability against single flood events in individual sections

selected from the total dataset. Figure 5.7 shows that the models for dune height and dune length, calibrated with average thresholds and adaptation constants, follow the trends observed in the dune development in Section 1 for the flood of 1995, in Section 2b for the flood of 1998, in Section 2c for the flood of 1997, and in Section 3 for the flood of 1997,

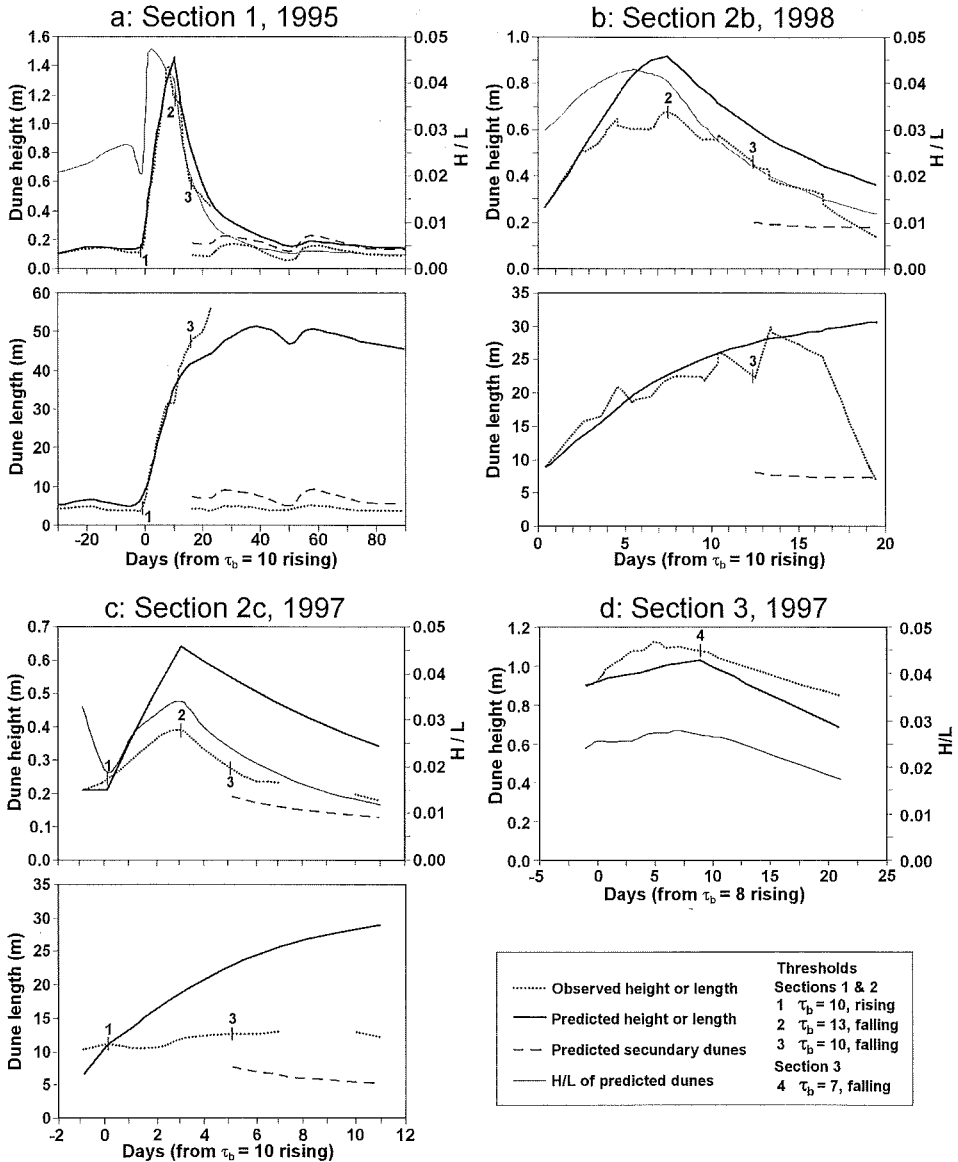


Figure 5.7: Examples of observed and predicted dune development:

- a) in the Bovenrijn (Section 1) for 1995
- b) the Pannerdensch Kanaal (Section 2b) for 1998
- c) the Waal near the Pannerdensch Kop (Section 2c) for 1997
- d) the Waal near Druten (Section 3) for 1997.

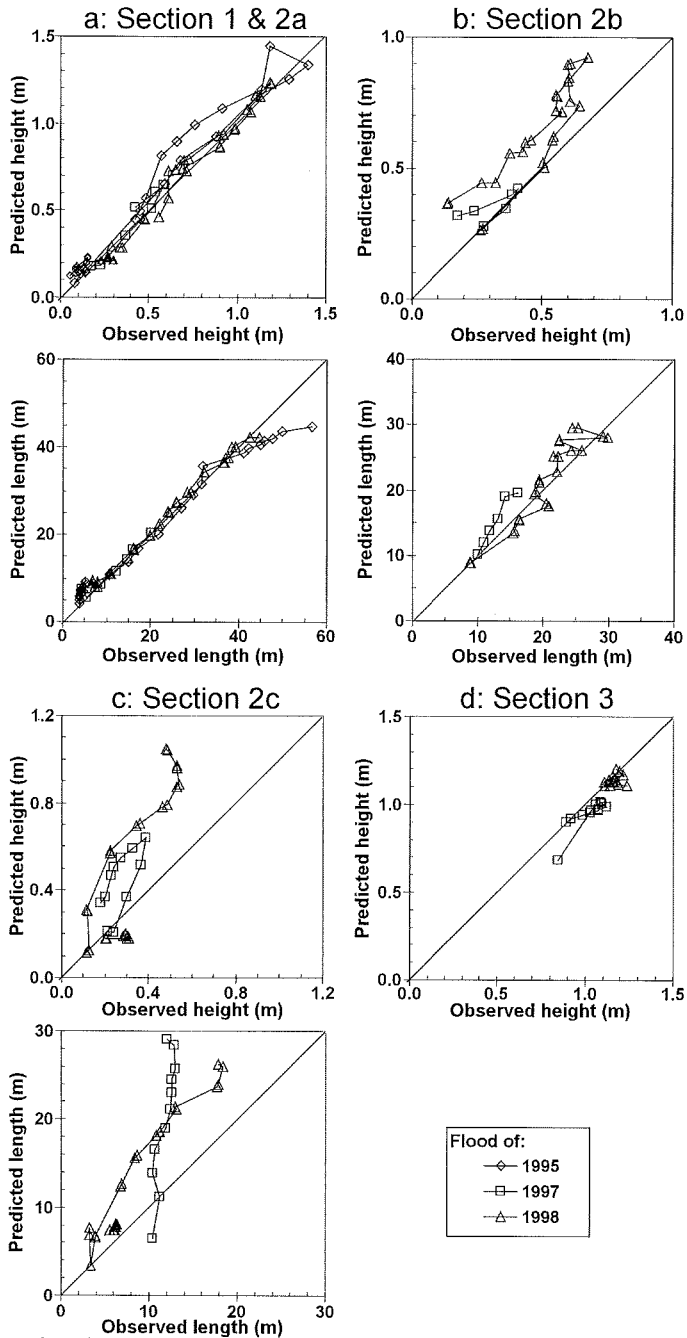


Figure 5.8: Comparison between observed and predicted dimensions. The line at a 45° angle denotes a perfect simulation.

- a) Bovenrijn (Sections 1 and 2a).
b) Pannerdensch Kanaal (Section 2b).
c) Waal near Pannerdensch Kop (Section 2c).
d) Waal near Druten (Section 3).

reasonably well. The moments when dunes start to grow, decline, or superposition occurs are simulated well. In some cases (fig 5.7a, b and d) even the observed dune height and lengths are approximated. Figure 5.8, however, shows that especially during high flows, the dune dimensions are over-predicted in Sections 1 and 2, while the dune height in Section 3 is always slightly under-predicted.

5.4 Discussion

A new prediction method was developed to predict the dune height and dune length during unsteady flows in the Rhine branches. Due to inherent differences between the development of dune height and length in the different river sections this new method resulted in three different calculation models. A comparison with individual flood events in individual river

sections shows that these models are applicable with reasonable accuracy. However, two aspects prohibit the general application of this method in any event anywhere in the Rhine or its branches. The first is that the adaptation constant seems to be different for individual branches, for rising or falling discharge, and for dune height and dune length. The second is that in using the available dataset from the Rhine branches, two predictors have to be used to calculate to equilibrium dune height or length, instead of one. In this section these two aspects will be discussed in more detail. Besides these two aspects, a reason has to be found to explain why no prediction method can be made for the dune length of the large dunes and the dimensions of the small dunes in Section 3.

5.4.1 Adaptation constant

In the analysis above, it was assumed that the adaptation constant could be averaged over all branches and over rising and falling flows. Statistically, there was no difference between the adaptation constants for rising and for falling flows, or for the adaptation constants in the different branches, because of the small number of measurements. However, the adaptation constant for dune height in Section 3 during the 1997 flood was much larger than the values in Section 2. In Sections 2b and 2c during falling discharges the values were higher than during rising discharges. This may indicate that a factor, influencing the adaptation constant, was ignored. As the grain size of the dune material was assumed constant during all events (due to lacking measurements), the grain size may be this lacking factor. The grain size in Section 3 is much finer than in Section 2. This could result in a faster adaptation, as is indicated by the larger adaptation constants. Also, Kleinhans (2002) showed that in Section 2c the grain size of bedload transport material decreased during the flood of 1998 making the material sandier during falling discharges than during rising discharges. These smaller grain sizes could result in a faster adaptation during falling discharges as is indicated by the larger adaptation values during falling discharge in Section 2c.

5.4.2 Two equilibrium predictors

The basis of the new prediction method is formed by eq. 5.1 and 5.2, with eq. 5.2 defining the function that describes the equilibrium dune dimensions. However, none of the existing predictors, that were tested, performed well during a complete flood event. Therefore a set of two different equations was used separated by arbitrary threshold conditions. The fact that none of the existing predictors could be used throughout a flood event is probably caused by the assumption of a constant grain size. The bed material of the Rhine branches is composed of a badly sorted, mostly bimodal, sand and gravel mixture (fig. 4.2), so it is plausible that the average grain size of the dunes changes during a flood. These changes in grain size are an important factor in the prediction (eq. 5.2).

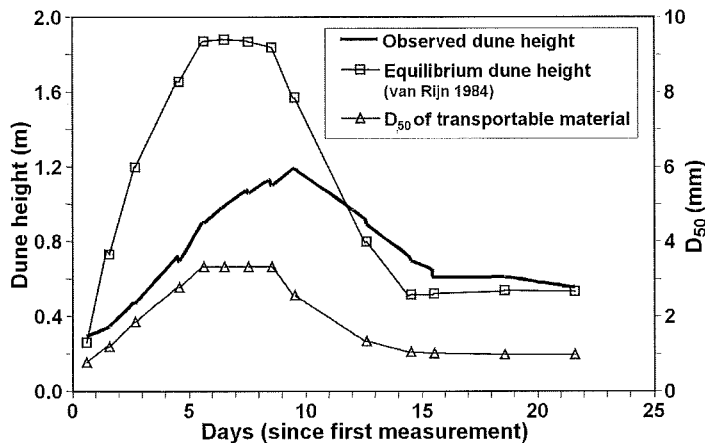


Figure 5.9: Influence on the prediction of equilibrium dune height of a hypothetical change in D_{50} of transportable material in the Bovenrijn (Section 2a) during the flood of 1998.

During low flows possibly an armour layer is formed (especially around the Pannerdensche kop) (Kleinhans, 2002), or at least the gravel part of the distribution becomes less mobile than the sandy part. It is likely that the dunes which are present during low flows are composed of more sandy material than the bed material below the dunes (Kleinhans *et al.*, 2002). During high flows the dunes will have more or less the same composition as the bed, transporting more gravel than during low flow. This expected change in the composition of the bedload material would imply a change in the equilibrium dimensions during a flood. This can be tested by introducing an hypothetical, but realistic, change in D_{50} . A single equilibrium equation then has to apply for both high and low flow conditions. That means that during rising flow, the predicted equilibrium dune dimension have to be larger than the measured values, while during falling flows, the predicted dimensions have to be smaller, otherwise the dunes would not grow during rising discharges and shrink during the falling limb of a flood. Figure 5.9 shows that, as the D_{50} is varied between 1 and 3.3 mm, the equation for predicting dune height by Van Rijn (1984) (Eq. 5.1.13, Appendix 5.I) indeed predicts lower than the observed values at low flows and higher during high flows. If such a variation in grain size was measured

during the floods, the new prediction model for dune height would only have needed one equilibrium equation and no threshold conditions to predict the changing dune height.

5.4.3 The Waal near Druten

During the formulation of the new prediction method, the development of the dune length in Section 3 appeared to be so different that it was decided to exclude it. The dune length of the large dunes, present only in the right half of the river (Chapter 4), does not change very much as the flow conditions change (fig. 4.2). The tests with the existing predictors in the review section also showed that none of the predictors predicted the observed dune lengths. However, what is the reason that the dune length of these large dunes does not changes very much.

Wilbers and Ten Brinke, (2003, Chapter 4) reported that due to the intensive shipping, the upper part of the bed in the left half (Southern) of the river in Section 3 is made of almost pure sand, while in the right half (Northern) the material is much more a mixture of sand and fine gravel (fig. 4.2). Fully loaded ships, going to Germany, travel only in the left half of the Waal, and thereby create additional turbulent currents that suck sandy material from between the groynes (Ten Brinke *et al.*, 1999; 2003). This difference in grain size is echoed in the dune dimensions. In the left half only small dunes (excluded from this analysis) consisting of merely sandy material are present. These small dunes are probably strongly influenced, during both low and high discharges, by the additional currents created by shipping, which keeps their dimensions constant (Chapter 2, Chapter 4). In the right half of the river large dunes are present, which consist mostly of a sand and gravel mixture. In the Waal near Druten, groynes are found on both sides of the river, almost paired opposite each other, and spaced about 200 m apart. From the echo-soundings it was determined that when two groynes oppose each other, the increase in flow velocity caused by the narrowing of the flow creates a fixed “trough” between the groynes (Chapter 4). Because each pair of opposing groynes has such a “trough” the space for large dunes between two groyne pairs is limited. In a space of 200 m only 5 or 6 dunes with a length of about 35-40 m can exist. If one dune grows in length, the other dunes have to become smaller to exist in this limited space. The average dune length will therefore remain almost constant, in spite of any change in flow conditions. Only in very low flows, when the dunes should have much smaller dune lengths, the actual dune lengths can decrease (as additional dunes are created within the available space). However, this low flow will have to persist for a very long time, because the large dunes will have to disappear first, which will take a long time during low sediment transport conditions.

5.5 Conclusion

The objective of the present analysis was to develop a method to predict dimensions of active dunes during unsteady, non-uniform flow conditions in the Rhine branches. A review of existing predictors showed that none of these could be directly used and therefore a new method was formulated. This new method incorporated the ideas on

reaction and relaxation (Allen, 1974; 1976a; 1976b), by using eq. 5.1 and 5.2 as its basis. However due to lack of measurement data on changes in grain size during flood events, the grain size had to be presumed constant. This resulted in the fact that not one equilibrium equation (eq. 5.2) but a set of two equilibrium equations had to be used, together with threshold values defining their use. The difference in the development of dune height and length also resulted in two different average adaptation constants, one for dune height and one dune length.

Together these necessary adaptations to the generic method resulted in three calculation models (a set of functions, thresholds and adaptation constants) for the Rhine branches (Appendix 5.II). There is a calculation model for the dune height and one for the dune length applicable in Section 1 and 2. And there is a calculation model for dune height, applicable in Section 3. A comparison between the simulations of the models and the observations from individual flood events in individual sections showed that the models accurately simulate the trends of dune development, the moments of maximum dune dimensions, and the occurrence of superposition of secondary dunes. Even the actual dune height and length was simulated accurately several cases.

The calculation models can therefore be used in future flood events to predict the dune dimensions in the three river sections used here. The basic method behind the calculation models should even make it possible to construct models for other parts of the Rhine branches or even to formulate a more general approach applicable throughout the Rhine, incorporating the grain-size as an additional parameter.

Acknowledgements

The author want to thank all persons and institutions that helped collecting and analysing the data used here. Special thanks goes out to the Meetdienst van de Directie Oost Nederland of the Dutch ministry of Waterways for carrying out the measurements during all the floods, and to Dr. J.H. van den Berg, Dr. E.A. Koster, Dr. M. Kleinhans, and Prof. Dr. Ir. L.C. van Rijn for their helpful suggestions on earlier drafts of this paper.

Notation

ν	=	kinematic viscosity
θ'	=	particle mobility parameter
β	=	roughness parameter
θ	=	Shields' parameter
Δ	=	specific density
ρ	=	water density [kgm^{-3}]
τ_b	=	bed shear stress [Nm^{-2}]
τ_b'	=	grain shear stress [Nm^{-2}]
θ_{cr}	=	critical Shields' parameter

ρ_s	=	sediment density [kgm^{-3}]
a	=	adaptation constant
C'	=	Chezy coefficient related to grains [$\text{ms}^{-0.5}$]
D	=	type of dune dimension
D_∞	=	equilibrium dune dimension
D^*	=	particle parameter
D_0	=	dune dimension at $t=0$
D_{50}	=	median grain size [m]
D_{65}	=	grain size at 65 percentile [m]
Fr	=	Froude number
g	=	gravitational acceleration [ms^{-2}]
H	=	dune height [m]
h	=	water depth [m]
H/L	=	dune steepness
i	=	slope
k	=	wave number [m^{-1}]
L	=	dune length [m]
t	=	time [s] (Δt however is in days)
T	=	particle mobility parameter
TC	=	temperature in Celsius
U	=	average flow velocity [ms^{-1}]
U_{top}	=	average flow velocity at dune crest [ms^{-1}]

References

- ALLEN, J.R.L. (1968) The nature and origin of bed form hierarchies. *Sedimentology*, 10, 161-182.
- ALLEN, J.R.L. (1974) Reaction, relaxation and lag in natural sedimentary systems: general principles, examples and lessons. *Earth-Science Reviews*, 10, 263-342.
- ALLEN, J.R.L. (1976a) Computational models for dune time-lag: an alternative boundary condition. *Sedimentary Geology*, 16, 255-279.
- ALLEN, J.R.L. (1976b) Computational models for dune time-lag: general ideas, difficulties and early results. *Sedimentary Geology*, 15, 1-53.
- ALLEN, J.R.L. (1976c) Computational models for dune time-lag: population structures and effects of discharge pattern and coefficient of change. *Sedimentary Geology*, 16, 99-130.
- ALLEN, J.R.L. (1978) Computational methods for dune time-lag: Calculations using Stein's rule for dune height. *Sedimentary Geology*, 20, 165-216.
- ANDERSON, A.G. (1953) The characteristics of sediment waves formed by flow in open channels. In: *Proceedings of the Third Midwestern Conference on fluid mechanics*, 379-395.
- FREDSØE, J. (1979) Unsteady flow in straight alluvial streams: modification of individual dunes. *Journal of Fluid Mechanics*, 91, 497-512.
- FREDSØE, J. (1980) The formation of dunes.
- FREDSØE, J. (1982) Shape and dimensions of stationary dunes in rivers. *Journal of the Hydraulics Division*, 108, 932-947.

- GILL, M.A. (1971) Height of sand dunes in open channel flows. *Journal of Hydraulic Engineering*, 97, 2067-2074.
- JULIEN, P.Y. & KLAASSEN, G.J. (1995) Sand-dune geometry of large rivers during floods. *Journal of Hydraulic Engineering*, 121, 657-663.
- KARIM, F. (1995) Bed configuration and hydraulic resistance in alluvial channel flows. *Journal of Hydraulic Engineering*, 121, 15-25.
- KARIM, F. (1999) Bed-form geometry in sand-bed flows. *Journal of Hydraulic Engineering*, 125, 1253-1261.
- KENNEDY, J.F. (1969) The formation of sediment ripples, dunes and antidunes. *Annual Review in Fluid Mechanics*, 1, 147-168.
- KENNEDY, J.F. & ODGAARD, A.J. (1990) An informal monograph on riverine sand dunes., 169, IIHR Ltd. Distribution, Iowa Inst. of Hydr. Res., University of Iowa, Iowa City, Iowa
- KLEINHANS, M.G. (2002) Sorting out sand and gravel: Sediment transport and deposition in sand-gravel bed rivers. *Netherlands Geographical Studies* 293,
- KLEINHANS, M.G. & TEN BRINKE, W.B.M. (2001) Accuracy of cross-channel sampled sediment transport in large sand-gravel-bed rivers. *Journal of Hydraulic Engineering*, 127, 258-269.
- KLEINHANS, M.G., WILBERS, A.W.E., DE SWAAF, A., & VAN DEN BERG, J.H. (2002) Sediment supply-limited bedforms in sand-gravel bed rivers. *Journal of Sedimentary Research*, 72, 629-640.
- MEYER-PETER, E. & MÜLLER, R. (1948) Formulas for bedload transport. In: *Proceedings of the second IAHR congress in Stockholm, Sweden* 2, 39-64.
- MOHRIG, D. (1994) Spatial evolution of dunes in a sandy river. University of Washington, 120 pp.
- RANGA RUJU, K.G. & SONI, J.P. (1976) Geometry of ripples and dunes in alluvial channels. *Journal of Hydraulic Research*, 14, 241-249.
- SHINOHARA, K. & TSUBAKI, T. (1959) On the characteristics of sand waves formed upon the beds of open channels and rivers. *Reports of Research Institute for Applied Mechanics*, 7, 15-45.
- STEIN, R.A. (1965) Laboratory studies of total load and apparent bed load. *Journal of Geophysical Research*, 70, 1831-1842.
- TEN BRINKE, W.B.M. (1997) De bodemsamenstelling van Waal en IJssel in de jaren 1966, 1976, 1984 en 1995., 97.009, RIZA: Rijksinstituut voor integraal zoetwaterbeheer en afvalwaterbehandeling, Arnhem
- TEN BRINKE, W.B.M., KRUYT, N.M., KROON, A., & VAN DEN BERG, J.H. (1999) Erosion of sediments between groynes in the Waal River due to navigation traffic, measured in situ. In: *Fluvial Sedimentology VI, Special Publication of the International Association of Sedimentologists* (Ed. by N.D. Smith & J. Rogers), 28, 147-160.
- TEN BRINKE, W.B.M., SCHULZE, F.H., & VAN DER VEER, P. (2003) Sand exchange between groyne field beaches along the Rhine and the main channel: the impact of navigation traffic versus river flow. *River Research and Applications*, submitted.
- TNO-NITG (2000) Descriptions and photographs of the vibrocores in the Niederrhein, Bovenrijn, Waal and Panterdensch Kanaal., Dutch Institute for Applied Geology (TNO-NITG), The Netherlands,
- TSUCHIYA, A. & ISHIZAKI, K. (1967) In: *Proceedings of the 12th congress of the international association of hydraulic research* No. 1, 479-486.
- VAN DEN BERG, J.H. & VAN GELDER, A. (1993) Prediction of suspended bed material transport in flows over silt and very fine sand. *Water Resources Research*, 29, 1393-1404.
- VAN DER VEEN, R. (2002) Calibratie en validatie van een hydraulisch model (SOBEK)., RIZA, Arnhem, The Netherlands,
- VAN RIJN, L.C. (1984) Sediment transport; Part 3: bed forms and alluvial roughness. *Journal of Hydraulic Engineering*, 110, 1733-1754.
- VAN RIJN, L.C. (1989) *Handboek sediment transport by currents and waves.*, report H461, Delft Hydraulics, Delft
- WILBERS, A.W.E. & TEN BRINKE, W.B.M. (2003) The response of subaqueous dunes to floods in sand and gravel bed reaches of the Dutch Rhine. *Sedimentology*, in press.
- YALIN, M.S. (1964) Geometrical properties of sand waves. *Journal of the Hydraulics Division*, 90, 105-119.
- YALIN, M.S. (1972) *Mechanics of sediment transport*. Pergamon Press, Oxford

Appendix 5.I

Shinohara & Tsubaki (1959)

Shinohara & Tsubaki (1959) created predictors for both dune height and dune length from their measurements in the Hii river. The predictors are valid in a range of θ' between 0.05 and 0.3. Shinohara & Tsubaki (1959) reported these predictors as two diagrams and Van Rijn (1989) used regression analyses to extract these equations from both diagrams:

$$H = 2.1 * h (\theta')^{1.2} \quad (5.I.1)$$

$$L = 4.2 * h \quad (5.I.2)$$

$$\theta' = \frac{\tau_b'}{(\rho_s - \rho)gD_{50}} \quad (5.I.3)$$

$$\tau_b' = \rho g \left(\frac{U}{C'} \right)^2 \quad (5.I.4)$$

$$C' = 18 \log \left(\frac{12h}{D_{65}} \right) \quad (5.I.5)$$

with h = water depth [m]; θ' = particle mobility parameter; ρ_s = sediment density [kgm^{-3}]; ρ = water density [kgm^{-3}]; g = gravitational acceleration [ms^{-2}]; D_{50} = median grain size [m]; τ_b' = grain shear stress [Nm^{-2}]; U = average flow velocity [ms^{-1}]; C' = Chezy coefficient related to grains [$\text{ms}^{-0.5}$]; D_{65} = grain size at 65 percentile [m].

Tsuchiya & Ishizaki (1967)

Tsuchiya & Ishizaki (1967) created predictors for both dune height and dune length from theoretical stability analyses.

$$H = h * Fr^2 * \left(\left(1 - \frac{1}{\beta^2} \right) + 2(1 - \beta) \right) \quad (5.I.6)$$

$$\beta = \frac{U}{U_{top}} \text{ about } 0.9 - 1.0 \text{ in } Fr \ll 1 \quad (5.I.7)$$

$$Fr = \frac{U}{\sqrt{gh}} \quad (5.I.8)$$

$$k = \frac{2\pi}{L} \quad (5.I.9)$$

$$Fr = \sqrt{\frac{2}{kh} \tanh(2kh)} - \sqrt{\frac{1}{kh} \tanh(kh)} \quad (5.I.10)$$

with Fr = Froude number; β = roughness parameter; U_{top} = average flow velocity at dune crest [ms^{-1}]; k = wave number [m^{-1}].

Allen (1968)

Allen (1968) created predictors for both dune height and dune length from measurements in several flumes, rivers and estuaries. The predictors are valid in a range of h between 0.6 and 40 m.

$$H = 0.086h^{1.19} \quad (5.I.11)$$

$$L = 1.16h^{1.55} \quad (5.I.12)$$

Van Rijn (1984)

Van Rijn (1984) created predictors for both dune height and dune length from measurements in several rivers and flumes. The predictors are valid in a range of T between 0 and 22 and of h between 0.1 and 16 m.

$$\frac{H}{h} = 0.11 \left(\frac{D_{50}}{h} \right)^{0.3} (1 - e^{-0.5T}) (25 - T) \quad (5.I.13)$$

$$L = 7.3h \quad (5.I.14)$$

$$T = \frac{\theta - \theta_{cr}}{\theta_{cr}} \quad (5.I.15)$$

$$\theta = \frac{\tau_b}{(\rho_s - \rho)gD_{50}} \quad (5.I.16)$$

$$\tau_b = \rho g h i \quad (5.I.17)$$

$$\theta_{cr} = f(D_*) \quad \text{relations listed by Van den Berg \& Van Gelder (1993)} \quad (5.I.18)$$

$$D_* = \left(\frac{(\Delta - 1)g}{\nu^2} \right)^{\frac{1}{3}} D_{50} \quad (5.I.19)$$

$$\Delta = \frac{\rho_s}{\rho} \quad (5.I.20)$$

$$\nu = (1.14 - 0.031(TC - 15) + 0.00068(TC - 15)^2) * 10^{-6} \quad (5.I.21)$$

with T = particle mobility parameter; θ = Shields' parameter; τ_b = bed shear stress [Nm^{-2}]; i = slope; θ_{cr} = critical Shields' parameter; D_* = particle parameter; Δ = specific density; ν = kinematic viscosity; TC = temperature in Celsius.

Appendix 5.II

In all models below Δt is in days

Dune height around Pannerdensche Kop

Initiation:

measured height or eq. 5.I.6

Rising Flood

If $\tau_b < 10$ Then

$$H(t) = H_{(t-1)} + (1 - e^{-0.12\Delta t})(H_{\infty,t} - H_{(t-1)})$$

with $H_{\infty,t}$ = eq. 5.I.6

If $\tau_b > 10$ and $\tau_b > 13$ (falling flood) Then

$$H(t) = H_{(t-1)} + (1 - e^{-0.12\Delta t})(H_{\infty,t} - H_{(t-1)})$$

with $H_{\infty,t}$ = eq. 5.I.13

Falling Flood

If $\tau_b < 13$ Then

$$H(t) = H_{(t-1)} + (1 - e^{-0.12\Delta t})(H_{\infty,t} - H_{(t-1)})$$

with $H_{\infty,t}$ = eq. 5.I.6

If $\tau_b < 10$ Then

superposition

with $H(t) = H_{\infty,t}$ (eq. 5.I.6)

If $H/L < 0.01$ Then

primary dunes disappear and secondary superimposed dunes become primary

Dune length around Pannerdensche Kop

Initiation:

measured length or eq. 5.I.10

Rising Flood

If $\tau_b < 10$ Then

$$L(t) = L_{(t-1)} + (1 - e^{-0.05\Delta t})(L_{\infty,t} - L_{(t-1)})$$

with $L_{\infty,t}$ = eq. 5.I.10

If $\tau_b > 10$ Then

$$L(t) = L_{(t-1)} + (1 - e^{-0.05\Delta t})(L_{\infty,t} - L_{(t-1)})$$

with $L_{\infty,t}$ = eq. 5.I.14

Falling Flood

If $H/L > 0.01$ Then

$$L(t) = L_{(t-1)} + (1 - e^{-0.05\Delta t})(L_{\infty,t} - L_{(t-1)})$$

with $L_{\infty,t}$ = eq. 5.I.14

If $\tau_b < 10$ Then

superposition

with $L(t) = L_{\infty,t}$ (eq. 5.I.10)

If $H/L < 0.01$ Then

primary dunes disappear and secondary superimposed dunes become primary

Dune height near Druten

Initiation:

measured height or eq. 5.I.11

Rising Flood

If $\tau_b < 7$ Then

$$H(t) = H_{(t-1)} + (1 - e^{-0.12\Delta t})(H_{\infty,t} - H_{(t-1)})$$

with $H_{\infty,t} = \text{eq. 5.I.11}$

If $\tau_b > 7$ and $\tau_b > 7$ (falling flood) Then

$$H(t) = H_{(t-1)} + (1 - e^{-0.12\Delta t})(H_{\infty,t} - H_{(t-1)})$$

with $H_{\infty,t} = \text{eq. 5.I.13}$

Falling Flood

If $\tau_b < 7$ Then

$$H(t) = H_{(t-1)} + (1 - e^{-0.12\Delta t})(H_{\infty,t} - H_{(t-1)})$$

with $H_{\infty,t} = \text{eq. 5.I.11}$

Part 2 The hydraulic roughness of subaqueous dunes

In part 2 of this thesis (Chapters 6 & 7) the main objective is the prediction of the hydraulic roughness caused by dunes using the characteristics of dune shape, size, and flow conditions. Dunes cause an increase in hydraulic roughness because they protrude from the bed into the flowing water, and because of their asymmetric longitudinal shape. The lee-side of a dune is so steep that the flow cannot follow it and separates from the bed. This flow separation creates large turbulent bursts in the flow which dissipate energy away from the flow thereby slowing it down. The amount of energy dissipation and thus the hydraulic roughness is probably related to the size and shape of the flow separation zone. In Chapter 6 this size and shape of the flow separation zone is therefore analysed in different conditions and for different bedforms. The relations between bedform shape and size and the shape and size of the flow separation zone are then used in Chapter 7.

In Chapter 7 three existing predictors of the hydraulic roughness of dunes are adapted to incorporate new knowledge on, a) which dune characteristics should be used, b) how grain roughness is to be treated, and c) how to sum the hydraulic roughness of primary and superimposed secondary dunes. The adapted predictors are tested to assess if they perform better than the original predictors. Finally, a stepwise method is described to predict the hydraulic roughness in the Rhine branches. In Chapter 8, the results of part 1 and 2 are brought together by combining the prediction methods of dune development and of hydraulic roughness.

6 Invariable flow separation zone characteristics at the lee sides of subaqueous bedforms

Abstract

At the lee-side of a subaqueous dune a flow separation zone exists, where large scale turbulence is created dissipating energy. It is therefore likely that the size and shape of this flow separation zone is directly related to the hydraulic roughness of the dune. To investigate which flow characteristics or dune dimensions influence the size and shape of the flow separation zone, measurements, previously reported in literature, were compiled and analysed.

The results show that the shape of flow separation zones is independent of flow conditions and dune dimensions, as in streamwise direction the zero velocity line always has an angle of 10 ± 1 degrees. The size of flow separation zones is directly related to the height of the flow separation point, which usually coincides with the brinkpoint of a dune. However, on sinuous or low-angle dunes it is likely that the flow will separate at the point on the lee-side where the slope-angle exceeds 10 degrees.

6.1 Introduction

Subaqueous dunes are present on the bed of many rivers. They form patterns of repetitive triangular undulations, several meters to hundreds of meters long and decimetres to meters high (Ashley, 1990), and form major roughness elements in open channel flow. This hydraulic roughness is caused by the generation of turbulence at the steep downstream side of the dunes. This lee-side of a dune is generally so steep that the flow is not able to adjust to the unfavourable pressure gradient caused by the changes in bed elevation and as a result separates, creating a flow separation zone (fig. 6.1; Buckles *et al.*, 1984; Chang, 1970b). The amount of turbulence that is created in this flow separation zone is probably linked to the general flow conditions and the shape and size of the flow separation zone (Vanoni & Hwang, 1967; Engel, 1981; Kornman, 1995; Yoon & Patel, 1996).

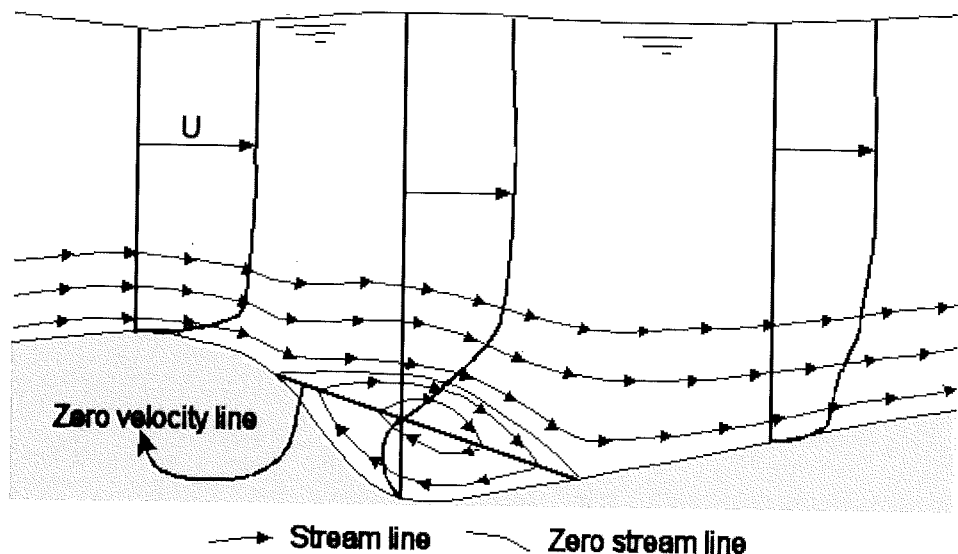


Figure 6.1: Example of the average flow over a dune (not to scale). The arrow lines indicate stream lines, while vertical lines show the location of velocity profiles.

The most common dunes are shaped as depicted in fig. 6.2, a gentle stoss-side of a few degrees leading up to a dune crest. Then, from the crest going down, a gentle curve to a brinkpoint where the lee-side angle suddenly changes into the angle of repose. And finally, this steep slope slowly changes into a gentler slope near the bottom of the trough. In time averaged flows, a flow separation zone starts at the brinkpoint (separation point) which is created by this flow separation. Due to separation, the flow shear at the bed becomes zero, which means bedload material can only move further downstream if the critical internal shearing threshold is surpassed by gravity whereby the material

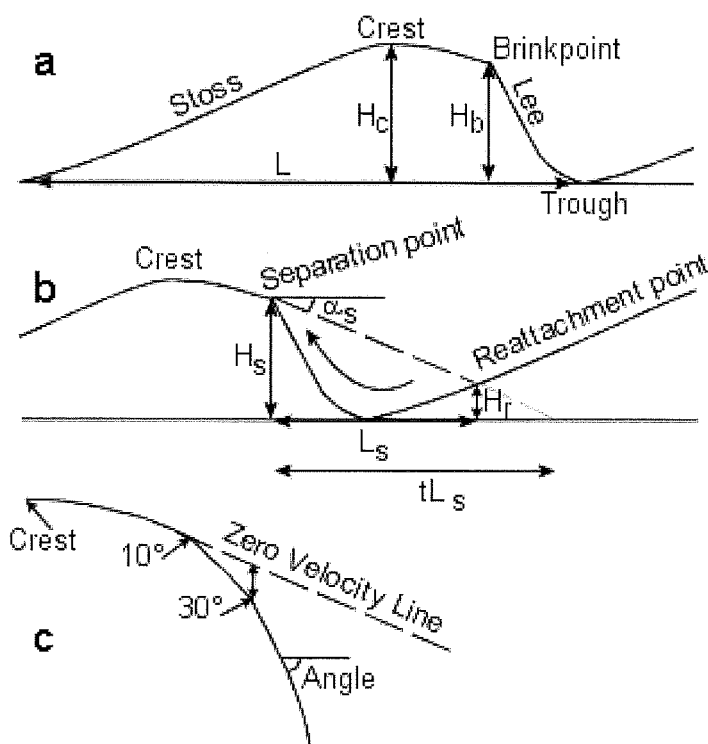


Figure 6.2: a) definition of the bed form characteristics.

b) definition of the separation zone characteristics.

c) detail of the upper part of a smoothly curving lee-side.

In all three figures the vertical scale is exaggerated compared to the horizontal scale.

avalanches down the lee-side creating a slope at the angle of repose (Van den Berg, 1982). The flow reattaches again somewhere on the lower stoss-side of the next dune at the reattachment point (fig. 6.2b). Between these two points, averaged over time, a zone of upstream moving flow is present, and at the boundary between the downstream and upstream moving water (fig. 6.1), large scale turbulence is created (Raudkivi, 1963; Chang, 1970b; Vittal *et al.*, 1976; Simpson, 1989; Kadota & Nezu, 1999).

The size and shape of the flow separation zone is probably governed by flow conditions and dune characteristics, but it is not clear how. Many investigators (Yalin, 1964; Vanoni & Hwang, 1967; Vittal, 1972; Vittal *et al.*, 1977; Engelund, 1977; Van Rijn, 1984) tried to predict the hydraulic roughness by using general dune characteristics instead of the size and shape of the flow separation zone. To a certain extent this approach may produce reasonable results (Julien *et al.*, 2002). However, in view of the better representation of the hydraulics involved, it may be expected that introducing flow separation zone related dune characteristics will provide an improvement. Therefore, the purpose of the present analysis is to investigate which characteristics of flow, and which dune dimensions govern the shape and size of the flow separation zone. The analysis involved a

parameterisation of flow separation zones from published data on flow measurements over various bedforms and other obstacles in both flumes and rivers (Table 6.1).

Table 6.1: Summary of the collected data sources. The bedforms are classified in 6 types, Backward step, Sinuous dune, Solid dune (dunes which are solidified forms of migration dunes, using glue, resin or cement, or artificial dune models with a more natural shape than Triangle dunes), Trench (not really a bedform but in shape similar to backward steps), Triangle dune (an artificial dune model with a triangular shape) and Migrating sand dune (dunes that are actively migrating downstream during the measurements). The abbreviations are used in fig. 6.4.

Reference	Abbreviation	Location / test situation	Data type	Bedform type
Etheridge & Kemp (1978)	ek	Flume	Paper	Backward step
Nakagawa & Nezu (1987)	nn	Flume	Paper	Backward step
Raudkivi (1963)	r	Flume	Paper	Backward step
Buckles et al. (1984)	bha	Flume	Paper	Sinuous dune
Bennett & Best (1995)	bb	Flume	Digital	Solid dune
Kadota & Nezu (1999)	kn	Flume	Digital	Solid dune
Raudkivi (1966).	r	Flume	Paper	Solid dune
Vanoni & Hwang (1967)	vh	Flume	Paper	Solid dune
Alfrink & Van Rijn (1983)	ar	Flume	Paper	Trench
Kornman (1995)	k	Flume	Report	Triangle dune
Lyn (1993)	L	Flume	Paper	Triangle dune
McLean <i>et al.</i> (1994)	mnw	Flume	Paper	Triangle dune
Rifai & Smith (1971)	rs	Flume	Paper	Triangle dune
Van Mierlo & De Ruiter (1988)	mr	Flume	Report	Triangle dune
Vittal <i>et al.</i> (1976)	vr	Flume	Paper	Triangle dune
Kostaschuk & Villard (1996)	kv	Lower Fraser River/Estuary, Canada	Paper	Migrating sand dune
Johns <i>et al.</i> (1993)	jsx	Taw Estuary, England	Paper	Migrating sand dune

6.2 Review of past research

In the past, a great deal of attention was paid to the structure of flows over backward-steps, bedforms of various shapes and other obstacles, mostly in flume experiments, and sometimes in river or estuarine situations (Table 6.1). These measurements were done for various reasons: a) to study hydraulic roughness, turbulence structures, or fluid-sediment interactions over bedforms, b) to test new equipment or modelling techniques, and c) to investigate the relation between dune dimensions or flow conditions and the size of the flow separation zone. The results of these latter investigations are mentioned here to enable comparison with the findings of the study.

6.2.1 Separation length versus dune dimensions

According to several investigators, there is a strong relation between dune height and separation length (Engel, 1981; Yoon & Patel, 1996). Many report a separation length (L_s), 3-5 times the dune height in case of dunes, and 5-10 times the height in case of backward steps. Several investigators therefore introduced the Dimensionless Separation

Length (DSL) as an almost constant quotient of L_s and H_c (L_s/H_c). Engel (1981) found a relation between the DSL and the form steepness (H/L), showing that the separation length of dunes (with the same height) decreases as the form steepness increases up to about 0.07 after that the DSL becomes constant at about 4.3 (fig. 6.7b).

6.2.2 Separation length versus flow and grain size

Other investigations have found that the separation length is also related to flow conditions and to the grain size of the bedform material. Karahan & Peterson (1980) suggested a relation between the separation length and the Froude number (Fr).

$$Fr = \frac{U}{\sqrt{gh}} \quad (1)$$

where U = average flow velocity [m/s], g = gravitational acceleration [m/s^2], and h = water depth [m]. This was opposed, however, by Engel (1981) who showed that the relation of Karahan & Peterson (1980) was the result of the low Reynolds numbers (Re) during the measurements and not by the low Froude numbers.

$$Re = \frac{Uh}{\nu} \quad (2)$$

where ν = kinematic viscosity [-]. Engel (1981) and Kadota & Nezu (1999) demonstrated that in cases with solitary bedforms (which means that only one bedform is present in a flume, for example a backward step) and Reynolds numbers below about 20000, the DSL decreases with increasing Reynolds number, reaching a constant value of about 6.5 at $Re > 20000$ (fig. 6.7a). In cases with multiple bedforms (which means that repetitive forms are present, for example dunes), they showed that the DSL is about 4.5 at any Reynolds number.

A relation between the DSL and grain size was reported by Engel (1981) and Yoon & Patel (1996), who showed that, in cases where the dune height remains constant, an increase in grain size results in a decrease of separation length (fig. 6.7b). This relation is physically based on the fact that small roughness elements create small-scale turbulence, dissipating energy, and thus hinder flow separation. In aeronautics, for example, this effect is used to prevent or control separation, by introducing small protrusions on airplane wings, preventing loss of lift Chang (1970a).

6.3 Parameterisation of the flow separation zone

The parameterisation of the size and shape of flow separation zones was primarily done by calculating (fig. 6.2b); the height of the separation point (H_s [m]), the height of the reattachment point (H_r [m]), the separation length (L_s [m]) as the distance between the separation point and the reattachment point; and the angle of the zero velocity line (α_s). This zero-velocity-line connects the points between the separation point and the reattachment point where the time-averaged (minutes) flow is going neither upstream nor downstream ($U_x = 0$). Zero velocity points were determined from vertical velocity

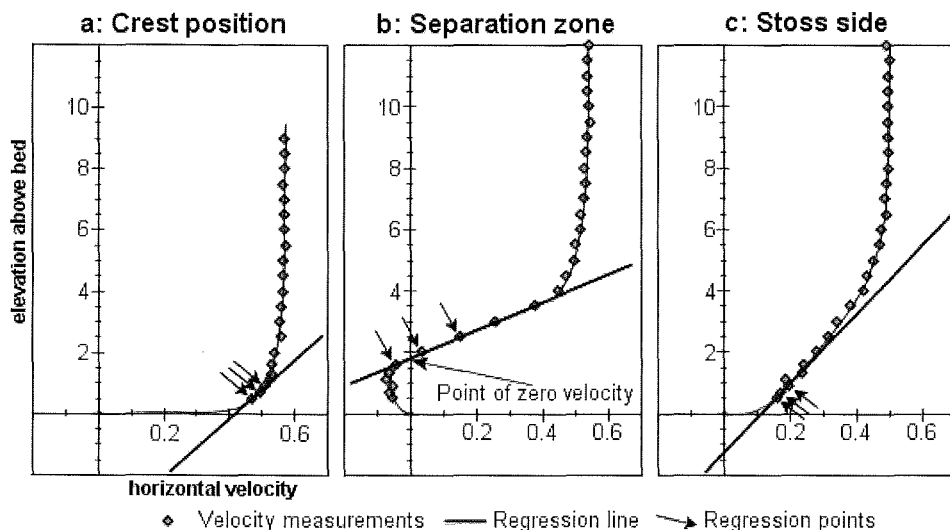


Figure 6.3: The point of zero velocity is calculated from vertical velocity profiles by calculating a regression line through the three points nearest to the zero velocity.

- a) a typical velocity profile near the crest of a dune.
- b) a typical velocity profile in the separation zone.
- c) a typical velocity profile on the stoss-side of a dune downstream of the reattachment point.

profiles that were measured and reported by previous investigations (Table 6.1). These velocity profiles were located in and around the flow separation zone (fig. 6.3), and the height of the zero velocity point was computed as follows: in every vertical velocity profile a linear regression line was drawn through the three measurement points closest to the zero velocity point. In vertical velocity profiles situated outside the region of separated flow (fig. 6.3a and c), these points were the lowest points, near the bed. In the region of flow separation (fig. 6.3b), one of the three points had a negative velocity and two points a positive velocity. The height at which this linear regression line indicated a zero streamwise velocity was defined as the height of the zero velocity point (fig. 6.3b).

In case of a vertical profile inside the flow separation zone, a zero velocity point is located above the bed, but outside this zone, zero velocity is always located at the bed surface. The method used here however produced virtual zero velocity points below the bed surface in regions outside the flow separation zone (fig. 6.3a & c). These virtual points are theoretically incorrect, but helped to determine the positions of the separation and reattachment points as these are points where the zero velocity coincides with the bed surface even in the calculation method used here. If a virtual zero velocity point just outside the flow separation zone is connected with a zero velocity point just inside the flow separation zone, the intercept of this line with the bed determines the position of the separation or reattachment point.

Finally the angle of the zero velocity line was determined by representing this line as a straight line connecting separation and reattachment point and calculating the angle it had with the average bed surface (fig. 6.2b).

6.3.1 Data quality

The quality of the data used in this study is expected to vary between the various sources (Table 6.1). Measurements came from flume experiments with a wide range of experimental setups and measurement equipment, or even from field measurements where accurate positioning of the measurement equipment is difficult. Some of the data was not even available as (digital) tables, but only as graphs, making accurate determination of zero velocity points difficult and diminishing the quality of the analyses. Therefore, the quality was classified as Sufficient, Good or Excellent, based on the average spacing between velocity profiles in the separation zone, the elevation above the bed of the lowest measurement point, the average distance between measurement points, and the quality of the measurement situation, equipment, and data presentation. The factor of the quality of the measurement situation, equipment, and data presentation was introduced to take into account unreliable equipment that was used in some cases, or the inaccurate representation of the data in the paper.

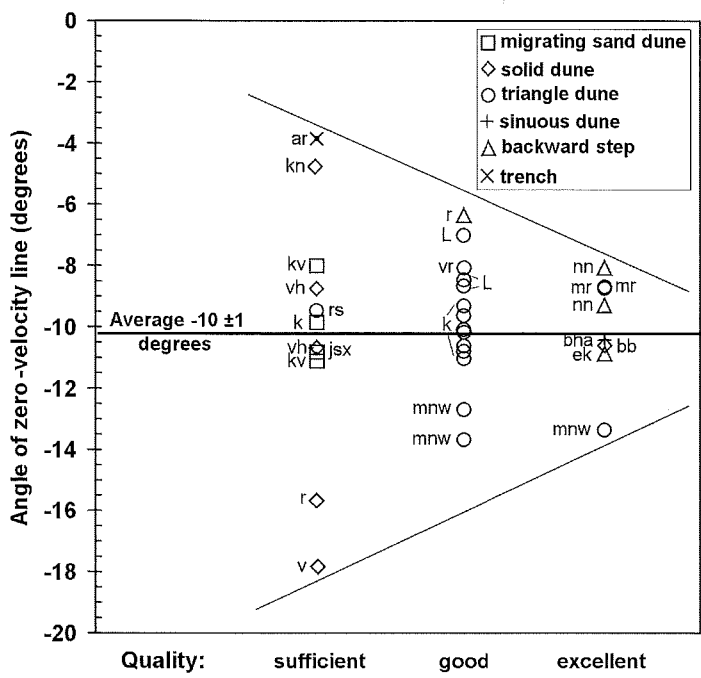


Figure 6.4: The angle of the zero velocity line in all measurements plotted against the quality of the data (see table 6.1 for abbreviations).

6.4 Results

When the quality of the analysed data is taken into account, fig. 6.4 shows that the angle of the zero velocity line is constant and independent of flow condition and bedform type. The angle averages around 10 degrees (± 1 degree) and the variation decreases as the

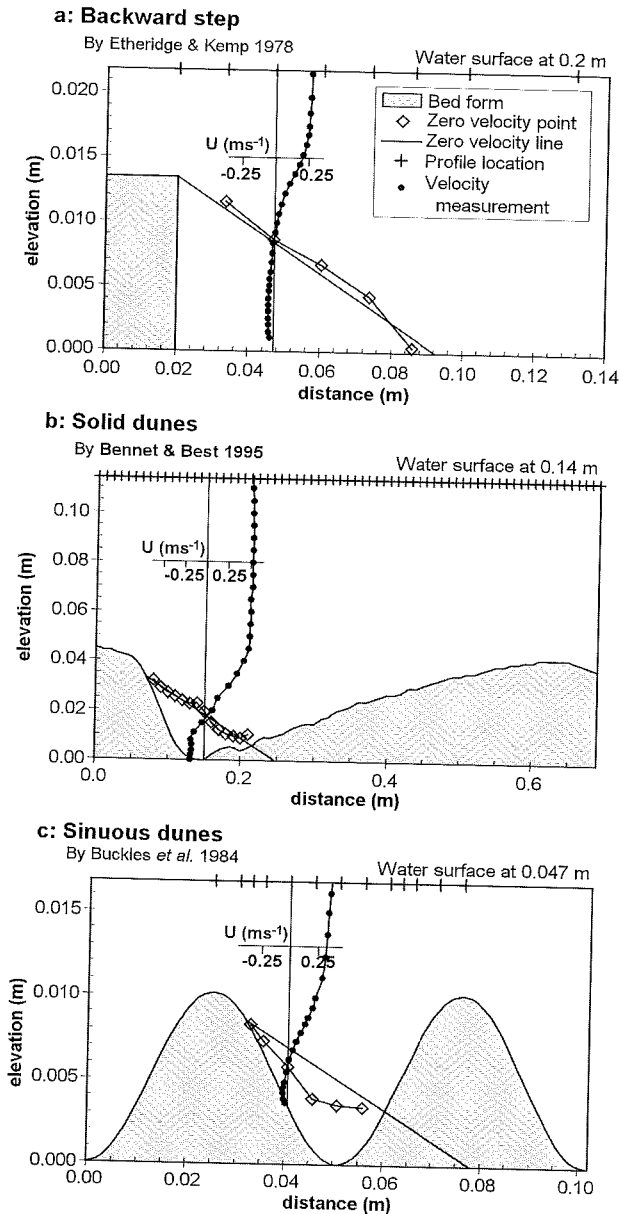


Figure 6.5: Examples of the shape of the flow separation zone in case of:
a) a solitary backward step.

b) multiple solid dunes.

c) a sinuous dune for a case without a free water surface.

The points along the vertical lines represent examples of velocity profiles which were measured at every location marked at the top of each figure. The points along the diagonal lines indicate the zero-velocity points at each velocity profile location. The diagonal lines approximate the zero-velocity lines by connecting the separation point and the reattachment point.

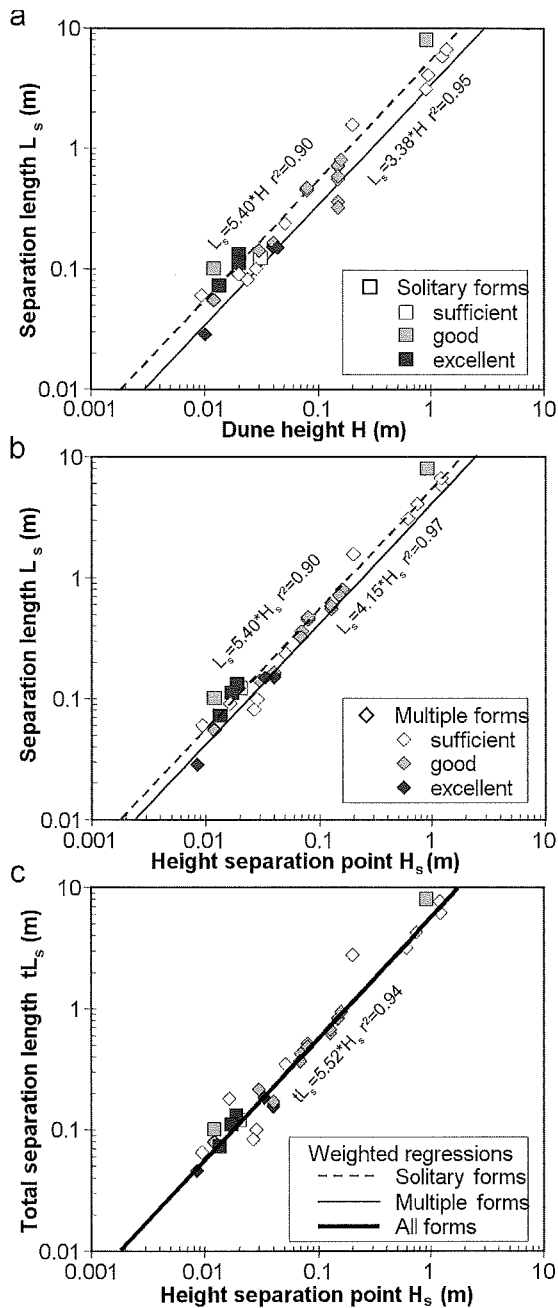


Figure 6.6: a) relation between the height of an obstacle and the separation length.

b) relation between the separation height and the separation length.

c) the relation between separation height and total separation length.

Solitary forms are represented by squares and multiple forms by diamonds, the grey filling indicating the quality of the data.

quality of the measurements increases. The zero velocity line itself is almost straight or sometimes a little convex (or in cases without a free water surface concave). Two good examples of similar flow separation zone shapes in very different conditions are shown in fig. 6.5a and b, while fig. 6.5c shows a flow separation zone in a case without a free water surface.

Figure 6.6a shows that the separation length is strongly related to the height of the bedform, but that there are different relations for solitary and multiple bedforms. These relations become stronger (fig. 6.6b) if not dune height is used but height of the separation point (brinkpoint height). The strongest relation (fig. 6.6c) is found between separation height and total separation length (tL_s , fig. 6.2b), which is the length of the separation zone, if the zero velocity line is extended all the way to the horizontal plane (fig. 6.2b). In that case, the data related to the solitary and multiple forms clearly plot closely together and have only one relation, because it treats the multiple forms as solitary individuals by ignoring the stoss-sides of the next forms.

The relations between DSL, Reynolds number, form steepness, and grain size are shown in fig. 6.7a & b. The present data analysis seems to support the relation between Reynolds number and solitary forms although there is much scatter (fig. 6.7a). The relations with form steepness and grain size are not reproduced by the present analysis (fig. 6.7b).

6.5 Discussion

The analysis of flow separation zones in this study indicates that the shape and size of such a zone only depends on the height of the separation point (brinkpoint). No other dune dimensions or any characteristics of flow influences the shape or size of the flow separation zone significantly. The strong relation between separation height and separation length (fig. 6.6), reported earlier and also found here, is directly caused by the fact that the angle of the zero velocity line is constant in any condition (fig. 6.4). The relation is stronger with separation height than with dune height because the separation point is also the point where the zero velocity line starts. The fact that two relations appear in figs 6.6a and b is not caused by any difference in flow separation between solitary and multiple form, but by the fact that with multiple forms, the zero velocity line is cut off early by the stoss side of a new bedform instead of going down all the way to the bottom. Both relations collapse into one if the total separation length is used because it treats all forms as solitary.

The differences in Dimensionless Separation Lengths, between solitary and multiple forms, also appear when they are related to the Reynolds number (fig. 6.7a). However, the fact, reported by Kadota & Nezu (1999), that the DSL decreases as Reynolds increases (up to about 20000) has no major consequences in most situations especially in natural settings where Reynolds numbers are normally over 10^5 .

The data points from this analysis in figure 6.7b do not show the relations between DSL and form steepness and grain size, as reported by Engel (1981). In the tests used in this analysis, the average form steepness (H/L) was higher than used by Engel indicating that his relations may hold for smaller values of form steepness but not for higher. Also, in

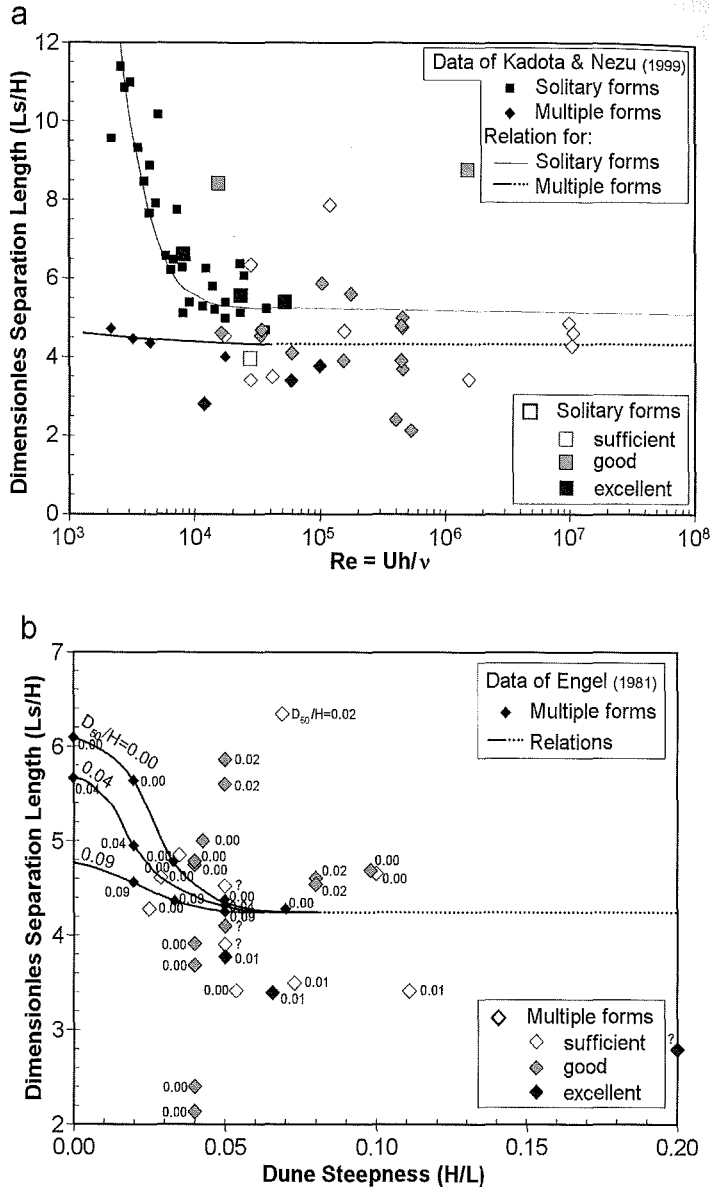


Figure 6.7: a) relation between dimensionless separation length (L_s/H) and the Reynold's number. The original figure was created by Kadota & Nezu (1999), but the results of the present analysis have been added. Solitary forms are thereby represented as squares and multiple forms as diamonds, the grey filling indicating the quality of the data. The small squares and diamonds are the data points of Kadota & Nezu, (1999) and the lines are the relations they created.

b) relation between dimensionless separation length (L_s/H) and form steepness (H/L). the original figure was created by Engel (1981), but the results of the present analysis have been added. Only the tests with multiple forms were used. The numbers beside each point show the dimensionless grain size (D_{50}/H), and the lines show the relations created by Engel (1981).

most of the tests used here, no sand grains were glued to the solid forms, and therefore the value of D_{50}/H was 0 in many cases. However, it is also possible that Engel's relation between the DSL and the form steepness is strong because he only changed the dune length of his forms. By increasing the length, while keeping the height and angle of the lee face the same, he increased the space inside the trough creating forms that began to resemble solitary forms, which therefore had much longer separation zones. In his experiments Engel made the grains coarser relative to the dune height, which probably meant that the flow began separating not at the top of his forms, but progressively lower on the lee-side, due to small scale turbulence, thereby decreasing the separation length.

6.5.1 Point of flow separation

In the introduction it was stated that the most common dunes slope smoothly down from the crest to the knick of the brinkpoint, where the slope suddenly increases up to the angle of repose, which is about 30 degrees in sand. Therefore, most investigators assume that the flow separates at an angle of about 30 degrees and thus construct their artificial dunes with this 30 degree lee-side. However, in natural conditions dunes have been found that did not possess lee-sides with 30 degree angles (Kostaschuk & Villard, 1996; Best & Kostaschuk, 2002). This may suggest that flow separation did not occur along these dunes. However, these dunes did generate a hydraulic roughness, that was much higher than could be expected without a flow separation (Van den Berg & Van Gelder, 1998). This indicates that these low angle dunes might have some sort of semi-permanent flow separation, or that the flow separates at much lower angles than 30 degrees.

In order to investigate these low-angle dunes with no flow separation but a higher than expected roughness, Best & Kostaschuk (2002) analysed the flow over a down-scaled model of such a low-angle dune from the Fraser River. They found no permanent flow reversal, only an occasional turbulent eddy shedding from the front of the dune, temporarily disturbing the flow. Therefore, they concluded that permanent flow separation does not occur over low-angle dunes but instead is replaced by a region of intermittent flow reversal which could explain the higher hydraulic roughness.

On the other hand, on a curving slope (fig. 6.2c), the flow may separate at any angle that becomes too high for the flow to follow. As the separated flow moves downstream at an angle of 10 degrees in the zero-velocity line, it is logical to assume that at the separation point, the angle of the lee-side slope is also about 10 degrees. This assumption is supported by Henn & Sykes (1999), who state that flow, over sinuous forms, separates when the form steepness (H/L) exceeds 0.05. A quick calculation shows that a sinuous form with a steepness of 0.06 or higher, has a point on its lee-side where the slope-angle exceeds 10 degrees. A point on the lee-side where the slope-angle exceeds 30 degrees is not present until a steepness of the sinuous forms exceeds 0.18, indicating the flow has to separate at a much lower angle than 30 degrees. The assumption of separation at a lower angle than 30 degrees is also supported by experiments of Formica (1955, in Te Chow, 1959). Formica shows that the hydraulic roughness decreases as the angle of a sudden change in flow width decreases from 90 degrees to 14 degrees and that in case of 14 degrees there is still some flow separation.

The tests used in this study, including those of Kostaschuk & Villard (1996) only showed a flow separation point at an angle higher than 25 degrees, not even if the forms had a curved lee-side, indicating that the conclusions of Best & Kostaschuk (2002) might be more correct than the assumption of separation at 10 degrees. However, there are two possible objections to this premature conclusion. First, re-examining the measurements of Johns *et al.* (1993) and Kostaschuk & Villard (1996) suggests that they did not find the flow separation zone because they did not measure close enough to the bed. Some of the low angle dunes could have had a flow separation zone of a few decimetres high, assuming flow separation at the 10 degrees point. However, the flow-velocity measurements that were done never reached inside these zones because the lowest measurement point was always 0.5 m above the bed, far above the possible zero velocity line.

A second possible reason that a flow separation point with an angle higher than 25 degrees was found, could be in the size of the bedforms during the flume experiments. These bedforms were only centimetres to decimetres high, and the zone defined by the point where the lee side is 10 degrees, the zero velocity line and the point of 30 degrees (fig. 6.2c), is in such a case at most a few millimetres high. This is much too small to measure any flow velocity that might represent a returning flow. Possibly this size problem also prevented Best & Kostaschuk (2002) to find a permanent flow separation zone over their down-scaled low angle dune. The separation zone in their model situation would, if a separation angle of 10 degrees is assumed, only extend 3.4 millimetres above the bed while the vertical velocity profile at this location indicates that the viscous sub-layer would be about 2 mm high. The measurements inside this probable separation zone therefore show the flow behaviour of the viscous sub-layer instead of the turbulent regime above it.

Reviewing all the indications and opinions, it is concluded that the flow separates at a slope-angle of about 10 degrees than at a higher angle, and that the idea that low-angle dunes only have intermittent flow separation is probably not correct. If the bedforms are measured in detail, and the flow separation point (in most cases the brinkpoint) is determined from these measurements, the shape and size of the flow separation zone can be calculated from the triangle between the separation point, the reattachment point, and the 10 degree angle of the zero velocity line.

6.6 Conclusions

The size and shape of the flow separation zone is governed by the height of the flow separation point, as the zero velocity line has a constant angle of 10 degrees (± 1 degree), independent of any difference in bedform characteristics or flow conditions. In theory, grain size may have some influence on the height of the flow separation zone because at large grain sizes, small-scale turbulence is created which results in a lowering of the separation height, but this was not shown by the results of the analysis.

The flow separation point is probably located at that point on a lee-slope where the angle of the slope exceeds 10 degrees. On dunes, this point normally coincides with the brinkpoint, where the loss of flow shear results in avalanching material, creating a break

from a gentle to a steep slope. The fact that in some investigations no permanent flow separation zones were found on low angle dunes was probably caused by measurement and scaling problems. Therefore the assumption that low-angle dunes only have intermittent flow separation causing hydraulic roughness is probably incorrect.

Acknowledgments

The author wishes to thank all persons that helped with the revisions of earlier drafts of this paper: Dr. J.H. van den Berg, Dr. E.A. Koster, Dr. M. Kleinhans, and Prof. Dr. Ir. L.C. van Rijn.

Notation

D_{50}	=	medium grain-size [m].
Fr	=	Froude number [-]
g	=	gravitational acceleration [ms^{-2}]
H	=	dune crest height [m]
h	=	water depth [m]
H_b	=	dune height [m].
H_c	=	dune crest height [m].
H_r	=	height of reattachment point [m].
H_s	=	height of separation point [m].
L	=	dune wavelength [m]
L_s	=	separation length [m].
Re	=	Reynolds number [-]
tL_s	=	total separation length [m].
U	=	average flow velocity [ms^{-1}]
U_x	=	flow velocity in x-direction [ms^{-1}]
α_s	=	angle of the zero velocity line [$^\circ$].
ν	=	kinematic viscosity [-]

References

- ALFRINK, B.J. & VAN RIJN, L.C. (1983) Two-equation turbulence model for flow in trenches. *Journal of Professional Issues in Engineering*, 109, 941-958.
- ASHLEY, G.M. (1990) Classification of large-scale subaqueous bedforms: a new look at an old problem. *Journal of Sedimentary Petrology*, 60, 160-172.
- BENNETT, S.J. & BEST, J.L. (1995) Mean flow and turbulence structure over fixed, two-dimensional dunes: implications for sediment transport and bedform stability. *Sedimentology*, 42, 491-513.
- BEST, J.L. & KOSTASCHUK, R.A. (2002) An experimental study of turbulent flow over a low-angle dune. *Journal of Geophysical Research*, 107, 18-1-18-19.
- BUCKLES, J., HANRATTY, T.J., & ADRIAN, R.J. (1984) Turbulent flow over large-amplitude wavy surfaces. *Journal of Fluid Mechanics*, 140, 27-44.

- CHANG, P.K. (1970a) Control of separation of flow. In: Separation of flow pp. 716-752. Pergamon Press, Oxford.
- CHANG, P.K. (1970b) Introduction to the problems of flow separation. In: Separation of flow pp. 1-54. Pergamon Press, Oxford.
- ENGEL, P. (1981) Length of flow separation over dunes. *Journal of the Hydraulics Division*, 107, 1133-1143.
- ENGELUND, F. (1977) Hydraulic resistance for flow over dunes. Progress Report of the Institute for hydrodynamic and hydraulic engineering, 44, Tech. Univ. Denmark, 19 pp.
- ETHERIDGE, D.W. & KEMP, P.H. (1978) Measurements of turbulent flow downstream of a rearward-facing step. *Journal of Fluid Mechanics*, 86, 545-566.
- FORMICA, G. (1955) Esperienze preliminari sulle perdite di carico nei canali, dovute a cambiamenti di sezione (preliminary test on head losses in channels due to cross-sectional changes). *L'Energia Elettrica*, 32, 554-568.
- HENN, D.S. & SYKES, R.I. (1999) Large-eddy simulation of flow over wavy surfaces. *Journal of Fluid Mechanics*, 383, 75-112.
- JOHNS, B., SOULSBY, R.L., & XING, J. (1993) A comparison of numerical model experiments of free surface flow over topography with flume and field observations. *Journal of Hydraulic Research*, 31, 215-228.
- JULIEN, P.Y., KLAASSEN, G.J., TEN BRINKE, W.B.M., & WILBERS, A.W.E. (2002) Case study: Bed resistance of the Rhine River during the 1998 flood. *Journal of Hydraulic Engineering*, 128, 1042-1050.
- KADOTA, A. & NEZU, I. (1999) Three-dimensional structure of space-time correlation on coherent vortices generated behind dune crest. *Journal of Hydraulic Research*, 37, 59-80.
- KARAHAN, M.E. & PETERSON, A.W. (1980) Visualization of separation over sand waves. *Journal of the Hydraulics Division*, 106, 1345-1352.
- KORNMAN, B.A. (1995) The effect of changes in the lee shape of dunes on the flow field, turbulence and hydraulic roughness. Report on measurements., R 95-1, Institute for marine and atmospheric research Utrecht,
- KOSTASCHUK, R.A. & VILLARD, P.V. (1996) Flow and sediment transport over large subaqueous dunes: Fraser River, Canada. *Sedimentology*, 43, 849-863.
- LYN, D.A. (1993) Turbulence measurements in open-channel flows over artificial bed forms. *Journal of Hydraulic Engineering*, 119, 306-325.
- MCLEAN, S.R., NELSON, J.M., & WOLFE, S.R. (1994) Turbulence structure over two-dimensional bed forms: implications for sediment transport. *Journal of Geophysical Research*, 99, 12729-12747.
- NAKAGAWA, H. & NEZU, I. (1987) Experimental investigation on turbulent structure of backward-facing step flow in an open channel. *Journal of Hydraulic Research*, 25, 67-88.
- RAUDKIVI, A.J. (1963) Study of sediment ripple formation. *Journal of the Hydraulics Division*, 89, 15-33.
- RAUDKIVI, A.J. (1966) Bed forms in alluvial channels. *Journal of Fluid Mechanics*, 26, 507-514.
- RIFAI, M.F. & SMITH, K.V.H. (1971) Flow over triangular elements simulating dunes. *Journal of the Hydraulics Division*, 97, 963-976.
- SIMPSON, R.L. (1989) Turbulent boundary-layer separation. *Annual Review in Fluid Mechanics*, 21, 205-234.
- TE CHOW, V. (1959) Open-channel hydraulics. McGraw-Hill Book Company, Inc., 1 pp.
- VAN DEN BERG, J.H. (1982) Migration of large-scale bedforms and preservation of cross-bedded sets in highly accretional parts of tidal channels in the Oosterschelde, SW Netherlands. *Geologie & Mijnbouw*, 61, 253-263.
- VAN DEN BERG, J.H. & VAN GELDER, A. (1998) Discussion: Flow and sediment transport over large subaqueous dunes: Fraser River, Canada. *Sedimentology*, 45, 217-221.
- VAN MIERLO, M.C.L.M. & DE RUITER, J.C.C. (1988) Turbulence measurements above artificial dunes Report on measurements., Q789, Delft hydraulics,
- VAN RIJN, L.C. (1984) Sediment transport; Part 3: bed forms and alluvial roughness. *Journal of Hydraulic Engineering*, 110, 1733-1754.
- VANONI, V.A. & HWANG, L.S. (1967) Relation between bed forms and friction in streams. *Journal of the Hydraulics Division*, 93, 121-144.
- VITTAL, N. (1972) Flow over triangular roughnesses in open channels. University of Roorkee, India,

- VITTAL, N., RANGA RUJU, K.G., & GARDE, R.J. (1976) Velocity distribution over triangular elements simulating ripples and dunes. *Irrigation and Power*, 33, 375-383.
- VITTAL, N., RANGA RUJU, K.G., & GARDE, R.J. (1977) Resistance of two dimensional triangular roughness. *Journal of Hydraulic Research*, 15, 19-36.
- YALIN, M.S. (1964) Geometrical properties of sand waves. *Journal of the Hydraulics Division*, 90, 105-119.
- YOON, J.Y. & PATEL, V.C. (1996) Numerical model of turbulent flow over sand dune. *Journal of Hydraulic Engineering*, 122, 10-18.

7 Predicting the hydraulic roughness of subaqueous dunes.

Abstract

The main part of the hydraulic roughness of a riverbed is determined by the size and shape of subaqueous dunes. This may be the reason that many hydraulic roughness predictors have been proposed, which use the dune height and length being the most prominent features of dune morphology. However, several investigators have suggested that the predictions could be improved by accounting for: 1) grain roughness, which is only present in the areas outside the flow separation zone, 2) height of flow separation (the brinkpoint height) instead of dune height, 3) the roughness of secondary dunes, if existing, in proportion to their abundance. In this study no new predictor is developed. Instead, three well known roughness predictors are adapted taking into account these three factors. These adapted predictors are tested with a dataset consisting of both flume and field measurements. The results show that the adapted predictors perform much better than their original forms. Especially over-prediction in low roughness situations and under-prediction in high roughness situations is improved significantly. The results also show that summing k_s values of grain roughness, form roughness, and superimposed form roughness, as assumed by Van Rijn (1984) is incorrect. A recalibration of the predictor of Vanoni & Hwang (1967), which was the best of the three selected predictors, performed only marginally better than the adapted one, meaning that either one can be used in the prediction of hydraulic roughness caused by subaqueous dunes.

7.1 Introduction

The hydraulic roughness of a riverbed is one of the most important and least known parameters in any flow model, especially in cases where the riverbed is covered with bedforms of many shapes and sizes. In those cases, predicting water levels during severe floods, poses a challenge for many engineers. Being able to accurately calculate the hydraulic roughness caused by bedforms would therefore mean a vast improvement in many flow models.

Hydraulic roughness is a measure that describes the amount of friction that an obstacle exerts on the water flowing over or past it. It is normally expressed in the roughness coefficients f or C defined in:

$$U = \sqrt{\frac{8g}{f}} \sqrt{Ri_e} = C \sqrt{Ri_e} \quad (7.1)$$

with; U = average flow velocity [ms^{-1}], g = gravitational acceleration coefficient [ms^{-2}], R = hydraulic radius [m], i_e = energy slope [-], f = Darcy-Weisbach friction factor [-] and C = Chezy coefficient [$\text{m}^{0.5}\text{s}^{-1}$]. The friction factor f was first used to describe the energy loss in pipe flow:

$$h_f = f \frac{L_p}{D} \frac{U^2}{2g} \quad (7.2)$$

where: h_f = energy loss [m], L_p is length of the pipe [m] and D = pipe diameter [m]. Introducing the hydraulic radius of a pipe $R = \frac{1}{4} D$ and the energy slope $i_e = h_f/L$, eq. 7.1 is seen to be obtained, which also applies to open channel flow. Substitution of eq. 7.1 in the bed shear stress expression $\tau = \rho g R i_e$ gives:

$$\tau = \frac{1}{8} f \rho U^2 = \frac{g}{C^2} \rho U^2 \quad (7.3)$$

with; τ = boundary shear stress [Nm^{-2}] and ρ = fluid density [kgm^{-3}]. This boundary shear stress can be divided into a stress related to the grains and a stress related to the bedforms. Therefore, it is also possible to express the hydraulic roughness in a separate hydraulic roughness for the grains of a riverbed and for the bedforms that cover the riverbed.

$$\tau = \tau' + \tau'' \quad \text{gives} \quad f = f' + f'' \quad (7.4)$$

where τ' = shear stress related to grains [Nm^{-2}], τ'' = shear stress related to bedforms [Nm^{-2}], f' = friction factor related to grains [-] and f'' = friction factor related to bedforms [-].

The hydraulic roughness of grains has been studied extensively in the past. One of the first was Nikuradse (1933), who studied the hydraulic roughness of pipes covered on the inside with grains of different sizes. He expressed the hydraulic roughness as k_s , the Nikuradse roughness height [m]. For a hydraulically rough bed the relation between k_s and the Chezy coefficient, according to Colebrook & White (1937), is:

$$C = 18 \log \left(\frac{12R}{k_s} \right) \quad (7.5)$$

Many investigators tried to identify the relation between grainsize and k_s , and the results were rather unequal. Based on data of various sources, the average values for plane bed

conditions are best represented by (Van Rijn, 1984; Kleinhans & Van Rijn, 2002):

$$k_s = 3D_{90} \quad \text{in case of a sand-bed river.} \quad (7.6)$$

$$k_s = 1D_{90} \quad \text{in case of a gravel-bed river.} \quad (7.7)$$

where D_{90} = the 90 percentile of the grainsize distribution [m].

Defining the hydraulic roughness of bedforms is even more difficult than with only grains, as is demonstrated by the large number of bedform roughness predictors that were created in the past. Methods proposed by Yalin (1964), Vanoni & Hwang (1967), Vittal (1972), Vittal *et al.* (1977), Engelund (1977), White *et al.* (1979), Brownlie (1981) and Van Rijn (1984), all tried to relate flow and bedform characteristics with the hydraulic roughness, with various success. In a later section, a more detailed description of some of these predictors is given.

Assessments by for example, Van Urk (1982), Ogink (1989), and Julien *et al.* (2002) of the quoted bedform roughness predictors resulted in very diverse and mostly unsatisfying results. One of the issues that was recognised as being a problem in most predictors is the way in which grain roughness, as part of the total roughness, is determined. Not only did each investigator use a different method of calculating this grain roughness, but in most cases it is assumed that the grain roughness is the same as in a case with no bedforms. However, both Yalin (1964) and Ogink (1989) realized correctly that grain roughness will be zero in the region of flow separation and Ogink also showed, using test results of Van Mierlo & De Ruiter (1988), that outside the flow separation zone the grain roughness is not constant either. Only near the top of a bedform, the shear stress reaches a value that is similar to flat bed situations. Over the stoss-side of a bedform the shear stress and thus the grain roughness slowly increases.

However, in case of large bedforms such as dunes the grain roughness represents only up to a few percent of the total hydraulic roughness. The largest part of the hydraulic roughness is related to the size and shape of the bedforms. Therefore, in most cases the bedform roughness is directly related to the bedform height. Some investigators on the other hand, realized that bedforms can also have a more symmetrical shape with lee-sides that do not reach a slope near the angle of repose. Vanoni & Hwang (1967) and Chang (1970) therefore proposed a correction coefficient called the exposure parameter, while Ogink (1989) and Kornman (1995) proposed the use of the effective dune height instead of the maximal dune height. Finally, Wilbers (Chapter 6) showed that this effective height, or the brinkpoint height as it can also be called, is in accordance with the height of the point of separation, which obviously is the best choice of height to be linked to the size and shape of the separation zone.

A final issue which complicates accurate calculations of the hydraulic roughness of dunes with existing predictors is the superposition of different-sized bedforms on top of each other. Superposition is mainly present in river settings and sometimes in flume situations. Most investigators ignored this superposition, but Ogink (1989) clearly showed that in case of superposition the hydraulic roughness is larger than can be expected of only the largest bedforms. It is, however, unclear how to account for these superimposed bedforms. Some investigators (Van Rijn, personal communication) proposed to simply calculate the roughness of these secondary form in the same way as is done with the primary ones and then add this roughness as a third friction factor. Others, especially

Ogink (1989), argued that as the larger forms are not totally covered with smaller forms the bedform roughness of the superimposed forms should be added only by a fraction, based on their spatial abundance.

In order to calculate the hydraulic roughness in the best way, a predictor should take into consideration that; (1) grain roughness is only of influence in the regions outside the separation zones; (2) the brinkpoint height or separation height rather than dune crest is linked to form roughness; (3) the roughness of superimposed bedforms should be added in accordance with their spatial abundance. In a first approximation, existing predictors will be used without major readjustments. In most formulas, probably only the empirical coefficients will need some readjustment but this can simply be done after a straightforward test has revealed which predictor is the best.

The goal of this study therefore is to test in what way the predictive capabilities of the original roughness predictors improve in case adaptations are included for: a) grain roughness, b) brinkpoint height, and c) superposition (fig. 7.1). This analyses is executed using flume test data of Ogink (1989) and Kornman (1995) concerning solid dunes, flume test data of Van Enckevoort & Van der Slikke (1996) with regard to migrating dunes in both steady and unsteady flows, flow and bedform measurements in 4 sections of the Nile, and flow and bedform measurements in the Rhine near the Pannerdensche Kop in the Netherlands.

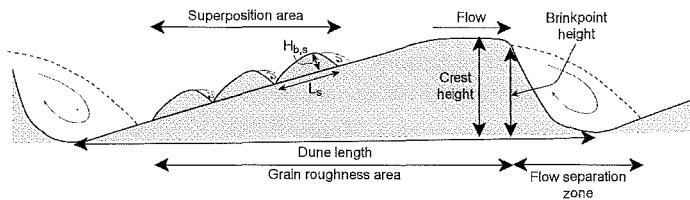


Figure 7.1: Definition of several dune characteristics, including the areas of superposition and grain roughness. $H_{b,s}$ and L_s are the brinkpoint height and dune length of the superimposed secondary forms.

7.2 Measurement data

To test the effect of the three adaptations to bedform roughness predictors, a dataset of measurements has to be available that meets the following conditions.

- Accurate measurements have to be available in different settings with different flow conditions, both steady and unsteady, and with different bedform sizes and shapes including superposition.
- The measurements have to include accurate characteristics of bedforms with special attention to brinkpoint height (separation height) both of the primary and secondary bedforms.
- Furthermore the measurements have to include accurate flow characteristics necessary to calculate the total hydraulic roughness, which includes; flow velocity, water depth and water surface slope, or even better energy slope.

The measurements used in the dataset for this analysis consisted of both flume (Ogink, 1989; Kornman, 1995; Van Enckevoort & Van der Slikke, 1996) and field (Nile and Rhine) conditions which all satisfy the above described requirements. As far as the authors know no other measurements have been reported in the literature so far that also comply to these requirements. So the analysis has to be performed with this dataset which is described in detail in the following section of this paper.

The most comprehensive way to calculate the total hydraulic roughness is to solve the one dimensional momentum equation:

$$\frac{1}{g} \frac{\partial U}{\partial t} + \frac{\partial}{\partial x} \left(\frac{U^2}{2g} + h_p \right) + \frac{U|U|}{C^2 R_b} = 0 \quad (7.8)$$

with U = the average flow velocity in a cross-section [ms^{-1}], h_p = water level relative to a horizontal plane, R_b = the hydraulic radius [m] corrected for the side wall effects according to the method of Vanoni & Brooks (1957). From eq. 7.8 for steady flow the hydraulic roughness is given by:

$$C = \frac{U}{\sqrt{R_b i_e}} \quad (7.9)$$

The energy slope can be replaced with the water-surface slope (i_w) provided that the velocity head does not vary in the measuring section. For a wide rectangular cross-section the adapted hydraulic radius can be substituted by the water depth yielding:

$$C = \frac{U}{\sqrt{h i_w}} \quad (7.10)$$

with h = average water depth [m] and i_w = water-surface slope [-].

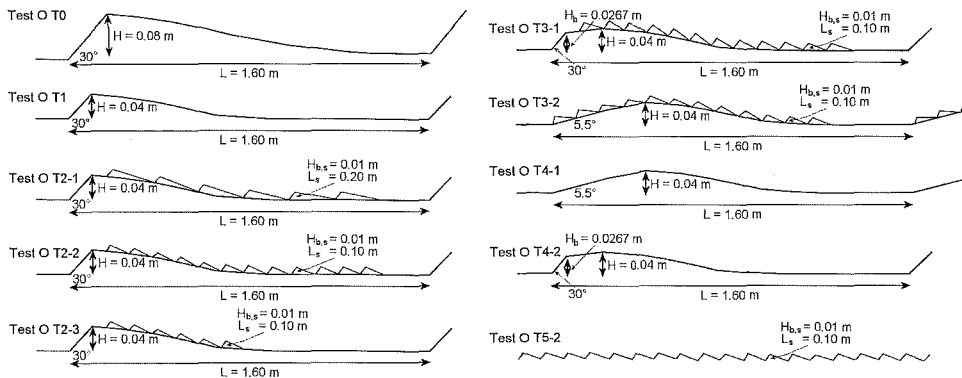


Figure 7.2: Bedform configurations in the tests of Ogink (1989).

7.2.1 Flume experiments

The flume experiments used in this study can be divided in tests concerning solid (made of wood or concrete) dunes and tests concerning migrating natural dunes in a sand bed. The tests over solid dunes were performed by Ogink (1989) and Kornman (1995), who

Table 7.1: Data on flow and bedform characteristics during the tests of Ogink (1989), Kornman (1995), Van Enckevoort & Van der Slikke (1996), and measurements in the Nile (Abdel-Fattah, 1997) and in the Rhine (Julien *et al.*, 2002; Wilbers and Ten Brinke, 2003; Chapter 4).

in the flume tests by Van Enckevoort & Van der Slikke, Kornman, and Ogink, R_b and I_e was used, in the other cases h and I_w .

* abundance during falling stages of the flood otherwise no secondary dunes present.

General		Flow				Primary dunes			Secondary dunes			
Author	Test or Location	U [ms ⁻¹]	R_b or h [m]	i_e or i_w [-] [#]	D_{90} [10 ⁻³ m]	H [m]	H_b [m]	L [m]	H_s [m]	$H_{b,s}$ [m]	L_s [m]	Abun. [%]
Ogink	T0	0.55	0.32	0.0010	1.70	0.08	0.08	1.6				
	T1	0.78	0.32	0.0010	0.85	0.04	0.04	1.6				
	T2-1	0.76	0.32	0.0010	0.85	0.04	0.04	1.6	0.01	0.01	0.2	75
	T2-2	0.71	0.32	0.0010	0.85	0.04	0.04	1.6	0.01	0.01	0.1	75
	T2-3	0.74	0.32	0.0010	0.85	0.04	0.04	1.6	0.01	0.01	0.1	38
	T3-1	0.76	0.32	0.0010	0.85	0.04	0.03	1.6	0.01	0.01	0.1	75
	T3-2	0.80	0.32	0.0010	0.85	0.04	0.00	1.6	0.01	0.01	0.1	75
	T4-1	0.95	0.32	0.0010	0.85	0.04	0.00	1.6				
	T4-2	0.93	0.32	0.0010	0.85	0.04	0.03	1.6				
	T5-2	0.72	0.28	0.0010	0.85	0.01	0.01	0.1				
Kornman	Shape 1	0.70	0.37	0.0004	0.25	0.15	0.10	3.8				
	Shape 2	0.69	0.48	0.0005	0.25	0.15	0.13	3.8				
	Shape 3	0.68	0.52	0.0007	0.25	0.15	0.15	3.8				
	Shape 4	0.67	0.55	0.0008	0.25	0.16	0.16	3.8				
Van Enckevoort and Van der Slikke	Test A	0.70	0.43	0.0014	0.25	0.17	0.17	4.1	0.03	0.02	1.7	18
	Test B	0.85	0.41	0.0016	0.25	0.19	0.18	6.3	0.03	0.01	1.6	1
	Test D	0.39	0.42	0.0004	0.25	0.17	0.15	6.3	0.02	0.02	0.2	89
	Test D	0.49	0.42	0.0006	0.25	0.17	0.16	6.5	0.02	0.02	0.2	87
	Test D	0.59	0.40	0.0006	0.25	0.17	0.16	6.5	0.01	0.01	0.3	85
	Test D	0.68	0.40	0.0011	0.25	0.16	0.15	5.7	0.02	0.02	0.5	46
	Test D	0.79	0.39	0.0013	0.25	0.16	0.15	5.7	0.03	0.03	1.6	13
	Test D	0.89	0.38	0.0018	0.25	0.15	0.15	6.0	0.04	0.04	2.1	7
Abdel-Fattah	Test D	1.00	0.38	0.0025	0.25	0.15	0.14	6.5				
	Aswan	0.53	5.1	3.5e-5	0.70	1.34	1.16	41.3	0.21	0.02	8.0	6
	Quena	0.52	4.1	4.2e-5	0.37	0.64	0.49	20.9	0.17	0.01	7.3	8
	Sohag	0.80	4.2	5.7e-5	0.58	0.34	0.22	8.7				
Julien <i>et al.</i>	Bani-Sweif	0.70	3.4	8.5e-5	0.82	0.33	0.21	6.5	0.17	0.07	2.8	23
	Rhine left	1.75	9.8	9.9e-5	11.3	0.73	0.62	25.8	0.28	0.17	6.6	56*
	Rhine centre	1.65	10.2	9.9e-5	9.8	0.78	0.66	25.0	0.27	0.17	7.0	41*
	Rhine right	1.75	10.7	9.9e-5	11.6	0.86	0.74	25.7	0.29	0.19	7.1	38*

both were trying to show the shortcomings of the existing roughness predictors. Ogink investigated three issues: 1) grain roughness should not be considered as constant over the full length of a dune, 2) using the effective dune height is a better characteristic than the crest height, and 3) the roughness of superimposed secondary forms should not be simply added to the hydraulic roughness of the primary dunes. He therefore constructed 11 different bedform configurations in a 50 m long and 1.5 m wide flume at the De Voorst Laboratory of WL|Delft Hydraulics. These configurations included flat bed, a bed

with ripples, beds comprised of dunes of different sizes and beds with dunes covered by ripples with different spatial abundance, see figure 7.2.

Because of the constructed bedforms, the bedform characteristics were known precisely. The tests therefore consisted of measuring the discharge, water depth and energy gradient. Uniform flow conditions were created by forcing the slope control system of the flume to maintain an energy gradient approximately equal to the average bottom slope of 10^{-3} by adjusting the tailgate under a preset discharge condition. The average flow velocity was known from the discharge, water depth and flume width while the water depth was measured as the average value of two pressure tubes located at 16,7 and 46,7 m along the flume. To keep the measurements of Ogink comparable to the other measurements used in the present analysis, it was decided to ignore the measurements in water depths larger than 0.35 m (as proposed by Ogink) and in very small water-depths. The measurements by Ogink used here are presented in table 7.1. The flat bed test has been omitted from this analysis. The total hydraulic roughness was calculated using eq. 7.9.

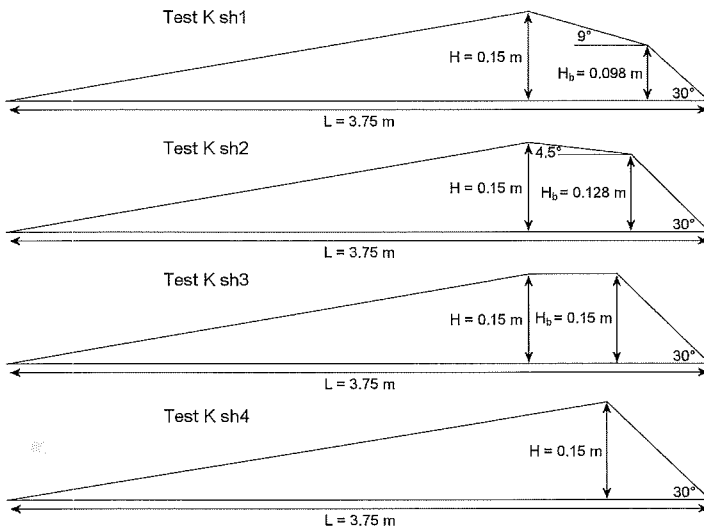


Figure 7.3: Bedform configurations in the tests of Kornman (1995).

Kornman (1995), set out to show that lowering the brinkpoint height of a dune results in a lowering of the hydraulic roughness produced by this dune. He therefore put 4 different bedforms in the same 50m long and 1.5m wide flume as mentioned above. These bedforms were constructed in such a way that the brinkpoint height started at 65% of the dune height and increased to 100% of the dune height while in the final test he eliminated the distance between the crest and the brinkpoint (fig. 7.3 and table 7.1). As was the case with the tests by Ogink, the bedform characteristics of the constructed bedforms were known precisely and the tests therefore consisted of measuring the discharge, water depth and energy gradient. In this case the tailgate was adjusted in such a way that the required depth-averaged velocities were reached with the highest possible water depth above the dunes, resulting in water depths of about 0.8 – 0.9 m at 47.33 m down the flume. In these steady but non-uniform flow conditions, the energy slope was not the same as the average

bottom slope (which was 10^{-3}) and therefore the total hydraulic roughness was calculated with eq. 7.9.

For the tests by Kornman an additional remark has to be made about the grain roughness. Contrary to the tests by Ogink, Kornman only glued sand, with a median diameter of 250 μm , to the middle 3 dunes in the flume, the other 10 dunes in the flume were left bare. As the total hydraulic roughness is calculated over the full length of the flume it is not correct to assume a constant grain roughness over all the dunes. Because of this, it was assumed in the further analysis that the grain roughness during these test was zero.

The flume experiments over migrating natural dunes in a sand bed were performed by Van Enckevoort & Van der Slikke (1996). They aimed at getting a better insight in the hydraulic roughness of different shaped dunes. The tests were performed in the same flume at the De Voorst Laboratory of WL|Delft Hydraulics, which was now narrowed to a width of 1.0 m. The bed of the flume was covered with a layer of sand with a median diameter of 200 μm (Fig. 7.4), which was automatically recirculated. The tests were

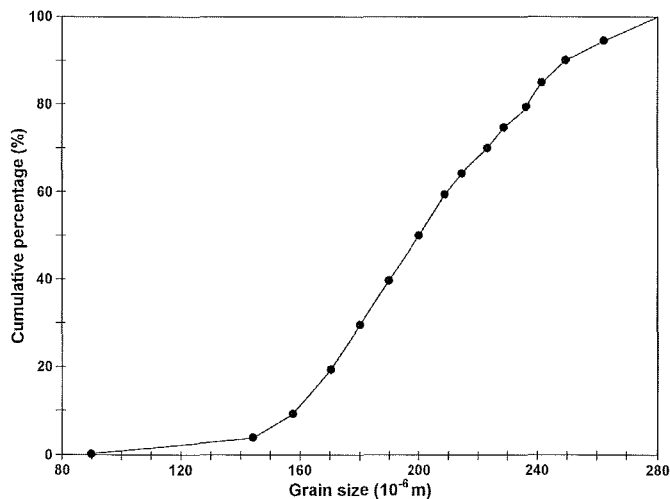


Figure 7.4: Grain-size distribution of the sand in the flume during the tests of Van Enckevoort & Van der Slikke (1996).

divided into two parts, steady flow experiments and unsteady flow experiments. In the steady flow experiments the flow velocity was held constant at about 0.7 ms^{-1} (test A) and about 0.9 ms^{-1} (Test B). During the unsteady flow experiments (Test D) the flow velocity was varied in steps of 0.1 ms^{-1} increasing and decreasing between 0.4 and 1.0 ms^{-1} . In all experiments, the water depth was held at a constant value of about 0.5 m by adjusting the tailgate, resulting in non-uniform flow conditions in the flume. During the steady flow experiments the measurements started only after the Chezy value remained more or less constant for the current flow velocity (table 7.1). In the unsteady flow experiments the flow velocities were held almost constant for only short periods to perform the measurements, without waiting for the Chezy value to become constant also. Both bed and flow characteristics were measured using a carriage that could automatically move up and down the flume. From this carriage a water profiler and three

bottom profilers measured the water surface and bed elevation at intervals of 1 cm. The three bottom profilers were positioned at 20, 50 and 80 cm, and the water profiler at 50 cm from either side of the flume. In this analyses only the information of the profilers at 50 cm were used. Using these measurements of the bed elevation and water-surface elevation along with the known discharge, the average water depth, flow velocity and water surface slope could be accurately determined. Moreover, the gathered information was also accurate enough to calculate the energy height, and deduce from this the energy slope. However because of the non-uniformity of the flow conditions along the flume, the dune dimensions, flow velocities and energy slope changed over the length of the flume. Figure 7.5 shows the flow velocities and energy heights along the flume for one of the tests. The flow velocities are clearly related to the bed configuration and the flow velocity slope is, along with the dune characteristics, therefore divided into three sections where it is markedly different from the overall velocity slope. This non-uniformity of the flow results in a non-linear energy slope over the length of the flume, therefore the energy slope is approximated separately for the three sections. In the calculations of the hydraulic roughness (eq. 7.9) the energy slope of the section with the most common dune size and shape was used.

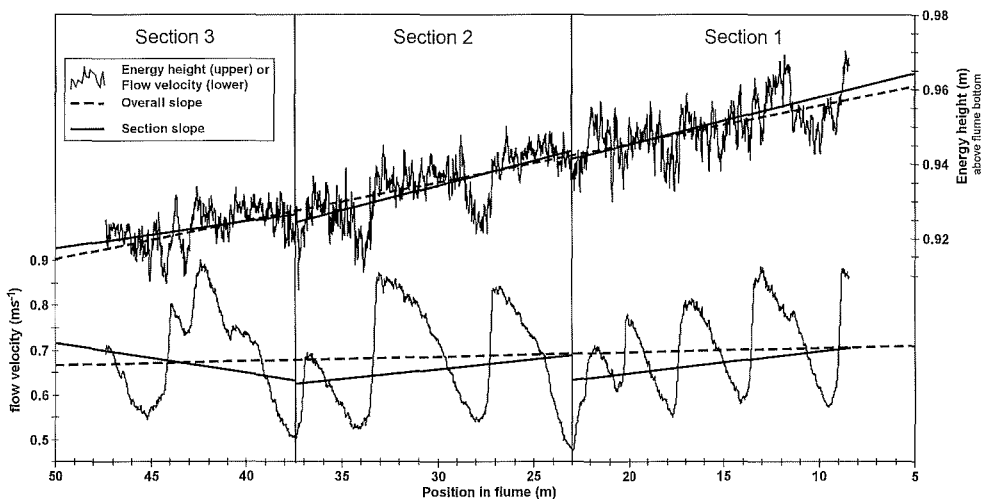


Figure 7.5: The non-linear energy height and velocity slopes in one of the tests of Van Enckevoort & Van der Slikke (1996). Due to non-uniform flow conditions resulting in differences in dune size along the flume, the velocity slope can be divided into 3 sections with slopes that differ from the overall slope. Along with this the energy slope can also be divided into 3 sections to approximate its non-linear shape. For this example the second section was used as the dominant part, and flow velocity, energy slope, and bed form characteristics were determined from this section. The average sand bed height was about 40 cm above the bottom of the flume.

The bedform characteristics of both primary and secondary forms (where present) were determined using the computer program DT2D (see Chapter 4 for further details). This program determines the dune height (difference between crest and trough elevation), length (distance between troughs on stoss and lee-side), lee and stoss-side slope of every individual dune in the centre profile of the flume. It is also used to determine the height

of the brinkpoint of a dune. This is done by locating that point on the lee-side of a dune where the slope becomes larger than 10 degrees. According to Wilbers (Chapter 6), a steeper slope than 10 degrees will initiate flow separation and therefore this point is the best location to use as the effective or brinkpoint height. In most natural dunes the point of flow separation is located at the brinkpoint where the loss of shear velocity and deposition of transported sediments induces avalanching of material down from this point, creating the characteristic lee-side slope at the angle of repose. If no point can be determined where the lee-side slope is more than 10 degrees, it is assumed that the flow did not separate and that the effective height of this dune was zero. The accurate determination of the brinkpoint is however strongly dependant on the measurement resolution. Just as is the case with dune height or length (Chapter 3), a low resolution can result in large errors in brinkpoint height. The distance between dune crest and dune trough is small compared to the total dune length. Therefore, determination of the point where the lee-slope exceeds 10 degrees requires very detailed observations (a high measurement resolution). In the flume tests of Van Enckevoort & Van der Slikke (1996), the bed was measured at intervals of 1 cm. So the resolution was high enough even for the accurate determination of the brinkpoint height of the superimposed dunes. For the three tests that were used in this analysis, the dune characteristics as determined with DT2D are summarized in table 7.1.

7.2.2 Field measurements

Two sets of useful field measurements were available for this analysis: (1) consisting of measurements done at four locations in the Nile (Egypt) in 1997, reported by Abdel-Fattah (1997; Abdel-Fattah *et al.*, 2003) and (2) consisting of extensive measurements during a large flood in 1998 in the Rhine (The Netherlands), reported by Julien *et al.* (2002) and Wilbers & Ten Brinke (2003, Chapter 4). In the Nile, at each of the four locations (table 7.1) the local water surface slope was determined by measuring the water level at two points about 1000m apart. The discharge was acquired from local gauging stations, while the local water depths and the flow velocities (propeller type current-meters) were measured at 4 to 6 location over the width of the river directly above the longitudinal profiles. The flow conditions were assumed to be uniform over the short distances and steady during the short time intervals, therefore the total hydraulic roughness was calculated using eq. 7.10. The bed was measured at each location by making 4 to 6 longitudinal profiles of at least 100 m length using a single-beam echosounder. These longitudinal profiles were recorded on paper (Van Rijn, *pers. comm.*), and subsequently digitized for analysis with DT2D. Using the program DT2D, the dune length, height, and brinkpoint height of each primary and secondary dune in the profiles was determined (table 7.1). The resolution of the analysed profiles was about 1 point per meter, meaning that the brinkpoint heights of the primary dunes were probably determined accurate enough, while the accuracy of the brinkpoint height of the secondary dunes is questionable.

The measurements in the Rhine were done in order to calculate the bedload transport in the Rhine near Pannerdensche Kop using the dune tracking technique. Over a period of 3 weeks a series of twice daily multi-beam echo-soundings were performed of the bed of

the Rhine along with flow velocity measurements across the river using ADCP-equipment (Acoustic Doppler Current Profiler). The water surface slope was determined from stage measurements at nearby automatic gauging stations spanning a section of 5 km. The echo-sounding transects themselves had a length of 1 km and spanned the full width of the river. The dune characteristics of both primary and secondary dunes were determined using DT2D in longitudinal profiles spaced 1 m apart. In this case the resolution was about 1 point per 0.4 - 0.6 m. Therefore it can be assumed that for the primary dunes the brinkpoint heights were determined accurately, while for the small secondary dunes the determined brinkpoint height are questionable. All the gathered data were averaged to obtain values for the centre of the river and for the positions 67m (about a quarter of the river width) left and right of the centre (table 7.1). Assuming the flow was almost uniform and steady, at least during the time it took to perform one complete measurement, the total hydraulic roughness was calculated using eq. 7.10.

7.3 Method of analysis

The goal of this study is to test in what way the predictive capabilities of original roughness predictors improves in case adaptations are included for: a) grain roughness, b) brinkpoint height, and c) superposition. Therefore, in this section several existing predictors are reviewed and three predictors are selected for analysis. Also, the methods used to calculate grain roughness and the roughness of superimposed forms are described.

As was shown in the introduction, many bedform roughness predictors have been created in the past (Yalin, 1964; Vanoni & Hwang, 1967; Vittal, 1972; Vittal *et al.*, 1977; Engelund, 1977; Brownlie, 1981; Van Rijn, 1984). The roughness predictor by Brownlie simply ignores the bedforms and related the hydraulic roughness to flow using different empirical coefficients in cases with or without bedforms. Therefore this predictor is of no use in this analysis and is therefore ignored.

Both Yalin (1964) and Vittal (Vittal, 1972; Vittal *et al.*, 1977) tried to relate bedforms and hydraulic roughness with dune steepness (H/L), relative water depth (H/h) and the drag (C_d) or loss (α) coefficient. These last two coefficients were shown also to be related to dune steepness and relative water depth.

$$f = f' + f'' = f_g \left(1 - \frac{H}{L} \cot g(\phi) \right) + 4\alpha \frac{H^2}{hL} \quad \text{with} \quad \alpha = F\left(\frac{h}{H}, \frac{H}{L}\right) \quad (7.11, \text{Yalin})$$

where f_g = plain bed friction factor and ϕ = angle of repose.

$$f = f' + f'' = \frac{0.0224}{\frac{H}{L} * \left(\frac{R_b}{k_s}\right)^{1/6} * R_e^{1/4}} + 4C_d \frac{H}{L} \quad \text{with} \quad C_d = F\left(\frac{H}{h}, \frac{H}{L}\right) \quad (7.12, \text{Vittal})$$

where $k_s = D_{65}$ of bed material [m] and R_e = Reynolds number [-]. It is, however, unknown how these drag and loss coefficients are influenced by the brinkpoint heights or superposition of dunes. No information is available to recalibrate the functions for C_d or α according to these influences. Therefore these roughness predictors are excluded from this analysis.

Vanoni & Hwang (1967) and Engelund (1977) also created roughness predictors which relate the hydraulic roughness of bedforms to the dune steepness and relative water depths.

$$f = f' + f'' = \frac{8g}{18 \log\left(\frac{12R_b}{D_{90}}\right)} + \left(\frac{1}{3.3 \log\left(\frac{R_b L}{H^2}\right) - 2.3} \right)^2 \quad (7.13, \text{Vanoni \& Hwang})$$

$$f = f' + f'' = \frac{8g}{18 \log\left(\frac{12R_b}{2D_{65}}\right)} + 10 \frac{H^2}{hL} * \exp\left(-2.5 \frac{H}{h}\right) \quad (7.14, \text{Engelund})$$

where $R_b' =$ hydraulic radius of the same channel with a plane bed, which carries the same amount of water as the dune covered bed; so $R_b' \leq R_b$. They however did not use any drag or loss coefficients (C_d , or α) and the dune steepness and relative water depth can simply be replaced by H_b/L and H_b/h (Appendix 7.I). Both these predictors were therefore selected for this analysis. It should however be stated that the predictor of Vanoni & Hwang (1967) shown in eq. 7.13 is a secondary derivative of their original predictor. In their original predictor they used an exposure parameter to incorporate the differences in dune lee-side slopes in a similar way as is done here by incorporating brinkpoint height. However this exposure parameter is impossible to determine in field situations and therefore they also provided a simplified predictor which is used here.

Finally, Van Rijn (1984) introduced the concept of splitting k_s into a grain and bedform part, in the same way as was done for f in eq. 7.4:

$$k_s = k_s' + k_s'' \quad (7.15)$$

with $k_s' =$ Nikuradse roughness height for grains [m] and $k_s'' =$ the roughness height for bedforms [m]. With this concept Van Rijn could then relate the hydraulic roughness of bedforms with only dune height and dune steepness and eliminate the relative water depth.

$$k_s = k_s' + k_s'' = 3D_{90} + 1.1H * \left(1 - \exp\left(-25 \frac{H}{L}\right)\right) \quad (7.16, \text{Van Rijn})$$

Later Van Rijn (1993) introduced a shape factor (γ) into eq. 7.16 to attempt to counteract an inherent tendency for overprediction that was observed:

$$k_s = k_s' + k_s'' = 3D_{90} + 1.1H\gamma * \left(1 - \exp\left(-25 \frac{H}{L}\right)\right) \quad (7.17, \text{Van Rijn})$$

With only limited data at his disposal, he suggested a value $\gamma = 0.7$ for field situations. However, it is unclear how to define this shape factor other than calculating it empirically. Therefore, this shape factor was not used in this paper. Instead, in this case the dune height and steepness was replaced with the brinkpoint height and H_b/L (Appendix 7.I), which give a better representation of the dune shape. This predictor was therefore also selected for the analysis in this paper.

The grain roughness was calculated both with the original methods provided by the authors of the different roughness predictors and with the new method given in eqs. 7.6 and 7.7. The original grain roughness predictors were applied over the full length of the dunes as was done by their authors, while eqs. 7.6 and 7.7 were only applied in the parts outside the flow separation zones. To also account for the steady increase in bed shear

stress from the point of reattachment to the dune crest, as suggested by Ogink (1989), was deemed impractical and therefore the grain roughness was considered constant over the stoss-side of a dune. To estimate the length of the separation zone and thus the proportion of grain roughness to the full length of a dune the observations of the analysis by Wilbers (Chapter 6) were used. Wilbers showed that from the point of separation a line can be drawn at an angle of 10 degrees and that the length of the flow separation zone is the distance between the point of separation and the point where this 10 degree line intersects the stoss-side. Simplified the separation length (L_{sep} [m]) can be calculated with:

$$L_{sep} = \frac{H_b}{\tan(10^\circ)} \quad (7.18)$$

and the proportion of grain roughness with:

$$\frac{(L - L_{sep})}{L} \quad (7.19)$$

In order to account for the added hydraulic roughness of the superimposed dunes the same method is adopted as was proposed by Ogink (1989). The hydraulic roughness of these secondary dunes is calculated with the same adjusted predictors as used for the primary dunes. The only difference is that the roughness of the secondary dunes is applied for only that part of the primary dunes that is covered with the secondary ones.

$$\frac{(N_s * L_s)}{L_{prof}} \quad (7.20)$$

where N_s = the number of secondary dunes in a profile [-]; L_s = the average length of the secondary dunes [m] and L_{prof} = the total length of the profile [m]. In cases where the secondary dunes totally cover the primary forms (eq. 7.20 is 100%) it can be assumed that the primary dune does no longer have a separation zone of it's own and therefore the hydraulic roughness of this primary dune is zero. In those cases the dune-related hydraulic roughness consists only of the hydraulic roughness of the secondary dunes. The adapted predictors and a complete method for predicting hydraulic roughness using these predictors are listed in Appendix 7.I.

7.3.1 Statistical analysis

To check if the adapted roughness predictors of Vanoni & Hwang, Engelund and Van Rijn, combined with the new method of adding both grain roughness and the roughness of superimposed dunes, significantly improved the prediction of the total hydraulic roughness, two separate statistical method were used. First the Root Mean Squared Error (RMSE) was calculated for all the points in the dataset.

$$RMSE = \sqrt{\frac{1}{N} \sum_{i=1}^N (p_i - o_i)^2} \quad (7.21)$$

with N = number of datapoints, p_i = predicted roughness of point i and o_i = observed roughness of point i . RMSE defines how close the data points are distributed around a perfect prediction. The smaller the RMSE is the better the predicted roughness approached the measured roughness. RMSE can also be split into the sum of the bias (B)

and the variance (V) of the errors ($p_i - o_i$).

$$RMSE = \sqrt{B^2 + V}$$

$$B = \frac{1}{N} \sum_{i=1}^N (p_i - o_i) \quad (7.22)$$

$$V = \frac{1}{N} \sum_{i=1}^N ((p_i - o_i) - B)^2$$

The bias describes how much the predictor on average over or under predicts the hydraulic roughness, while \sqrt{V} describes the standard deviation of the errors around the perfect prediction. In a perfect prediction all three measures, RMSE, B and \sqrt{V} , will be zero.

The second method of testing the adapted predictors is by linear regression. In a perfect case the regression of the predicted values against the observed values should result in:
 $p = a + b * o$ (7.23)

with a = the intercept being zero and b = the slope being 1. To get a realistic intercept that says how much the predictor on average over or under predicts (similar to the bias) the dataset was normalised in such a way that the observed values were evenly distributed around zero. The central observed roughness value was thereby defined as zero and subtracted from all other observed roughness values.

7.4 Results

The results of predicting the hydraulic roughness using both the original predictors of Vanoni & Hwang, Engelund and Van Rijn and the adapted predictors are shown in figures 7.6 to 7.8. The plots of predicted against observed roughness show that in the dataset f ranges from about 0.02 to about 0.12 and k_s from about 0.01 to about 1 m. A visual comparison between the plots of the original predictors and the adapted predictors also shows a clear improvement in the predictions in case of the adapted predictors. In all three cases the scatter around the line of perfect agreement clearly diminishes. Statistically this is shown by all 5 measures (table 7.2), thereby the k_s values of the Van Rijn predictor have been recalculated into f values. Especially the RMSE and \sqrt{V} strongly decrease while the regression slope (b) moves closer to 1. Except for Engelund, the Bias also decreases. The RMSE, Bias and \sqrt{V} are however relatively much larger in case of the predictor of Van Rijn.

The regressions of the predicted roughness against the observed roughness clearly show that the adapted predictors better predict the total hydraulic roughness especially in low and high roughness conditions, where all three original predictors respectively over- and under-predicted the hydraulic roughness. This effect can be shown even more clearly by using the results for two specific tests individually. In all three cases the data from the tests of Kornman and of test D from Van Enckevoort & Van der Slikke show clear deviations from the line of perfect agreement in the original predictors. The roughness with the data from Kornman is generally overestimated, whereas with the data from test D it is mostly underestimated. The regression slopes are very low and sometimes even

Flume data		River data		Regression lines
Ogink	Kornman	Nile		— Pred. = Obs.
○ O T0	□ K sh1	◇ Aswan		— All data
○ O T1	□ K sh2	◇ Quena		- - Test D
○ O T2-1	□ K sh3	◇ Sohag		· · · Kornman
○ O T2-2	■ K sh4	◇ Bani-Sweif		sh1-sh4
● O T2-3				
○ O T3-1	Van Enckevoort			
○ O T3-2	& Van der Slikke	Rhine		
○ O T4-1	× Test A	△ Rijn left		
○ O T4-2	× Test B	△ Rijn center		
● O T5-2	+ Test D	△ Rijn right		

161

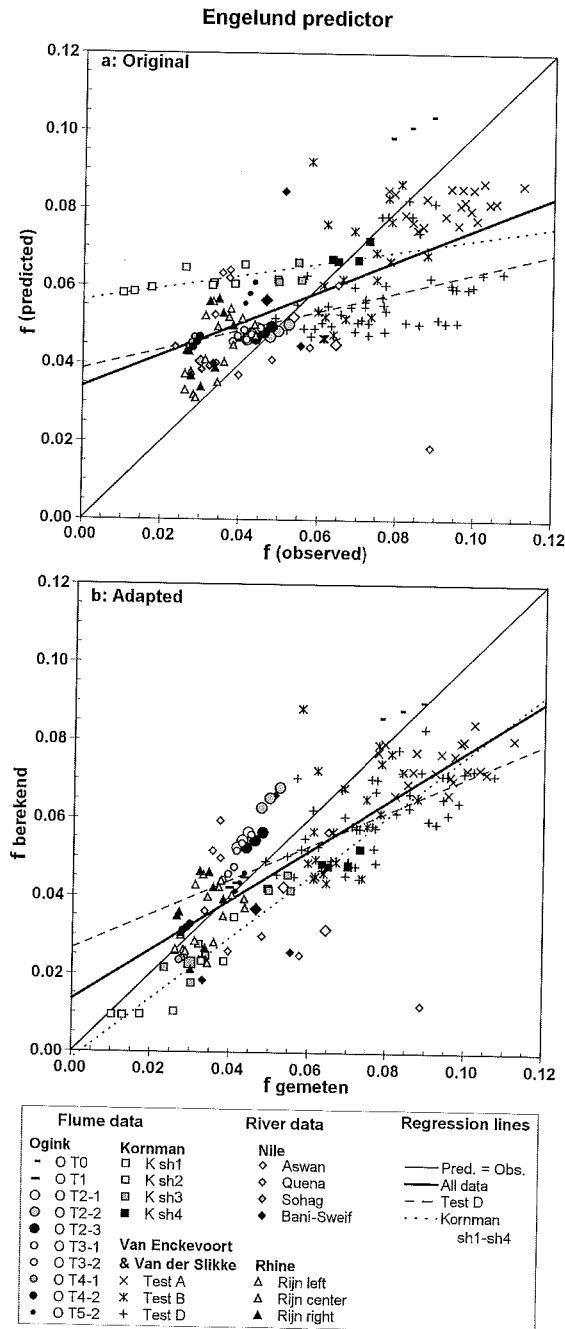


Figure 7.7: Predicted roughness versus observed roughness using the original (a) and the adapted (B) predictor of Engelund (1977). The larger diamonds in the cases from the Nile indicate the average values over the full width of the river.

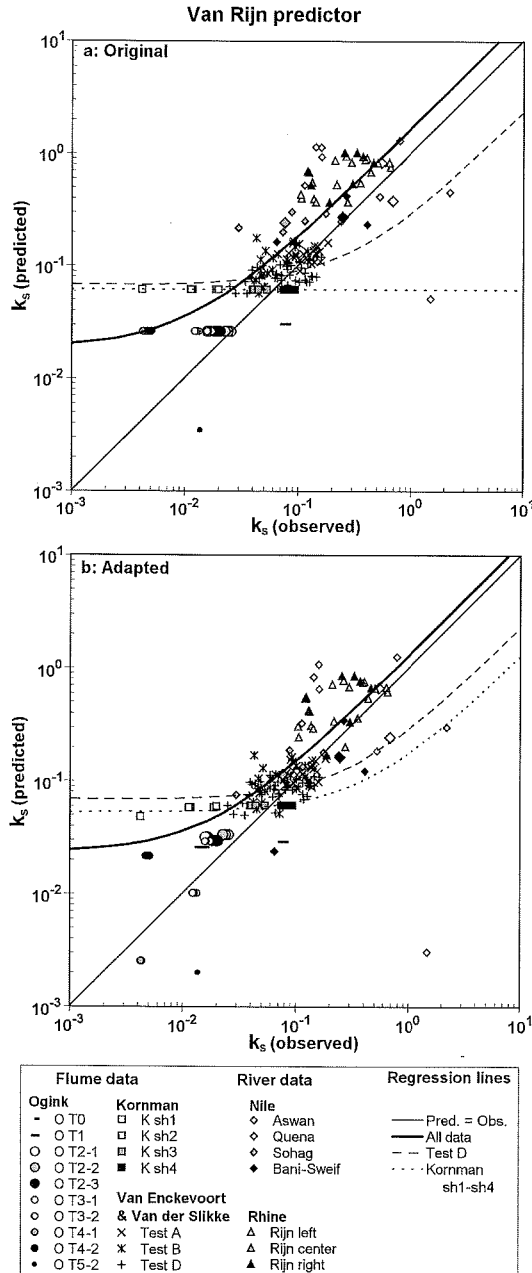


Figure 7.8: Predicted roughness versus observed roughness using the original (a) and the adapted (b) predictor of Van Rijn (1984). The larger diamonds in the cases from the Nile indicate the average values over the full width of the river.

negative, which indicates an opposite relation (table 7.3). With the adapted predictors the regression slopes increase strongly and in most cases approach the perfect value of 1.

Table 7.2: Statistical results on all data points. The centre values for f and k_s of all observed roughness values are 0.073 and 0.325 respectively.

Formula	version	RMSE	Bias	\sqrt{V}	slope	intercept
Vanoni and Hwang (1967)	original	0.022	0.0061	0.021	0.57	0.0006
	adapted	0.017	0.0052	0.016	0.85	0.0038
Engelund (1977)	original	0.020	-0.0020	0.020	0.41	-0.0094
	adapted	0.018	-0.0089	0.016	0.64	-0.0132
Van Rijn (1984)	original	0.215	0.0913	0.195	1.66	0.2327
	adapted	0.160	0.0534	0.150	1.27	0.1121

Table 7.3: Statistical results on the data points of test D and the tests by Kornman. The centre values for f and k_s of Test D are 0.078 and 0.093 respectively, and for the tests by Kornman, 0.042 and 0.047.

Formula	version	Test D		Kornman	
		slope	intercept	slope	intercept
Vanoni and Hwang (1967)	original	0.15	-0.0072	-0.32	0.0377
	adapted	0.44	0.0035	0.65	0.0063
Engelund (1977)	original	0.25	-0.0201	0.16	0.0213
	adapted	0.44	-0.0173	0.78	-0.0111
Van Rijn (1984)	original	0.23	-0.0039	0.00	0.0143
	adapted	0.22	-0.0042	0.12	0.0117

7.5 Discussion

Adapting the hydraulic roughness predictors of Vanoni & Hwang, Engelund and Van Rijn (Appendix 7.I), by: 1) calculating grain roughness only in the regions outside the separation zones, 2) substituting dune height with brinkpoint height, and 3) adding the hydraulic roughness of superimposed dunes according to their spatial abundance, significantly improves the predicted total hydraulic roughness. It is not the overall prediction of the hydraulic roughness that is impressively improved, as the RMSE values are already low for the original predictors, but it is the direction of the regressions that improves strongly. This proves that the adapted predictors much less overpredict in low roughness conditions and much less underpredict in high roughness conditions compared to the original predictors.

Overprediction in low roughness conditions occur most likely in situations where dunes have a small steepness (H/L). Those dunes are more symmetrical and have gentle lee-side slopes far below the angle of repose. Therefore, their dune height is much larger than the brinkpoint height (there may be no brinkpoint at all), resulting in the overprediction of the form roughness. This is clearly shown by the data from Kornman. The original predictors result in equal roughness values for all four different bedform shapes, while the observed values shows an increasing roughness along with the increasing brinkpoint height. The adapted predictors use these lower brinkpoint heights for the first two dune shapes and thereby predict a much smaller dune roughness than the original roughness predictors. Especially with the adapted predictors of Vanoni & Hwang and Engelund this

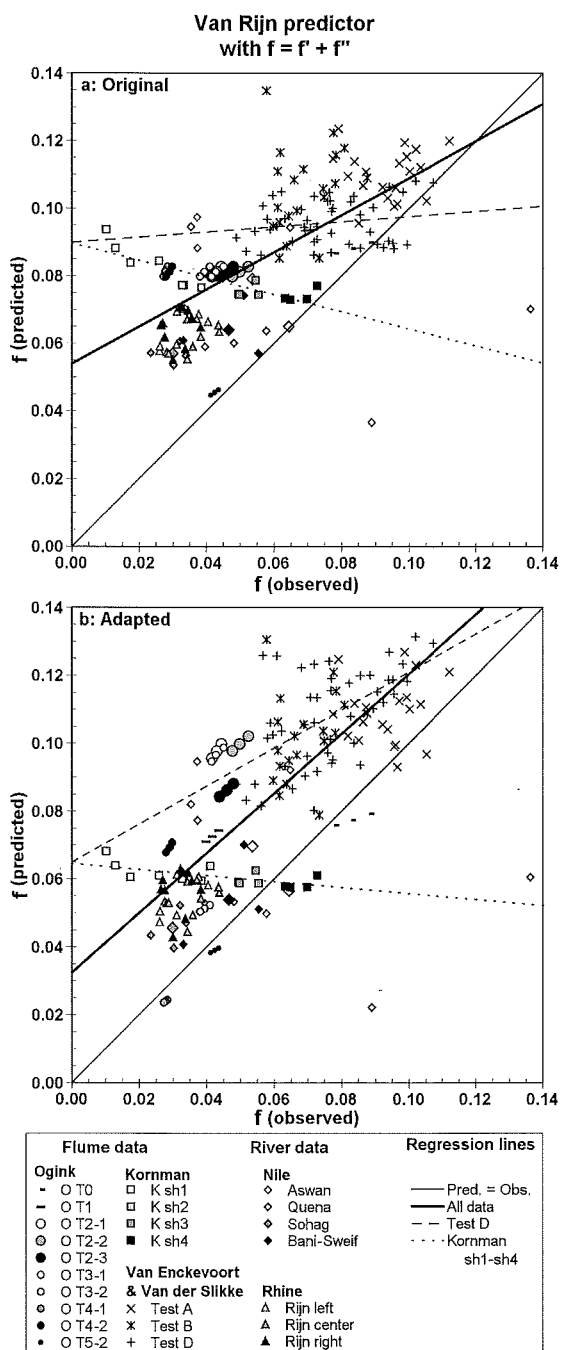


Figure 7.9: Predicted roughness versus observed roughness using the original (a) and the adapted (b) predictor of Van Rijn (1984) but now with $f = f' + f''$ instead of $k_s = k_s' + k_s''$.

strongly improves the regression slopes (table 7.3). Clearly, using the brinkpoint height in stead of dune height for long, low, and maybe symmetrical dunes with gentle lee-side slopes, greatly improves the prediction of the hydraulic roughness.

Underpredicting the hydraulic roughness in cases where the observed hydraulic roughness was high is probably closely connected to the occurrence of superposition. The original predictors ignore superposition and therefore do not account for this extra roughness part. A good example of this case is Test D by Van Enckevoort & Van der Slikke. The dunes in this test had brinkpoint heights which were only 5 % lower than the dune height so the influence of substituting the brinkpoint height was only small. However, during the low flow velocities in this test, the larger dunes were extensively covered with smaller dunes, while during the higher flows, the dunes were bare of any superimposed forms. The superimposed dunes covered on average about 75% of the larger dunes and therefore probably constituted a substantial added roughness. The results of the original predictors therefore showed a regression slope that strongly deviated from 1 (table 7.3) as they predicted the roughness during high flows quite well, but underestimated the roughness during low flows. The adapted predictors again showed a strong improvement of the regression slope because now the predictions during low flows improved very much (fig. 7.6). Thus, adding the hydraulic roughness of superimposed bedforms in the proposed way (eq. 7.19, Appendix 7.I), greatly improves the prediction of the hydraulic roughness in cases where superposition is present.

7.5.1 Summing k_s

The results from fig. 7.9 and tables 7.2 and 7.3 clearly show that adapting the predictor of Van Rijn does not improve the prediction very much. This is possibly caused by the incorrect assumption of Van Rijn (1984) that k_s is simply a sum of k_s' and k_s'' (eq. 7.15) as is the case with f (eq. 7.4). Summing the k_s in the correct way clearly shows the falseness of this assumption:

$$f = f' + f''$$

$$\frac{1}{C^2} = \frac{1}{C'^2} + \frac{1}{C''^2}$$

$$\text{using Strickler, stating } C :: \frac{1}{k_s^{1/6}}, \text{ hence: } \frac{1}{C^2} :: k_s^{1/3} \quad (7.24)$$

$$\text{so: } k_s = \left\{ (k_s')^{1/3} + (k_s'')^{1/3} \right\}^3 \text{ and not } k_s = k_s' + k_s''$$

It should however, be mentioned here that Van Rijn (1982) initially did not propose to sum k_s' and k_s'' , this was only later introduced (Van Rijn, 1984; Kornman, 1995). Van Rijn (1982) suggested to only calculate k_s' in case of flat bed, and k_s'' in case of a dune covered bed. In the latter case the k_s' could be ignored as it would be only a small fraction of the total k_s .

To see if the assumption of summing k_s is the basis of the bad improvement of the adapted Van Rijn predictor, the analyses was repeated. Now the individual k_s' and k_s'' values were first converted into f' and f'' values before summing them (eq. 7.24). Figure 7.9 and table 7.4 show that the predictions of both the original predictor and the adapted

Table 7.4: Statistical results on a comparison between using $k_s=k_s'+k_s''$ or $f=f'+f''$ in the method of Van Rijn (1984). The centre values for f and k_s of all observed roughness values are 0.073 and 0.325 respectively.

Formula	version	$f=f'+f''$		$k_s=k_s'+k_s''$	
		original	adapted	original	adapted
	RMSE	0.033	0.031	0.215	0.160
	Bias	0.0265	0.0241	0.0913	0.0534
	\sqrt{V}	0.019	0.020	0.195	0.150
All data	slope	0.55	0.88	1.66	1.27
	intercept	0.0209	0.0235	0.2327	0.1121
Test D	slope	0.08	0.56	0.23	0.22
	intercept	0.0179	0.0306	-0.0039	-0.0042
Kornman	slope	-0.25	-0.09	0.00	0.12
	intercept	0.0375	0.0193	0.0143	0.0117

predictor are markedly improved relative to the centre values of the observed f and k_s , in case of summing f . The RMSE, bias and \sqrt{V} are much lower and the regression slope is much closer to 1. Table 7.4 also shows that the adapted predictor of Van Rijn in case of summing f is much better than the original version. The regression slope is closest to 1 of all the adapted predictors however the bias is very large stating that the hydraulic roughness is always overpredicted.

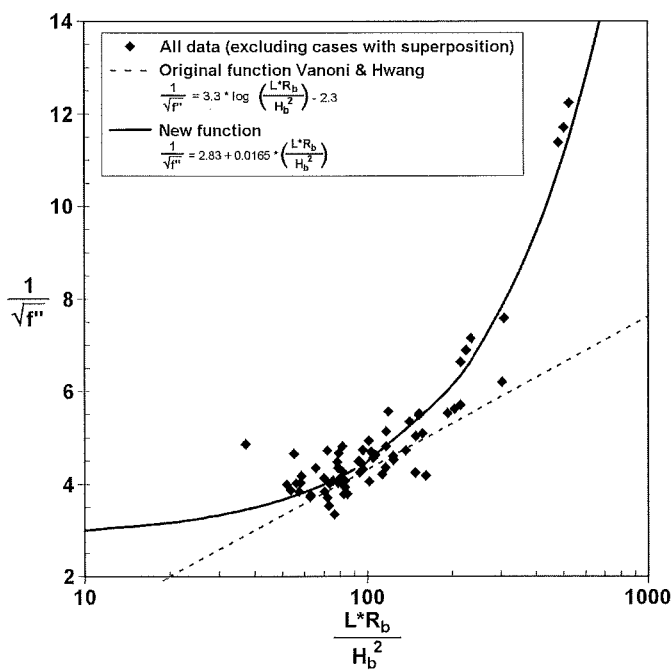


Figure 7.10: Observed roughness of bedforms versus dune characteristics and water depth similarly to Vanoni & Hwang (1967).

7.5.2 Improving the Vanoni & Hwang predictor

The result from the analyses with the predictors of Vanoni & Hwang, Engelund and Van Rijn show that the adapted predictor of Vanoni & Hwang performs best in predicting the hydraulic roughness. However this adaptation constituted a simple substitution of dune height with brinkpoint height. The empirical coefficients given by Vanoni & Hwang (3.3 and 2.3 in eq. 7.13) were not adapted at all. This can however be done now using part of the dataset of this analyses. This part of the dataset constitutes of those measurements where no superposition occurred and only the brinkpoint height differed. As was done by Vanoni & Hwang the observed hydraulic roughness of the bedforms was calculated by subtracting the grain roughness (calculated with eqs. 7.6 and 7.7) from the observed total roughness, and this bedform roughness was plotted against $R_b L / H_b^2$ (fig. 7.10). A regression was fitted through the dataset which resulted in an improved predictor for bedform roughness:

$$f'' = \left(\frac{1}{2.83 + 0.0165 * \left(\frac{R_b L}{H_b^2} \right)} \right)^2 \quad (7.25)$$

Fitting this regression showed that a quadratic function was much better ($r=0.96$) than a logarithmic function like Vanoni & Hwang ($r=0.84$). Table 7.5 shows that this improved predictor results in similar values for RMSE and \sqrt{V} . The bias is somewhat larger but negative. But the regression slope improved to 0.9 for the whole dataset and 0.78 for the Kornman tests. For Test D the regression slope did not improve. This refitted predictor of Vanoni & Hwang thus performs only marginally better than the adapted version and the use of either one is acceptable (Appendix 7.I).

Table 7.5: Statistical results on improving the predictor of Vanoni & Hwang (1967). The centre value for f of all observed roughness values is 0.073.

Formula	version	RMSE	Bias	\sqrt{V}	All data		Test D		Kornman	
					slope	intercept	slope	intercept	slope	intercept
Vanoni & Hwang (1967)	original	0.022	0.0061	0.021	0.57	0.0006	0.15	-0.0072	-0.32	0.0377
	adapted	0.017	0.0052	0.016	0.85	0.0038	0.44	0.0035	0.65	0.0063
	refitted	0.018	-0.0074	0.017	0.90	-0.0079	0.20	-0.0083	0.78	-0.0009

7.5.3 Field situations

In those cases where the dunes on the bed of a river are measured with high resolution measurements (for example using multibeam echosounders) it will be possible to determine accurately the brinkpoint heights of all the dunes and the spatial abundance of the superimposed dunes (if at all present). In some cases, such high resolution data will however not be available, and than only dune crest height and dune length can be accurately determined. Without information on brinkpoint height and spatial abundance

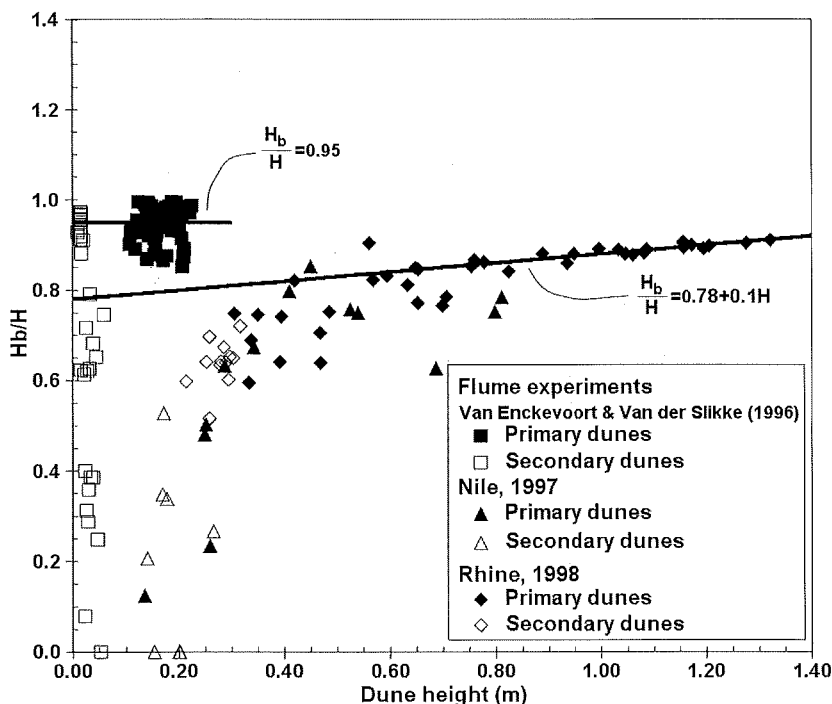


Figure 7.11: Relation between the brinkpoint height as a proportion of the dune height and the dune height. The fitted functions were created after assuming that the points which plot beneath the lines can be ignored due to low measurement resolution.

of superimposed dunes the three adapted predictors perform less well. However, the data from the flume experiments of Van Enckevoort & Van der Slikke (1996), and data from the Nile and Rhine may provide information on how to estimate both these factors from information on dune height and length. Figure 7.11 shows the relation between brinkpoint height and dune height for both the primary and secondary dunes from the flume experiments and the field measurements. There exists two distinct relations, one for the flume data and one for the field data. In a flume situation the brinkpoint appears to be closer to the dune crest than in a field situation. Secondly, it appears that the brinkpoint heights of small dunes (especially secondary dunes) are relatively smaller compared to the brinkpoint heights of larger dunes. However, as was explained above, the measurement resolution has a significant effect on the accurate detection of the brinkpoint. The measurement resolution in both the flume and field measurements was high, but not high enough to calculate the brinkpoint heights accurately. The brinkpoint heights of the small dunes are therefore probably underestimated. Therefore, in the creation of formulations to estimate the brinkpoint height from dune height as shown in fig. 7.11, the brinkpoint heights of the superimposed dunes were ignored, as were the smaller dunes in the field situations. For flume experiments this resulted in:

$$\frac{H_b}{H} = 0.95 \quad (7.26)$$

while for field situations:

$$\frac{H_b}{H} = 0.78 + 0.1H \quad (7.27)$$

can be used.

Figure 7.12 shows the abundance of secondary dunes superimposed on a primary dune in relation to the dune steepness (H/L) of the primary dune. In this case there is also a clear distinction between relation for the flume data and for the field data. In the flume data the abundance of superposition decreases at a larger steepness than in field situations. For flume situations the abundance can therefore be estimated with:

$$\frac{(N_s * L_s)}{L_{prof}} = 0.0014 \left(\frac{H}{L} \right)^{-1.67} \quad (7.28)$$

when H/L is larger than 0.02. For field situation the abundance can be estimated with:

$$\frac{(N_s * L_s)}{L_{prof}} = 0.0014 \left(\frac{H}{L} \right)^{-1.41} \quad (7.29)$$

when H/L is larger than 0.01.

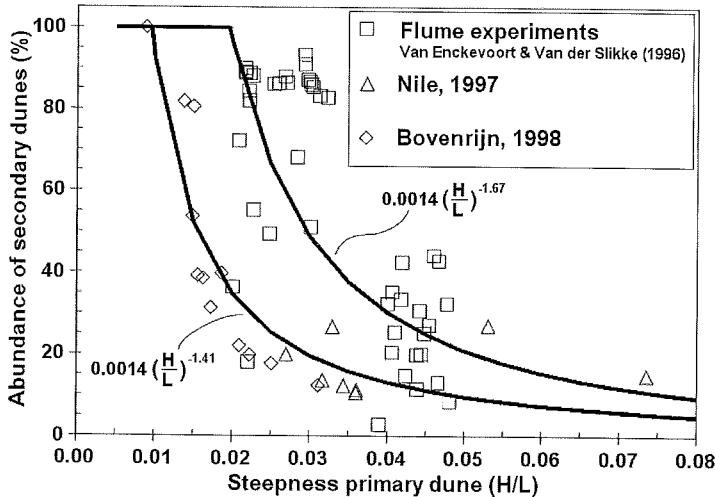


Figure 7.12: Relations between the abundance of superimposed dunes and the steepness of the primary dunes for both flume and field situations.

7.6 Conclusion

The results of the analyses that were performed show that adapting the hydraulic roughness predictors of Vanoni & Hwang (1967), Engelund (1977) and Van Rijn (1984) significantly improves the predicted total hydraulic roughness (Appendix 7.I), after introducing: 1) calculation of grain roughness only in the regions outside the separation zones, 2) substitution of dune height with brinkpoint height, 3) the addition of the hydraulic roughness of superimposed dunes according to their spatial abundance. Not only the overall prediction is improved, but especially the predictions in cases where

brinkpoint heights are much smaller than dune heights, and in cases where the dunes are superimposed by smaller bedforms. In those cases the original predictors over-, respectively underpredict the total hydraulic roughness. Therefore in many field situations where dunes come in various shapes and sizes and also superimposed on each other these adapted predictors are much more useful than the original ones. Even without recalibrating the coefficients of the Vanoni and Hwang predictor, which performed best in the analyses, the total hydraulic roughness of the bed can be predicted only on the bases of knowing the average shape and size of the dunes and the grain size of the bed. With the help of high resolution echo-sounder equipment and computer programs such as DT2D the necessary shape and size characteristics of both primary and secondary dunes can be easily determined.

The results also show that the assumption made by Van Rijn (1984), that k_s values can simply be summed, is incorrect and should be avoided. Summing the roughness in the correct way (eq. 7.24) improves the predictions of both the roughness predictor made by Van Rijn and of the adapted predictor. Finally, the predictor of Vanoni & Hwang, was recalibrated into a refitted predictor for the hydraulic roughness of bedforms, incorporating the use of brinkpoint height instead of dunes height. It performed only marginally better than the adapted original predictor. Therefore, either form of this predictor can be used to calculate the total hydraulic roughness in a river with a bed covered with dunes (Appendix 7.I).

Acknowledgements

The authors want to thank all persons and institutions that helped collecting and analysing the data used here. Special thanks goes out to Dr. J.H. van den Berg, Dr. M. Kleinhans, Dr. E.A. Koster, and Dr. Ir. L.C. van Rijn for valuable discussions and constructive criticism on drafts of the paper.

Notation

τ	=	boundary shear stress [Nm^{-2}]
τ'	=	shear stress related to grains
τ''	=	shear stress related to bedforms
ρ	=	fluid density [kgm^{-3}]
α	=	loss coefficient [-]
ϕ	=	angle of repose
γ	=	shape factor of Van Rijn, (1993)
a	=	regression intercept
Abun.	=	spatial abundance of superimposed dunes [%]
b	=	regression slope
B	=	bias
C	=	Chezy coefficient [$\text{m}^{0.5}\text{s}^{-1}$]
C'	=	Chezy coefficient related to grains [$\text{m}^{0.5}\text{s}^{-1}$]

C''	=	Chezy coefficient related to bedforms [$m^{0.5}s^{-1}$]
C_d	=	the drag coefficient [-]
D	=	pipe diameter [m]
D_{50}	=	50 percentile of the grain-size distribution [m]
D_{90}	=	90 percentile of the grain-size distribution [m]
f	=	Darcy-Weisbach friction factor [-]
f'	=	friction factor related to grains
f''	=	friction factor related to bedforms
f_s''	=	friction factor related to superimposed bedforms
f_g	=	plain bed friction factor [-]
g	=	gravitational acceleration coefficient [ms^{-2}]
h	=	average water depth [m]
h_f	=	energy loss [m]
h_p	=	water level relative to a horizontal plane [m]
H	=	height of dune crest [m]
H_b	=	brinkpoint height [m]
$H_{b,s}$	=	brinkpoint height of superimposed dune [m]
H_s	=	height of dune crest of superimposed dunes [m]
H/h	=	relative water depth [-]
H/L	=	dune steepness [-]
i_w	=	water-surface slope [-]
i_e	=	energy slope [-]
k_s	=	Nikuradse roughness height [m]
k_s'	=	Nikuradse roughness height for grains [m]
k_s''	=	Nikuradse roughness height for bedforms [m]
k_s'''	=	Nikuradse roughness height for superimposed bedforms [m]
L	=	dune length [m]
L_p	=	length of the pipe [m]
L_{prof}	=	total length of the profile [m]
L_s	=	average length of the superimposed dunes [m]
L_{sep}	=	separation length [m]
RMSE	=	Root Mean squared Error
N	=	number of datapoints
N_s	=	number of secondary dunes in a profile [-]
o_i	=	observed roughness of point i
p_i	=	predicted roughness of point i
R	=	hydraulic radius [m]
R_b	=	adapted hydraulic radius [m]
R_b'	=	hydraulic radius of the same channel with a plane bed
Re	=	Reynolds number [-]
U	=	average flow velocity [ms^{-1}]
V	=	variance of the errors
\sqrt{V}	=	standard deviation of the variance

A

References

- ABDEL-FATTAH, S. (1997) Field measurements of sediment load transport in the Nile river at Quena., Technical Report, HRI, Delta Barrage, Egypt
- ABDEL-FATTAH, S., AMIN, A., & VAN RIJN, L.C. (2003) Sand transport in Nile River, Egypt. *Journal of Hydraulic Engineering*, in prep.
- BROWNIE, W.R. (1981) Prediction of flow depth and sediment discharge in open channels., KH-R-43A, W. M. Keck Laboratory of Hydraulics and Water Resources Division of Engineering and Applied Science, California Institute of Technology, Pasadena, California, 1 pp.
- CHANG, F.F.M. (1970) Ripple concentration and friction factor. *Journal of the Hydraulics Division*, 96, 417-430.
- COLEBROOK, C.F. & WHITE, C.M. (1937) Experiments with fluid friction in roughened pipes. *Proceedings of the Royal Society of London*, 161, 367-381.
- ENGELUND, F. (1977) Hydraulic resistance for flow over dunes. *Progress Report of the Institute for hydrodynamic and hydraulic engineering*, 44, Tech. Univ. Denmark, 19 pp.
- JULIEN, P.Y., KLAASSEN, G.J., TEN BRINKE, W.B.M., & WILBERS, A.W.E. (2002) Case study: Bed resistance of the Rhine River during the 1998 flood. *Journal of Hydraulic Engineering*, 128, 1042-1050.
- KORNMAN, B.A. (1995) The effect of changes in the lee shape of dunes on the flow field, turbulence and hydraulic roughness. *Report on measurements.*, R 95-1, Institute for marine and atmospheric research Utrecht,
- NIKURADSE, J. (1933) Strömungsgesetze in rauhen rohren. *Forschung auf dem Gebiete de Ingenieurwesens*, 361.
- OGINK, H.J.M. (1989) Hydraulic roughness of single and compound bedforms part XI, report on model investigations., M 1314-XI/Q 786, Delft Hydraulics,
- VAN ENCKEVOORT, I. & VAN DER SLIKKE, A. (1996) Changes in hydraulic roughness of dunes under varying high flow velocities., University of Utrecht, Utrecht
- VAN MIERLO, M.C.L.M. & DE RUITER, J.C.C. (1988) Turbulence measurements above artificial dunes *Report on measurements.*, Q789, Delft hydraulics,
- VAN RIJN, L.C. (1982) Equivalent roughness of alluvial bed. *Journal of the Hydraulics Division*, 108, 1215-1218.
- VAN RIJN, L.C. (1984) Sediment transport; Part 3: bedforms and alluvial roughness. *Journal of Hydraulic Engineering*, 110, 1733-1754.
- VAN RIJN, L.C. (1993) *Principles of sediment transport in Rivers, Estuaries and Coastal seas.* Aqua Publications, Amsterdam
- VAN URK, A. (1982) Bedforms in relation to hydraulic roughness and unsteady flow in the Rhine branches (The Netherlands). In: *The mechanics of sediment transport*, Euromech 156, 151-156.
- VANONI, V.A. & BROOKS, N.H. (1957) Laboratory studies of the roughness and suspended load of alluvial streams., E-68, Sedimentation Laboratory, California Institute of Technology, New York
- VANONI, V.A. & HWANG, L.S. (1967) Relation between bedforms and friction in streams. *Journal of the Hydraulics Division*, 93, 121-144.
- VITTAL, N. (1972) Flow over triangular roughnesses in open channels. University of Roorkee, India,
- VITTAL, N., RANGA RUJU, K.G., & GARDE, R.J. (1977) Resistance of two dimensional triangular roughness. *Journal of Hydraulic Research*, 15, 19-36.
- WHITE, W.R., PARIS, E., & BETTESS, R. (1979) A new general method for predicting the frictional characteristics of alluvial streams., IT 187, Hydraulic Research Station Wallingford, Wallingford, England, 1 pp.
- WILBERS, A.W.E. & TEN BRINKE, W.B.M. (2003) The response of subaqueous dunes to floods in sand and gravel bed reaches of the Dutch Rhine. *Sedimentology*, in press.
- YALIN, M.S. (1964) Geometrical properties of sand waves. *Journal of the Hydraulics Division*, 90, 105-119.

Appendix 7.1

The prediction of the hydraulic roughness of the river bed, from measured dune characteristics can be done like this:

1. Determine the flow, grain size and dune characteristics necessary for the predictors. Flow characteristics: water depth (h), and hydraulic radius (R_b). Grain size characteristics: 90 percentile of the grain size distribution (D_{90}). Dune characteristics: dune length (L) and brinkpoint height (H_b) of both primary and superimposed secondary dunes. When the brinkpoint height cannot be determined from the field measurements it can be estimated with:

$$\frac{H_b}{H} = 0.78 + 0.1H \quad (7.1.1)$$

2. Calculate grain roughness.
in the case of a sand-bed river ($D_{50} \leq 0.002\text{m}$) the grain roughness is:

$$f' = \frac{L - L_{sep}}{L} * \frac{8 * g}{\left(18 \log \left(\frac{12R_b}{3D_{90}} \right) \right)^2} \quad (7.1.2)$$

while in case of a gravel-bed river ($D_{50} > 0.002\text{m}$) the grain roughness is:

$$f' = \frac{L - L_{sep}}{L} * \frac{8 * g}{\left(18 \log \left(\frac{12R_b}{D_{90}} \right) \right)^2} \quad (7.1.3)$$

Where g = gravitational acceleration coefficient, R_b = adapted hydraulic radius, L = dune length, L_{sep} = length of the separation zone, and D_{90} = 90 percentile of the grain size distribution. L_{sep} can be estimated with:

$$L_{sep} = \frac{H_b}{\tan(10^\circ)} \quad (7.1.4)$$

where H_b = brinkpoint height.

3. The form roughness of the primary dunes can be calculated with either:

$$f'' = \left(\frac{1}{3.3 \log \left(\frac{R_b L}{H_b^2} \right) - 2.3} \right)^2 \quad (7.1.5, \text{Vanoni and Hwang, 1967})$$

$$f'' = \left(\frac{1}{2.83 + 0.0165 * \left(\frac{R_b L}{H_b^2} \right)} \right)^2 \quad (7.1.6, \text{recalibrated Vanoni \& Hwang})$$

$$f'' = 10 \frac{H_b^2}{hL} * \exp \left(-2.5 \frac{H_b}{h} \right) \quad (7.1.7, \text{Engelund, 1977})$$

$$f'' = \frac{8 * g}{\left(18 \log \left(\frac{12 R_b}{k_s''} \right) \right)^2}$$

$$\text{with } k_s'' = 1.1 H_b * \left(1 - \exp \left(-25 \frac{H_b}{L} \right) \right) \quad (7.1.8, \text{Van Rijn, 1984})$$

where h = water depth, and k_s'' = Nikuradse roughness height for dunes.

4. The form roughness of superimposed secondary dunes can be calculated with either:

$$f_s'' = \frac{(N_s * L_s)}{L_{prof}} * \left(\frac{1}{3.3 \log \left(\frac{R_b L_s}{H_{b,s}^2} \right) - 2.3} \right)^2 \quad (7.1.9, \text{Vanoni and Hwang, 1967})$$

$$f_s'' = \frac{(N_s * L_s)}{L_{prof}} * \left(\frac{1}{2.83 + 0.0165 * \left(\frac{R_b L_s}{H_{b,s}^2} \right)} \right)^2 \quad (7.1.10, \text{recalibrated Vanoni \& Hwang})$$

$$f_s'' = \frac{(N_s * L_s)}{L_{prof}} * 10 \frac{H_{b,s}^2}{h L_s} * \exp \left(-2.5 \frac{H_{b,s}}{h} \right) \quad (7.1.11, \text{Engelund, 1977})$$

$$f_s'' = \frac{(N_s * L_s)}{L_{prof}} * \frac{8 * g}{\left(18 \log \left(\frac{12 R_b}{k_s'''} \right) \right)^2}$$

$$\text{with } k_s''' = 1.1 H_{b,s} * \left(1 - \exp \left(-25 \frac{H_{b,s}}{L_s} \right) \right) \quad (7.1.12, \text{Van Rijn, 1984})$$

where f_s'' = friction factor related to superimposed bedforms, N_s = the number of secondary dunes in a profile, L_s = the average length of the secondary dunes, L_{prof} = the total length of the profile, $H_{b,s}$ = brinkpoint height of secondary dunes, and k_s''' = Nikuradse roughness height for secondary dunes. When the abundance of the superimposed dunes cannot be determined from the field measurements it can be estimated with:

$$\frac{(N_s * L_s)}{L_{prof}} = 1 \text{ if } H/L \leq 0.01 \quad (7.1.13)$$

$$\frac{(N_s * L_s)}{L_{prof}} = 0.0014 \left(\frac{H}{L} \right)^{-1.41} \text{ if } H/L > 0.01 \quad (7.1.14)$$

5. The total hydraulic roughness of the river bed can then be calculated by:

$$f = f' + f'' + f_s'' \quad \text{or} \quad C = \sqrt{\frac{8g}{f}} \quad (7.1.15)$$

8 Synthesis, application of the results and implications for future research

8.1 Introduction

Subaqueous dunes are prominent features on the bed of many rivers. They obstruct the flow, thereby increasing the water levels especially during floods, and they may hinder navigation on rivers at low flow stages. The development of these subaqueous dunes and their related hydraulic roughness have therefore long been important subjects in many river studies. Dunes have been observed in many rivers, from small to large, and with fine to coarse bed material (Gabel, 1993; Nordin & Perez-Hernandez, 1989; Dinehart, 1989). From those observations the dune development was related to different flow characteristics (Shinohara & Tsubaki, 1959; Allen, 1978; Van Rijn, 1984) and the dune related hydraulic roughness appeared to be related to the dune dimensions (Van Rijn, 1984; Julien *et al.*, 2002). Several researchers also recognised that there is a strong feedback loop (fig. 8.1) between the flow conditions, sediment transport and dune development in a river (Simons & Sentürk, 1992; Best, 1993; Kleinhans, 2002). As the flow velocity increases, for example due to a flood wave, the sediment transport rates increases. This increase in sediment transport causes a growth in the dune dimensions, and because larger dunes have a higher hydraulic roughness, they slow down the flow velocity, decreasing the sediment transport.

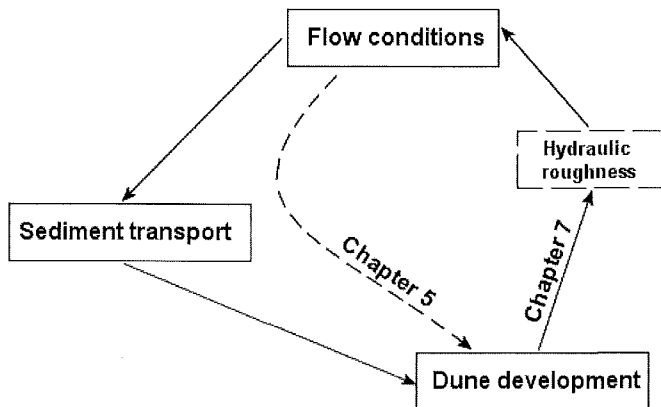



Figure 8.1: A visual representation on how the predictors formulated in Chapters 5 and 7 of this thesis fit into the feedback loop between flow conditions, sediment transport, and dune development.

However, dune characteristics, flow factors, and sediment transport rates are difficult to measure in field situations, especially in medium to large rivers like the Rhine branches in the Netherlands (Kleinhans & Ten Brinke, 2001). Factors such as slope, bed shear

stress, and overall hydraulic roughness are difficult to ascertain during a flood wave in a large river, with a bed covered with large dunes and heavy shipping on the river. Only recently, technical innovations made it possible to measure dune characteristics with high spatial resolution using multibeam echosounding systems and to automatically process the large amounts of data from these measurements with computers (Ten Brinke *et al.*, 1999). Also the ongoing development of sophisticated flow models has provided the possibility of utilizing reliable predicted flow parameters (Van der Veen, 2002), instead of labour intensive and inaccurate parameters measured in the field.

These improvements in measurement techniques and flow models make it possible to further investigate the dune development and related hydraulic roughness in field situations, which are the two objectives of this thesis. In accordance with these two goals this thesis is divided in two parts. Part 1 is focused on the influence of the flow on the dune development and of the dune migration on the sediment transport. Part 2 is mainly focused on the influence of the dunes on the flow through the hydraulic roughness. In the introduction of this thesis the following research questions were formulated:

Part 1

- How do sediment transport and dunes interact and how can the migration of dunes be used to calculate the bedload transport?
- How do the dunes in the Dutch rivers change during the unsteady flow conditions and how can these changes be predicted? 

Part 2

- What is the relation between dune shape and size, the dimensions of the flow separation zone, and the hydraulic roughness of a dune?
- How can the hydraulic roughness of dunes be predicted with dune characteristics?
- What is the cause of the superposition of dunes in the Dutch rivers and how does this superposition influence the bedload transport, dune development, and hydraulic roughness?

The aim of this synthesis is to summarize the answers to these research questions and to discuss to what extent these answers are an improvement of previous work. A second aim is to assess how well the proposed prediction methods for dune development (part 1) and hydraulic roughness (part 2) can be combined. Finally, some suggestions are given for future research on the topics of dune development and hydraulic roughness.

8.2 Conclusions of this thesis

8.2.1 Bedload transport and migrating dunes

The first research question of part 1 of this thesis is addressed in Chapter 3. It shows that, as was previously described by Allen (1965) and Bennett & Best (1995), the flow pattern over dunes is very complex which results in complex pathways of sediment transport and

different interactions between sediment transport and the dune surface. Over the stoss-side of a dune, sediment transport is divided into bedload and suspended transport. But over the lee-side, where the flow is separated from the bed surface, sediment is either deposited in avalanches on the lee-slope, or transported in semi-suspension to the next dune, or it goes into or falls out of suspension.

All these interactions play a role in dune migration and thereby influence the determination of bedload transport, which is called dune tracking. Several investigators (Van den Berg, 1987; Jinchi, 1992; Ten Brinke *et al.*, 1999; Dinehart, 2002) have already shown that this dune tracking technique is a useful tool in field situations. However neither of them made a thorough assessment of the factors that influence the reliability of this technique in field situations. The analysis in Chapter 3 shows that factors such as measurement resolution, the calculation of a form factor, and suspended or semi-suspended transport of material over a dune are important in dune tracking. When precautions are taken, most of the factors mentioned in Chapter 3 can be assumed to be of negligible influence or appear to cancel each other out. Only the migration rate, dune height and the dune shape factor are parameters that have to be known accurately before the bedload transport rate can be calculated.

It is shown that with detailed measurements of dunes, the bedload transport rate in a river can be determined accurately. However, in many cases it is desirable to know not only the bedload transport rate, but also the amount of suspended sediment and the grain-size composition of the transported material. In those cases, just as was done in the Rhine branches (Kleinhans & Ten Brinke, 2001; Kleinhans, 2002), direct measurements of both suspended and bedload sediment transport and dune tracking must be combined.

8.2.2 Observed and predicted dune development

The second research question is answered in Chapters 4 and 5. In Chapter 4 all the measurements of dunes done in different Rhine branches are described and analysed. From these measurements the dune development in those branches is deduced and an analysis is made in how far and why the dune development differed in the various river sections. It is concluded that both the grain-size differences between the sections and the variable discharge distribution over the main channel and the flood plain are the major factors causing the differences in dune development. The differences in shape and duration of the flood waves appear to be of less importance. Also in Chapter 4, a first attempt of predicting dune development is made. In order to avoid the difficulties associated with hystereses only the information during rising discharges is used. The results show that during rising discharges the development of dune height, length and migration rate is related strongly to both the dimensionless bed shear stress and grain related shear stress.

In Chapter 5 a method is presented that enables a satisfactory prediction of dune characteristics at any stage in the Rhine branches. This method is based on ideas of Allen (1976a, 1976b, 1976c), Fredsøe (1979), and Van Rijn (1989). It consists of three different calculation models, one for dune height and one for dune length in the river sections near the Pannerdensche kop, and one for dune height in the river section near Druten. These

calculation models are transcribed in Appendix 5.II. The calculation models have been calibrated with the average results from all available data, and they were tested against the data from individual floods in the same dataset. As compared to the existing methods of Allen (1976a), Fredsøe (1979), and Van Rijn (1989), the advantage of the proposed new method is that it contains only one calibration coefficient (the adaptation constant) which is easily determinable from time series of dune dimensions and flow conditions. However, the new method has still one major drawback. Due to a lack of information on the grain-size composition of the bed during a flood wave, the grain-size could only be assumed constant. This constant grain-size however necessitated the introduction of several thresholds distinguishing between the different equilibrium predictors. As these thresholds are only valid for certain sections of the Rhine branches, in other sections new thresholds have to be defined. Better information on the grain-size composition during flood waves will probably improve the new prediction method and eliminate the need for defining these thresholds.

8.2.3 The relation between flow separation and hydraulic roughness

The first research question of part 2, “What is the relation between dune shape and size, the dimensions of the flow separation zone, and the hydraulic roughness of a dune?” is studied in Chapter 6. In this chapter measurements of the flow separation zone over various bedforms are analysed to investigate the relation between dune shape, flow condition, and the shape and size of the flow separation zone. This analysis follows the assumption made by several investigators, such as Vanoni & Hwang (1967), Engel (1981), Kornman (1995), and Yoon & Patel (1996), that the shape and size of the separation zone is directly related to the amount of turbulence that is formed in the flow and therefore also directly related to the hydraulic roughness of the dunes.

The results of the analysis show that the size of the flow separation zone is strongly related to the height of the bedform, even more so than was assumed and described by Engel (1981) and Yoon & Patel (1996). Especially when the bedforms are viewed as solitary forms, then the length of the flow separation zone is 5.5 times the height of the point of separation. This can be explained by the fact that the zero velocity line, which connects the separation and the reattachment points, always has a constant angle of 10 degrees (± 1 degree) independent of flow condition or bedform shape. This fact was never recognised before and implies that size and shape of the flow separation zone can be approximated from the height of the point of flow separation. On steep-sided dunes this point of flow separation coincides with the brinkpoint, while on low angle dunes and other bedform shapes the flow is shown to separate at the point where the angle of the bed exceeds 10 degrees.

8.2.4 Predicting the hydraulic roughness of dunes

After analysing the relation between dune shape, flow separation and hydraulic roughness the final question of part 2 and the second goal of the thesis is considered in Chapter 7. Several predictors exist for the hydraulic roughness related to subaqueous dunes (Yalin, 1964; Vanoni & Hwang, 1967; Vittal, 1972; Vittal *et al.*, 1977; Engelund, 1977; White *et al.*, 1979; Brownlie, 1981; Van Rijn, 1984). However, none of these predictors use the height of flow separation or the brinkpoint height as a major parameter. Most of them just use the height of the dune crest as an approximation. Moreover, none of these predictors considers superimposed dunes as a major factor contributing to the total hydraulic roughness. Although in most cases the grain roughness is considered as part of the total hydraulic roughness it is not taken into account that the grain roughness is negligible in the region of flow separation. Ogink (1989) showed that all these factors are of influence on the accuracy of predictions of hydraulic roughness. Following his ideas a new dune-related hydraulic roughness predictor might be constructed. However, due to a lack of flume and field data such a new predictor can not yet be established. Therefore, it is decided to use the predictors of Vanoni & Hwang (1967), Engelund (1977), and Van Rijn (1984) and replace the dune height in these predictors with brinkpoint height. Simultaneously, the way in which grain roughness and the roughness of superimposed dunes is accounted for in these predictors is changed. However, the empirical coefficients of the roughness predictors are not recalibrated.

The results of testing these adapted predictors against a varied dataset from flume experiments and field measurements, reported in Chapter 7, show that using the brinkpoint height and adding the roughness of the superimposed dunes according to their abundance greatly improves the predictions. Especially in conditions with very low or very high hydraulic roughness the prediction improved significantly. It appeared that the adapted predictor of Vanoni & Hwang (1967) performed best of all. A recalibration of the empirical coefficients of this predictor did not further improve the results. The total procedure, of how to predict the hydraulic roughness in the Rhine branches, including the adapted equations, are transcribed in Appendix 7.I.

8.2.5 Superposition of subaqueous dunes

Although the issue of superposition of dunes is not considered separately in this thesis, it is shown to be relevant in almost every chapter. In Chapter 3 it is concluded that in case superimposed dunes are present in a river it is important to select the right dune type for dune tracking. In cases where the superimposed dunes cover both the lee and the stoss-sides of the primary dunes, the superimposed dunes should be used for calculating the bedload transport rate. In other cases either dune type will do for dune tracking. It is also concluded that superposition makes it more difficult to correctly determine the migration rates of the selected dune type, possibly reducing the reliability of the dune tracking technique.

In Chapter 4 it is shown that superposition occurs in all sections of the Rhine branches. Near the Pannerdensche kop, superposition occurs during falling discharges as the

primary dunes lengthen and decrease in height. In the Waal near Druten superposition is always present as several dune sizes are present on top of each other. The reason how and why this superposition occurs in those sections is unclear but from Chapter 5 it can be concluded that at least near the Pannerdensche kop superposition is related to the hystereses in the development of primary dunes. In these sections, superposition occurs during the falling stages as the bed shear stress declines below 10 Nm^{-2} , and the primary dunes disappear all together when their steepness (H/L) reduces below 0.01. The primary dunes obviously can not follow the fast decline in flow strength during the falling stages and therefore become inactive as small superimposed dunes take over (Chapter 4).

Finally in Chapter 7 superposition is shown to be an important factor in predicting the total hydraulic roughness. Especially the abundance of superimposed dunes is important. When the primary dune is totally covered with secondary dunes, the hydraulic roughness of the primary dunes is no longer of importance, only the hydraulic roughness of the secondary dunes contributes to the total hydraulic roughness. Adding the abundance of the superimposed dunes to the calculation of the hydraulic roughness greatly improves the performance of the predictions, especially in conditions with high values for total hydraulic roughness.

However, the question how and why superposition occurs remains. It is obvious that it occurs only when there is enough space and time to develop small forms on larger ones (Ashley, 1990), but it is unclear how the flow makes this possible. Stability diagrams (Chapter 2) suggest that in a particular combination of flow and grain-size, only one type of bedform can exist, and it should therefore be impossible to get other bedforms such as ripples on dunes. One possible explanation for superposition is that it occurs when the primary dunes become inactive due to hystereses (as described above; Chapters 4 and 5; Allen & Collinson, 1974). It is suggested that the dimensions of the primary dunes grow out of phase with the development of the flow during the falling stages of a flood and consequently these dunes cannot be supported anymore. These dunes will become lower, longer, more symmetrical, and their migration rate decreases as they become inactive. The bedload transport activity is then taken over by new, smaller secondary dunes that develop on top of these disappearing primary ones. These secondary dunes cover the complete primary dune including their lee-sides.

However, there has to be a second possible explanation for superposition because in other situations, for example in the Waal near Druten or in the flume experiments by Van Enckevoort & Van der Slikke (1996) superposition occurs with both primary and secondary dunes migrating actively. The secondary dunes in these cases only cover part of the stoss-side of the dune (sometimes almost up to the dune crest). This type of superposition is therefore not related to the hystereses in dune development, it probably is more related to the local structure of the flow over a primary dune. Each subaqueous dune has a flow separation zone on its lee side where large turbulent eddies are created which are shed into the flow. These eddies create two different flow regions over the stoss side of the next dune, which are divided by an internal shear layer (Bennett & Best, 1995; fig. 3.1). The overall flow shear, related to average flow and found in the upper region, causes the primary form. However, the existence of the internal shear layer creates a different local flow-shear over the stoss-side of a primary dune (Van Mierlo & De Ruiter, 1988; Bennett & Best, 1995) which may cause secondary dunes to develop.

This internal shear layer and its consequences for the flow over the stoss have been studied before (Bennett & Best, 1995). However, it is not clear how it is related to the occurrence of superposition. This latter phenomenon has not yet been studied.

8.3 Combining predictors

In the introduction of this chapter it is concluded that there is a strong feedback loop between the flow conditions, the sediment transport and the dune development in a river (fig. 8.1). Later on two prediction methods have been proposed that can be used to describe some of the interactions in this feedback loop. First, the prediction method for dune development, proposed in Chapter 5, describes the relation between flow conditions and dune development. By incorporating a time-lag between flow and dune characteristics, the method bypasses the relations between flow conditions and sediment transport and sediment transport and dune development. This is done because those relations are difficult to define due to the complex processes of grain-size sorting (Kleinhans, 2002). Secondly, the prediction method for hydraulic roughness, proposed in Chapter 7, describes part of the relation between dune development and flow conditions. Together these two prediction methods can be used to predict the changes in hydraulic roughness during extreme flood events using flow prediction from currently available numerical models. As in these models the hydraulic roughness is not calculated dynamically but is used as a calibration factor, a comparison between the dynamically predicted hydraulic roughness and the hydraulic roughness from a flow model during an extreme flood could indicate the reliability of the predictions made by such a flow model.

A good example of a flood event that can be used for such a comparison, is the extreme “design” flood that is used in The Netherlands as the basis for flood protection plans. This flood event has a discharge of $16,000 \text{ m}^3\text{s}^{-1}$ and an estimated occurrence of once every 1250 years. The flow model SOBEK, calibrated for the Rhine in The Netherlands, is one of the tools used to calculate the water levels for these extreme conditions. The comparison between the hydraulic roughness from the calibrated SOBEK model and the hydraulic roughness predicted from the dune development is done in five successive

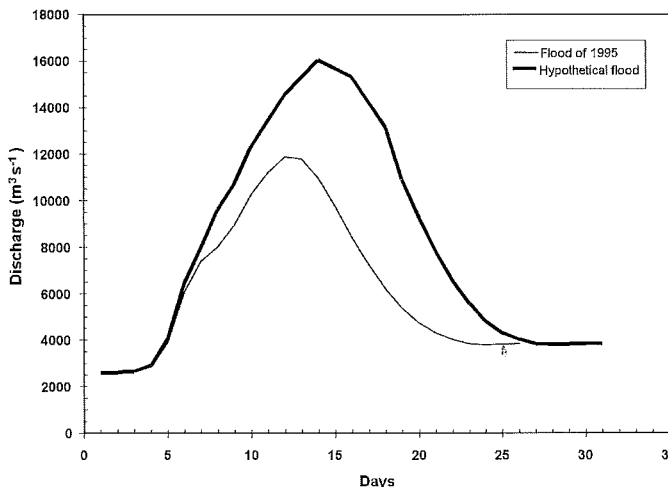


Figure 8.2: A hypothetical flood wave with a maximum of $16,000 \text{ m}^3\text{s}^{-1}$, defined according to the largest known flood wave in the Rhine at the Dutch-German border from 1995.

steps: 1) define a hypothetical flood wave for the Bovenrijn (Section 2A, fig. 4.1) with a maximal discharge of $16,000 \text{ m}^3\text{s}^{-1}$, 2) calculate the water depth, flow velocity, bed shear stress, and hydraulic roughness using the SOBEK model, 3) use the method of Chapter 5 and the data on water depths, flow velocities, and bed shear stresses from SOBEK to predict dune length and dune height, 4) use the predicted dune dimensions together with the method of Chapter 7 and the data on water depths, flow velocities, and bed shear stresses from SOBEK to predict the dynamic hydraulic roughness, and 5) compare the calculated hydraulic roughness of SOBEK with the predicted values.

8.3.1 Step 1

A hypothetical flood wave was defined using the flood wave of 1995 as an example. In 1995 the discharge rose from about $2500 \text{ m}^3\text{s}^{-1}$ to $12,000 \text{ m}^3\text{s}^{-1}$ and decreased again to about $3800 \text{ m}^3\text{s}^{-1}$ over a period of 24 days. The hypothetical wave also starts at about $2500 \text{ m}^3\text{s}^{-1}$ but rises to $16,000 \text{ m}^3\text{s}^{-1}$ and then falls to $3800 \text{ m}^3\text{s}^{-1}$ over a period of 30 days (fig. 8.2).

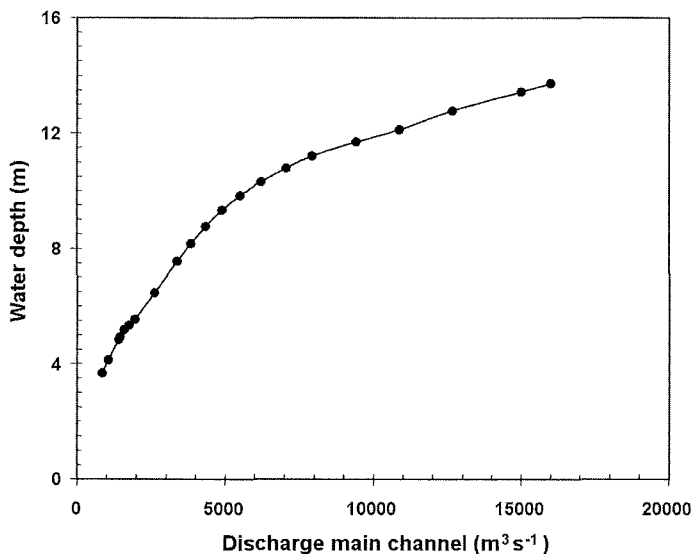


Figure 8.3: The relation between the discharge and the water depth of the main channel according to SOBEK-calculations.

8.3.2 Step 2

Using the SOBEK model, the flow conditions were determined for different stable discharges in 21 steps ranging from 838 to $16,000 \text{ m}^3\text{s}^{-1}$. This resulted in several functions describing the relation between the discharge of the main channel and the water depth (fig. 8.3), flow velocity, bed shear stress and Chezy value, also of the main

channel. Using these functions, the development of these parameters was calculated during the hypothetical flood wave. Figure 8.4 shows that the water depth, flow velocity, and bed shear stress, derived from SOBEK, all rise and fall in a similar way as the discharge. However, the Chezy value as derived from SOBEK, shows a very different development. After a decrease at the start (day 5) of the flood wave (this corresponds to an increase in the hydraulic roughness), there is a small increase and subsequent decrease during main part of the flood (between day 6 and 22), followed by a pronounced increase at the end of the flood (corresponding to a decrease in the hydraulic roughness). The variation in hydraulic roughness, however, is small as the Chezy value only varies between 49 and 53 $\text{m}^{1/2}\text{s}^{-1}$.

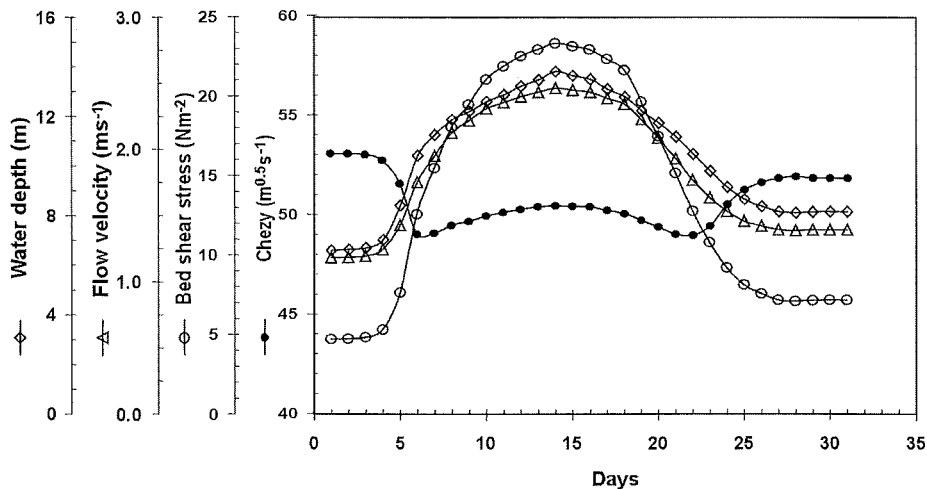


Figure 8.4: Development of water depth, flow velocity, bed shear stress, and Chezy value during the hypothetical flood wave according to SOBEK-calculations.

8.3.3 Step 3

The models for predicting dune height and length in the Bovenrijn (Chapter 5) are strongly related to the bed shear stress development. Because no other information on bed shear stress is available, the bed shear stress values from SOBEK are used. At the same time, the grain-size is assumed constant at a D_{50} of $3.34 \cdot 10^{-3}$ m. To calculate the dune height and length the models transcribed in Appendix 5.II were used, which resulted in the hypothetical dune development shown in fig. 8.5. Dune height and length start increasing after day 5. At day 22, 8 days after the peak discharge, the dune height is maximal, and after that the dune height starts decreasing again. The dune length however, keeps on increasing throughout the flood wave. At day 24, superimposed small dunes appear on the large primary ones. The dimensions of these secondary dunes do not change very much thereafter.

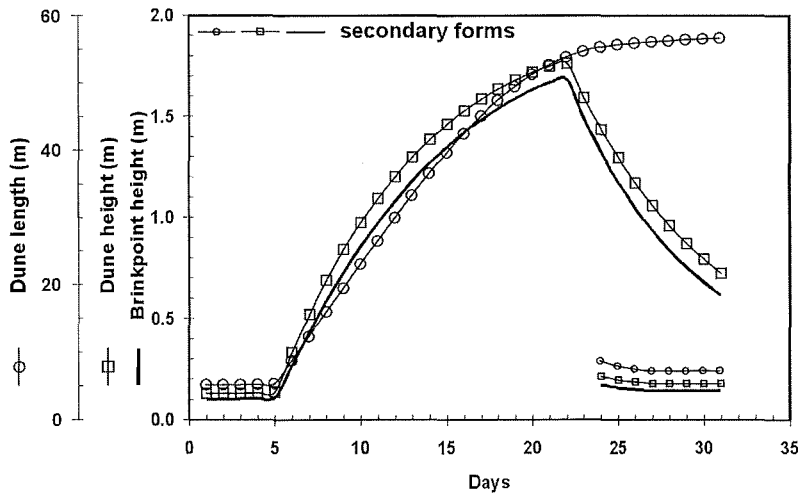


Figure 8.5: Development of dune length and height of primary and secondary dunes as predicted with the models described in Chapter 5. The development of the brinkpoint height was calculated with the function shown in fig. 8.6.

8.3.4 Step 4

The model for calculating the hydraulic roughness of dunes, developed in Chapter 7, uses the brinkpoint height of the dunes and the spatial abundance of the superimposed dunes. Both factors are, however, not calculated with the models of Chapter 5. From the data of the Rhine used in Chapter 7, two functions can be created to help determine these parameters. Figure 8.6 shows the strong relation between brinkpoint height and dune height for both primary and secondary dunes in the Bovenrijn during the flood of 1998. For dunes higher than 0.6m this relation follows a straight line. Smaller dunes, however, seem to have increasingly smaller brinkpoint height in proportion to the dune height. However, in Chapter 7 it was already explained that the measurement resolution has a significant effect on the accurate detection of the brinkpoint. The measurement resolution of the data from the Rhine was such that for small dunes, in this case especially the secondary dunes, the calculated brinkpoint height are most likely to be small. In this analyses therefore it was assumed that the relation between dune height and brinkpoint height followed the straight line and can be calculated with the function shown in fig. 8.6. Figure 8.7 shows the abundance of secondary dunes superimposed on a primary dune as a function of the dune steepness (H/L) of the primary dune for the Bovenrijn during the flood of 1998. If the primary dune has a steepness of 0.01 or smaller, then the secondary dunes cover the whole primary one including the lee-side and the abundance is 100%. Otherwise the abundance of superimposed secondary dunes in the Bovenrijn can be estimated with the function shown in fig. 8.7.

Using the two functions for brinkpoint height and abundance of superposition, together with the information on dune dimensions and flow conditions, the adapted method of Vanoni & Hwang (1967), described in Appendix 7.I, was used to calculate the dynamic

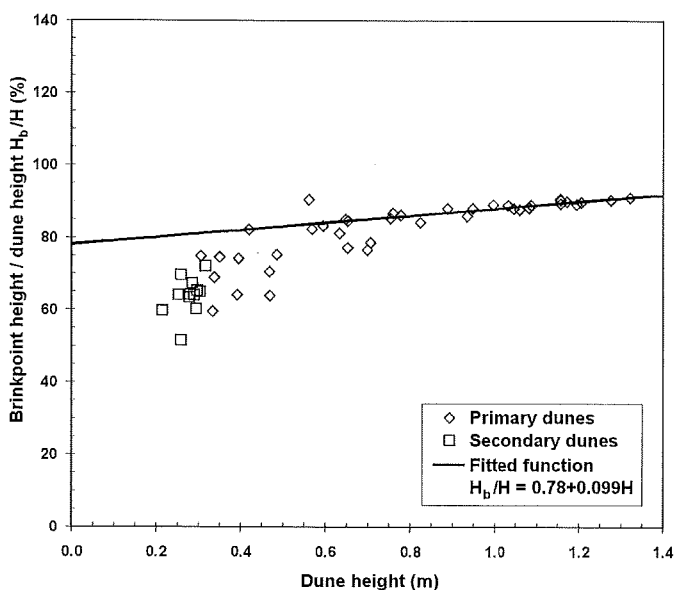


Figure 8.6: Relation between the brinkpoint height as a proportion of the dune height and the dune height. The fitted function indicates the relation used in the analysis, after assuming that the points which plot beneath the line can be ignored due to low measurement resolution.

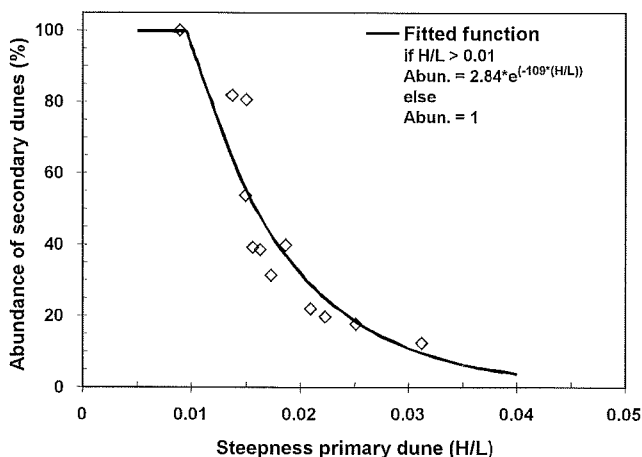


Figure 8.7: Relation between the abundance of superimposed dunes and the steepness of the primary dunes for the Bovenrijn during the flood of 1998.

hydraulic roughness (Chezy value) during this hypothetical flood wave. Figure 8.8 shows that the hydraulic roughness is small before the flood wave starts (indicated by a large Chezy value) and that it increases strongly as the dunes grow in size. After the dune height decreases again (8 days after the peak discharge) the hydraulic roughness decreases again slowly. Therefore a strong hystereses loop is predicted between the

hydraulic roughness during the rising limb of the flood and the falling limb, contrary to the predictions of SOBEK. The Chezy value in this case ranges from 41 to 59.5 $\text{m}^{1/2}\text{s}^{-1}$ during the hypothetical flood wave.

8.3.5 Step 5

The hydraulic roughness (Chezy) predicted according to the estimated dimensions of the dunes has a much larger variation during the hypothetical flood wave than the hydraulic roughness predicted by the SOBEK model (fig. 8.8). However, because the predictions of dune dimensions and dune related roughness used some of the results from the SOBEK model as measured data are absent, it is not possible to say that the predicted dynamic hydraulic roughness is correct. Actually, if the hydraulic roughness in the SOBEK model would vary as much as is predicted based on the dune predictions, than the flow velocities, water depths and bed shear stresses would be very different from the ones used here. How much different and how this would influence the predictions made here is, however, unknown. But, the fact that there is a great discrepancy between the Chezy values of SOBEK and the values predicted from the dunes indicates that there may be a problem with the prediction from SOBEK for such an extreme flood event. During the peak discharge of an extreme flood event the hydraulic roughness could be as much as 20% higher (resulting in lower Chezy values). This much higher hydraulic roughness would most probably result in much higher water levels than ever predicted with SOBEK. In that case, the implementation of the prediction models for dune development and dune-related hydraulic roughness in models such as SOBEK will have important implications for the redevelopment plans for the Rhine branches.

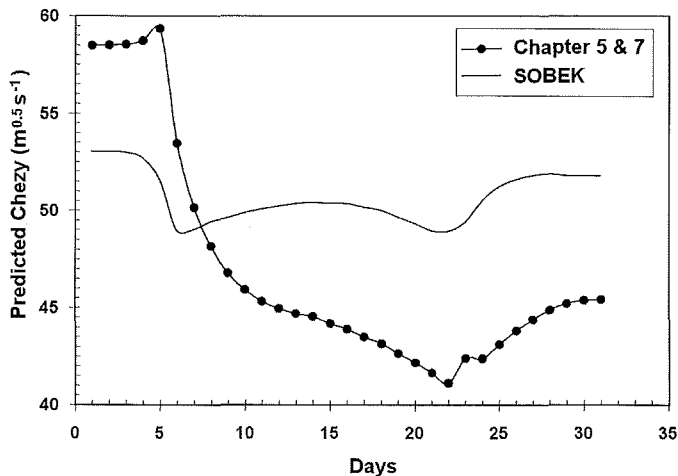


Figure 8.8: Development of the Chezy value during the hypothetical flood wave according to the models of Chapter 5 and 7 describing the dune development and dune related hydraulic roughness and also according to the SOBEK-calculations.

8.4 Conclusions

The main goals of this thesis are to propose methods to predict the dune development and the dune-related hydraulic roughness in a large river. These goals are reached, as in both cases a prediction method was successfully formulated and applied. The method for predicting dune development uses the flow strength and grain-size as major parameters together with the notion that the dunes are always developing toward an equilibrium dune dimension at a rate depending on the difference between their actual size and the equilibrium size. The method for predicting dune-related hydraulic roughness uses the shape of the dunes in the form of the brinkpoint height, and the composition of the dune field in the form of the abundance of superimposed forms. However, the generic use of these two prediction methods is limited because the major part of the analyses in this thesis was based on data from the Rhine branches gathered in the last decade. No information of the same high quality was available from other rivers and therefore the resulting predictors, as described in Chapters 5 and 7, are only applicable in certain sections of the Rhine branches.

The major contribution to the research field of subaqueous dunes of this thesis is therefore probably not the two prediction methods but the appreciation of the importance of the basic principles behind the two prediction methods. The ideas, that dune development is not related directly to the current flow conditions but more to the history of previous conditions, and that the hydraulic roughness of dunes is not related to dune height but to the height of flow separation, are not new, but are for the first time incorporated in applicable prediction methods. The possibility of combining the two prediction methods to analyse the development of hydraulic roughness during a hypothetical flood wave is also useful. A trial calculation, which is done above, shows that the combined prediction methods predict a much higher variation of the hydraulic roughness than is predicted by a well-known and well-calibrated flow model for the Rhine branches. This indicates that flow models will benefit from the use of these prediction methods or the concepts behind them to improve the calculation of the hydraulic roughness. This will result in more reliable water levels especially during discharges far beyond the calibration region, where flow conditions have to be extrapolated.

With respect to the research field of subaqueous dunes, the technique of dune tracking has shown to be a reliable and simple way of determining the bedload transport rate in a river. The measurements with high resolution multibeam echosounding equipment are shown to be very valuable for this technique. These multibeam echosoundings are also essential in determining the dune development and dune shapes in the Rhine branches during several floods. The analysis on the interrelations of flow separation, dune shape and hydraulic roughness shows that a flow separation zone is even more stable in shape than was suspected by several investigators. It also reveals that the point of flow separation coincides with the place where the lee-side slope exceeds an angle of 10 degrees. This notion could have important implications in situations where the bed is covered with symmetrical dunes whose lee-side angles are low, and for flow-turbulence models that are used in cases with subaqueous dunes. Finally, in most chapters the superposition of different dune types plays a distinct role. It influences the dune

development, significantly increases the hydraulic roughness and complicates the use of dune tracking. Two types of superposition are recognised, but more research is necessary to determine how and why superposition occurs.

8.5 Future research

The relations between flow conditions and dune development and vice versa that were investigated and converted into two prediction methods are part of the feedback loop (fig. 8.1). As was described before, this feedback loop describes the relations between flow conditions, sediment transport, and dune development. Of the two prediction methods that were formulated, only the one between the dune development and flow conditions, through hydraulic roughness, directly fits into the feedback loop. The prediction method for the relation between the flow conditions and the dune development for a large part simplified the relations between flow conditions and sediment transport and between sediment transport and dune development. Implicitly, these relations were incorporated in the notion of dune development lagging behind on the development of flow as it takes time to transport enough material to transform the dunes. The prediction methods from this thesis on their own therefore can not explain the complete feedback loop. However, the relation of flow conditions and dune development with sediment transport was extensively investigated by Kleinhans (2002) and Blom (2003). In their theses they investigated the processes behind these relations. The combination of their conclusions with the results of this thesis should make it possible to describe the feedback loop (fig. 8.1) in great detail and it may even be possible to formulate a flow model that incorporates all the relation of this feedback loop. The results from the comparison of the SOBEK data and the predictors of this thesis above, already showed that the correct implementation of the feedback loop could improve the prediction concerning extreme cases significantly.

However, the prediction methods in this thesis have important restrictions. The dune development prediction for example is river section specific because of the lack of information on how the grain-size composition of the bed material changed during a flood. Also the reliability of both the dune development and hydraulic roughness prediction is uncertain because no proper validation could be performed due to lack of sufficient data. And finally, the uncertainty of the predicted hydraulic roughness is difficult to assess because the formulation of the predictor depended largely on uncertain measurements of the actual hydraulic roughness. In future research, these factors for dune development and hydraulic roughness should be resolved along with the many problems that were stated by both Kleinhans and Blom.

Future research that comes forth from this thesis and that focuses on the detailed processes involved with dune development and measurements is suggested below:

1. *Investigating the three dimensional dune shapes and the dune development using the spatial information of multibeam measurements.* In this thesis the spatial information on dune shapes and size variation was ignored and averaged into single values per river section. However, a multibeam measurement provides a detailed picture of the riverbed in a section. This detailed information could

provide the basis to investigate the selective transport pathways in a river. To use this spatial aspect of the multibeam data, a new method has to be defined to identify dunes, not in a profile but in a three-dimensional image. Such an algorithm does currently not exist.

2. *Investigating the relations between shipping, grain-size and dunes.* From the situations found in the Waal near Druten it was concluded that there is a strong relation between the heavy shipping on the Waal, the grain-size of the bed and the size and shape of the dunes. However, it is unclear how the interactions between these three factors work, and if and to what extent these relations are important in other river sections. This could provide vital knowledge for other rivers in the world that function as important shipping routes.
3. *Assessing the dependency of the adaptation coefficient in the dune development predictor for influences such as variations in grain-size and flow conditions.* The dataset that was used in Chapter 5 to determine the adaptation coefficient was insufficient to provide anything better than an average value for dune length and dune height. However, the results did indicate that other factors may influence the adaptation coefficient. Investigations on factors such as rising and falling flow, or grain-size of the bed could be important, improving the prediction capabilities of the prediction method formulated in Chapter 5.
4. *Investigating at which angle the flow separates from a curved surface and how this is influenced by grain-size and flow conditions.* The discussion of Chapter 6 showed that it is unclear exactly at which point the flow will separate from a curved angle. The precise location of this point is important for the correct determination of the hydraulic roughness of a dune as was shown in Chapter 7. However, this separation point can only be investigated on large dune shapes, similar in size to natural dunes, because otherwise the size of turbulent bursts can complicate the detection of the flow separation zone. This definition of the point of flow separation is also relevant in turbulent flow models, such as k- ϵ models (Rodi, 1984). If the point of flow separation is not predicted correctly in such a model the model will also not provide a correct account of the turbulence and hydraulic roughness created by the flow separation.
5. *Assessing the relation between the size of a flow separation zone and the hydraulic roughness of a dune.* As explained in Chapter 6, no information is currently available to investigate this relationship. In virtually none of the cases, the flow separation zone and the hydraulic roughness were measured at the same time, and if they were, the conditions of the test deviated so much from common field situations that the relation was useless. Knowing the relation between the size and shape of the flow separation zone and the hydraulic roughness could improve the understanding of how dunes create hydraulic roughness and which dune and flow parameters are most important in predicting the hydraulic roughness.
6. *Performing accurate measurements of hydraulic roughness over naturally shaped dunes with many different shapes, sizes, abundance of superposition and grain-sizes.* One of the major problems in Chapter 7 was that a predictor, incorporating

brinkpoint height, superposition, and flow separation zone information, could not be defined because no really accurate datasets were available. Such datasets should satisfy the three conditions listed in Chapter 7: 1) accurate measurements have to be available in different settings with different flow conditions, both steady and unsteady, and with different bedform sizes and shapes, including superposition, 2) the measurements have to include accurate characteristics of bedforms with special attention to brinkpoint height (separation height) both of the primary and secondary bedforms, and 3) the measurements have to include accurate flow characteristics necessary to calculate the total hydraulic roughness, which includes: flow velocity, water depth and energy slope. New comprehensive tests that satisfy these conditions would probably provide information necessary for the development of a new predictor for dune-related hydraulic roughness that performs even better than the adapted version of Vanoni and Hwang used in Chapter 7.

7. *Assessing how the brinkpoint height is related to grain-size, flow conditions and suspended sediment concentrations.* Chapter 6 and 7 proved that the brinkpoint height of a dune is a major factor in determining the hydraulic roughness of this dune. However, in this thesis it was not investigated how this brinkpoint height depends on grain-size, flow conditions and suspended sediment concentrations. Some investigators suspect that the brinkpoint height of a dune is strongly related to the flow strength and the concentration of suspended material. It is suspected that the brinkpoint height of a dune will decrease as the flow velocity increases very much or when the sediment concentrations become very high (Dr. J.H. van den Berg, personal communication). However, as this has never been investigated, it is unclear if these processes really take place, and if so, at what flow velocity or suspended sediment concentration. As it is difficult to determine the brinkpoint height from echo sounder measurements, it could be useful to be able to predict the brinkpoint height from the dunes without direct measurements.

8.6 References

- ALLEN, J.R.L. (1965) Sedimentation to the lee of small underwater sand waves: an experimental study. *Journal of Geology*, 73, 95-116.
- ALLEN, J.R.L. (1976a) Computational models for dune time-lag: an alternative boundary condition. *Sedimentary Geology*, 16, 255-279.
- ALLEN, J.R.L. (1976b) Computational models for dune time-lag: general ideas, difficulties and early results. *Sedimentary Geology*, 15, 1-53.
- ALLEN, J.R.L. (1976c) Computational models for dune time-lag: population structures and effects of discharge pattern and coefficient of change. *Sedimentary Geology*, 16, 99-130.
- ALLEN, J.R.L. (1978) Computational methods for dune time-lag: Calculations using Stein's rule for dune height. *Sedimentary Geology*, 20, 165-216.
- ALLEN, J.R.L. & COLLINSON, J.D. (1974) The superposition and classification of dunes formed by unidirectional aqueous flows. *Sedimentary Geology*, 12, 169-178.
- ASHLEY, G.M. (1990) Classification of large-scale subaqueous bedforms: a new look at an old problem. *Journal of Sedimentary Petrology*, 60, 160-172.
- BENNETT, S.J. & BEST, J.L. (1995) Mean flow and turbulence structure over fixed, two-dimensional dunes: implications for sediment transport and bedform stability. *Sedimentology*, 42, 491-513.

- BEST, J.L. (1993) On the Interactions between turbulent flow structure, sediment transport and bedform development: some considerations from recent experimental research. In: *Turbulence: perspectives on flow and sediment transport* (Ed. by N.J. Clifford *et al.*), pp. 61-92. Wiley and Sons, Chichester.
- BLOM, A. (2003) A vertical sorting model for rivers with non-uniform sediment and dunes. Ph.D. thesis, University of Twente, The Netherlands
- BROWNLIE, W.R. (1981) Prediction of flow depth and sediment discharge in open channels., KH-R-43A, W. M. Keck Laboratory of Hydraulics and Water Resources Division of Engineering and Applied Science, California Institute of Technology, Pasadena, California, 1 pp.
- DINEHART, R.L. (1989) Dune migration in a steep, coarse-bedded stream. *Water Resources Research*, 25, 911-923.
- DINEHART, R.L. (2002) Bedform movement recorded by sequential single-beam surveys in tidal rivers. *Journal of Hydrology*, 258, 25-39.
- ENGEL, P. (1981) Length of flow separation over dunes. *Journal of the Hydraulics Division*, 107, 1133-1143.
- ENGELUND, F. (1977) Hydraulic resistance for flow over dunes. Progress Report of the Institute for hydrodynamic and hydraulic engineering, 44, Tech. Univ. Denmark, 19 pp.
- FREDSØE, J. (1979) Unsteady flow in straight alluvial streams: modification of individual dunes. *Journal of Fluid Mechanics*, 91, 497-512.
- GABEL, S.L. (1993) Geometry and kinematics of dunes during steady and unsteady flows in the Calamus River, Nebraska, USA. *Sedimentology*, 40, 237-269.
- JINCHI, H. (1992) Application of sandwave measurements in calculating bed load discharge. In: *Erosion and Sediment transport monitoring programmes in river basins* 210, 63-70.
- JULIEN, P.Y., KLAASSEN, G.J., TEN BRINKE, W.B.M., & WILBERS, A.W.E. (2002) Case study: Bed resistance of the Rhine River during the 1998 flood. *Journal of Hydraulic Engineering*, 128, 1042-1050.
- KLEINHANS, M.G. (2002) Sorting out sand and gravel: Sediment transport and deposition in sand-gravel bed rivers. *Netherlands Geographical Studies* 293,
- KLEINHANS, M.G. & TEN BRINKE, W.B.M. (2001) Accuracy of cross-channel sampled sediment transport in large sand-gravel-bed rivers. *Journal of Hydraulic Engineering*, 127, 258-269.
- KORNMAN, B.A. (1995) The effect of changes in the lee shape of dunes on the flow field, turbulence and hydraulic roughness. Report on measurements., R 95-1, Institute for marine and atmospheric research Utrecht,
- NORDIN, C.F. & PEREZ-HERNANDEZ, D. (1989) Sand waves, bars and wind-blown sand of the Rio Orinoco, Venezuela and Colombia. US Geological Survey Water supply Paper, 2326-A.
- OGINK, H.J.M. (1989) Hydraulic roughness of single and compound bed forms part XI, report on model investigations., M 1314-XI/Q 786, Delft Hydraulics,
- RODI, W. (1984) Turbulence models and their application in hydraulics. International association for hydraulic research, Delft
- SHINOHARA, K. & TSUBAKI, T. (1959) On the characteristics of sand waves formed upon the beds of open channels and rivers. Reports of Research Institute for Applied Mechanics, 7, 15-45.
- SIMONS, D.B. & SENTÜRK, F. (1992) Sediment transport technology: water and sediment dynamics. Water Resources Publications, Littleton
- TEN BRINKE, W.B.M., WILBERS, A.W.E., & WESSELING, C. (1999) Dune growth, decay and migration rates during a large-magnitude flood at a sand and mixed sand-gravel bed in the Dutch Rhine river system. In: *Fluvial Sedimentology VI*, Special Publication of the International Association of Sedimentologists (Ed. by N.D. Smith & J. Rogers), 28, 15-32.
- VAN DEN BERG, J.H. (1987) Bedform migration and bedload transport in some rivers and tidal environments. *Sedimentology*, 34, 681-698.
- VAN DER VEEN, R. (2002) Calibratie en validatie van een hydraulisch model (SOBEK)., RIZA, Arnhem, The Netherlands,
- VAN ENCKEVOORT, I. & VAN DER SLIKKE, A. (1996) Changes in hydraulic roughness of dunes under varying high flow velocities., University of Utrecht, Utrecht
- VAN MIERLO, M.C.L.M. & DE RUITER, J.C.C. (1988) Turbulence measurements above artificial dunes Report on measurements., Q789, Delft hydraulics,
- VAN RIJN, L.C. (1984) Sediment transport; Part 3: bed forms and alluvial roughness. *Journal of Hydraulic Engineering*, 110, 1733-1754.

- VAN RIJN, L.C. (1989) Handboek sediment transport by currents and waves., report H461, Delft Hydraulics, Delft
- VANONI, V.A. & HWANG, L.S. (1967) Relation between bed forms and friction in streams. Journal of the Hydraulics Division, 93, 121-144.
- VITTAL, N. (1972) Flow over triangular roughnesses in open channels. University of Roorkee, India,
- VITTAL, N., RANGA RUJU, K.G., & GARDE, R.J. (1977) Resistance of two dimensional triangular roughness. Journal of Hydraulic Research, 15, 19-36.
- WHITE, W.R., PARIS, E., & BETTESS, R. (1979) A new general method for predicting the frictional characteristics of alluvial streams., IT 187, Hydraulic Research Station Wallingford, Wallingford, England, 1 pp.
- YALIN, M.S. (1964) Geometrical properties of sand waves. Journal of the Hydraulics Division, 90, 105-119.
- YOON, J.Y. & PATEL, V.C. (1996) Numerical model of turbulent flow over sand dune. Journal of Hydraulic Engineering, 122, 10-18.

Appendix A

Data on flow and bedform characteristics of the measurements in the Dutch Rhine branches as described in Chapter 4. U is the cross-section averaged flow velocity provided by the SOBEK-model of the Rhine.

Section	Name	Date & Time	Q			U	D ₅₀	D ₉₀	Primary dunes			Secondary dunes		
			(local)	h	(local)				H	L	c	H	L	c
			[m ³ s ⁻¹]	[m]	[m]	[ms ⁻¹]	[x10 ⁻³ m]	[x10 ⁻³ m]	[m]	[m]	[m/day]	[m]	[m]	[m/day]
1	Bovenrijn	13-01-94	5415	8.48	1.61	3.34	11.30	0.78	57.1	8.6				
1	Bovenrijn	14-01-94	4788	7.97	1.53	3.34	11.30	0.56	34.2	3.2				
1	Bovenrijn	20-01-94	3640	6.80	1.36	3.34	11.30	0.35	32.2					
1	Bovenrijn	20-12-94	1999	4.53	1.05	3.43	11.25	0.08	3.8					
1	Bovenrijn	05-01-95	3775	6.95	1.35	3.43	11.25	0.13	4.7					
1	Bovenrijn	13-01-95	3071	6.07	1.24	3.43	11.25	0.14	3.9					
1	Bovenrijn	20-01-95	2588	5.41	1.16	3.43	11.25	0.11	3.8					
1	Bovenrijn	24-01-95	3903	7.01	1.37	3.43	11.25	0.14	4.1					
1	Bovenrijn	26-01-95	7397	9.74	1.86	3.34	11.30	0.45	10.7					
1	Bovenrijn	27-01-95	8015	10.05	1.93	3.34	11.30	0.59	15.1	41.3*				
1	Bovenrijn	28-01-95	8961	10.49	2.05	3.34	11.30	0.68	17.2	47.5*				
1	Bovenrijn	29-01-95	10283	11.05	2.21	3.34	11.30	0.88	21.8					
1	Bovenrijn	31-01-95	11885	11.63	2.43	3.34	11.30	1.11	27.0	50.0*				
1	Bovenrijn	01-02-95	11790	11.60	2.42	3.34	11.30	1.29	29.8	41.5*				
1	Bovenrijn	02-02-95	10944	11.32	2.30	3.34	11.30	1.40	31.6	30.0*				
1	Bovenrijn	04-02-95	8395	10.25	1.98	3.34	11.30	1.18	31.8	17.3				
1	Bovenrijn	06-02-95	6177	9.02	1.71	3.34	11.30	1.14	41.1	11.1				
1	Bovenrijn	07-02-95	5359	8.43	1.60	3.34	11.30	0.92	42.4	8.3				
1	Bovenrijn	08-02-95	4715	7.89	1.51	3.34	11.30	0.76	45.0	6.5				
1	Bovenrijn	09-02-95	4293	7.49	1.45	3.34	11.30	0.66	45.8	5.2				
1	Bovenrijn	10-02-95	4024	7.22	1.41	3.34	11.30	0.57	47.7			0.10	4.1	
1	Bovenrijn	14-02-95	3836	7.01	1.36	3.43	11.25	0.49	50.0	0.09	4.1			

Section	Name	Date & Time	Q _h (local) [m ³ s ⁻¹]	U _h (local) [m/s]	D ₅₀ [x10 ⁻³ m]	D ₉₀ [x10 ⁻³ m]	Primary dunes			Secondary dunes		
							H	L	c	H	L	c
			[m]	[ms ⁻¹]	[x10 ⁻³ m]	[x10 ⁻³ m]	[m]	[m]	[m/day]	[m]	[m]	[m/day]
1	Bovenrijn	17-02-95	3937	7.11	1.37	3.43	11.25	0.42	56.8	0.09	3.9	
1	Bovenrijn	21-02-95	5277	8.35	1.56	3.43	11.25			0.16	4.8	
1	Bovenrijn	03-03-95	4631	7.81	1.47	3.43	11.25			0.15	4.6	
1	Bovenrijn	10-03-95	3476	6.59	1.30	3.43	11.25			0.09	3.8	
1	Bovenrijn	17-03-95	2502	5.28	1.14	3.43	11.25			0.06	4.1	
1	Bovenrijn	23-03-95	5454	8.48	1.58	3.43	11.25			0.16	5.1	
1	Bovenrijn	11-04-95	3153	6.21	1.25	3.43	11.25			0.10	3.9	
1	Bovenrijn	26-04-95	2968	5.96	1.22	3.43	11.25			0.09	4.0	
2a	Bovenrijn	27-02-97	3740	6.75	1.40	3.32	10.55	0.18	4.5			
2a	Bovenrijn	28-02-97	5013	7.98	1.59	3.32	10.55	0.23	5.5			
2a	Bovenrijn	01-03-97	6237	8.99	1.75	3.32	10.55	0.37	8.7			
2a	Bovenrijn	02-03-97	6926	9.49	1.84	3.32	10.55	0.52	12.2			
2a	Bovenrijn	03-03-97	6596	9.28	1.80	3.32	10.55	0.58	14.8	31.6		
2a	Bovenrijn	04-03-97	5655	8.57	1.68	3.32	10.55	0.54	16.0			
2a	Bovenrijn	06-03-97	4190	7.25	1.47	3.32	10.55	0.42	20.2			
2a	Bovenrijn	06-03-97	4190	7.25	1.47	3.32	10.55	0.13	4.6			
2a	Bovenrijn	06-03-97	2888	5.73	1.26	3.32	10.55	0.10	3.8			
2a	Bovenrijn	29-10-98	4077	7.13	1.45	3.32	10.55	0.29	7.4			
2a	Bovenrijn	30-10-98	4783	7.81	1.55	3.32	10.55	0.34	7.8	48.1*		
2a	Bovenrijn	30-10-98	4931	7.94	1.57	3.32	10.55	0.35	8.0			
2a	Bovenrijn	31-10-98	6180	8.97	1.74	3.32	10.55	0.48	11.0	60.9		
2a	Bovenrijn	31-10-98	6234	9.01	1.75	3.32	10.55	0.47	10.8			
2a	Bovenrijn	02-11-98	8119	10.13	1.98	3.32	10.55	0.72	16.0	56.8		
2a	Bovenrijn	02-11-98	8225	10.18	1.99	3.32	10.55	0.70	16.2			
2a	Bovenrijn	03-11-98	9045	10.55	2.08	3.32	10.55	0.90	20.0	54.9		
2a	Bovenrijn	03-11-98	9114	10.58	2.09	3.32	10.55	0.90	20.0			
2a	Bovenrijn	04-11-98	9464	10.73	2.13	3.32	10.55	0.98	21.9	50.6		

Section	Name	Date & Time	Q _h (local) [m ³ s ⁻¹]	U _h (local) [m/s]	D ₅₀ [x10 ⁻³ m]	D ₉₀ [x10 ⁻³ m]	Primary dunes			Secondary dunes		
							H	L	c	H	L	c
			[m]	[ms ⁻¹]	[m]	[m]	[m]	[m]	[m/day]	[m]	[m]	[m/day]
2a	Bovenrijn	04-11-98 12:30	9476	10.73	2.13	3.32	10.55	0.99	22.2			
2a	Bovenrijn	05-11-98 10:37	9149	10.60	2.09	3.32	10.55	1.07	24.3	40.7		
2a	Bovenrijn	05-11-98 13:10	9068	10.56	2.08	3.32	10.55	1.06	24.0			
2a	Bovenrijn	06-11-98 10:02	8267	10.20	2.00	3.32	10.55	1.13	26.0	30.8		
2a	Bovenrijn	06-11-98 13:00	8119	10.13	1.98	3.32	10.55	1.10	25.8			
2a	Bovenrijn	07-11-98 10:57	7273	9.70	1.88	3.32	10.55	1.19	29.2	24.6		
2a	Bovenrijn	07-11-98 12:45	7204	9.66	1.87	3.32	10.55	1.19	28.3			
2a	Bovenrijn	10-11-98 12:35	5640	8.55	1.67	3.32	10.55	0.92	32.3	18.4		
2a	Bovenrijn	10-11-98 14:32	5603	8.51	1.67	3.32	10.55	0.89	32.3			
2a	Bovenrijn	12-11-98 09:32	5122	8.10	1.60	3.32	10.55	0.72	36.9	15.0	0.27	6.8
2a	Bovenrijn	12-11-98 12:25	5087	8.08	1.60	3.32	10.55	0.70	36.5	0.27	6.8	
2a	Bovenrijn	13-11-98 09:45	4851	7.87	1.56	3.32	10.55	0.65	37.1	13.8	0.26	6.7
2a	Bovenrijn	13-11-98 12:22	4823	7.85	1.56	3.32	10.55	0.61	37.6	0.27	6.6	
2a	Bovenrijn	16-11-98 10:30	4522	7.57	1.52	3.32	10.55	0.61	39.3	15.2	0.29	6.6
2a	Bovenrijn	16-11-98 13:52	4505	7.56	1.51	3.32	10.55	0.61	38.5	0.30	6.6	
2a	Bovenrijn	19-11-98 11:09	4527	7.58	1.52	3.32	10.55	0.56	42.6	19.6	0.23	7.5
2a	Bovenrijn	19-11-98 14:05	4527	7.58	1.52	3.32	10.55	0.56	44.8	0.23	7.3	
2b	Pannerdensch Kanaal	28-02-97	1716	5.48	1.48	6.89	16.56	0.28	10.1			
2b	Pannerdensch Kanaal	01-03-97	2126	6.45	1.62	6.89	16.56	0.36	11.0			
2b	Pannerdensch Kanaal	02-03-97	2323	6.92	1.69	6.89	16.56	0.41	11.9			
2b	Pannerdensch Kanaal	03-03-97	2178	6.76	1.64	6.89	16.56	0.39	13.1			
2b	Pannerdensch Kanaal	06-03-97	1344	4.89	1.35	6.89	16.56	0.24	14.3			
2b	Pannerdensch Kanaal	07-03-97	1174	4.39	1.28	6.89	16.56	0.18	16.2			
2b	Pannerdensch Kanaal	31-10-98 09:31	2039	6.20	1.59	6.89	16.56	0.26	8.8	61.6		
2b	Pannerdensch Kanaal	31-10-98 10:53	2052	6.23	1.59	6.89	16.56	0.27	9.0			
2b	Pannerdensch Kanaal	02-11-98 12:18	2749	7.51	1.85	6.89	16.56	0.51	15.6	53.9		
2b	Pannerdensch Kanaal	02-11-98 15:36	2793	7.57	1.87	6.89	16.56	0.50	15.8			

Section	Name	Date & Time	Q (local) [m ³ s ⁻¹]	h (local) [m]	U [ms ⁻¹]	D ₅₀ [x10 ⁻³ m]	D ₉₀ [x10 ⁻³ m]	Primary dunes			Secondary dunes		
								H	L	c	H	L	c
								[m]	[m]	[m/day]	[m]	[m]	[m/day]
2b	Pannerdensch Kanaal	03-11-98 09:44	3048	7.82	2.00	6.89	16.56	0.54	16.4	42.8			
2b	Pannerdensch Kanaal	03-11-98 12:42	3099	7.87	2.02	6.89	16.56	0.54	16.4				
2b	Pannerdensch Kanaal	04-11-98 11:56	3291	8.02	2.13	6.89	16.56	0.64	20.8	44.9			
2b	Pannerdensch Kanaal	04-11-98 14:59	3314	8.02	2.15	6.89	16.56	0.61	20.5				
2b	Pannerdensch Kanaal	05-11-98 10:21	3150	7.91	2.05	6.89	16.56	0.60	18.7	38.1			
2b	Pannerdensch Kanaal	05-11-98 13:25	3103	7.88	2.02	6.89	16.56	0.60	18.9				
2b	Pannerdensch Kanaal	06-11-98 10:57	2714	7.59	1.84	6.89	16.56	0.60	19.5	30.8			
2b	Pannerdensch Kanaal	06-11-98 14:17	2641	7.52	1.81	6.89	16.56	0.61	19.5				
2b	Pannerdensch Kanaal	07-11-98 13:10	2373	7.13	1.70	6.89	16.56	0.68	22.2				
2b	Pannerdensch Kanaal	09-11-98 11:41	2019	6.45	1.58	6.89	16.56	0.56	22.4	20.3			
2b	Pannerdensch Kanaal	09-11-98 13:59	1999	6.41	1.57	6.89	16.56	0.56	21.7				
2b	Pannerdensch Kanaal	10-11-98 09:07	1890	6.15	1.54	6.89	16.56	0.55	24.3	27.3			
2b	Pannerdensch Kanaal	10-11-98 11:37	1869	6.12	1.53	6.89	16.56	0.58	26.0				
2b	Pannerdensch Kanaal	12-11-98 10:23	1680	5.69	1.47	6.89	16.56	0.46	22.5	12.0			
2b	Pannerdensch Kanaal	12-11-98 14:11	1679	5.65	1.47	6.89	16.56	0.44	22.5				
2b	Pannerdensch Kanaal	13-11-98 09:59	1582	5.48	1.43	6.89	16.56	0.43	29.9	10.9			
2b	Pannerdensch Kanaal	13-11-98 12:24	1573	5.46	1.43	6.89	16.56	0.38	29.2				
2b	Pannerdensch Kanaal	16-11-98 10:26	1478	5.18	1.40	6.89	16.56	0.32	25.4	13.4			
2b	Pannerdensch Kanaal	16-11-98 12:45	1472	5.17	1.39	6.89	16.56	0.27	24.5				
2b	Pannerdensch Kanaal	19-11-98 09:46	1480	5.18	1.40	6.89	16.56	0.14	7.0				
2b	Pannerdensch Kanaal	19-11-98 12:46	1487	5.17	1.40	6.89	16.56	0.14	6.8				
2c	Waal	27-02-97	2510	6.82	1.31	2.86	13.24	0.21	10.3				
2c	Waal	28-02-97	3297	7.98	1.44	2.86	13.24	0.24	11.2				
2c	Waal	01-03-97	4111	8.95	1.57	2.86	13.24	0.30	10.5				
2c	Waal	02-03-97	4603	9.42	1.66	2.86	13.24	0.36	10.6				
2c	Waal	03-03-97	4418	9.26	1.62	2.86	13.24	0.39	11.8				
2c	Waal	04-03-97	3786	8.63	1.52	2.86	13.24	0.33	12.4				

Section	Name	Date & Time	Q ^h (local) [m ³ s ⁻¹]	U ^h (local) [ms ⁻¹]	D ₅₀ [x10 ⁻³ m]	D ₉₀ [x10 ⁻³ m]	Primary dunes			Secondary dunes		
							H	L	c	H	L	c
			[m]				[m]	[m]	[m/day]	[m]	[m]	[m/day]
2c	Waal	05-03-97	3280	8.00	1.44	2.86	13.24	0.27	12.6			
2c	Waal	06-03-97	2846	7.39	1.37	2.86	13.24	0.24	12.5			
2c	Waal	07-03-97	2528	6.89	1.31	2.86	13.24	0.23	13.0			
2c	Waal	10-03-97	1986	5.90	1.21	2.86	13.24	0.20	12.9			
2c	Waal	11-03-97	1865	5.65	1.19	2.86	13.24	0.18	12.0			
2c	Waal	29-10-98	2734	7.21	1.36	2.86	13.24	0.12	3.3	77.2*		
2c	Waal	30-10-98	3166	7.83	1.43	2.86	13.24	0.12	3.3			
2c	Waal	30-10-98	3249	7.96	1.44	2.86	13.24	0.12	3.3			
2c	Waal	31-10-98	4056	8.92	1.57	2.86	13.24	0.12	3.9	86.1		
2c	Waal	31-10-98	4093	8.95	1.58	2.86	13.24	0.11	3.9			
2c	Waal	02-11-98	5363	9.98	1.81	2.86	13.24	0.22	6.8	70.6		
2c	Waal	02-11-98	5446	10.04	1.82	2.86	13.24	0.22	6.9			
2c	Waal	03-11-98	5946	10.38	1.93	2.86	13.24	0.34	8.4	93.1		
2c	Waal	03-11-98	5976	10.39	1.94	2.86	13.24	0.36	8.7			
2c	Waal	04-11-98	6168	10.51	1.98	2.86	13.24	0.47	10.9	73.0		
2c	Waal	04-11-98	6177	10.52	1.98	2.86	13.24	0.49	11.2			
2c	Waal	05-11-98	6002	10.41	1.94	2.86	13.24	0.53	13.1	59.1		
2c	Waal	05-11-98	5961	10.38	1.93	2.86	13.24	0.54	12.9			
2c	Waal	06-11-98	5536	10.10	1.84	2.86	13.24	0.53	17.8	45.0	0.36	9.25
2c	Waal	06-11-98	5451	10.04	1.82	2.86	13.24	0.53	17.8		0.36	9.14
2c	Waal	07-11-98	4863	9.64	1.71	2.86	13.24	0.49	18.3	57.5	0.34	8.65
2c	Waal	07-11-98	4838	9.63	1.71	2.86	13.24	0.48	17.9		0.37	8.53
2c	Waal	10-11-98	3770	8.61	1.53	2.86	13.24				0.30	6.57
2c	Waal	10-11-98	3749	8.59	1.52	2.86	13.24				0.29	6.55
2c	Waal	12-11-98	3436	8.19	1.47	2.86	13.24				0.29	6.32
2c	Waal	12-11-98	3414	8.17	1.47	2.86	13.24				0.30	6.27
2c	Waal	13-11-98	3267	7.98	1.44	2.86	13.24				0.28	6.07
												44.2*

Section	Name	Date & Time	Q _h (local) [m ³ s ⁻¹]	U _h (local) [m/s]	D ₅₀ [x10 ⁻³ m]	D ₉₀ [x10 ⁻³ m]	Primary dunes			Secondary dunes		
							H [m]	L [m]	c [m/day]	H [m]	L [m]	c [m/day]
2c	Waal	13-11-98 12:22	3250	7.96	1.44	2.86	13.24			0.30	6.22	
2c	Waal	16-11-98 10:30	3045	7.68	1.41	2.86	13.24			0.31	5.98	46.7*
2c	Waal	16-11-98 13:52	3037	7.67	1.41	2.86	13.24			0.30	6.03	
2c	Waal	19-11-98 11:09	3042	7.67	1.41	2.86	13.24			0.20	5.58	41.5*
2c	Waal	19-11-98 14:05	3038	7.67	1.41	2.86	13.24			0.21	5.52	
3 North	Waal (Druuten)	23-01-89	1232	4.50	1.06	1.62	5.08	0.66	38.6	4.7		
3 North	Waal (Druuten)	25-01-89	1201	4.47	1.05	1.62	5.08	0.63	39.4	4.9		
3 North	Waal (Druuten)	26-01-89	1194	4.40	1.05	1.62	5.08	0.59	38.7			
3 North	Waal (Druuten)	13-02-89	970	3.78	0.99	1.62	5.08	0.44	39.0	3.9		
3 North	Waal (Druuten)	14-02-89	962	3.74	0.99	1.62	5.08	0.48	38.8	3.4		
3 North	Waal (Druuten)	15-02-89	966	3.85	0.99	1.62	5.08	0.46	38.0			
3 North	Waal (Druuten)	14-03-89	1645	5.56	1.18	1.62	5.08	0.71	42.3	5.4		
3 North	Waal (Druuten)	15-03-89	1563	5.38	1.15	1.62	5.08	0.64	35.0	6.4		
3 North	Waal (Druuten)	16-03-89	1491	5.19	1.13	1.62	5.08	0.65	37.4			
3 North	Waal (Druuten)	11-04-89	1774	5.80	1.22	1.62	5.08	0.73	41.9	4.6		
3 North	Waal (Druuten)	12-04-89	1719	5.69	1.20	1.62	5.08	0.74	40.7	7.3		
3 North	Waal (Druuten)	13-04-89	1686	5.62	1.19	1.62	5.08	0.72	38.1			
3 North	Waal (Druuten)	09-05-89	1453	5.08	1.12	1.62	5.08	0.78	39.5	5.6		
3 North	Waal (Druuten)	10-05-89	1410	5.00	1.11	1.62	5.08	0.75	39.1	5.1		
3 North	Waal (Druuten)	11-05-89	1354	4.83	1.09	1.62	5.08	0.76	41.7			
3 North	Waal (Druuten)	13-06-89	1154	4.31	1.04	1.62	5.08	0.51	39.7	5.1		
3 North	Waal (Druuten)	14-06-89	1136	4.27	1.04	1.62	5.08	0.53	39.9	4.6		
3 North	Waal (Druuten)	15-06-89	1121	4.22	1.03	1.62	5.08	0.53	38.8			
3 North	Waal (Druuten)	25-07-89	1049	4.02	1.02	1.62	5.08	0.54	37.2	5.9		
3 North	Waal (Druuten)	26-07-89	1051	4.07	1.02	1.62	5.08	0.55	39.6	4.4		
3 North	Waal (Druuten)	27-07-89	1056	4.06	1.02	1.62	5.08	0.54	37.5			
3 North	Waal (Druuten)	04-09-89	1096	4.21	1.03	1.62	5.08	0.52	41.1	4.6		

Section	Name	Date & Time	Q _h			Primary dunes						Secondary dunes		
			(local) [m ³ s ⁻¹]	(local) [m]	U [ms ⁻¹]	D ₅₀ [x10 ⁻³ m]	D ₉₀ [x10 ⁻³ m]	H [m]	L [m]	c [m/day]	H [m]	L [m]	c [m/day]	
3 North	Waal (Druuten)	05-09-89	1078	4.18	1.02	1.62	5.08	0.52	39.1	4.1				
3 North	Waal (Druuten)	06-09-89	1060	4.13	1.02	1.62	5.08	0.52	36.8					
3 North	Waal (Druuten)	28-11-89	798	3.47	0.95	1.62	5.08	0.47	36.9	3.9				
3 North	Waal (Druuten)	01-12-89	750	3.28	0.94	1.62	5.08	0.46	39.3					
3 North	Waal (Druuten)	08-01-90	1071	4.15	1.02	1.62	5.08	0.64	37.5	3.9				
3 North	Waal (Druuten)	09-01-90	1033	4.05	1.01	1.62	5.08	0.59	36.9	6.1				
3 North	Waal (Druuten)	10-01-90	1007	3.96	1.00	1.62	5.08	0.61	39.5					
3 North	Waal (Druuten)	12-03-90	2104	6.44	1.28	1.62	5.08	0.89	39.0	6.4				
3 North	Waal (Druuten)	13-03-90	1941	6.14	1.26	1.62	5.08	0.83	38.2	5.6				
3 North	Waal (Druuten)	14-03-90	1813	5.89	1.23	1.62	5.08	0.75	40.9					
3 North	Waal (Druuten)	24-03-92	1894	5.93	1.25	1.62	5.08	0.63	43.1	6.9				
3 North	Waal (Druuten)	25-03-92	2019	6.16	1.27	1.62	5.08	0.65	38.3	8.4				
3 North	Waal (Druuten)	26-03-92	2311	6.67	1.31	1.62	5.08	0.70	35.5					
3 North	Waal (Druuten)	17-01-94	2956	7.60	1.38	1.62	5.08	0.74	37.4	10.5				
3 North	Waal (Druuten)	18-01-94	2865	7.48	1.37	1.62	5.08	0.91	40.6	8.1				
3 North	Waal (Druuten)	18-01-94	2865	7.48	1.37	1.62	5.08	0.79	38.4					
3 North	Waal (Druuten)	19-01-94	2787	7.38	1.36	1.62	5.08	1.26	38.3					
3 North	Waal (Druuten)	21-01-94	2486	6.95	1.33	1.62	5.08	0.71	39.6					
3 North	Waal (Druuten)	27-01-95	5175	9.43	1.47	1.62	5.08	1.04	36.9	10.1				
3 North	Waal (Druuten)	29-01-95	6357	10.17	1.32	1.62	5.08	1.09	36.4					
3 North	Waal (Druuten)	02-02-95	7008	10.57	1.34	1.62	5.08	1.14	37.1	9.5				
3 North	Waal (Druuten)	04-02-95	5866	9.88	1.46	1.62	5.08	1.07	37.6	15.3				
3 North	Waal (Druuten)	05-02-95	5232	9.48	1.47	1.62	5.08	1.11	37.1	11.1				
3 North	Waal (Druuten)	06-02-95	4653	9.10	1.51	1.62	5.08	1.07	35.5	11.3				
3 North	Waal (Druuten)	08-02-95	3601	8.28	1.47	1.62	5.08	1.14	37.4	11.7				
3 North	Waal (Druuten)	09-02-95	3242	7.93	1.42	1.62	5.08	1.09	37.3					
3 North	Waal (Druuten)	21-02-95	3595	8.27	1.47	1.62	5.08	1.07	37.1					

Section	Name	Date & Time	Q (local) [m ³ s ⁻¹]	h (local) [m]	U [ms ⁻¹]	D ₅₀ [x10 ⁻³ m]	D ₉₀ [x10 ⁻³ m]	Primary dunes			Secondary dunes		
								H [m]	L [m]	c [m/day]	H [m]	L [m]	c [m/day]
3 North	Waal (Druuten)	27-02-97	2277	6.60	1.31	1.62	5.08	0.90	37.3	8.9			
3 North	Waal (Druuten)	28-02-97	2871	7.46	1.37	1.62	5.08	0.92	36.1	9.3			
3 North	Waal (Druuten)	01-03-97	3751	8.39	1.45	1.62	5.08	0.99	37.0	9.7			
3 North	Waal (Druuten)	02-03-97	4436	8.93	1.55	1.62	5.08	1.03	37.3	10.7			
3 North	Waal (Druuten)	03-03-97	4660	9.10	1.56	1.62	5.08	1.08	37.6	8.9			
3 North	Waal (Druuten)	03-03-97	4660	9.10	1.56	1.62	5.08	1.09	35.8	8.3			
3 North	Waal (Druuten)	04-03-97	4212	8.78	1.52	1.62	5.08	1.08	36.5	7.7			
3 North	Waal (Druuten)	04-03-97	4212	8.78	1.52	1.62	5.08	1.14	38.7	7.4			
3 North	Waal (Druuten)	05-03-97	3600	8.28	1.44	1.62	5.08	1.13	36.3	7.2			
3 North	Waal (Druuten)	05-03-97	3600	8.28	1.44	1.62	5.08	1.12	35.6	6.9			
3 North	Waal (Druuten)	06-03-97	3110	7.79	1.39	1.62	5.08	1.09	36.7	6.6			
3 North	Waal (Druuten)	06-03-97	3110	7.79	1.39	1.62	5.08	1.14	36.9	6.7			
3 North	Waal (Druuten)	07-03-97	2732	7.31	1.36	1.62	5.08	1.09	36.4				
3 North	Waal (Druuten)	07-03-97	2732	7.31	1.36	1.62	5.08	1.13	37.3				
3 North	Waal (Druuten)	10-03-97	2057	6.23	1.27	1.62	5.08	1.06	37.6	8.2			
3 North	Waal (Druuten)	10-03-97	2057	6.23	1.27	1.62	5.08	1.09	36.9	8.5			
3 North	Waal (Druuten)	11-03-97	1928	5.99	1.24	1.62	5.08	1.03	37.0				
3 North	Waal (Druuten)	11-03-97	1928	5.99	1.24	1.62	5.08	1.06	36.1	7.6			
3 North	Waal (Druuten)	12-03-97	1746	5.72	1.20	1.62	5.08	1.07	36.9	6.4			
3 North	Waal (Druuten)	13-03-97	1641	5.48	1.17	1.62	5.08	1.05	37.6	7.0			
3 North	Waal (Druuten)	14-03-97	1574	5.28	1.16	1.62	5.08	1.02	37.6				
3 North	Waal (Druuten)	21-03-97	1405	4.82	1.12	1.62	5.08	0.85	39.2				
3 North	Waal (Druuten)	01-11-98	4373	8.89	1.54	1.62	5.08	1.11	36.6	10.6			
3 North	Waal (Druuten)	02-11-98	5079	9.38	1.55	1.62	5.08	1.14	37.3	11.2			
3 North	Waal (Druuten)	03-11-98	5814	9.85	1.38	1.62	5.08	1.11	37.2	10.3			
3 North	Waal (Druuten)	04-11-98	6135	10.04	1.31	1.62	5.08	1.16	36.4	10.0			
3 North	Waal (Druuten)	05-11-98	6127	10.04	1.31	1.62	5.08	1.20	36.7	9.9			

Section	Name	Date & Time	Q ^h (local) [m ³ s ⁻¹]	Q ^h (local) [m]	U [ms ⁻¹]	D ₅₀ [x10 ⁻³ m]	D ₉₀ [x10 ⁻³ m]	Primary dunes			Secondary dunes		
								H	L	c	H	L	c
								[m]	[m]	[m/day]	[m]	[m]	[m/day]
3 North	Waal (Druuten)	06-11-98	5809	9.84	1.38	1.62	5.08	1.18	35.9				
3 North	Waal (Druuten)	08-11-98	4840	9.22	1.57	1.62	5.08	1.22	36.3				
3 North	Waal (Druuten)	10-11-98	4166	8.74	1.51	1.62	5.08	1.17	36.6	7.7			
3 North	Waal (Druuten)	11-11-98	3872	8.51	1.47	1.62	5.08	1.14	36.6				
3 North	Waal (Druuten)	13-11-98	3457	8.14	1.42	1.62	5.08	1.16	38.1				
3 North	Waal (Druuten)	16-11-98	3154	7.83	1.39	1.62	5.08	1.19	39.1	7.2			
3 North	Waal (Druuten)	17-11-98	3066	7.73	1.39	1.62	5.08	1.16	39.2				
3 North	Waal (Druuten)	23-11-98	2579	7.09	1.35	1.62	5.08	1.19	39.7	6.7			
3 North	Waal (Druuten)	24-11-98	2358	6.75	1.32	1.62	5.08	1.24	40.6				
3 South	Waal (Druuten)	17-01-94	2956	7.60	1.38	0.73	4.15	0.36	9.1				
3 South	Waal (Druuten)	18-01-94	2865	7.48	1.37	0.73	4.15	0.37	9.2				
3 South	Waal (Druuten)	18-01-94	2865	7.48	1.37	0.73	4.15	0.36	9.2				
3 South	Waal (Druuten)	19-01-94	2787	7.38	1.36	0.73	4.15	0.40	9.3				
3 South	Waal (Druuten)	21-01-94	2486	6.95	1.33	0.73	4.15	0.32	9.0				
3 South	Waal (Druuten)	27-01-95	5175	9.43	1.47	0.73	4.15	0.44	9.6				
3 South	Waal (Druuten)	29-01-95	6357	10.17	1.32	0.73	4.15	0.40	9.5				
3 South	Waal (Druuten)	02-02-95	7008	10.57	1.34	0.73	4.15	0.39	8.9				
3 South	Waal (Druuten)	04-02-95	5866	9.88	1.46	0.73	4.15	0.40	9.2				
3 South	Waal (Druuten)	05-02-95	5232	9.48	1.47	0.73	4.15	0.41	9.1				
3 South	Waal (Druuten)	06-02-95	4653	9.10	1.51	0.73	4.15	0.41	9.1				
3 South	Waal (Druuten)	08-02-95	3601	8.28	1.47	0.73	4.15	0.39	9.4				
3 South	Waal (Druuten)	09-02-95	3242	7.93	1.42	0.73	4.15	0.37	9.4				
3 South	Waal (Druuten)	21-02-95	3595	8.27	1.47	0.73	4.15	0.40	8.9				
3 South	Waal (Druuten)	27-02-97	2277	6.60	1.31	0.73	4.15	0.36	8.8				
3 South	Waal (Druuten)	28-02-97	2871	7.46	1.37	0.73	4.15	0.37	8.8				
3 South	Waal (Druuten)	01-03-97	3751	8.39	1.45	0.73	4.15	0.36	8.9				
3 South	Waal (Druuten)	02-03-97	4436	8.93	1.55	0.73	4.15	0.36	9.0				

		Primary dunes										Secondary dunes			
Section	Name	Date & Time	Q (local) [m ³ s ⁻¹]	h (local) [m]	U [ms ⁻¹]	D ₅₀ [x10 ⁻³ m]	D ₉₀ [x10 ⁻³ m]	H	L	c	[m/day]	H	L	c	[m/day]
3 South	Waal (Druten)	03-03-97	4660	9.10	1.56	0.73	4.15	0.36	8.7						
3 South	Waal (Druten)	03-03-97	4660	9.10	1.56	0.73	4.15	0.51	7.5						
3 South	Waal (Druten)	04-03-97	4212	8.78	1.52	0.73	4.15	0.34	9.2						
3 South	Waal (Druten)	04-03-97	4212	8.78	1.52	0.73	4.15	0.52	8.0						
3 South	Waal (Druten)	05-03-97	3600	8.28	1.44	0.73	4.15	0.34	9.0						
3 South	Waal (Druten)	05-03-97	3600	8.28	1.44	0.73	4.15	0.56	9.7						
3 South	Waal (Druten)	06-03-97	3110	7.79	1.39	0.73	4.15	0.34	9.1						
3 South	Waal (Druten)	06-03-97	3110	7.79	1.39	0.73	4.15	0.55	9.4						
3 South	Waal (Druten)	07-03-97	2732	7.31	1.36	0.73	4.15	0.35	8.9						
3 South	Waal (Druten)	07-03-97	2732	7.31	1.36	0.73	4.15	0.54	9.5						
3 South	Waal (Druten)	10-03-97	2057	6.23	1.27	0.73	4.15	0.34	8.9						
3 South	Waal (Druten)	10-03-97	2057	6.23	1.27	0.73	4.15	0.50	9.9						
3 South	Waal (Druten)	11-03-97	1928	5.99	1.24	0.73	4.15	0.36	9.1						
3 South	Waal (Druten)	11-03-97	1928	5.99	1.24	0.73	4.15	0.50	10.5						
3 South	Waal (Druten)	12-03-97	1746	5.72	1.20	0.73	4.15	0.50	10.7						
3 South	Waal (Druten)	13-03-97	1641	5.48	1.17	0.73	4.15	0.48	10.3						
3 South	Waal (Druten)	14-03-97	1574	5.28	1.16	0.73	4.15	0.45	10.5						
3 South	Waal (Druten)	21-03-97	1405	4.82	1.12	0.73	4.15	0.35	8.4						
3 South	Waal (Druten)	01-11-98	4373	8.89	1.54	0.73	4.15	0.52	8.7						
3 South	Waal (Druten)	02-11-98	5079	9.38	1.55	0.73	4.15	0.54	8.8						
3 South	Waal (Druten)	03-11-98	5814	9.85	1.38	0.73	4.15	0.47	9.0						
3 South	Waal (Druten)	04-11-98	6135	10.04	1.31	0.73	4.15	0.46	9.1						
3 South	Waal (Druten)	05-11-98	6127	10.04	1.31	0.73	4.15	0.45	8.6						
3 South	Waal (Druten)	06-11-98	5809	9.84	1.38	0.73	4.15	0.46	8.6						
3 South	Waal (Druten)	08-11-98	4840	9.22	1.57	0.73	4.15	0.49	8.8						
3 South	Waal (Druten)	10-11-98	4166	8.74	1.51	0.73	4.15	0.44	9.6						
3 South	Waal (Druten)	11-11-98	3872	8.51	1.47	0.73	4.15	0.43	9.5						

Section	Name	Date & Time	Q (local) [m ³ s ⁻¹]	h (local) [m]	U [ms ⁻¹]	D ₅₀ [x10 ⁻³ m]	D ₉₀ [x10 ⁻³ m]	Primary dunes			Secondary dunes		
								H	L	c	H	L	c
3 South	Waal (Druten)	13-11-98	3457	8.14	1.42	0.73	4.15	0.44	9.6				
3 South	Waal (Druten)	16-11-98	3154	7.83	1.39	0.73	4.15	0.47	8.8				
3 South	Waal (Druten)	17-11-98	3066	7.73	1.39	0.73	4.15	0.45	9.0				
3 South	Waal (Druten)	23-11-98	2579	7.09	1.35	0.73	4.15	0.47	8.9				
3 South	Waal (Druten)	24-11-98	2358	6.75	1.32	0.73	4.15	0.48	8.9				

* uncertain determination of migration rate, rates could be half or twice this value.

Appendix B

Data on flow and bedform characteristics during different tests and measurements as described in Chapter 7.

Author	Test or location	Primary dunes							Secondary dunes				
		U [ms ⁻¹]	R _b or h [m]	i _e or i _w [*10 ⁻⁵]	D ₉₀ [*10 ⁻³ m]	H [m]	H _b [m]	L [m]	H _{sec} [m]	H _{bsec} [m]	L _{sec} [m]	Abun. [%]	
	a50	0.71	0.43	14.9	0.25	0.19	0.19	4.8	0.02	0.01	0.4	3	
	a51	0.71	0.43	14.7	0.25	0.21	0.21	5.3	0.06	0.04	2.0	35	
	a52	0.70	0.43	14.8	0.25	0.20	0.20	4.3	0.04	0.03	1.8	27	
	a53	0.71	0.42	14.2	0.25	0.16	0.16	4.0	0.03	0.01	2.7	20	
	a54	0.72	0.41	14.2	0.25	0.16	0.17	4.2					
	a55	0.75	0.40	15.0	0.25	0.18	0.18	4.7					
	a57	0.72	0.40	12.7	0.25	0.17	0.16	3.8					
	a58	0.68	0.42	11.1	0.25	0.22	0.21	4.9	0.03	0.01	1.7	31	
	a59	0.68	0.45	14.8	0.25	0.22	0.21	4.8	0.05	0.01	2.4	25	
	a60	0.67	0.44	12.5	0.25	0.14	0.12	2.9	0.03	0.02	0.8	8	
	a61	0.66	0.44	11.9	0.25	0.15	0.14	3.1	0.03	0.02	0.8	32	
	a62	0.69	0.42	12.2	0.25	0.13	0.12	3.0	0.02	0.01	0.8	42	
	a63	0.68	0.43	12.2	0.25	0.17	0.17	4.0	0.04	0.03	2.6	20	
	a64	0.69	0.43	13.6	0.25	0.19	0.18	4.5	0.03	0.02	1.4	15	
	a65	0.69	0.44	14.3	0.25	0.19	0.18	4.5	0.04	0.01	1.9	33	
	a66	0.70	0.43	15.0	0.25	0.15	0.14	3.4					
	a67	0.70	0.42	14.4	0.25	0.16	0.15	3.7					
	a68	0.70	0.43	14.5	0.25	0.19	0.19	4.3	0.05	0.00	3.9	20	
	a69	0.69	0.43	13.7	0.25	0.15	0.14	3.7	0.03	0.01	1.4	32	
	a70	0.70	0.41	12.2	0.25	0.17	0.15	4.2	0.02	0.01	0.8	25	
	b18	0.81	0.41	12.8	0.25	0.19	0.19	4.8					
	b19	0.82	0.42	14.2	0.25	0.18	0.17	4.7					
	b20	0.84	0.42	15.9	0.25	0.18	0.17	5.1					

Van Enckevoort and Van der Slikke

Author	Test or location	Primary dunes					Secondary dunes					
		U [ms ⁻¹]	R ₀ or h [m]	i _c or i _{sv} [*10 ⁻⁵]	D ₉₀ [*10 ⁻³ m]	H [m]	H _b [m]	L [m]	H _{sec} [m]	H _{hsec} [m]	L _{sec} [m]	Abun. [%]
Van Enckevoort and Van der Slikke	b21	0.86	0.41	17.0	0.25	0.18	0.18	6.1				
	b22	0.90	0.39	19.3	0.25	0.12	0.11	4.6				
	b23	0.94	0.36	19.1	0.25	0.12	0.12	5.8				
	b24	0.93	0.37	19.0	0.25	0.14	0.14	6.7				
	b25	0.88	0.39	16.3	0.25	0.21	0.20	10.9				
	b26	0.87	0.38	15.5	0.25	0.21	0.21	10.8				
	b27	0.87	0.40	16.2	0.25	0.19	0.18	8.2				
	b28	0.92	0.36	17.7	0.25	0.14	0.13	5.7				
	b29	0.87	0.38	15.7	0.25	0.16	0.16	6.8				
	b30	0.88	0.38	16.0	0.25	0.20	0.19	6.9				
	b31	0.82	0.40	12.4	0.25	0.22	0.22	4.4				
	b32	0.79	0.45	14.0	0.25	0.23	0.22	5.1	0.02	0.002	1.5	11
	b33	0.79	0.46	14.0	0.25	0.21	0.19	4.4	0.03	0.01	1.7	13
	b34	0.80	0.46	15.4	0.25	0.21	0.22	6.4				
	b35	0.81	0.45	14.7	0.25	0.21	0.21	5.3				
	b36	0.83	0.41	14.1	0.25	0.20	0.19	6.7				
	b37	0.83	0.43	15.9	0.25	0.20	0.19	5.9				
	d10	0.65	0.44	10.7	0.25	0.14	0.14	3.1	0.02	0.02	0.5	44
	d11	0.65	0.43	10.1	0.25	0.14	0.13	3.1	0.02	0.02	0.6	43
d12	0.75	0.42	13.0	0.25	0.14	0.13	3.1					
d13	0.74	0.42	12.5	0.25	0.15	0.14	3.3					
d14	0.85	0.43	18.2	0.25	0.15	0.15	3.6					
d15	0.86	0.42	19.0	0.25	0.14	0.13	3.4					
d16	1.02	0.38	24.9	0.25	0.11	0.10	3.7					
d17	1.06	0.35	26.5	0.25	0.12	0.12	4.6					
d18	0.92	0.34	16.5	0.25	0.11	0.10	4.5					
d19	0.93	0.35	17.7	0.25	0.11	0.10	4.5					

Author	Test or location	Primary dunes							Secondary dunes				
		U [ms ⁻¹]	R ₀ or h [m]	i _e or i _w [*10 ⁻⁵]	D ₉₀ [*10 ⁻³ m]	H [m]	H _b [m]	L [m]	H _{sec} [m]	H _{base} [m]	L _{sec} [m]	Abun. [%]	
Van Enckevoort and Van der Slikke	d20	0.79	0.35	11.1	0.25	0.12	0.12	4.6					
	d21	0.79	0.36	11.9	0.25	0.13	0.12	4.6					
	d22	0.68	0.40	10.2	0.25	0.14	0.14	4.7	0.01	0.01	0.3	51	
	d23	0.68	0.40	10.6	0.25	0.13	0.13	4.6	0.01	0.01	0.4	68	
	d24	0.58	0.38	6.3	0.25	0.15	0.15	4.6	0.01	0.01	0.2	83	
	d25	0.57	0.42	7.8	0.25	0.14	0.14	4.6	0.02	0.01	0.3	85	
	d26	0.47	0.43	5.8	0.25	0.14	0.14	4.6	0.02	0.02	0.2	83	
	d27	0.47	0.44	6.1	0.25	0.14	0.14	4.6	0.02	0.02	0.2	86	
	d28	0.37	0.43	3.9	0.25	0.14	0.14	4.6	0.02	0.01	0.2	87	
	d29	0.37	0.44	4.1	0.25	0.14	0.14	4.6	0.02	0.01	0.2	87	
	d82	0.40	0.41	4.6	0.25	0.15	0.14	7.1	0.02	0.01	0.2	89	
	d83	0.40	0.41	4.8	0.25	0.15	0.14	7.1	0.02	0.01	0.2	90	
	d84	0.50	0.41	6.9	0.25	0.16	0.15	7.1	0.02	0.01	0.2	89	
	d85	0.50	0.41	6.6	0.25	0.15	0.16	7.1	0.02	0.01	0.2	89	
	d86	0.60	0.41	9.1	0.25	0.16	0.15	7.1	0.02	0.02	0.3	84	
	d87	0.60	0.40	8.4	0.25	0.16	0.14	7.1	0.02	0.02	0.4	82	
	d88	0.70	0.40	11.9	0.25	0.15	0.16	7.2	0.03	0.03	0.9	72	
	d89	0.71	0.37	10.3	0.25	0.16	0.15	7.1	0.02	0.03	0.7	88	
	d90	0.82	0.38	15.7	0.25	0.16	0.17	7.1	0.03	0.03	1.4	55	
	d91	0.82	0.38	15.4	0.25	0.17	0.18	7.0	0.03	0.05	1.7	49	
	d92	0.91	0.36	17.1	0.25	0.18	0.16	8.8	0.04	0.06	1.8	36	
	d93	0.90	0.36	16.9	0.25	0.16	0.18	7.0	0.04	0.04	2.3	18	
	d94	0.97	0.40	21.9	0.25	0.19	0.18	9.3					
	d95	0.97	0.39	21.6	0.25	0.17	0.16	8.2					
	d96	0.89	0.39	17.9	0.25	0.18	0.18	8.0					
	d97	0.89	0.38	17.1	0.25	0.18	0.17	8.0					
	d98	0.80	0.40	15.9	0.25	0.19	0.18	7.9					

Author	Test or location	Primary dunes					Secondary dunes					
		U [ms ⁻¹]	R _b or h [m]	i _c or i _w [*10 ⁻⁵]	D ₉₀ [*10 ⁻³ m]	H [m]	H _b [m]	L [m]	H _{1sec} [m]	H _{5sec} [m]	L _{sec} [m]	Abun. [%]
Van Enckevoort and Van der Slikke	d99	0.81	0.40	15.9	0.25	0.20	0.19	7.9				
	d100	0.70	0.38	9.9	0.25	0.19	0.19	7.9				
	d101	0.70	0.38	10.2	0.25	0.20	0.19	7.8				
	d102	0.60	0.40	8.2	0.25	0.20	0.19	7.8	0.01	0.01	0.3	86
	d103	0.60	0.40	8.6	0.25	0.20	0.19	7.8	0.01	0.01	0.3	86
	d104	0.50	0.42	7.3	0.25	0.21	0.19	7.8	0.02	0.02	0.3	86
	d105	0.50	0.42	7.5	0.25	0.21	0.18	7.8	0.02	0.02	0.3	88
	d106	0.40	0.42	4.9	0.25	0.21	0.18	7.1	0.02	0.02	0.2	93
	d107	0.40	0.43	5.0	0.25	0.21	0.18	7.1	0.02	0.02	0.2	91
	Aswan 1	0.48	4.98	0.4	0.49	0.69	0.43	21.9				
Abdel-Fattah	Aswan 2	0.49	5.72	0.4	0.58	2.17	2.12	68.5	0.20	0.00	7.25	13
	Aswan 3	0.59	4.78	0.4	0.58	1.42	1.14	39.5	0.27	0.07	7.67	11
	Aswan 4	0.62	5.02	0.4	0.64	1.80	1.48	52.3	0.15	0.00	9.00	12
	Aswan 5	0.59	4.82	0.4	1.20	1.85	1.79	57.0				
	Aswan 6	0.42	5.70	0.4	0.74	0.14	0.02	8.5				
	Quena 1	0.67	4.65	0.4	0.43	0.80	0.60	22.2	0.20	0.00	10.5	11
Abdel-Fattah	Quena 2	0.60	4.40	0.4	0.39	0.54	0.40	20.0	0.14	0.03	4.0	20
	Quena 3	0.49	3.55	0.4	0.35	0.41	0.33	12.8				
	Quena 4	0.31	4.03	0.4	0.32	0.81	0.64	28.5				
	Sohag 1	0.77	4.58	0.6	0.59	0.34	0.23	7.9				
Abdel-Fattah	Sohag 2	0.88	4.13	0.6	0.99	0.25	0.13	4.3				
	Sohag 3	0.78	4.19	0.6	0.41	0.25	0.12	4.9				
	Sohag 4	0.75	4.12	0.6	0.33	0.53	0.40	17.9				
	Bani-Sweif 1	0.71	4.28	0.9	0.70	0.29	0.18	5.4	0.17	0.06	2.7	27
Abdel-Fattah	Bani-Sweif 2	0.66	3.40	0.9	0.54	0.45	0.38	6.1	0.17	0.09	3.5	15
	Bani-Sweif 3	0.74	2.76	0.9	1.22	0.26	0.06	7.9	0.18	0.06	2.2	27
	Shape 1	0.39	0.31	0.6	0.25	0.15	0.10	3.8				
Korman												

Author	Test or location	Primary dunes							Secondary dunes				
		U [ms ⁻¹]	R _b or h [m]	i _e or i _w [*10 ⁻⁵]	D ₉₀ [*10 ⁻³ m]	H [m]	H _b [m]	L [m]	H _{sec} [m]	H _{hsec} [m]	L _{sec} [m]	Abun. [%]	
Ogink	T5-2	0.68	0.26	10.0	0.85	0.01	0.01	0.1					
	T5-2	0.72	0.28	10.0	0.85	0.01	0.01	0.1					
	T5-2	0.76	0.30	10.0	0.85	0.01	0.01	0.1					
Ogink	T2-1	0.73	0.30	10.0	0.85	0.04	0.04	1.6	0.01	0.01	0.2	75	
	T2-1	0.76	0.32	10.0	0.85	0.04	0.04	1.6	0.01	0.01	0.2	75	
	T2-1	0.80	0.34	10.0	0.85	0.04	0.04	1.6	0.01	0.01	0.2	75	
Ogink	T2-2	0.67	0.30	10.0	0.85	0.04	0.04	1.6	0.01	0.01	0.1	75	
	T2-2	0.71	0.32	10.0	0.85	0.04	0.04	1.6	0.01	0.01	0.1	75	
	T2-2	0.75	0.34	10.0	0.85	0.04	0.04	1.6	0.01	0.01	0.1	75	
Ogink	T2-3	0.70	0.30	10.0	0.85	0.04	0.04	1.6	0.01	0.01	0.1	38	
	T2-3	0.74	0.32	10.0	0.85	0.04	0.04	1.6	0.01	0.01	0.1	38	
	T2-3	0.78	0.34	10.0	0.85	0.04	0.04	1.6	0.01	0.01	0.1	38	
Ogink	T3-1	0.72	0.30	10.0	0.85	0.04	0.03	1.6	0.01	0.01	0.1	75	
	T3-1	0.77	0.32	10.0	0.85	0.04	0.03	1.6	0.01	0.01	0.1	75	
	T3-1	0.80	0.34	10.0	0.85	0.04	0.03	1.6	0.01	0.01	0.1	75	
Ogink	T3-2	0.76	0.30	10.0	0.85	0.04	0.00	1.6	0.01	0.01	0.1	75	
	T3-2	0.80	0.32	10.0	0.85	0.04	0.00	1.6	0.01	0.01	0.1	75	
	T3-2	0.84	0.34	10.0	0.85	0.04	0.00	1.6	0.01	0.01	0.1	75	
Brinke and Wilbers Julien, Klaassen, Ten	Rhine left 29-10-98		8.22	0.9	11.30	0.31	0.23	6.5					
	Rhine left 30-10-98		8.98	0.9	11.30	0.35	0.26	6.7					
	Rhine left 31-10-98	1.80	9.90	1.1	11.30	0.49	0.37	10.4					
	Rhine left 1-11-98	1.85	10.63	1.2	11.30								
	Rhine left 2-11-98	1.90	11.17	1.3	11.30	0.65	0.50	13.9					
	Rhine left 3-11-98	1.88	11.54	1.4	11.30								
	Rhine left 4-11-98	1.79	11.72	1.4	11.30	1.05	0.92	22.3					
	Rhine left 5-11-98	1.81	11.60	1.4	11.30	1.16	1.04	24.8					
	Rhine left 6-11-98	1.78	11.23	1.2	11.30	1.21	1.08	25.8					

Author	Test or location	U [ms ⁻¹]	Primary dunes					Secondary dunes				
			R _b or h [m]	i _e or i _w [*10 ⁻⁵]	D ₉₀ [*10 ⁻³ m]	H [m]	H _b [m]	L [m]	H _{sec} [m]	H _{bsec} [m]	L _{sec} [m]	Abun. [%]
Julien, Klaassen, Ten Brinke and Wilbers	Rhine left 7-11-98	1.73	10.79	1.1	11.30	1.17	1.05	27.8				
	Rhine left 8-11-98	1.69	10.41	1.0	11.30							
	Rhine left 9-11-98	1.65	10.04	0.9	11.30							
	Rhine left 10-11-98	1.59	9.71	0.9	11.30	0.82	0.69	35.6				
	Rhine left 11-11-98	1.54	9.45	0.8	11.30							
	Rhine left 12-11-98		9.25	0.8	11.30	0.65	0.55	37.7	0.29	0.18	6.7	31
	Rhine left 13-11-98		9.03	0.8	11.30	0.60	0.50	38.1	0.29	0.19	6.5	39
	Rhine left 14-11-98		8.89	0.8	11.30							
	Rhine left 15-11-98		8.83	0.8	11.30							
	Rhine left 16-11-98		8.74	0.8	11.30	0.57	0.47	38.1	0.30	0.20	6.6	54
	Rhine left 17-11-98		8.66	0.8	11.30							
	Rhine left 18-11-98		8.70	0.8	11.30							
	Rhine left 19-11-98		8.74	0.8	11.30	0.42	0.34	47.2	0.22	0.13	6.8	100
	Rhine centre 29-10-98		8.63	0.9	9.80	0.33	0.20	7.5				
	Rhine centre 30-10-98		9.39	0.9	9.80	0.39	0.25	8.4				
	Rhine centre 31-10-98	1.60	10.31	1.1	9.80	0.47	0.33	10.9				
	Rhine centre 1-11-98	1.70	11.04	1.2	9.80							
	Rhine centre 2-11-98	1.80	11.58	1.3	9.80	0.71	0.56	16.1				
	Rhine centre 3-11-98	1.82	11.95	1.4	9.80	0.89	0.78	20.1				
	Rhine centre 4-11-98	1.75	12.13	1.4	9.80	1.00	0.89	22.8				
Julien, Klaassen, Ten Brinke and Wilbers	Rhine centre 5-11-98	1.71	12.01	1.4	9.80	1.09	0.97	24.4				
	Rhine centre 6-11-98	1.71	11.64	1.2	9.80	1.16	1.05	26.0				
	Rhine centre 7-11-98	1.68	11.20	1.1	9.80	1.16	1.03	28.8				
	Rhine centre 8-11-98	1.65	10.82	1.0	9.80							
	Rhine centre 9-11-98	1.63	10.45	0.9	9.80							
	Rhine centre 10-11-98	1.58	10.12	0.9	9.80	0.93	0.80	32.8				
	Rhine centre 11-11-98	1.53	9.86	0.8	9.80							

Author	Test or location	U [ms ⁻¹]	R _b or h [m]	i _e or i _w [*10 ⁻⁵]	D ₉₀ [*10 ⁻³ m]	Primary dunes				Secondary dunes			
						H [m]	H _b [m]	L [m]	H _{sec} [m]	H _{bsec} [m]	L _{sec} [m]	Abun. [%]	
Julien, Klaassen, Ten Brinke and Wilbers	Rhine centre 12-11-98	1.48	9.66	0.8	9.80	0.78	0.67	34.9	0.28	0.18	6.9	20	
	Rhine centre 13-11-98	1.43	9.44	0.8	9.80	0.76	0.66	36.2	0.25	0.16	6.8	22	
	Rhine centre 14-11-98		9.30	0.8	9.80								
	Rhine centre 15-11-98		9.24	0.8	9.80								
	Rhine centre 16-11-98		9.15	0.8	9.80	0.65	0.55	39.8	0.28	0.18	6.6	38	
	Rhine centre 17-11-98		9.07	0.8	9.80								
	Rhine centre 18-11-98		9.11	0.8	9.80								
	Rhine centre 19-11-98		9.15	0.8	9.80	0.56	0.51	40.8	0.26	0.18	7.7	82	
	Rhine right 29-10-98		9.12	0.9	11.60	0.34	0.23	7.6					
	Rhine right 30-10-98		9.88	0.9	11.60	0.40	0.29	8.5					
	Rhine right 31-10-98	1.75	10.80	1.1	11.60	0.47	0.30	11.3					
	Rhine right 1-11-98	1.85	11.53	1.2	11.60								
	Rhine right 2-11-98	1.90	12.07	1.3	11.60	0.70	0.54	16.7					
	Rhine right 3-11-98	1.86	12.44	1.4	11.60								
	Rhine right 4-11-98	1.91	12.62	1.4	11.60	1.03	0.92	21.7					
	Rhine right 5-11-98	1.93	12.50	1.4	11.60	1.20	1.07	25.6					
Julien, Klaassen, Ten Brinke and Wilbers	Rhine right 6-11-98	1.81	12.13	1.2	11.60	1.28	1.15	26.6					
	Rhine right 7-11-98	1.77	11.69	1.1	11.60	1.32	1.20	29.5					
	Rhine right 8-11-98	1.74	11.31	1.0	11.60								
	Rhine right 9-11-98	1.71	10.94	0.9	11.60	1.06	0.93	31.8					
	Rhine right 10-11-98	1.65	10.61	0.9	11.60								
	Rhine right 11-11-98	1.60	10.35	0.8	11.60								
	Rhine right 12-11-98	1.55	10.15	0.8	11.60	1.08	0.96	34.7	0.32	0.23	6.8	12	
	Rhine right 13-11-98	1.50	9.93	0.8	11.60	0.95	0.83	37.7	0.29	0.19	6.7	18	
	Rhine right 14-11-98		9.79	0.8	11.60								
	Rhine right 15-11-98		9.73	0.8	11.60								
	Rhine right 16-11-98		9.64	0.8	11.60	0.75	0.64	40.4	0.30	0.19	6.7	40	

Author	Test or location	Primary dunes						Secondary dunes				
		U [ms ⁻¹]	R _b or h [m]	i _e or i _w [*10 ⁻⁵]	D ₉₀ [*10 ⁻³ m]	H [m]	H _b [m]	L [m]	H _{sec} [m]	H _{bsec} [m]	L _{sec} [m]	Abun. [%]
Julien, Klaassen, Ten Brinke and Wilbers	Rhine right 17-11-98		9.56	0.8	11.60							
	Rhine right 18-11-98		9.60	0.8	11.60							
	Rhine right 19-11-98		9.64	0.8	11.60	0.63	0.51	42.1	0.26	0.13	8.1	81

* In the flume tests by Van Enckevoort and Van der Slikke, Komman, and Ogink, R_b and i_e was used, in other cases h and i_w.

The development and hydraulic roughness of subaqueous dunes

Summary

Objectives

Natural alluvial rivers by definition bear the threat of flooding. However, the presence of water and the fertility of floodplains was the reason the areas next to these rivers are presently heavily populated. Now, as a climate change is predicted with more extreme precipitation, these heavily populated areas have to be protected from catastrophic floods. In order to take appropriate measures to reduce the risk of flooding, it is necessary to know what water levels will occur during such extreme events. This implies knowledge of the hydraulic resistance at high flood stages. A major part of this flow resistance, or hydraulic roughness, is formed by obstacles found on the bed of the main channel. In many rivers these obstacles are natural dunes shaped by transport of loose bed material. Dunes are transverse bedforms which can be found in channelized environments, where flow conditions are sub-critical and the viscous sub-layer is smaller than the maximum grain size (Chapter 2). Dunes are related to the vertical flow patterns and therefore dune dimensions are strongly related to the water depth. In medium sized rivers this means that dunes are several to tens of meters long and several decimetres to a few meters high.

It is a better understanding of the development and the roughness of these dunes that formed the general aim of this PhD-project. More specifically, this study was focused on the development and hydraulic roughness of dunes in non-steady flows during floods in medium-sized rivers with sand or sand-gravel beds like the Rhine and Meuse. The specific goals were:

1. The prediction of the development of dune shape and size in non-steady flows during floods,
2. The prediction of the hydraulic roughness caused by dunes, using the characteristics of dune shape, size, and flow conditions.

To achieve these goals the following research questions were answered, bearing in mind the dynamic interaction between flow, sediment transport and dune development:

- How do sediment transport and dunes interact and how is the migration of dunes related to the bed load transport?
- How do the dunes in the Dutch rivers change during unsteady flow conditions and how can these changes be predicted?
- What is the relation between dune shape and size, the dimensions of the flow separation zone, and the hydraulic roughness of a dune?
- How can the hydraulic roughness of dunes be predicted based on dune characteristics?

- What is the cause of the superposition of dunes in the Dutch rivers and how does this superposition influence the bed load transport, dune development, and hydraulic roughness?

Interaction between dune migration and bedload transport

The flow pattern over dunes is very complex which results in complex pathways of sediment transport and different interactions between sediment transport and the dune surface. Over the stoss-side of a dune, sediment transport is divided into bedload and suspended transport. Over the lee-side, where the flow is separated from the bed surface, sediment is either deposited in avalanches on the lee-slope, or transported in semi-suspension to the next dune, or it goes into or falls out of suspension.

All these interactions play a role in dune migration and thereby influence the determination of bedload transport using dune migration, which is called dune tracking. The analyses of various difficulties in using this dune tracking technique in field situations (Chapter 3) shows, that dune tracking can produce reliable results even without direct measurements. However, to use dune tracking correctly several factors have to be taken into account:

- the location of the sounded profiles should be in an almost straight stretch of river and their direction should be parallel to the banks but perpendicular to the dune crests,
- the spatial and temporal resolution of the measurements should be based on expected dune characteristics and dune migration rates. The chosen resolutions should be high enough to accurately determine dune height, length, volume and migration rate, for example a spatial resolution of more than 15 points per dune and a temporal resolution that allows the dunes to migrate 20% to 80% of their dune length between two measurements,
- finally, in case of superposition of dunes, those dunes (either the primary or the secondary) have to be used in dune tracking, that are most active in transporting bedload material as they migrate downstream.

If all these factors are accounted for, the bedload transport rate (including pore space) can be calculated from the height and celerity of the migrating dunes (Chapter 4).

Prediction of dune development in unsteady flow

In Chapter 4 the growth and decay of dunes in the Dutch Rhine is analysed from echo soundings collected during several floods and during periods of low to moderate discharge. The evolution of dune shape and dimension during a river flood appears to be very different for various sections of the Rhine. This appears to be primarily due to grain-size differences and a variable discharge distribution over the main channel and the floodplain. The influence of differences in shape and duration of a flood wave is less

important. The variable discharge distribution of the studied river over channel and floodplain causes a clearly different development of bed shear stress and grain-related shear stress in the main channel, which is reflected in the way dunes develop. Combining the differences in grain-size and the differences in the shear stress exerted by the river bed results in reasonably good power relations that predict dune height, length and migration rate for during rising discharges.

During falling discharges the development of the dunes show a clear hysteresis (Chapter 4). This hysteresis cannot be predicted directly from the changes in bed shear stress and therefore, in Chapter 5, a method to predict dimensions of active dunes during unsteady, non-uniform flow conditions in the Rhine branches is proposed. A review of existing predictors showed that none of these can be directly used. In the proposed method effects of reaction time and relaxation in dune development are incorporated. Unfortunately, due to lack of measurement data concerning changes in grain size during flood events, no prediction model could be presented that is applicable everywhere in the Rhine. The prediction models that were formulated are only applicable in certain sections of the Rhine. The analysis also showed that separate models are necessary for dune height and length because dune height adapts much faster to new flow conditions than dune length.

Despite these problems, a comparison between the model simulations and the observations from individual flood events in individual sections showed that the models accurately simulate the trends of dune development, the moments of maximum dune dimensions, and the occurrence of superposition of secondary dunes. Even the actual dune height and length was simulated accurately in several cases. The models can therefore be used in future flood events to predict the dune dimensions in the three river sections used here. The physical basis of the proposed method implies its potential for future application in other parts of the Rhine branches. By incorporation of the grain-size as an additional parameter the method can be made more generic.

The relation between dunes, flow separation and hydraulic roughness

The hydraulic roughness of a dune is caused by the generation of turbulence at the steep downstream side, where the flow separates from the bed to reattach again on the stoss side of the next dune. The amount of turbulence that is created in the flow separation zone is probably linked to the general flow conditions and the shape and size of the flow separation zone. The size and shape of the flow separation zone is governed by the height of the flow separation point, as the zero velocity line has a constant angle of 10 degrees (± 1 degree), independent of any difference in bedform characteristics or flow conditions (Chapter 6). The flow separation point is probably located at that point on a lee-slope where the angle of the slope exceeds 10 degrees. On dunes, this point normally coincides with the brinkpoint, where the loss of flow shear results in avalanching material, creating a break from a gentle to a steep slope.

Predicting hydraulic roughness of dunes

The total hydraulic resistance of the river bed consists of the roughness of the grains (skin friction), and the form resistance of dunes (form roughness). In the case of dunes the hydraulic roughness is directly related to the size of the flow separation, which in turn is directly related to the height of the flow separation point. The analysis of Chapter 7 showed that existing hydraulic roughness predictors significantly improved by restricting grain roughness to the area outside the separation zone, substitution of dune height by brinkpoint height and the incorporation of the hydraulic roughness of superimposed dunes according to their spatial abundance. Especially in the case that the brinkpoint heights were much smaller than dune heights, and in cases where the dunes are superimposed by smaller bedforms the original predictors over-, respectively under predicted the total hydraulic roughness. Therefore, the total hydraulic roughness of the riverbed can be accurately predicted if data is available on the average shape and size of the dunes and the median grain size of the bed.

Superposition of dunes

The issue of superposition of dunes was not considered separately in this thesis. However, it was shown to be relevant in almost every chapter. In Chapter 3 it was concluded that in case superimposed dunes are present in a river it is important to select the right dune type for dune tracking. In Chapter 4 it was shown that superposition occurs in all sections of the Rhine branches. Finally in Chapter 7 superposition was shown to be an important factor in predicting the total hydraulic roughness. The question how and why superposition occurs was addressed shortly in Chapter 8. Here it was concluded that superposition may be related to the hysteresis in the dune development, resulting in secondary dunes on top of degrading primary dunes. However, superposition can also be due to local flow conditions over the stoss-side of a dune being very different from the general flow conditions in the river. With this type of superposition, conversely to hysteresis case, both primary and secondary dunes are active.

General conclusion

Both for the dune development as well as for the hydraulic roughness of dunes a prediction method was successfully formulated and applied. The method for predicting dune development is based on the principle that the dunes are always developing toward an equilibrium dune dimension at a rate depending on the difference between their actual size and the equilibrium size. Flow strength and bed material grain-size are the key parameters. The proposed method for predicting dune-related hydraulic roughness uses the shape of the dunes in the form of the brinkpoint height, and the composition of the dune field in the form of the abundance of superimposed forms. The method is generic, and should be applicable in many rivers. For the time being however, the use of these two

prediction methods is limited to the Rhine branches as information of the same high quality from other rivers is still lacking.

De ontwikkeling en de hydraulische ruwheid van duinen op de rivierbodem

Samenvatting

Inleiding

De vele voordelen van het wonen aan een rivier, vruchtbaar land, een handelsroute, en de beschikbaarheid van water is er de oorzaak van dat vele beschavingen zijn ontstaan langs laaglandrivieren, ondanks het risico van overstromingen. Voor de toekomst wordt er een klimaatsverandering voorspeld waarbij er veel meer neerslag zal vallen. Daarom zullen de dichtbevolkte gebieden langs de rivieren beter moeten worden beschermd tegen catastrofale overstromingen. Om de benodigde voorzieningen te treffen die de overstromingsrisico's moeten verminderen is het noodzakelijk om te weten wat voor waterstanden er tijdens zulke extreme situaties zullen optreden. De waterstanden die worden bereikt zijn afhankelijk van de aangevoerde hoeveelheid water, maar ook van de mate van opstuwing door allerlei obstakels in de rivier. Het belangrijkste deel van deze opstuwing wordt veroorzaakt door de weerstand die wordt uitgeoefend door obstakels op de bodem van de rivier. Hoe ruwer de bodem, hoe meer weerstand er wordt geboden aan het stromende water en hoe meer het water wordt opgestuwd. In de meeste rivieren zijn (onderwater) duinen, gevormd door het transport van los bodemmateriaal, de belangrijkste obstakels op de bodem van de rivier. Duinen zijn zandgolfpatronen met een asymmetrisch profiel (de stroomafwaartse zijde is veel steiler dan de stroomopwaartse). Ze komen vooral voor in situaties waar het water door geulen stroomt, waarbij de duinkammen dan loodrecht georiënteerd zijn op de stroming. Duinen zijn sterk gerelateerd aan verticale stromingspatronen en daarom is de duingrootte gerelateerd aan de waterdiepte. In middelgrote rivieren betekent dit dat duinen enkele meters tot tientallen meters lang zijn en enkele decimeters tot een paar meter hoog.

De aanleiding voor dit promotie onderzoek was te komen tot een beter begrip van het ontstaan en de ontwikkeling van deze duinen en in het bijzonder van de stromingsweerstand die zij veroorzaken. Om deze doelstellingen te verwezenlijken werd het onderzoek gericht op de beantwoording van de volgende onderzoeksvragen:

- Wat is de interactie tussen sedimenttransport en duinen. En hoe kan de migratie van duinen gerelateerd worden aan het transport van materiaal over de bodem?
- Hoe veranderen de duinen in de Nederlandse rivieren tijdens een hoogwater. En hoe kunnen deze veranderingen worden voorspeld?
- Wat is de relatie tussen de duinvorm, duingrootte, de grootte van de stroomseparatie zone en de hydraulische ruwheid van een duin?
- Hoe kan de hydraulische ruwheid van duinen worden voorspeld met behulp van de duinkarakteristieken?

- Wat is de oorzaak van de superpositie van duinen in de Nederlandse rivieren. En hoe beïnvloedt deze superpositie het bodemtransport, de duinontwikkeling en de hydraulische ruwheid?

De interactie tussen duinmigratie en bodemtransport

De stroming over duinen is zeer complex en veroorzaakt daardoor verschillende interacties tussen het sedimenttransport en het oppervlak van de duin. Boven de loefzijde (de stroomopwaartse zijde) van een duin is het sedimenttransport verdeeld over bodem- en suspensietransport. Aan de lijzijde (de stroomafwaartse zijde) laat de stroming los van de bodem en wordt het sediment afgezet op de steile helling, of stroomafwaarts getransporteerd naar het volgende duin, of het wordt hoger de waterkolom in geblazen en blijft daar in suspensie.

Al deze interacties spelen een rol in de migratie van duinen en dus zijn ze van invloed op het berekenen van het bodemtransport met behulp van de duinmigratie, ook wel “dune tracking” genoemd. De analyse van verschillende problemen die optreden bij het gebruik van deze “dune tracking” techniek in veld situaties (Hoofdstuk 3), laat zien dat het bodemtransport hiermee goed kan worden berekend zonder dat daar directe metingen van het sedimenttransport voor nodig zijn. Er dient dan wel voldaan te worden aan de volgende voorwaarden:

- Het deel van de rivier waarin de profielen van de bodem worden gemeten moet zo recht mogelijk zijn, de richting van de profielen moet parallel zijn aan de oevers en de profielen moeten loodrecht op de kammen van de duinen staan.
- De keuze van de meetresolutie en de tijd tussen twee metingen moet zo goed mogelijk aansluiten bij de te verwachten duindimensies en migratiesnelheden. De gekozen meetresolutie moet groot genoeg zijn om de duinhoogte, lengte, volume en migratiesnelheid nauwkeurig te bepalen. Bijvoorbeeld: een meetresolutie van 15 meetpunten per duin en een tijdspanne tussen twee metingen waarin de duinen tussen de 20 tot 80% van hun duinlengte zijn verplaatst.
- Ten slotte, in het geval van gesuperponeerde duinen moet er gekozen worden voor dat duintype (primaire of daarop gesuperponeerde secundaire duinen) dat het meest actief het bodemmateriaal transporteert terwijl ze stroomafwaarts verplaatsen.

Het voorspellen van duinontwikkeling tijdens een hoogwater

In hoofdstuk 4 is met behulp van metingen, uitgevoerd tijdens verschillende hoogwaters en tijdens perioden met lage of gemiddelde debieten, het groter en kleiner worden van de duinen in de Rijn in Nederland geanalyseerd. De ontwikkeling van de duinvorm en grootte tijdens een hoogwater blijkt duidelijk anders te zijn in verschillende delen van de Rijn. Dit wordt vooral veroorzaakt door een verschil in samenstelling van het

bodemmateriaal en door verschillen in de verdeling van het debiet over de hoofdgeul en de uiterwaarden tijdens hoogwater. De verschillen in vorm en duur van een hoogwatergolf zijn veel minder belangrijk. De variabele verdeling van het debiet over de hoofdgeul en de uiterwaarden in de verschillende delen van de Rijn veroorzaakt duidelijke verschillen in de krachten die uitgeoefend worden op de rivierbodem in de hoofdgeul, wat zijn weerslag heeft op de ontwikkeling van de duinen op die rivierbodem. Door rekening te houden met de samenstelling van het bodemmateriaal en met de krachten die daarop worden uitgeoefend door het stromende water blijkt het goed mogelijk te zijn om te voorspellen hoe de duinen veranderen, ten minste tijdens het stijgende deel van een hoogwatergolf.

Als de debieten weer afnemen vertonen de duinen een duidelijke naijling in hun grootte. Dat betekent dat bij eenzelfde debiet als tijdens het stijgende deel, de duinen nu groter of kleiner zijn (Hoofdstuk 4). Deze hysteresis kan niet direct verklaard worden met de veranderingen in de krachten aan de rivierbodem. In Hoofdstuk 5 wordt daarom een andere methode voorgesteld om de duinontwikkeling tijdens een hoogwater te voorspellen. In de nieuwe methode wordt rekening gehouden met het moment van de eerste reactie en aanpassingstijd van de duinen op veranderingen in de stroming. De aanpassingstijd is een maat voor hoe lang het duurt voordat een duin helemaal is aangepast aan de nieuwe stromingssituatie vanaf het moment van de eerste verandering. Vanwege het niet beschikbaar zijn van informatie over de veranderingen in de samenstelling van het bodemmateriaal tijdens een hoogwater kon in Hoofdstuk 5 geen rekenmodel worden gemaakt dat toepasbaar was in de hele Rijn. De rekenmodellen die worden voorgesteld zijn alleen bruikbaar in bepaalde delen van de Rijn. De analyse toonde ook aan dat er aparte modellen nodig zijn voor de duinhoogte en duinlengte omdat de duinhoogte sneller wordt aangepast aan een nieuwe stromingssituatie dan de duinlengte.

Ondanks deze problemen bleek uit een vergelijking tussen de voorspellingen en de metingen dat de voorgestelde rekenmodellen redelijk goed de trend van de duinontwikkeling en het moment van maximale duingrootte konden voorspellen. Ook de werkelijke duingrootte werd in vele gevallen goed voorspeld. Deze rekenmodellen kunnen daarom gebruikt worden om te voorspellen wat de duindimensies tijdens toekomstige hoogwaters zullen zijn in de drie delen van de Rijn. Met behulp van informatie over de veranderingen van de samenstelling van de rivierbodem kan de methode zodanig worden aangepast dat deze ook toepasbaar zal zijn in andere delen van de Rijn en mogelijk zelf in andere rivieren.

De relatie tussen duinen, stroomseparatie en hydraulische ruwheid

De hydraulische ruwheid van een duin wordt veroorzaakt door turbulente stroming in een neer aan de steile stroomafwaartse zijde van een duin. In deze neer is er een netto retourstroming langs de bodem. Boven de neer vervolgt de van de bodem “losgelaten”, gesepareerde hoofdstroom zijn weg, om pas weer bodem te “voelen” op de stroomopwaartse zijde van de volgende duin (Hoofdstuk 6). De hoeveelheid turbulentie

die wordt geproduceerd in deze separatiezone is waarschijnlijk gerelateerd aan de algemene stromingscondities en de vorm en grootte van de separatiezone. Deze wordt op haar beurt bepaald door de hoogte van het loslaatpunt, omdat de lijn tussen loslaatpunt en aanhechtpunt altijd een helling heeft van 10 graden (± 1 graad), onafhankelijk van de vorm van de duin of de heersende stromingscondities. Het loslaatpunt van de stroming is waarschijnlijk te vinden op de plek waar de helling van de lijzijde groter wordt dan 10 graden. Bij duinen is op dit punt vaak een knik te vinden in het profiel, het “brinkpoint”, waar het verlies van stroomkracht ervoor zorgt dat het sediment naar beneden rolt over de lijzijde, zodat er een knik ontstaat van een flauw naar een steile helling.

Het voorspellen van de ruwheid van duinen

De totale hydraulische ruwheid van de rivierbodem bestaat uit een combinatie van de weerstand van de korrels waaruit de bodem bestaat (korrelruwheid) en de weerstand van de duinen (vormruwheid). In het geval van duinen is de hydraulische ruwheid direct gerelateerd aan de grootte van de zone van stroomseparatie, die op haar beurt is gerelateerd aan de hoogte van het loslaatpunt. De analyse in Hoofdstuk 7 laat zien dat bestaande voorspellers voor de ruwheid beter presteren als alleen de korrelruwheid in rekening wordt gebracht van het gebied buiten de zone van stroomseparatie, de duinhoogte wordt vervangen door de hoogte van het loslaatpunt (de hoogte van het brinkpoint) en door rekening te houden met de bijdrage aan de weerstand door gesuperponeerde duinen. De bestaande ruwheidsvoorspellers gaven te hoge ruwheden in die gevallen waar de hoogte van het brinkpoint veel kleiner is dan de duinhoogte en voorspelden te lage ruwheden in die gevallen waarbij de primaire duinen bedekt waren met kleinere secundaire duinen. Met de aangepaste voorspellers kan de totale hydraulische ruwheid van de rivierbodem dus worden voorspeld mits er nauwkeurige informatie beschikbaar is over de duinvorm en grootte en de samenstelling van het bodemmateriaal.

Superpositie van duinen

Het onderwerp superpositie is niet afzonderlijk behandeld in dit proefschrift, maar de relevantie van superpositie werd aangetoond in vrijwel elk hoofdstuk. In Hoofdstuk 3 werd aangetoond dat als er gesuperponeerde duinen voorkomen in een rivier het belangrijk is om goed te kiezen welk duintype voor “dune tracking” gebruikt wordt. In Hoofdstuk 4 is aangetoond dat superpositie veelvuldig voorkomt in verschillende delen van de Rijn. En in Hoofdstuk 7 werd aangetoond dat superpositie een belangrijke factor is bij het voorspellen van de hydraulische ruwheid. De vraag van hoe en waarom er superpositie optreedt, wordt kort behandeld in Hoofdstuk 8. Daar wordt geconcludeerd dat superpositie gerelateerd kan zijn aan de hysteresis in de duinontwikkeling waardoor er secundaire duinen ontstaan op de verdwijnende primaire duinen. Superpositie kan echter ook worden veroorzaakt door lokale stromingscondities over de stroomopwaartse zijde van een duin, die duidelijk afwijken van de algemene stromingscondities in de rivier. Bij

dit type superpositie zijn, in tegenstelling tot het hysteresese type, beide duintypen even actief in het verplaatsen van bodemmateriaal.

Algemene conclusies

Voor zowel de ontwikkeling van duinen als de hydraulische ruwheid van duinen is in dit promotieonderzoek een voorspellingsmethode ontwikkeld en toegepast. De methode voor het voorspellen van de duinontwikkeling is gebaseerd op het idee dat duinen zich ontwikkelen naar een evenwicht met een snelheid die afhangt van het verschil tussen de actuele grootte en de evenwichtsgrootte. De krachten uitgeoefend door de stroming en de samenstelling van het bodemmateriaal zijn daarbij de belangrijkste factoren. De voorgestelde methode voor het voorspellen van de hydraulische ruwheid van duinen maakt gebruik van de vorm van het duin, meer specifiek van de brinkpointhoogte, en van de samenstelling van het duinenveld op de rivierbodem, in het bijzonder de aanwezigheid van gesuperponeerde vormen. De methode is algemeen en zou daarom geldig moeten zijn in elke rivier. Voorlopig zijn de beide voorspellingsmethodes echter alleen bruikbaar zijn in enkele Rijntakken omdat er geen informatie beschikbaar is uit andere rivieren met dezelfde hoge kwaliteit die een calibratie voor die rivieren mogelijk maakt.

Curriculum Vitae



Antoine Wilbers was born on 13 January, 1973 in Asten (The Netherlands). He went through primary and secondary education in this village and then moved to Zoetermeer (The Netherlands) in 1992. Between 1992 and 1997, he studied Physical Geography at Utrecht University, with a specialisation in Riverine Morphodynamics. During an internship at RIZA-Arnhem he studied bedlevel changes and sediment transport over a period of about 25 years in the Border-Meuse (The Netherlands), and graduated (Msc equivalent level) on a field study of the general morphology and river patterns of the Allier River (France).

In 1997 and 1998, Antoine conducted several investigations on dune development and bedload transport at Utrecht University under contract of Rijkswaterstaat, RIZA-Arnhem. As a result of these investigations, in 1998, he wrote the proposal for this PhD study. The proposal was accepted and partially funded by the department of Physical Geography at Utrecht University. In addition, during the PhD-study Antoine worked under various contracts from Rijkswaterstaat to provide additional funding. The results of these contracts were partly incorporated in this thesis.

During the PhD study Antoine attended a conference of the International Association of Hydraulic Research (IAHR) in Genua (Italy) in 1999 and a conference of the International Association of Sedimentology in Lincoln, Nebraska (USA) in 2001. Antoine also attended measurement expeditions on the Rhine (in 1998), the Merwede (2002), and the Mississippi (2002), as well as assisting with the field studies of Msc-students in the Allier River (France) in the summers of 1999 to 2002.

In 2001 Antoine married Bianca le Large, with whom he had been together for 10 years, and on 13 October 2003 his daughter Caithlyn was born. Antoine spends his spare time with building web pages, editing videos and creating animations, doing some DIY or gardening, or going out for some metal-detecting.

Publications by Antoine Wilbers

Peer-reviewed publications

- WILBERS, A.W.E. & TEN BRINKE, W.B.M. (accepted) The response of subaqueous dunes to floods in sand and gravel bed reaches of the Dutch Rhine. *Sedimentology*.
- JULIEN, P.Y., KLAASSEN, G.J., TEN BRINKE, W.B.M. & WILBERS, A.W.E. (2002) Case study: Bed resistance of the Rhine River during the 1998 flood. *Journal of hydraulic engineering*, 128, 1042-1050.
- KLEINHANS, M.G., WILBERS, A.W.E., de SWAAF, A. & VAN DEN BERG, J.H. (2002) Sediment supply-limited bedforms in sand-gravel bed rivers. *Journal of sedimentary research*, 72, 629-640.
- TEN BRINKE, W.B.M., WILBERS, A.W.E., & WESSELING, C. (1999) Dune growth, decay and migration rates during a large-magnitude flood at a sand and mixed sand-gravel bed in the Dutch Rhine river system. In: *Fluvial Sedimentology VI*, Special Publication of the International Association of Sedimentologists (Ed. by N.D. SMITH and J. ROGERS), 28, 15-32.

Conference publications

- WILBERS, A.W.E. & TEN BRINKE, W.B.M. (1999) Development of subaqueous dunes in the Rhine and Waal, the Netherlands. A preliminary note. In: *IAHR Symposium on river, coastal and estuarine morphodynamics 1*, 303-312.
- TEN BRINKE, W.B.M. & WILBERS, A.W.E. (1999) Spatial and temporal variability of dune properties and bedload transport during a flood at a sand bed reach of the Dutch Rhine river system. In: *IAHR Symposium on river, coastal and estuarine morphodynamics 2*, 309-318.

Professional publications

- WILBERS, A.W.E. (2000) De bewegende bodem van de Waal. *Aarde en Mens* 4, 39-42.
- VAN DEN BERG, J.H., DE KRAMER, J., KLEINHANS, M.G., & WILBERS, A.W.E. (2000) De Allier als morfologisch voorbeeld voor de Grensmaas. I: vergelijkbaarheid en rivierpatroon. *Natuurhistorisch maandblad juli 2000*, 118-122. Maastricht.
- DE KRAMER, J., WILBERS, A.W.E., VAN DEN BERG, J.H. & KLEINHANS, M.G. (2000) De Allier als morfologisch voorbeeld voor de Grensmaas. II: oevererosie en meadermigratie. *Natuurhistorisch maandblad augustus 2000*, 189-198. Maastricht.
- KLEINHANS, M.G., VAN DEN BERG, J.H., WILBERS, A.W.E & DE KRAMER, J. (2000) De Allier als morfologisch voorbeeld voor de Grensmaas. III: sedimenttransport en afpleistering. *Natuurhistorisch maandblad september 2000*, 202-207. Maastricht.

Reports

- KLEINHANS, M.G., WILBERS, A.W.E. & VAN DEN BERG, J.H. (2001) Effect van het getij op het sedimenttransport in de Merwede: Proefmeting splitsingspunt. ICG: Netherlands Centre for Geo-ecological Research, 01/6, Utrecht University, Utrecht
- WILBERS, A.W.E. & VAN DEN BERG, J.H. (2001) Beddingvormen en baggerwerk in de Waal. ICG: Netherlands Centre for Geo-ecological Research, 01/7, Utrecht University, Utrecht
- WILBERS, A.W.E. (1999) Bodemtransport en duinontwikkeling in de Rijntakken: bodempeilingen hoogwater november 1998. ICG: Netherlands Centre for Geo-ecological Research, 99/10, Utrecht University, Utrecht

- WILBERS, A.W.E. & KLEINHANS, M.G. (1999) Gevoeligheidsanalyse dune tracking in 2 dimensies. ICG: Netherlands Centre for Geo-ecological Research, 99/8, Utrecht University, Utrecht, the Netherlands
- WILBERS, A.W.E. (1998a) Bodemtransport en duinontwikkeling tijdens afvoergolven in de Rijn en Waal. ICG: Netherlands Centre for Geo-ecological Research, 98/12, Utrecht University, Utrecht
- WILBERS, A.W.E. (1998b) Ruimtelijke variabiliteit van duinkarakteristieken in de Waal tijdens een afvoergolf in 1997. ICG: Netherlands Centre for Geo-ecological Research, 98/19, Utrecht University, Utrecht.
- WILBERS, A.W.E. (1997) Duinkarakteristieken en dune tracking tijdens een hoogwater in de Rijntakken. ICG: Netherlands Centre for Geo-ecological Research, 97/8, Utrecht University, Utrecht

- 280 K T HOUWMAN Tide, wind- and wave-driven flow processes in the nearshore zone; field measurements Terschelling and modelling -- Utrecht 2000: Knag/Faculteit Ruimtelijke Wetenschappen Universiteit Utrecht. 256 pp, 139 figs, 10 figs. ISBN 90-6809-307-X, Dfl 40,00
- 281 G BOLT Wooncarrières van Turken en Marokkanen in ruimtelijk perspectief -- Utrecht 2001: Knag/Faculteit Ruimtelijke Wetenschappen Universiteit Utrecht. 224 pp, 13 figs, 55 tabs. ISBN 90-6809-308-8, Dfl 47,50
- 282 A BONGENAAR Corporate governance and public private partnership; the case of Japan -- Utrecht 2001: Knag/Faculteit Ruimtelijke Wetenschappen Universiteit Utrecht. 190 pp, 29 figs, 31 tabs. ISBN 90-6809-313-4, Dfl 50,00
- 283 E STOUTHAMER Holocene avulsions in the Rhine-Meuse delta, The Netherlands -- Utrecht 2001: Knag/Faculteit Ruimtelijke Wetenschappen Universiteit Utrecht. 224 pp, 69 figs, 5 tabs + 1 folded full colour map. ISBN 90-6809-314-2, Dfl 51,50
- 284 A DE WIT Runoff controlling factors in various sized catchments in a semi-arid Mediterranean environment in Spain -- Utrecht 2001: Knag/Faculteit Ruimtelijke Wetenschappen Universiteit Utrecht. 240 pp, 123 figs, 33 tabs. ISBN 90-6809-318-5, Dfl 43,80
- 285 C N UZUN Gentrification in Istanbul; a diagnostic study -- Utrecht 2001: Knag/Faculteit Ruimtelijke Wetenschappen Universiteit Utrecht. 220 pp, 33 figs, 36 tabs. ISBN 90-6809-319-3, Dfl 42,00
- 286 R WINTJES Regionaal-economische effecten van buitenlandse bedrijven; een onderzoek naar verankering van Amerikaanse en Japanse bedrijven in Nederlandse regio's -- Utrecht 2001: Knag/Faculteit Ruimtelijke Wetenschappen Universiteit Utrecht. 192 pp, 14 figs, 38 tabs. ISBN 90-6809-320-7, Dfl 39,50
- 287 T A BOGAARD Analysis of hydrological processes in unstable clayey slopes -- Utrecht 2001: Knag/Faculteit Ruimtelijke Wetenschappen Universiteit Utrecht. 208 pp, 77 figs, 33 tabs. ISBN 90-6809-321-5, Dfl 42,50
- 288 I M J VAN ENCKEVORT Daily to yearly nearshore bar behaviour -- Utrecht 2001: Knag/Faculteit Ruimtelijke Wetenschappen Universiteit Utrecht. 186 pp, 89 figs, 12 tabs. ISBN 90-6809-322-3, Dfl 35,00
- 289 I J TERLUIJN Rural regions in the EU; exploring differences in economic development -- Utrecht/Groningen 2001: Knag/Faculteit Ruimtelijke Wetenschappen Rijksuniversiteit Groningen. 276 pp, 76 figs, 13 tabs. ISBN 90-6809-324-X, Euro 27,50
- 290 J WALLINGA The Rhine-Meuse System in a new light: optically simulated luminescence dating and its application to fluvial deposits -- Utrecht 2001: Knag/Faculteit Ruimtelijke Wetenschappen Universiteit Utrecht. 192 pp, 75 figs, 19 tabs. ISBN 90-6809-325-8, Dfl 45,00
- 291 P J KORTEWEG Veroudering van kantoorgebouwen: probleem of uitdaging? -- Utrecht 2002: Knag/Faculteit Ruimtelijke Wetenschappen Universiteit Utrecht. 206 pp, 33 figs, 40 tabs. ISBN 90-6809-326-6, Euro 22,40
- 292 A W HESSELINK History makes a river; morphological changes and human interference in the river Rhine, The Netherlands -- Utrecht 2002: Knag/Faculteit Ruimtelijke Wetenschappen Universiteit Utrecht. 190 pp, 58 figs, 22 tabs. ISBN 90-6809-327-4, Euro 20,80
- 293 M G KLEINHANS Sorting out sand and gravel; sediment transport and deposition in sand-gravel bed rivers -- Utrecht 2002: Knag/Faculteit Ruimtelijke Wetenschappen Universiteit Utrecht. 320 pp, 120 figs, 19 tabs. ISBN 90-6809-328-2, Euro 36,80
- 294 R VAN BEEK Assessment of the influence of changes in climate and land use on landslide activity in a Mediterranean environment -- Utrecht 2002: Knag/Faculteit Ruimtelijke Wetenschappen Universiteit Utrecht. 366 pp, 105 figs, 98 tabs. ISBN 90-6809-329-0, Euro 30,50
- 295 R KRANENBURG Buurteconsolidatie en urbane transformatie in El Alto; een longitudinaal onderzoek naar veranderingsprocessen in de voormalige periferie van La Paz, Bolivia -- Utrecht 2002: Knag/Faculteit Ruimtelijke Wetenschappen Universiteit Utrecht. ca 240 pp. ISBN 90-6809-330-4, Euro 24,00
- 296 L L BRONS Ondernemersgedrag en de dialectiek van cultuur en economie -- Utrecht/Groningen 2002: Knag/Faculteit der Ruimtelijke Wetenschappen Rijksuniversiteit Groningen. 126 pp, 20 figs, 23 tabs. ISBN 90-6809-331-2, Euro 12,00
- 297 C J PEN Wat beweegt bedrijven? Besluitvormingsprocessen bij verplaatste bedrijven -- Utrecht/Groningen 2002: Knag/Faculteit der Ruimtelijke Wetenschappen Rijksuniversiteit Groningen. 352 pp, 49 figs, 75 tabs. ISBN 90-6809-332-0, Euro 25,00
- 298 D DE MORRÉE Cooperación campesina en los Andes; un estudio sobre estrategias de organización para el desarrollo rural en Bolivia -- Utrecht 2002: Knag/Faculteit Ruimtelijke Wetenschappen Universiteit Utrecht. 182 pp, 5 figs, 17 tabs. ISBN 90-6809-333-9, Euro 17,60
- 299 G NIJENHUIS Decentralisation and popular participation in Bolivia; the link between local governance and local development -- Utrecht 2002: Knag/Faculteit Ruimtelijke Wetenschappen Universiteit Utrecht. 208 pp, 15 figs, 41 tabs. ISBN 90-6809-334-7, Euro 22,50
- 300 IGU SECTION THE NETHERLANDS Dutch geography and Africa -- Utrecht 2002: Knag. 168 pp, 37 figs. ISBN 90-6809-336-3, Euro 20,00
- 301 D GENELETTI Ecological evaluation for environmental impact assessment -- Utrecht/Amsterdam 2002: Knag/Faculteit der Economische Wetenschappen en Econometrie, Vrije Universiteit Amsterdam. 224 pp, 70 figs, 41 tabs. ISBN 90-6809-337-1, Euro 27,00
- 302 B T GRASMEIJER Process-based cross-shore modelling of barred beaches -- Utrecht 2002: Knag/Faculteit Ruimtelijke Wetenschappen Universiteit Utrecht. 254 pp, 149 figs, 27 tabs. ISBN 90-6809-338-X, Euro 28,80
- 303 J VAN DIJK, P ELHORST, J OOSTERHAVEN & E WEVER (eds) Urban regions: governing interacting economic, housing, and transport systems -- Utrecht 2002: Knag/Faculteit Ruimtelijke Wetenschappen Universiteit Utrecht. ca 416 pp. ISBN 90-6809-339-8, Euro 41,50

- 304 R DANKERS Sub-arctic hydrology and climate change; a case study of the Tana River Basin in Northern Fennoscandia -- Utrecht 2002: Knag/Faculteit Ruimtelijke Wetenschappen Universiteit Utrecht. 240 pp, 92 figs, 31 tabs. ISBN 90-6809-340-1, Euro 24,00
- 305 D KARSSENBERG Building dynamic spatial environmental models -- Utrecht 2002: Knag/Faculteit Ruimtelijke Wetenschappen Universiteit Utrecht. 224 pp, 76 figs, 18 tabs. ISBN 90-6809-341-X, Euro 21,00
- 306 H P BROERS Strategies for regional groundwater quality monitoring -- Utrecht 2002: Knag/Faculteit Ruimtelijke Wetenschappen Universiteit Utrecht. 236 pp, 97 figs, 41 tabs. ISBN 90-6809-342-8, Euro 24,50
- 307 R HESSEL Modeling soil erosion in a small catchment on the Chinese Loess Plateau; applying LISEM to extreme conditions -- Utrecht 2002: Knag/Faculteit Ruimtelijke Wetenschappen Universiteit Utrecht. 320 pp, 87 figs, 60 tabs. ISBN 90-6809-343-6, Euro 32,00
- 308 S VAN DER LINDEN Icy rivers heating up; modelling hydrological impacts of climate change in the (sub)arctic - Utrecht 2002: Knag/Faculteit Ruimtelijke Wetenschappen Universiteit Utrecht. 176 pp, 45 figs, 25 tabs. ISBN 90-6809-347-9, Euro 19,90
- 309 T HAARTSEN Platteland: boerenland, natuurerrein of beleidsveld? Een onderzoek naar veranderingen in functies, eigendom en representaties van het Nederlandse platteland -- Utrecht/Groningen 2002: Knag/Faculteit Ruimtelijke Wetenschappen Rijksuniversiteit Groningen. 188 pp, 40 figs, 13 tabs. ISBN 90-6809-346-0, Euro 20,00
- 310 K P FABBRI A framework for structuring strategic decision situations in integrated coastal zone management -- Utrecht/Amsterdam 2002: Knag/ Faculteit der Economische Wetenschappen en Econometrie, Vrije Universiteit Amsterdam. ca 268 pp. ISBN 90-6809-348-7, Euro 29,00
- 311 K PFEFFER Integrating spatio-temporal environmental models for planning ski runs: applied to the ski area of Sölden, Austria -- Utrecht 2003: Knag/Faculteit Ruimtelijke Wetenschappen Universiteit Utrecht. 240 pp, 83 figs, 27 tabs. ISBN 90-6809-349-5, Euro 21,50
- 312 F L J FAAL, J H L NIEMANS & H J VERDONK (red) Creatief ruimtegebruik; de rol van de overheid ondersteboven -- Utrecht 2003: Knag/Vereniging van Utrechtse Geografie Studenten VUGS/Kennisnetwerk Habiforum. ca 128 pp. ISBN 90-6809-350-9, Euro 12,00
- 313 A J F HOITINK Physics of coral reef systems in a shallow tidal embayment -- Utrecht 2003: Knag/Faculteit Ruimtelijke Wetenschappen Universiteit Utrecht. ca 144 pp. ISBN 90-6809-351-7, Euro 15,00
- 314 J SCHOKKER Patterns and processes in a Pleistocene fluvio-acolian environment (Roer Graben, south-eastern Netherlands) -- Utrecht 2003: Knag/Faculteit Ruimtelijke Wetenschappen Universiteit Utrecht. 144 pp. ISBN 90-6809-352-5, Euro 16,00
- 315 J HIN Ethnic and civic identity: incompatible loyalties? The case of the Armenians in Post-Soviet Georgia -- Utrecht/Amsterdam 2003: Knag/Faculteit of Social and Behavioral Sciences, Department of Geography and Planning Universiteit van Amsterdam. ca 200 pp. ISBN 90-6809-353-3, Euro 20,00
- 316 K M COHEN Differential subsidence within a coastal prism; Late-Glacial - Holocene tectonics in the Rhine-Meuse delta, The Netherlands -- Utrecht 2003: Knag/Faculteit Ruimtelijke Wetenschappen Universiteit Utrecht. 176 pp. ISBN 90-6809-354-1, Euro 28,00
- 317 M GIELCZEWSKI The Narew River Basin: A model for the sustainable management of agriculture, nature and water supply -- Utrecht 2003: Knag/Faculteit Ruimtelijke Wetenschappen Universiteit Utrecht. ca 192 pp. ISBN 90-6809-355-X, Euro 21,00
- 318 V MILLIGAN How different? Comparing housing policies and housing affordability consequences for low income households in Australia and The Netherlands -- Utrecht 2003: Knag/Faculteit Ruimtelijke Wetenschappen Universiteit Utrecht. ca 208 pp. ISBN 90-6809-356-8, Euro 22,50
- 319 E WEVER (ed) Recent urban and regional developments in Poland and the Netherlands. Papers presented at the Dutch-Polish economic geography seminar in Utrecht, 12-16 November 2001 -- Utrecht 2003: Knag/Faculteit Ruimtelijke Wetenschappen Universiteit Utrecht. 94 pp. ISBN 90-6809-357-6, Euro 13,00
- 320 M MIRANDA QUIROS Institutional capacities for sustainable progress: Experiences from Costa Rica -- Utrecht 2003: Knag/Faculteit Ruimtelijke Wetenschappen Universiteit Utrecht. ca 200 pp. ISBN 90-6809-360-6, Euro 21,00
- 321 P J VAN HELVOORT Complex confining layers. A physical and geochemical characterization of heterogeneous unconsolidated fluvial deposits using a facies-based approach -- Utrecht 2003: Knag/Faculteit Ruimtelijke Wetenschappen Universiteit Utrecht. ca 160 pp. ISBN 90-6809-359-2, Euro 20,00
- 322 J UITERMARK De sociale controle in achterstandswijken; een beleidsgenetisch perspectief -- Utrecht/Amsterdam 2003: Knag/Faculteit Maatschappij- en Gedragwetenschappen, afdeling Geografie en Planologie, Universiteit van Amsterdam. ca 150 pp., 7 figs, 6 tabs. ISBN 90-6809-358-4, Euro 19,00
- 323 A W E WILBERS The development and hydraulic roughness of subaqueous dunes -- Utrecht 2004: Knag/Faculteit Geowetenschappen Universiteit Utrecht. ca 224 pp. ISBN 90-6809-361-4, Euro 22,00

For a complete list of NGS titles please visit www.knag.nl/index.html. Publications of this series can be ordered from KNAG / NETHERLANDS GEOGRAPHICAL STUDIES, P.O. Box 80123, 3508 TC Utrecht, The Netherlands (Fax +31 30 253 5523; E-mail KNAG@geog.uu.nl). Prices include packing and postage by surface mail. Orders should be prepaid, with cheques made payable to "Netherlands Geographical Studies". Please ensure that all banking charges are prepaid. Alternatively, American Express, Eurocard, Access, MasterCard, BankAmericard and Visa credit cards are accepted (please specify card number, name as on card, and expiration date with your signed order).